AHTD TRC TRANSPORTATION RESEARCH COMMITTEE

TRC1504

Alternative Uses for Ground Penetrating Radar (GPR) in Highway Construction Maintenance

Hanan Mahdi, Amin Akhnoukh

Final Report

2016

<table>
<tr><td>1.Report No.</td><td>2.Government Association No.</td><td colspan="2">3. Recipient Catalog No.</td></tr>
<tr><td colspan="2" rowspan="2">4. Title and Subtitle
Alternative Uses for Ground Penetrating Radar (GPR) in Highway Construction Maintenance</td><td colspan="2">5. Report Date Sept. 2016</td></tr>
<tr><td colspan="2">6. Performing Organization code
AHTD TRC 1504</td></tr>
<tr><td colspan="2">7. Authors
Hanan Mahdi (PI), and Amin Akhnoukh</td><td colspan="2">8. Performing Organization report No.</td></tr>
<tr><td colspan="2" rowspan="2">9. Performing Organization Name and Address
University of Arkansas at Little Rock
2801 South University Ave.
Little Rock, AR 72204</td><td colspan="2">10. Work Unit No. (TRAIS)</td></tr>
<tr><td colspan="2">11. Contract or Grant No.</td></tr>
<tr><td colspan="2" rowspan="2">12. Sponsoring Agency Name and Address
Arkansas Highway and Transportation Department
P.O. Box 2261
Little Rock, AR 72203</td><td colspan="2">13. Type of Report
Final Report</td></tr>
<tr><td colspan="2">14. Sponsoring Agency Code</td></tr>
<tr><td colspan="4">15. Supplementary Notes:
Supported by a grant from the Arkansas Highway and Transportation Department</td></tr>
<tr><td colspan="4">16. Abstract
The primary objective of this research project was to recommend and purchase a GPR system to be used for alternative AHTD activities in highway construction maintenance, such as detecting underground utilities, unmarked graves, and soil anomalies. Currently, AHTD uses GPR for pavement studies only, using two airborne 2GHz antennas. The GPR system evaluated for accuracy in terms of system frequency, site conditions, soil types, depth of ground water table, and required depth of penetration. This project included an extensive literature review using different GPR equipment by other highway state agencies for different alternative applications. Based on the review of literature and the results of the different GPR fieldwork to cover wide range of applications, a GPR list of equipment acquired and purchased. This list of GPR equipment included a GSSI SIR-4000 control unit, 1600 MHz, 400 MHz, 200 MHz antennas, and Radan 7 software package. A training workshop on GPR methodology and equipment was conducted in the AHTD headquarters.</td></tr>
<tr><td>17. Key Words
Ground Penetration Radar, Site Conditions, Water Table, Antenna.</td><td colspan="3">18. Distribution Statement
No restrictions.</td></tr>
<tr><td>19. Security Classif.

Unclassified</td><td>20. Security Class (of this page)

Unclassified</td><td>21. No. of Pages
155</td><td>22. Price

N/A</td></tr>
</table>

Table of Contents

List of Acronyms

1. AHTD: Arkansas Highway and Transportation Department
2. FHWA: Federal Highway Administration
3. DOT: Department of Transportation
4. GPR: Ground Penetrating Radar
5. TRB: Transportation Research Board
6. ASR: Alkali-Silica reactivity

Chapter 1: Introduction

1.1 Introduction:

Ground Penetrating Radar (GPR) has been used over the past forty years for shallow subsurface investigation. It is a high resolution electromagnetic (EM) method that uses the differences in dielectric properties of subsurface objects to detect and locate features. GPR's transmitter antenna sends high rate EM waves (10-2000 MHz) (Davis and Annan, 1989) toward the ground and the backscattered and reflected signals are detected by the receiver antenna. The GPR technique has been used to detect and locate subsurface anomalies such as air, water, or clay-filled cavities, and animal burrows within the levee's body, which may affect the levee integrity and place its structure at risk. The reflected electromagnetic energy could also be used to detect low density and high permeability zones, which are common weakness zones in levees (Chlaib et al., 2013). GPR technology has also been used to provide information on pavement structure and layer thickness, detect various forms of pavement deterioration, voids and regions of excessive subsurface moisture, tunnels (< 10 m depth), concrete integrity studies and inspection, locating rebar in concrete, pavement integrity studies, detection of voids beneath pavement, and detection of bodies of sub-grade in which moisture content is anomalously high, as a precursor to development of pitting and potholes (Anderson and Cardimona, 2000).

1.2 Problem Statement

Ground Penetrating Radar (GPR) has long been known to be a good non-destructive method for collecting pavement data. AHTD is currently using GPR to evaluate pavement thickness on Arkansas highways. However, it may be possible to utilize GPR for other types of evaluations. Some of these uses include detecting and locating underground utilities, unmarked graves, and soil anomalies. AHTD's current GPR system utilizes two airborne, 2 GHz antennas. Other low frequency GPR systems may be more effective for meeting AHTD's needs. Being able to locate these items will significantly increase the productivity of design for AHTD.

1.3 Research Objectives

The main objective of this research project is to recommend a new GPR system to be used in AHTD activities with high accuracy. Specific project objectives are:

a) Different GPR systems, available at the University of Arkansas at Little Rock, will be used in detecting and locating underground utilities, unmarked graves, and soil anomalies
b) Evaluate different GPR systems for their accuracy, given the system frequency, site conditions, soil type, depth of ground water table, depth of penetration, lateral and vertical resolution
c) Evaluate result changes due to seasonal variations, such as large changes in temperature and different level of water saturation in both pavement and soil
d) Recommending the most efficient GPR system for the specific highway department activities. The most efficient GPR device will be purchased and used in conducting required fieldwork as per the AHTD project personnel.

e) Conclusive report and workshop will be held to train the AHTD personnel on the new GPR system

This report is presented to attain the above objectives. The following sections of the report are divided into 5 chapters as follows:

Chapter 2- Background and Literature Review
This chapter presents different studies performed on the use of GPR systems on a national and international level. It presents work done on using different types of GPR equipment in various projects to determine locations of underground utilities, soil anomalies, quality of construction projects, and the effect of different parameters of GPR signal quality. Appendix 1 presents a comprehensive list of the use of GPR technology for highway related problems.

Chapter 3- GPR Methodology
This chapter introduces the theoretical GPR background and the practical equations to calculate the target depth. It also presents the procedures for data processing, the target material properties and the phase of GPR signal, in addition to the trade-off between resolution and antenna frequency

Chapter 4- GPR Fieldwork
This chapter introduces the efforts of the research team in conducting the GPR fieldwork and presents the result of GPR profiles performed in different sites and site conditions. It also presents a study of the different parameters affecting the GPR signal recording and how GPR signal was affected.

Chapter 5- GPR Equipment Purchase and Training
This chapter presents a recommendation of the equipment that matches the AHTD applications given different site conditions and a list for the purchased equipment. Appendix 2 presents a training manual summary on the use of the purchased equipment.

Chapter 6- Conclusion and Recommendation for Future Research
This chapter presents the most significant conclusion developed throughout this project. Recommendation for future research is included in this chapter. Recommendation for future research covers additional aspects to be considered in GPR applications relevant to different highway construction projects and the potential use of GPR equipment in highway applications including the non-destructive testing of bridge girders and non-destructive testing of bridge decks conditions, especially decks poured against stay-in-place metal forms.

Chapter 2: Background and Literature Review

GPR is a non-destructive, high-resolution, continuous, and high-speed geophysical tool to investigate subsurface conditions and structure using electromagnetic waves. GPR has evolved over the past forty years (Daniels, 2000). GPR technology was developed during World War II for military applications. In the late 1960s, the US military used the first GPR, developed at MIT, for subsurface tunnel investigations in Vietnam. The first commercially developed GPR was first used in 1970 (Loken, 2007). GPR has been applied in wide range of applications and has been widely successful in many applications (Sato, 2001). Below are some of these applications:

- Hydrology: GPR is used widely in hydrogeological studies such as, ground water table determination (Travassos and Menezes, 2004), Ground water contamination (Hyndman and Tronicke, 2005), aquifers hydraulic properties (Lu and Sato, 2007), monitoring of the ground water flow (Kowalsky *et al*., 2004), vadose zone and its water content (Loeffler and Bano, 2004), water infiltration monitoring (Saintenoy *et al*., 2008), and ground water salinity (Tsoflias and Becker, 2008).
- Historical and Archaeological applications: this field includes many investigations such as buried archaeological structures, graves, headstones, ancient roads, pathways, fire hearth, building foundations detection (Riley and Johnson, 2004), crypt investigation (Nuzzo, 2004), and buried wood artifacts (Conyers, 2004).
- Highway and road investigations: this application has quickly developed during the past 26 years, which includes pavement layers thicknesses (Wu *et al*., 2002), in-situ pavement layers and road materials dielectric constant determination (Benedetto and Pensa, 2007), detection of pavement problems and defects such as voids, rutting, stripping, sinkholes, cracking, etc. (Scullion and Saarenketo, 1998), bridge deck evaluations (Scullion and Saarenketo, 1998); asphalt density, and moisture content base coarse quality (Loken, 2007).
- Geological applications: paleoseismological research, fault detection, liquefaction features and sand blows (Al-Shukri *et al*., 2006); joint detection, karst and sinkhole detection, layer type, layer thickness, grain size distribution, bedrock-soil interface, and mineral exploration. (Hickin *et al*., 2009); geologic material properties (water content, porosity, permeability… etc.) (Lambot *et al*., 2004; Kowalsky *et al.*, 2004).
- Environmental applications: liquid (e.g. oil) contaminations (Daniels *et al*., 1995); water leaks (Eyuboglu, 2005); military devices and unexploded ordnance (Peters *et al*., 1994).
- Civil engineering and geotechnical problems: locating utilities (water pipes, underground vaults, buried tanks, and rebar mapping) (Peters *et al*., 1994; Mellett, 1995, Grandjean *et al*., 2000); rock stability (Maerz and Kim, 2000; Fish and Lane, 2002; Francke and Utsi., 2009); levee and river embankment evaluations (Yang *et al*., 2009; Golebiowski, 2010; Miele *et al*., 2009; Prinzio *et al*., 2010; Chlaib *et al.*, 2013; Chlaib *et al.*, 2014a,b).

Due to its importance as a non-destructive testing technique for soil and material investigation to various depths, GPR has been used by the Federal Highway Administration (FHWA) and State Departments of Transportation (DOTs) to enhance their construction performance. Multiple research projects across the United States, European Countries, and China researched the different parameters affecting GPR measurement, factors affecting the accuracy of GPR readings,

and possible uses for different GPR equipment, different antennas and frequencies. A detailed literature review for previous research and research findings are included in Appendix 1 which summarizes a comprehensive search of literatures published by other DOTs related to using the GPR technology for highway applications.

Chapter 3: GPR Methodology

3.1 GPR Principles

GPR employs electromagnetic signals at a very high rate to map near subsurface anomalies (Davis and Annan, 1989). Mono-static GPR antennas usually consist of a transmitter through which an electromagnetic pulse is transmitted to the ground and reflected to the surface to be detected by the receiving antenna. The electromagnetic signal travels through the subsurface with velocities that are a function of the electromagnetic properties of the medium. The velocity of the electromagnetic signal is a function of the dielectric constant (ε_r) and the electrical conductivity (σ) (Davis and Annan, 1989; Kirsch, 2006; Milsom, 2003; Annan and Cosway, 1992; Chlaib el. al. 2014).

The dielectric constant (ε_r) is the relative measure of dielectric permittivity of the medium (ε) to the dielectric permittivity of a vacuum (ε_0 = 8.89*10^{-12} F (Farad)/m) (Olhoeft, 1998; Jol, 2009; Reynolds, 1998; Milsom, 2003; Davis and Annan, 1989; Kirsch, 2006):

$$\varepsilon_r = \frac{\varepsilon}{\varepsilon_0} \qquad \text{(Eq.1)}$$

Dielectric constant values of the material are affected by many factors such as chemical composition, texture, porosity, density, and water content. Due to the high dielectric constant of water (ε_r=80), water content within the layer will increase the material's dielectric constant. Also, clay content within the layer increases the conductivity which increases the dielectric constant of the layer.

The velocity of the EM wave (v m/ns) in a medium can be represented as (Kirsch, 2006; Davis and Annan, 1989; Reynolds, 1998; Yoshino, 1967; Sato, 2001; USACE, 1995; Sutinen, 1992):

$$v = \frac{c}{\sqrt{\varepsilon_r}} \qquad \text{(Eq.2)}$$

Where c is the speed of light in vacuum (0.3 m/ns). EM wave velocity can be calculated by examining the GPR signal. If the target depth (D) and the signal travel time (t) are known:

$$v = \frac{2 \cdot D}{t} \qquad \text{(Eq.3)}$$

Where t is the two-way travel time, which represents the duration of the pulse propagation from the surface, reaching the target, reflecting and returning to the surface. t is measured from the GPR profile. It is also possible to calculate the target's depth, D, if the dielectric constant is known (Sato, 2001; Sutinen, 1992):

$$D = \frac{c \cdot t}{2\sqrt{\varepsilon_r}} \qquad \text{(Eq.4)}$$

3.2 Procedures for Data Processing

The raw GPR data was processed using GSSI RADAN 7.4.15.0427 software with the application of the following procedures:

1- Time Zero correction:
   An important process operation is to ensure that the mean value of the A-scan is near to zero (Daniels, 2004). The place in time where the radar pulse leaves the antenna, and enters the subsurface is considered as "Time Zero". The zero time may not have been detected precisely by the instrument in the field and should therefore be repicked to ensure correct depths in the profile (M. Szymczyk and P. Szymczyk, 2013).
2- Background Removal:
   Background Removal is a filter, formally called a Horizontal Background Removal FIR Filter, which removes horizontal bands of noise. Sometimes 'real' horizontal reflectors cause these bands, but they can also be caused by low frequency noise such as antenna ringing. These layers can obscure other 'real' horizontal or point source reflectors (RADAN 7 manual).
3- Migration procedure:
   Migration is a technique that moves dipping reflectors, which appear as hyperbolic tails, to their true subsurface positions and collapses hyperbolic diffractions. There are two Migration methods available in RADAN 7: Hyperbolic Summation and Kirchhoff Migration. We used the kirchhof migration as it is also applying a correction factor to the averaged value derived by summing along a hyperbola based upon the angle of incidence and distance to the feature. It also applies a filter to compensate for the summation process (RADAN 7 manual).
4- Low and High pass filters:
   The low pass filter will eliminate high frequency noise; it will reject frequencies below an established threshold. While the high pass filter eliminates the low frequency noise; it will reject frequencies above an established threshold (RADAN 7 manual).

3.3 Target Material Properties and the Phase of GPR Signal

Under Ideal subsurface condition and high signal to noise ratio, it is possible to identify the target material by examining the phase of the GPR signal of the target. Voids and small cavities (air) are characterized by their low dielectric media, and accordingly, GPR signal will exhibit negative-positive-negative (N-P-N) signal or black-white-black (B-W-B) using the gray scale presentation. High dielectric materials, such as clasts of silt, clay, metallic objects, and water-filled voids, result in GPR signal of P-N-P (W-B-W). Though, we have to emphasize that we should use this with caution in case of deep targets and low signal to noise ratio as we will show later in the section.

Figure 3.3.1 is a laboratory experiment schematic showing 2 PVC pipes at 20 cm depth and 20 cm apart imbedded in dry sand. 1.5 GHZ antenna was used to collect the data. Data processed for Time Zero and Background Removal. Left upper panel shows polarity of the water filled PVC (P-N-P) to the left (circled blue) and the air filled (empty) PVC (N-P-N) to the right (circled red). Upper middle panel shows a single scan across the water filled PVC and the upper right shows the single scan across the empty PVC. Lower panel is a schematic of the experiment setting.

Figure 3.3.2 is a laboratory experiment schematic showing steel rebar at 30 cm depth imbedded in dry sand. 1.5 GHZ antenna was used to collect the data. Data processed for Time Zero and Background Removal. Middle panel shows the radargram of the rebar. Right panel shows a single scan across the rebar with a polarity of P-N-P. Left panel is a schematic of the experiment setting.

Figure 3.3.3 shows the GPR profile that was conducted over a PVC pipe. Left panel is the radargram for the PVC pipe that was buried at 40 cm depth with a diameter of about 18 inches. Data was collected on UALR Campus on February 04, 2016 from north-east to south-west direction using 400 MHz antenna and SIR-3000 GSSI equipment. Middle panel show a picture for the pipe. Right panel is a single scan showing the pipe's anomaly and the N-P-N polarity of the GPR signal, which is indicative of an empty PVC pipe.

Figure 3.3.4 shows the GPR profile that was conducted over a metal pipe. Left Panel is the radargram of the metallic pipe buried at 1 m (3.3 ft.) depth with a diameter of about 12 inches. Data was collected using 400 MHz antenna and SIR-3000 GSSI equipment from north to south direction over asphalt pavement. Middle panel is a picture of the pipe and right panel is a single scan across the pipe anomaly showing the phase of the target as P-N-P indicative of metallic pipe.

For deeper targets, the 200 MHz antenna has more capability of resolving the target anomaly than the 400 MHz antenna because of longer wavelength. In addition, the increased effects of the noise and water saturation with depth make the 400 MHz antenna less efficient. Figure 3.3.5 shows a comparison between the 200 and 400 MHz antennas. The Upper panel is the GPR profile using 400 MHz antenna conducted on UALR Campus. The Lower panel is same GPR profile using 200 MHz antenna. The 400 MHz antenna was unable to resolve the phase of the target material correctly, which was a group of insulated metal pipes, because of the deterioration of signal to noise ration.

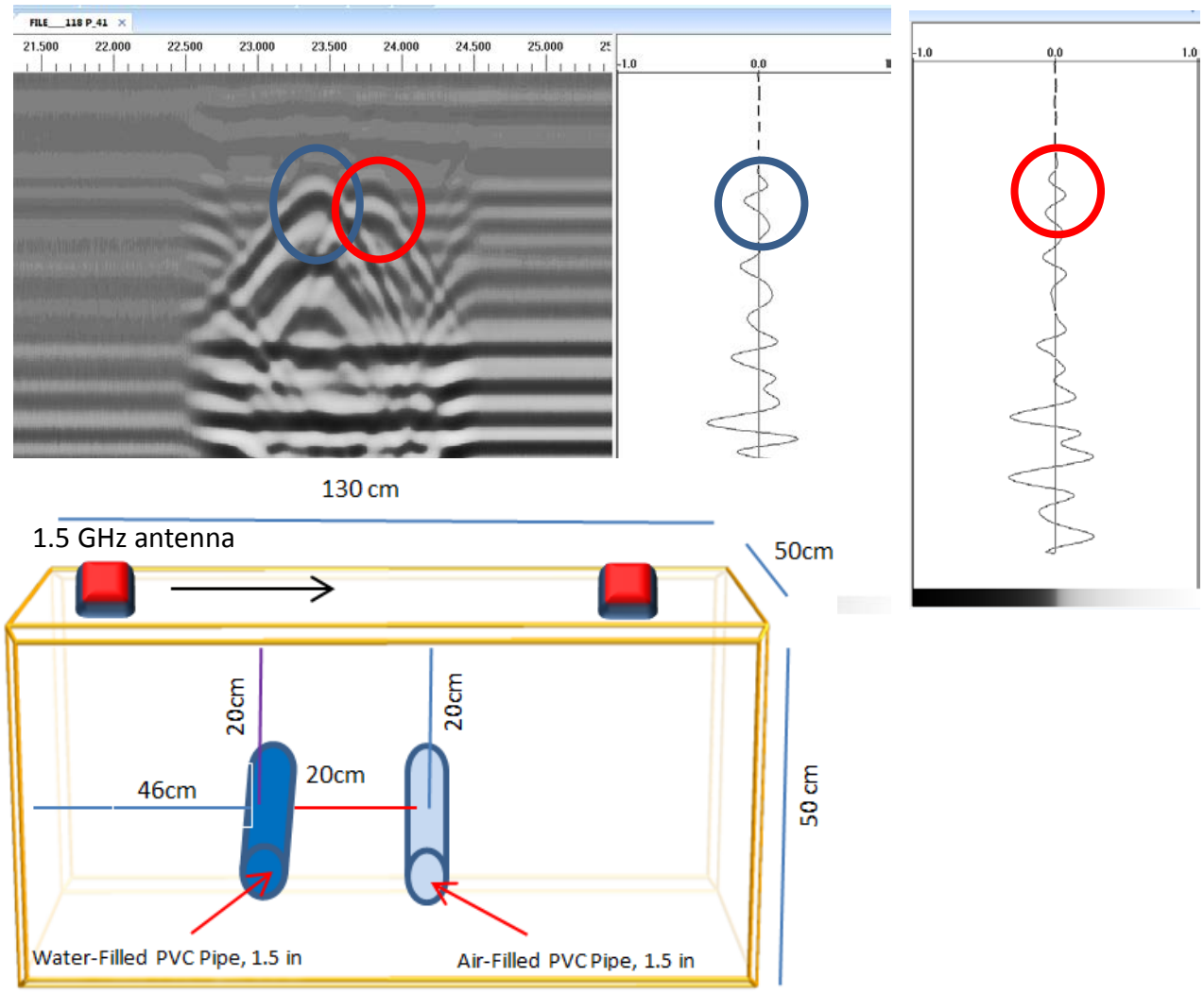

Figure 3.3.1: Two PVC pipes at 20 cm depth and 20 cm apart imbedded in dry sand. Data processed for Zero Time and Background Removal. Upper left panel show polarity of the water filled PVC (circled blue) and the air filled (empty) PVC (circled red). Upper middle panel shows a single scan across the water filled PVC and the upper right shows a single scan across the empty PVC. Lower panel is a schematic of the experiment setting.

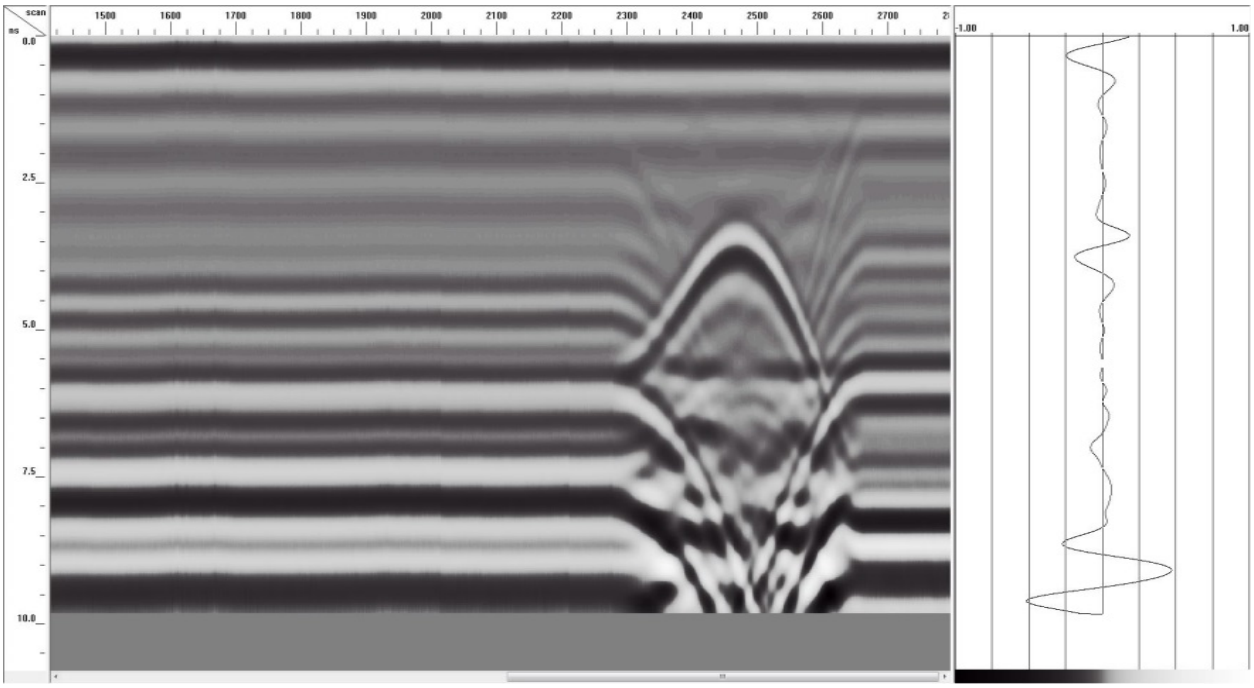

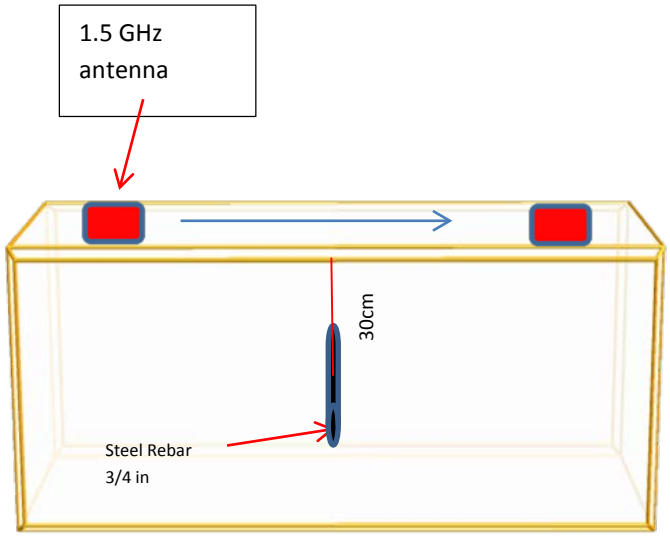

Figure 3.3.2: Steel rebar at 30 cm depth imbedded in dry sand. Data processed for Zero Time and Background Removal. Upper panel shows the radargram of the rebar. To the right of the upper panel is a single scan across the rebar with a polarity of P-N-P. Lower panel is a schematic of the experiment setting.

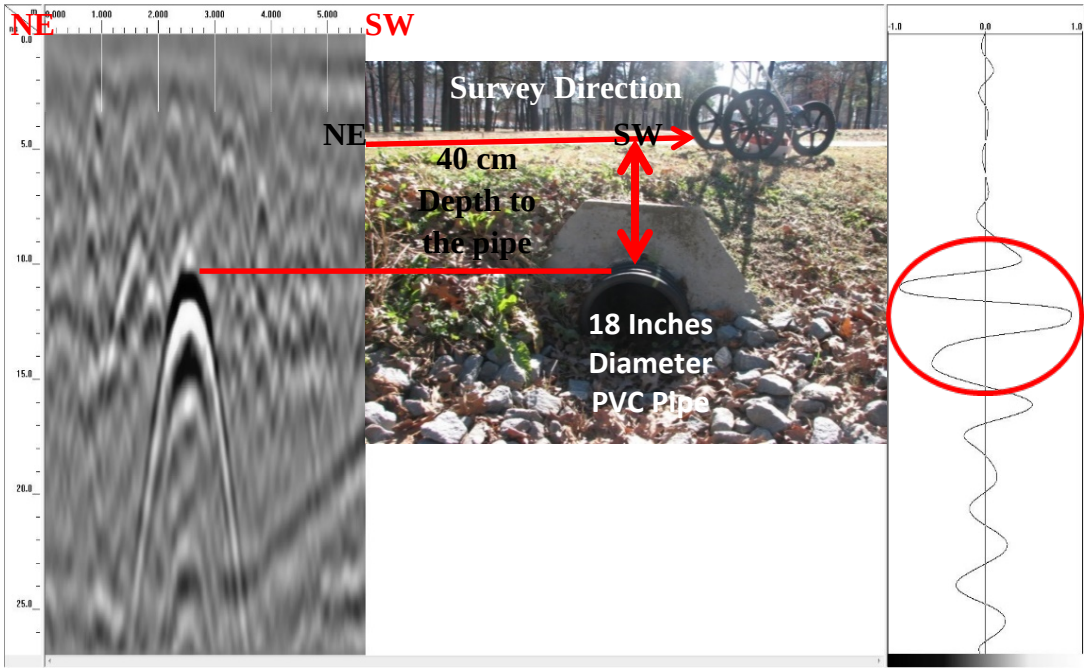

Figure 3.3.3: Left panel is a radargram for a PVC pipe buried at 40 cm depth with a diameter of about 18 inches. Middle panel show a picture for the pipe. Right panel is a single scan across the pipe anomaly showing the N-P-N polarity of the GPR signal, which is indicative of an empty PVC pipe.

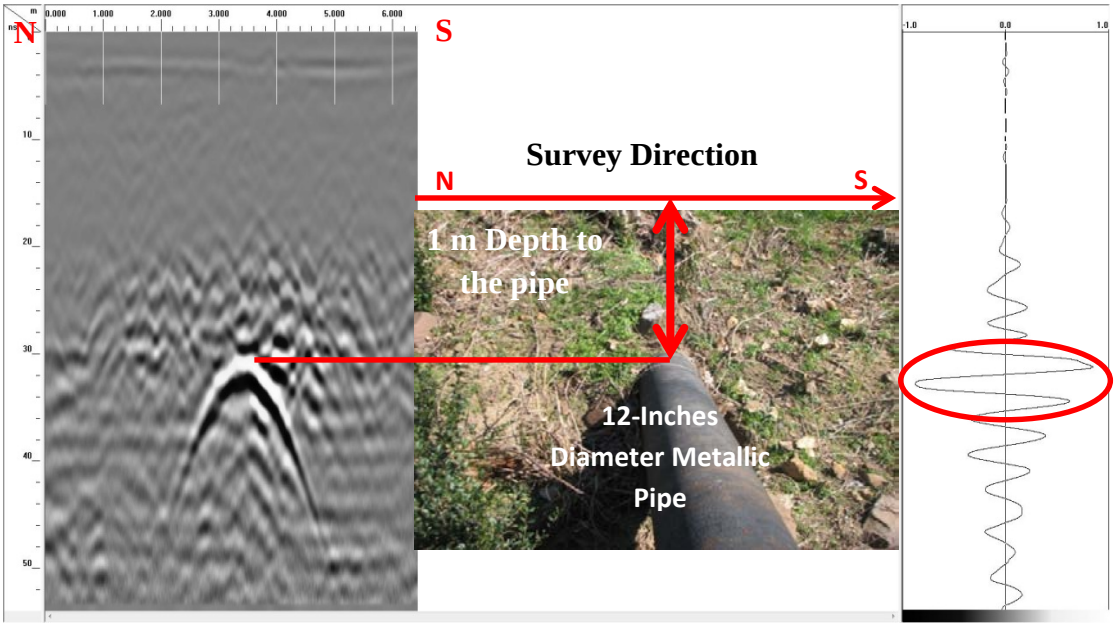

Figure 3.3.4: Left is a radargram of a metallic pipe located at a depth of 1 m (3.3 ft) with a diameter of about 12 inches. Data was collected on February 04, 2016 at UALR Campus from north to south direction over asphalt pavement. In the middle is a photograph of the pipe and to the right is a single scan of the pipe anomaly showing the phase of the target as P-N-P indicative of metallic pipe.

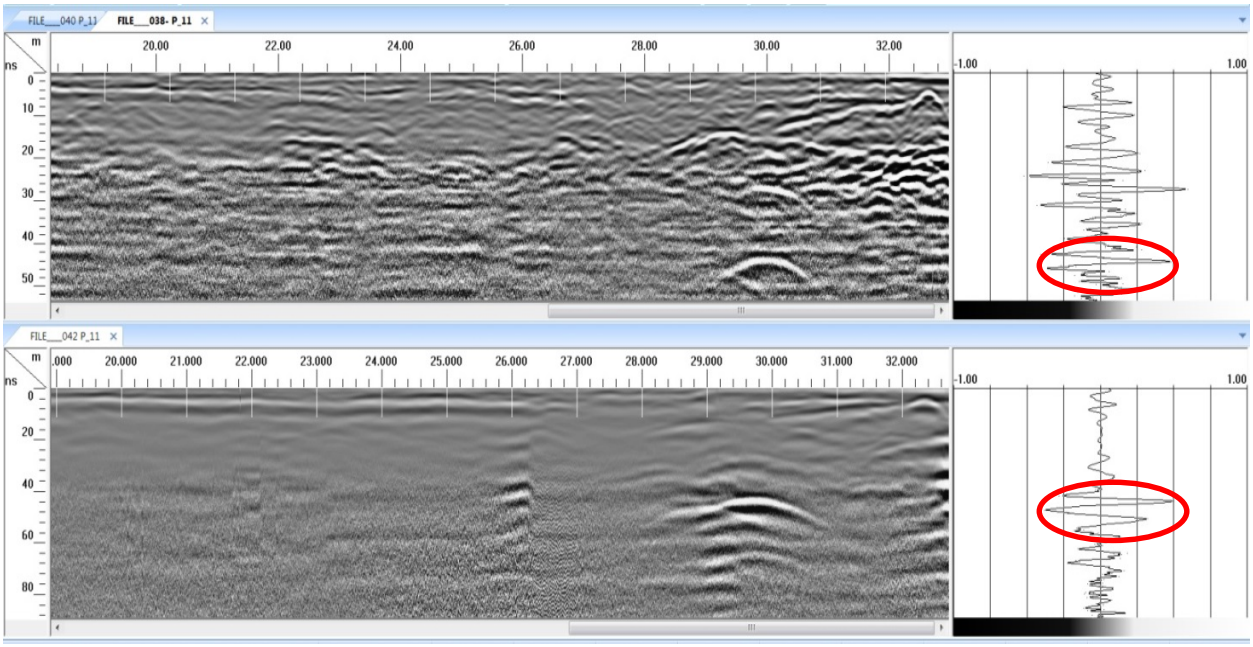

Figure 3.3.5: Upper panel GPR profile using 400 MHz antenna on UALR Campus. Lower panel is same GPR profile using 200 MHz antenna.

3.4 The Radar Antenna Frequency: Trade-Off Resolution and Antenna Frequency

There is a trade-off between resolution and antenna frequency. Larger size low frequency antennas produce less resolution data; however, increased penetration depth. High frequency antennas produce high resolution data; however, decreased penetration depth.

Figure 3.4.1 shows the beginning section of three GPR profiles run from ETAS Building, UALR Campus, toward the Creek on August 17th 2015 (Files 38, 40, and 42). Left panel represents the 400MHz radargram, middle 270MHz and right is the 200MHz. GPR data were processed for Time Zero and Background Removal. This example shows that the shallow anomaly was better resolved using the 400 MHz antenna than the other two antennas. Figure 3.4.2 shows the end part of the same three profiles (Figure 3.4.1). We were interested in verifying the antenna frequency capability in resolving the anomaly of group of insulated metal pipes buried underground. As seen in the figure, all the antennas were able to resolve this anomaly around a depth of 1.75 m (5.75 ft.). However, the 200 MHz antenna better resolved this anomaly due to the increased level of noise and water saturation.

Table 3.4.1 lists antenna frequencies and penetrating depth (Rister and Graves, 2008**)** along with typical applications.

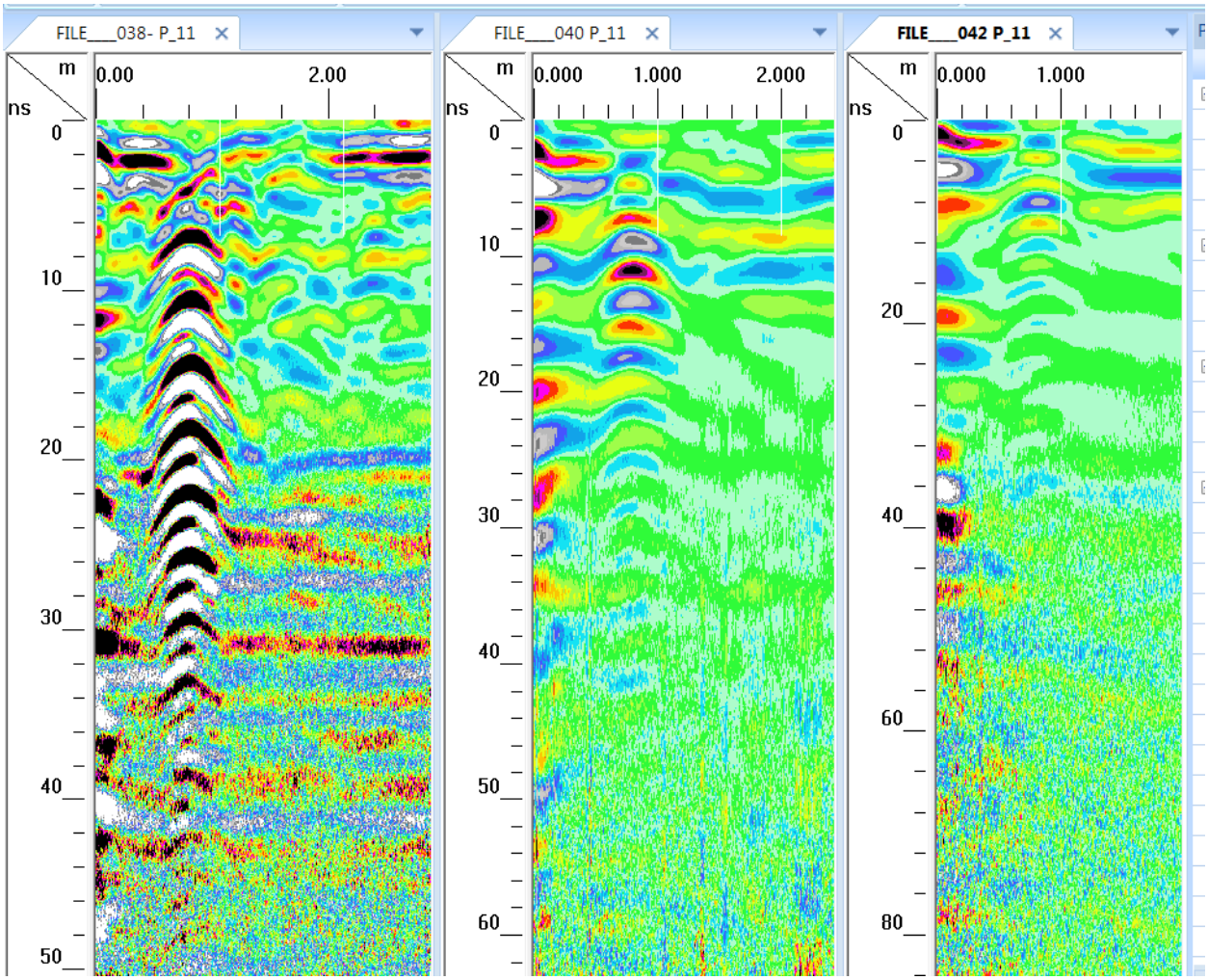

Figure 3.4.1: Beginning part of three GPR Profiles run from ETAS Building, UALR Campus, toward the Creek on August 17 2015 (Files 38, 40, and 42). Left panel is GPR data using 400MHz, middle 270MHz, and the right panel is the 200MHz. GPR data processed for Time Zero and Background Removal.

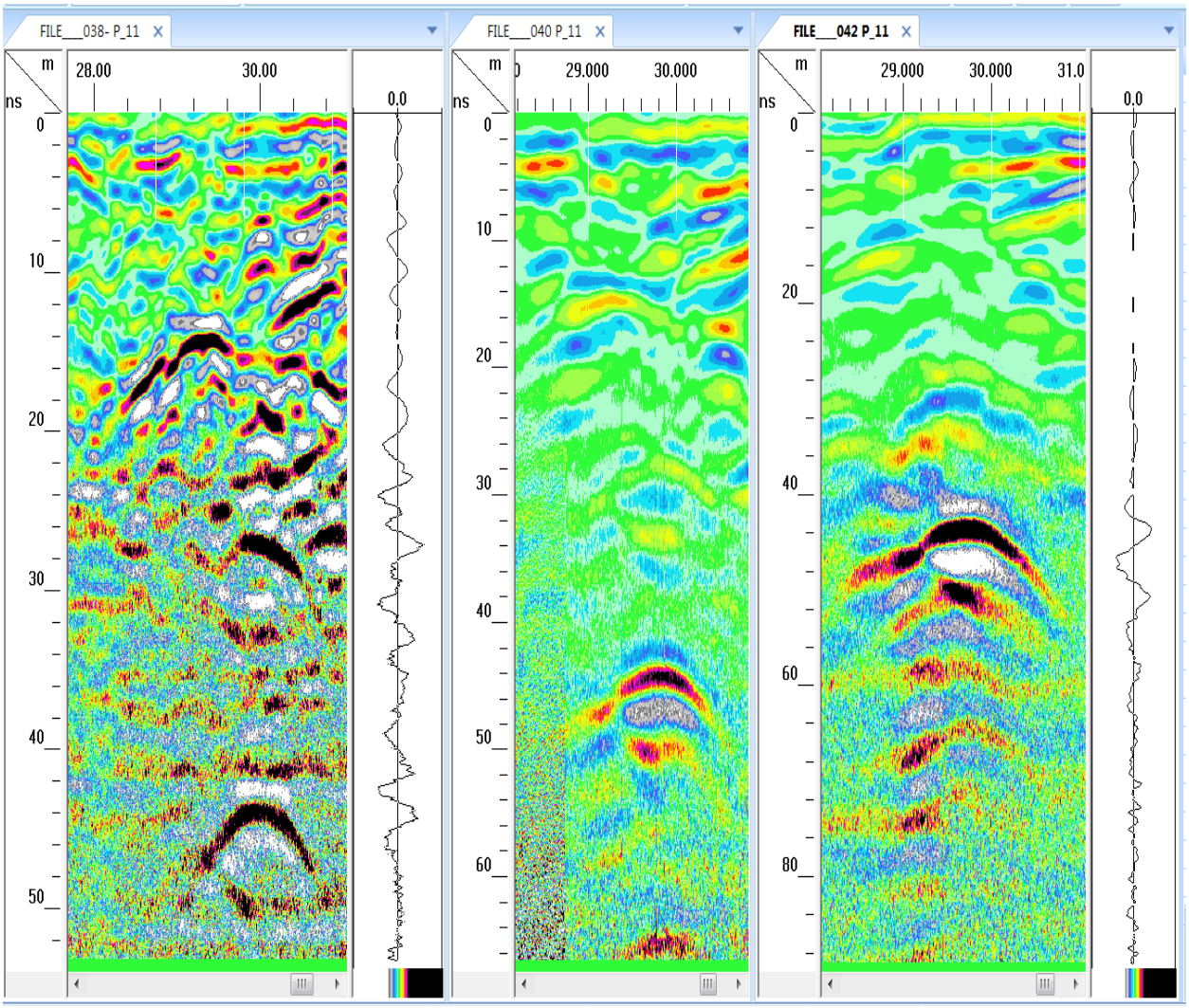

Figure 3.4.2: End part of three Profiles run from ETAS Building, UALR Campus, toward the Creek on August 17 2015 (Files 38, 40, and 42). Left panel is the 400MHz, middle 270MHz and the right panel is the 200MHz. GPR data processed for Time Zero and Background Removal.

Table 3.4.1: Antenna frequencies and penetrating depth (Rister and Graves, 2008)

Center Frequency	Depth of Penetration*	Typical Applications
2600 MHz	to 0.4 m (12 in)	Concrete Evaluation
2.0 GHz	0-.75 m (0-2.5 ft)	Pavement Thickness and Road Condition Assessment
1600 MHz	to 0.5 m (18 in)	Concrete Evaluation
1.0 GHz	0-.9 m (0-3 ft)	Highway and Bridge Deck Evaluations
900 MHz	0-1 m (0-3 ft)	Concrete Evaluation, Void Detection
400 MHz	0-4 m (0-12 ft)	Utility, Engineering, Environmental, Void Detection
270 MHz	0-6 m (0-18 ft)	Utility, Engineering, Geotechnical
200 MHz	0-9 m (0-30 ft)	Geotechnical, Engineering,
100 MHz	2-15 m (5-50 ft)	Geotechnical, Engineering, Mining
16-80 MHz	0-50 m (0-150 ft)	Geotechnical

*Penetration depths may vary depending on soil conditions.

Chapter 4: GPR Fieldwork

4.1 Using Ground Penetrating Radar to Detect Underground Utility Pipes: GPR Surveys on AHTD-Site 1, 2 & 3

UALR geophysics team collected a series of GPR profiles near 12300 and 12915 Cantrell Rd; and near the I-30 River Bridge in downtown, Little Rock in August 2015 with the intent of detecting buried ductile iron pipes (DIPs) as requested by the AHTD. These areas are named as Site-1, Site-2 and Site-3 respectively. Although, the DIP material is responsive to the electromagnetic wave, the presence of the high water content around the pipes was very challenging to the research team since the pipes were located at least in one site at the bottom of the troughs, where the water gathers and saturates the soil.

In order to overcome the challenges mentioned above, and in coordination with AHTD personnel, a set of surveys were repeated in February of 2016 during a period of less vegetation and cold dry weather. Both 200 MHz and 400 MHz antennas were used for the survey. The survey parameters were optimized for best possible result. For site-2, we extended the survey beyond the previous area to the west in order to constraint and enhance the results. As for Site-3, we conducted another survey on the same extension of the same pipe hoping to avoid high moisture areas and obtain better results.

As a general rule, the research team conducts a preliminary survey to determine the suitable antenna type(s) and the best possible data collection parameters. The second phase of the surveying continues with comprehensive GPR survey once the antenna is selected and the surveying parameters are set for the area. This enables a fair comparison of signal between the different GPR profiles. However, due to the complexity of the soil, some of the parameters may require additional adjustments for specific profiles in order to reduce the noise and increase the signal strength.

4.1.1 Site-1

The Google satellite image shows the location of the Site-1 to the north of HWY 10 near 12300 Cantrell Rd (Figure 4.1.1). The layout map provided by the AHTD shows the prospective location of the utility pipes (Figure 4.1.1) to be detected while the zoomed-in section shows the area surveyed with GPR marked in a red rectangle. The total size of the survey area was 10 m (32.8 ft) by 30 m (98.4 ft).

According to the layout map, prospective pipe(s) buried parallel to the road, therefore, the GPR profiles were collected perpendicular to the direction of the pipe(s) in order to locate the pipes and measure their depth(s). This survey setup is ideal to detect the pipes under favorable conditions because the pipe(s) would create hyperbolas in the GPR images. Figure 4.1.2A shows the locations of the profiles in a satellite image and a more detailed survey scheme

is provided in the zoomed-in portion (Figure 4.1.2B). In total, 31 profiles were planned and collected in NS orientation, which are 1m (3.2) ft apart from each other (Figure-4.1.2B). The total length of all the profiles for Site-1 is 312 m (1,023 ft).

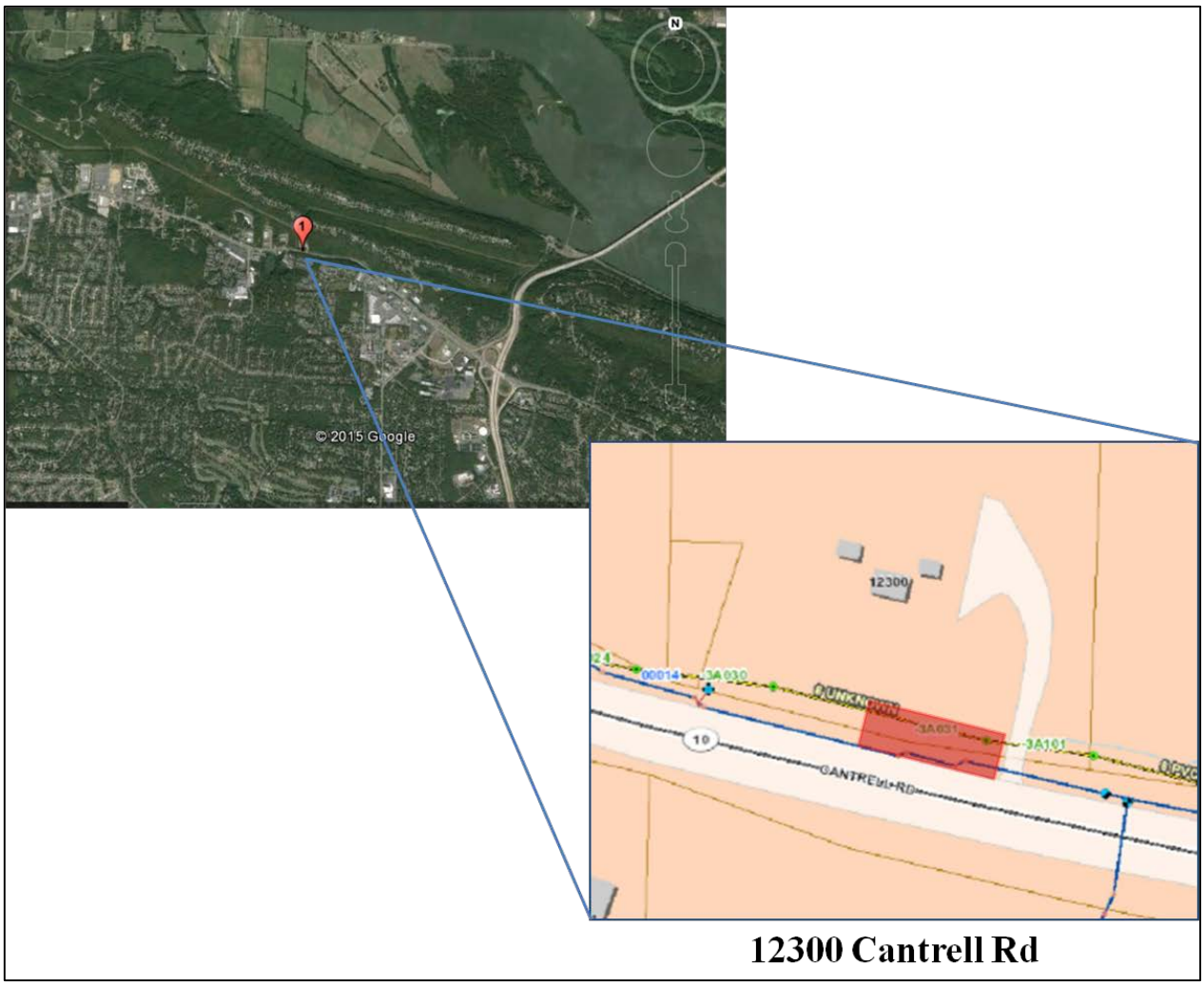

Figure 4.1.1 - Google satellite image showing the location of the Site-1 on Cantrell Rd (upper left) and the layout map provided by the AHTD showing the location of the utility pipes and the surveyed area in red rectangle in the zoomed-in section (lower right).

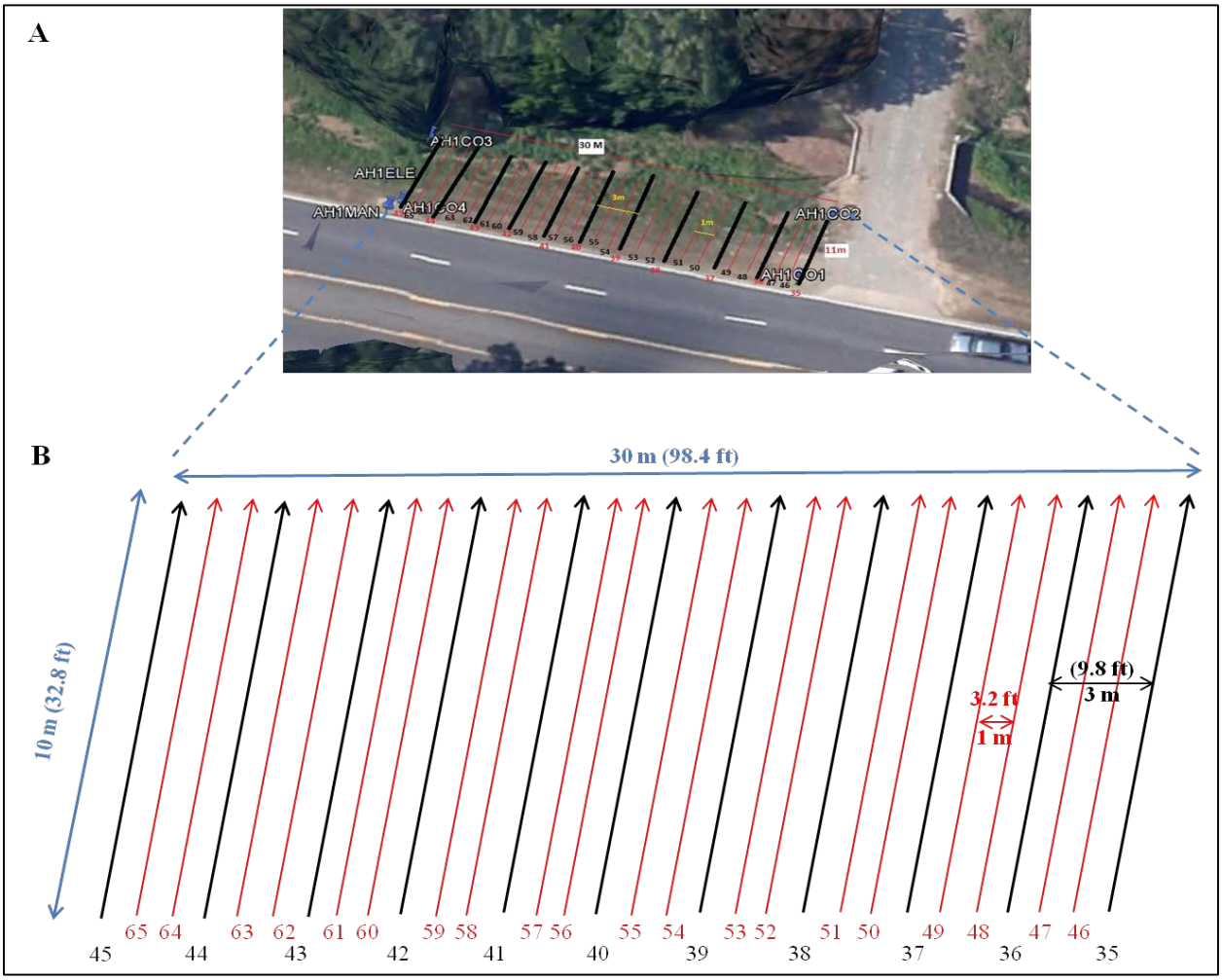

Figure 4.1.2 – (A) Google satellite image showing the locations of the profiles in Site-1. (B) A more detailed survey plan showing the numbers and the directions of the profiles.

For this site, GSSI SIR-3000 control unit with 400 MHz mono-static antenna was used due to its higher-resolution and the shallow depth of the prospective pipe(s). According to the preliminary survey, 50 ns time-range was sufficient to detect the pipes and possible other anomalies below the pipes. Therefore, 50 ns was selected as the time-range for this site. The soil had relatively high moisture content because of the widespread roots of the weeds and the area being close to a water source. Figure 4.1.3 shows this water channel close to the survey area. The presence of water in the immediate vicinity of the survey area is not desired since it reduces the signal to noise ratio (SNR).

Figure 4.1.3 - A small water channel is shown close to the survey area in Site-1.

Due to the presence of water, a high pass IIR filter was applied to the data to minimize the noise in addition to the standard data reduction methods such as Background Removal and time-zero correction. Although, SIR-3000 allows the operator to select additional FIR/IIR filters during data collection in addition to the built in filters, research team most often prefers to further process the data in the laboratory depending on the type of the noise content.

Figure **4.1.4** shows a comparison of raw (left) and processed (right) data collected along profile 35, which is the farthest east profile closest to the water channel. The high-frequency noise shown in the raw data is removed from the signal after the processing. The single scan from the processed profile shows this result (right). It is also important to select a color scheme and color form that highlights the subsurface features of interest. This is shown in the

Figure **4.1.4** as the anomalies in the processed data are more prominent compared to the raw data. However, the anomaly that represent the pipe is masked in this profile due to the complexity of the reworked top soil above 20 ns and the high water content below the 20 ns and since it is the closest to the small water channel shown in Figure 4.1.3.

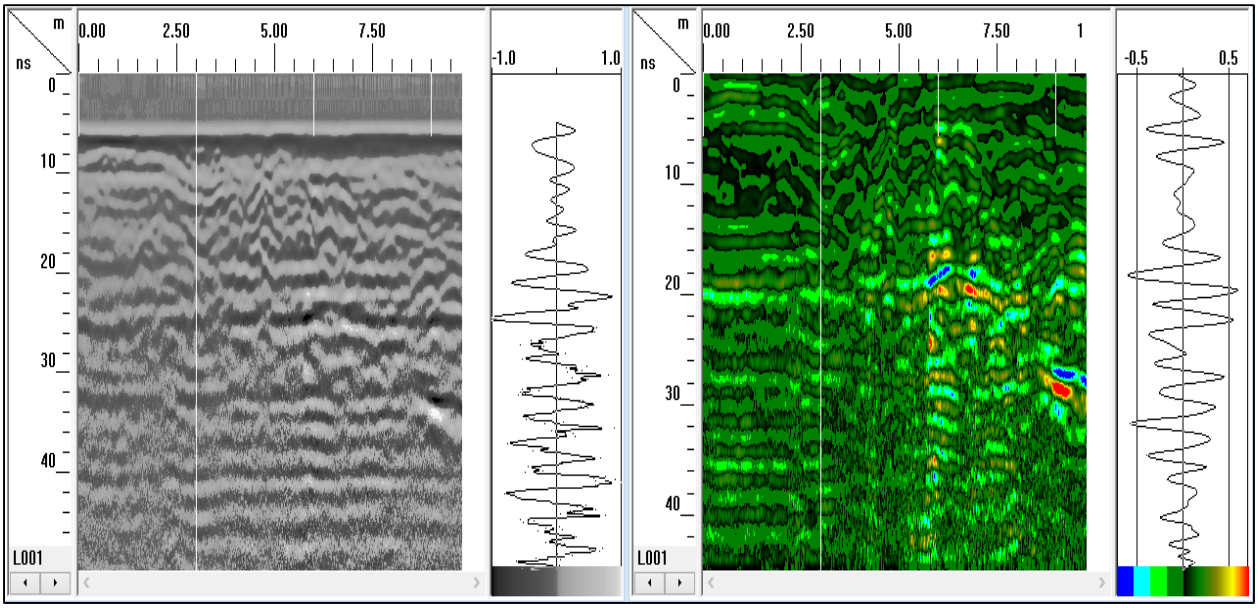

Figure 4.1.4 - 400 MHz data collected along the profile 35. The profile on the left is the raw data and the profile on the right is processed data.

Figure 4.1.5 shows the GPR profiles 55 (A) and 58 (B), which are 4.5 m (15 ft) apart from each other. The prospective pipe's location is circled in yellow and the corresponding single scan from this location is provided to the right of the profiles. The red arrows over the distance markers on top of the profiles show exactly where these scans are located in the profiles. According to these results, the DIP is at 20 ns below the surface, right above the water saturated zone where water starts to dominate the signal below this depth. Due to the reworked top soil, signal quickly diminishes close to the surface however; DIP produces a very prominent reflection as shown in single scans. Although, the data collection parameters were standardized, the reflections from DIP in profiles 55 and 58 have different strengths. This could be related to the following reasons or the combination of those at the same time,

a. The differential compaction of the soil above pipes causing a change in electromagnetic contrast between the layers
b. The antenna losing contact with the ground intermittently due to the roughness of the surface
c. The changes in reworked soil texture changing the absorption and scattering of electromagnetic waves.
d. The differential corrosion of the material causing a change in the electromagnetic properties.

A distinct hyperbolic reflection is also observed next to the reflection circled in yellow in figure 4.1.5A. This reflection has almost the same strength as the neighboring reflection caused by the DIP. It is probable that this reflection might be caused by a junction (or turn) in DIP as depicted in the layout map because the depth and the location of this anomaly matches approximate position of the junction in DIP.

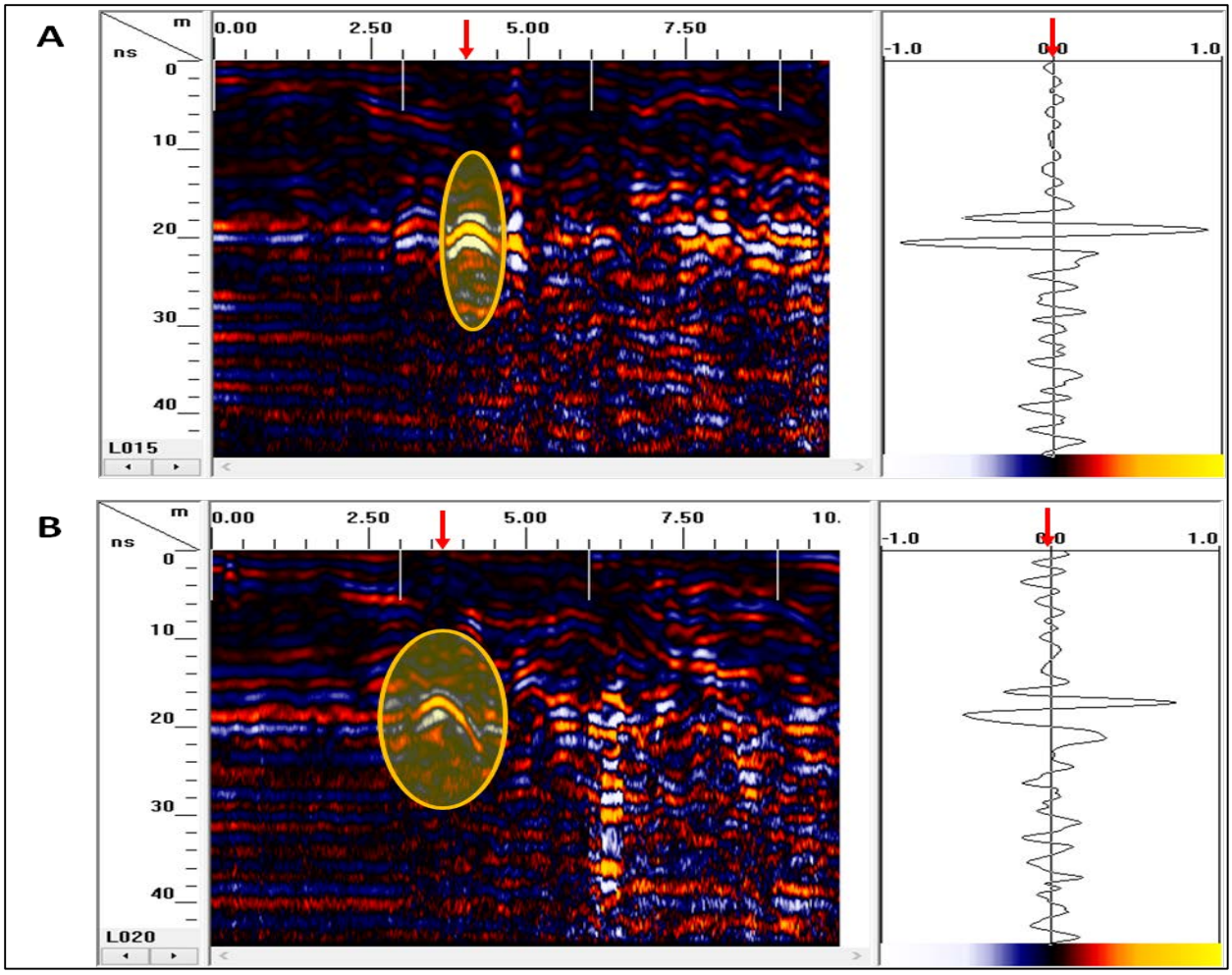

Figure 4.1.5 – Profile 55(A) and 58 (B) with the corresponding single scans. The prospective pipe's location circled in yellow and the corresponding single scan from this location provided to the right of the profiles. The red arrows over the distance markers on top of the profiles show exactly where these scans are located in the profiles.

Figure 4.1.6 shows profiles 42 (A) and 44 (B), respectively, which are further west of profiles 55 and 58 (**Figure 4.1.2**), and 5.5 m (18 ft) apart from each other. Similar to the previous examples, the location of the prospective pipe circled in yellow and the corresponding single scan from this location is provided on the right hand side. According to the radargrams, the DIP is around 18 ns below the surface and slightly above the water saturated zone. This is approximately two ns above the location of the DIP in profile 55 and 58. In addition, the soil texture differs from this location to the other above the pipe, which results in different reflection characteristics for the same pipe.

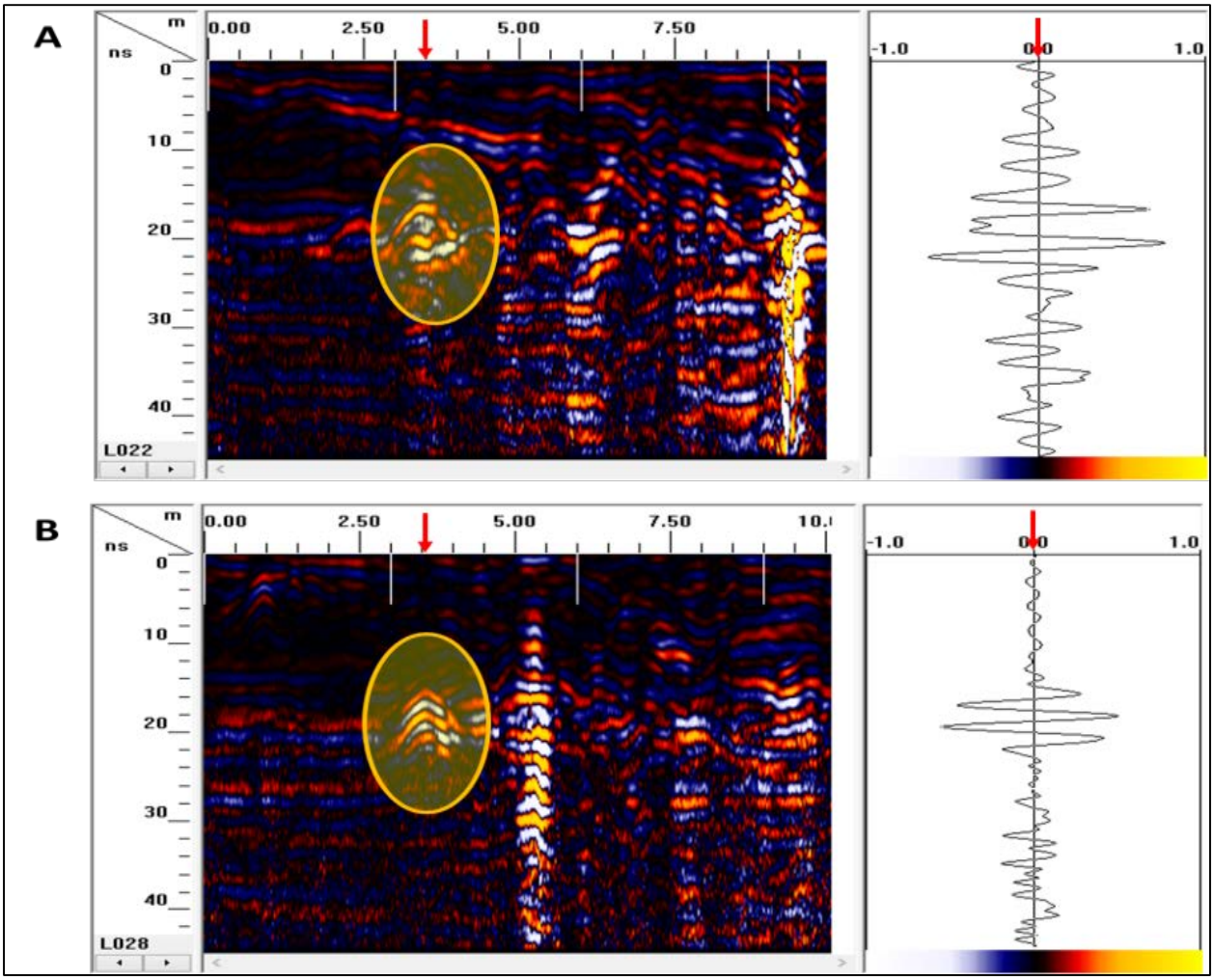

Figure 4.1.6 - Profile 42(A) and 44 (B) with the corresponding single scans. The prospective pipe's location circled in yellow and the corresponding single scan from this location provided to the right of the profiles. The red arrows over the distance markers on top of the profiles show exactly where these scans are located in the profiles.

In order to calculate the true depth of the DIP, an accurate estimation of dielectric constant is required. However, this is not an easy task due to the numerous factors affecting this parameter. The most accurate method of determining the dielectric constant is using ground-truth data, which is often referring to a buried object with a known depth. If this method is not applicable, a known value (wet clayey soil) is preferred to be representative of the dielectric constant. Using a dielectric constant value of 10, the estimated avearge depth of the DIP was 0.8 m (2.6 ft).

Site-1 Winter Survey

We repeated the GPR survey in this area using the same profile layout as the summer survey. An area 30 by 8 m (98.4 by 26.2 ft) was cleared for the survey to be conducted. SIR-3000 GPR system with a 400-MHz was used in the survey. Thirty-one profiles (109 through 139) were collected for this area on Feb 10, 2016 from South to the North direction.

Comparison between the GPR Surveys during Different Seasons and Subsurface Moisture Contents

Both GPR surveys reveal the existence of at least one DIP water pipe (blue) extends parallel to Cantrell and about 3.5 m (11.5 ft) away from the curb. The second anomaly, two meters to the north of the blue pipe, represents the anomaly of fiber optic line (orange) which extends parallel to the blue pipe. Figures 4.1.7 and 4.1.8 show two S-N GPR profiles radargram during summer time. The middle panels of the figures is 3-D presentation of the GPR survey data with the cross hair indicating survey lines crossing the underground DIP at two different locations. The right panels of the figures show the GPR survey parameters. Figures 4.1.9 and 4.1.10 represent the GPR survey for the same areas during wintertime. GPR data were processed for Time Zero and Background Removal. Comparing GPR data collected at the same area under two different seasonal conditions reveal the following:

1. We expect the DIP to lay horizontal and the depth values are the same along the different GPR profiles. Data revealed that the depth of the DIP varied from one profile to another within the survey area for the same season. Although we conducted GPR surveys in dry periods with no rain for many days, we found that in summer survey the depth variations along different profiles were much less than in winter survey. Depth values were more consistent in summer. These depth variations reflect that moisture content variations are more prominent in winter than in summer. For summer survey, using dielectric constant of 10.0, the depth of DIP is ranging from 0.76 m-0.94 m (2.5-3.1 ft.). The average depth of the DIP is 0.84m (2.75 ft.). For winter data using the same dielectric constant of 10.0, the depth values ranging from 0.76 m – 1.14m (2.5-3.75 ft.) with average depth of 1m (3.3 ft.).
2. In general, the average depth value in summer is shallower than in winter. Drier subsurface with less moisture content will cause higher velocity which in turns leads to shorter two way travel time that results in a shallower depth of the target. In addition, the less moisture variation within an area, the more consistent the target depth values.
3. The subsurface moisture caused the GPR data in summer survey to look less noisy than in winter survey. In addition, the amplitude of the GPR reflection from the target, as it shown in the left panel of the figures, is higher in summer than in winter. Although the gain for collecting the data during summer was a little higher than in winter, we think that part of this reduction in amplitude is due to signal attenuation due to the increase in moisture content.
4. For any successful GPR survey, choosing the appropriate dielectric constant value is essential to the correct determination of the target depth value. For a target, in specific subsurface condition, using different dielectric constant values will result in different depth values. For the same target, using the same dielectric constant value in different moisture conditions will result in incorrect depth value. Figure 4.1.11 and 4.1.12 show the radargram of profile L014

during summer and winter survey respectively. For the summer survey (fig. 4.1.11), the depth to the top of the DIP is 17.26 ns. Using dielectric constant value of 10.0 will result in a depth value of 0.82m (2.7 ft.). At the same location, the winter survey revealed that the depth to the same pipe is 19.73 ns. This difference in depth values (2.47 ns) is the result of the difference of the moisture content. The more the moisture, the slower the GPR signal, the longer is the two way travel time. Accordingly using the same dielectric constant of 10.0 will result in an incorrect depth of 0.94 m (3.08 ft.). In order to obtain the correct depth value (0.82 m) for this pipe at this location, the dielectric constant value should be at least 13.0. Thus, this shows that GPR results will not be affected by different weather temperature conditions but rather what control the outcome of a GPR survey is the amount of moisture in the subsurface and the appropriate dielectric constant value used to calculate the depth of target.

In order to ground truth the GPR data in this area, a GPR profile using 400 MHz antenna was collected, across a visible drainage pipe located at the immediate vicinity west of the survey area to determine an average value for the dielectric constant of the area. Using the measured depth of the drainage pipe (0.38 m), the dielectric constant value was calculated as 15.0. Figure 4.1.13 shows the GPR profile and a single scan (right panel) across the visible drainage pipe shown in the photograph to the left.

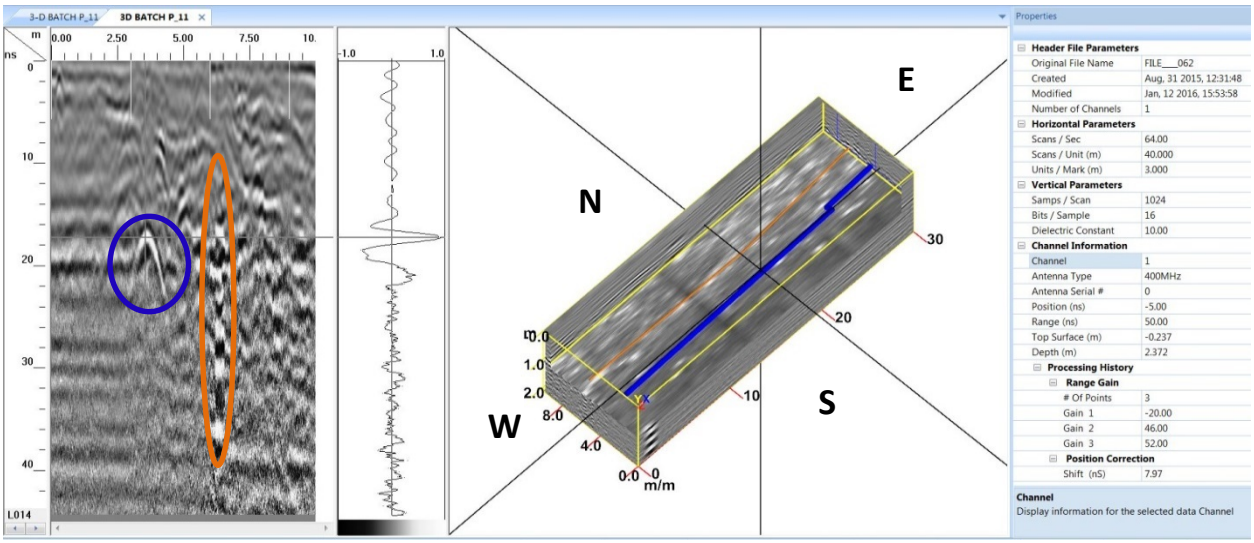

Figure 4.1.7: GPR radargram of profile L014 collected in summer of 2015 using 400 MHz antenna. Left panel is the GPR processed data for Time Zero and Background Removal. Blue circled anomaly represents the DIP and the orange represents the fiber optics anomaly. To the right of the panel shows the single scan across blue DIP anomaly. The middle panel represents the 3-D block diagram of the survey area. The blue pipe represents the DIP and the orange one is the fiber optic wire. The cross-hair shows the location of the GPR profile within the survey area. The right panel shows the different GPR parameters that were used during collecting the GPR data.

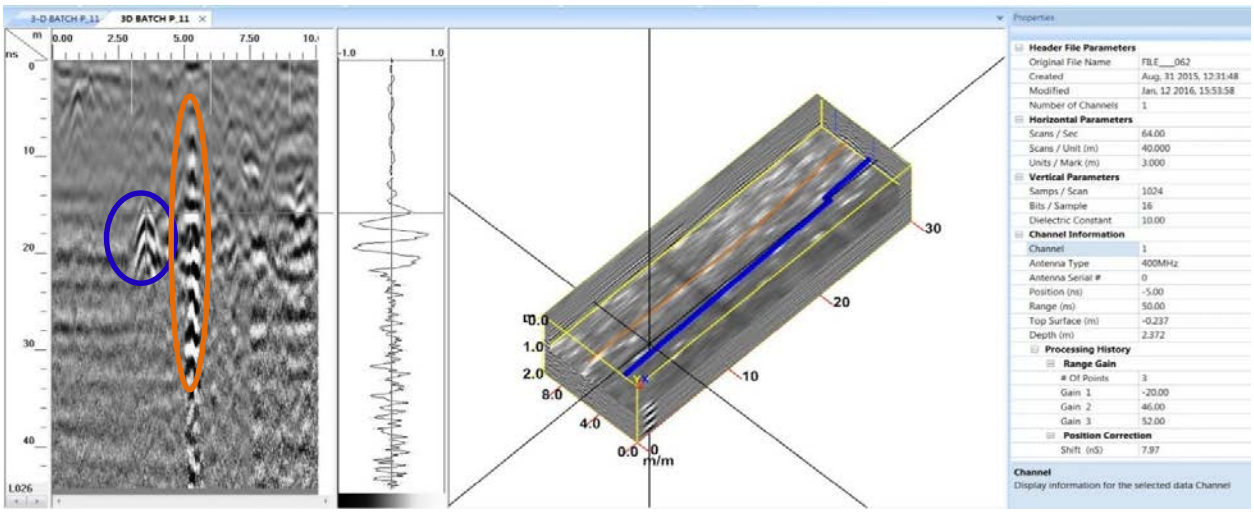

Figure 4.1.8: GPR radargram of profile L026 collected in summer of 2015 using 400 MHz antenna. Left panel is the GPR processed data for Time Zero and Background Removal. Blue circled anomaly represents the DIP and the orange represents the fiber optics anomaly. To the right of the panel shows the single scan across the blue DIP anomaly. The middle panel represents the 3-D block diagram of the survey area. The blue pipe represents the DIP and the orange one is the fiber optic wire. The cross-hair shows the location of the GPR profile within the survey area. The right panel shows the different GPR parameters that were used during collecting the GPR data.

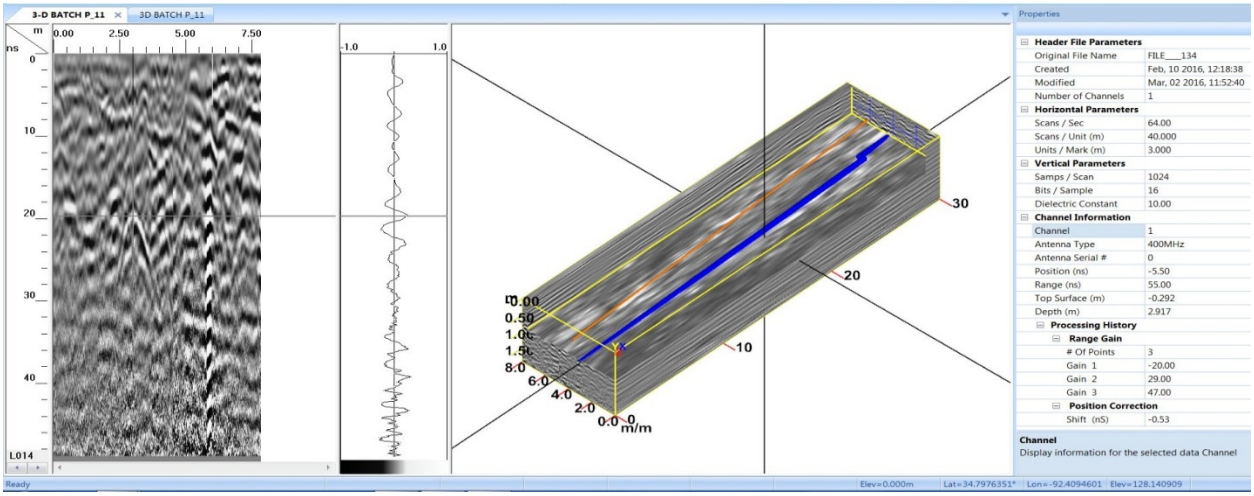

Figure 4.1.9: GPR radargram of profile L014 collected in winter of 2016 using 400 MHz antenna. Left panel is the GPR processed data for Time Zero and Background Removal. Blue circled anomaly represents the DIP and the orange represents the fiber optics anomaly. To the right of the panel shows the single scan of the blue DIP anomaly. The middle panel represents the 3-D block diagram of the survey area. The blue pipe represents the DIP and the orange one is the fiber optic wire. The cross-hair shows the location of the GPR profile within the survey area. The right panel shows the different GPR parameters that were used during collecting the GPR data.

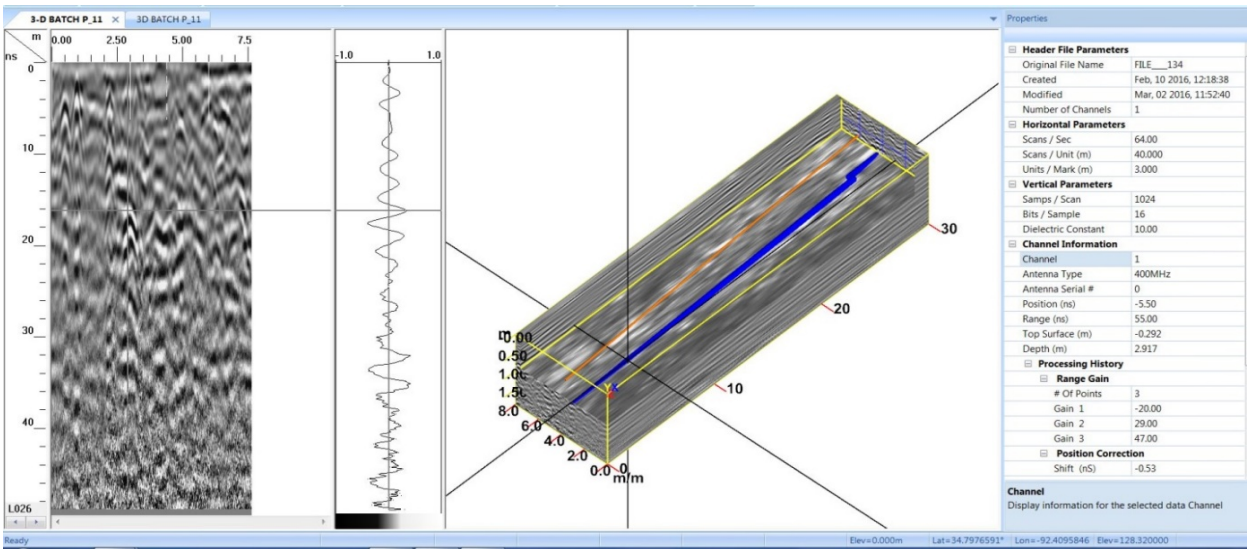

Figure 4.1.10: GPR radargram of profile L026 collected in winter of 2016 using 400 MHz antenna. Left panel is the GPR processed data for Time Zero and Background Removal. Blue circled anomaly represents the DIP and the orange represents the fiber optics anomaly. To the right of the panel shows the single scan across the blue DIP anomaly. The middle panel represents the 3-D block diagram of the survey area. The blue pipe represents the DIP and the orange one is the fiber optic wire. The cross-hair shows the location of the GPR profile within the survey area. The right panel shows the different GPR parameters that were used during collecting the GPR data.

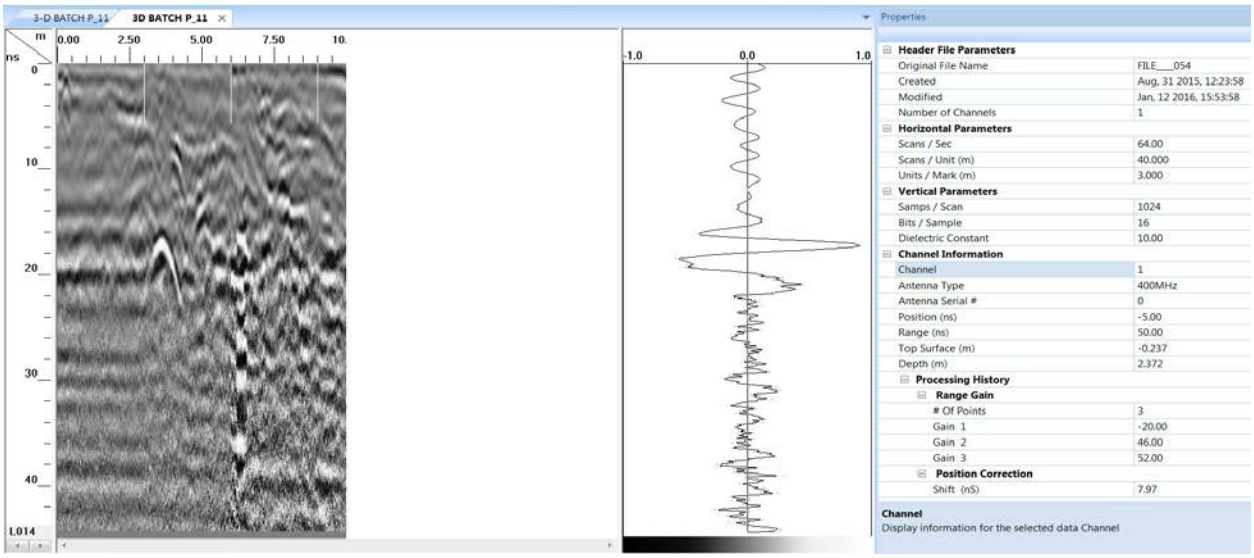

Figure 4.1.11: Radargram, single scan, and parameters (left to right respectively) of profile L014 collected during summer 2015.

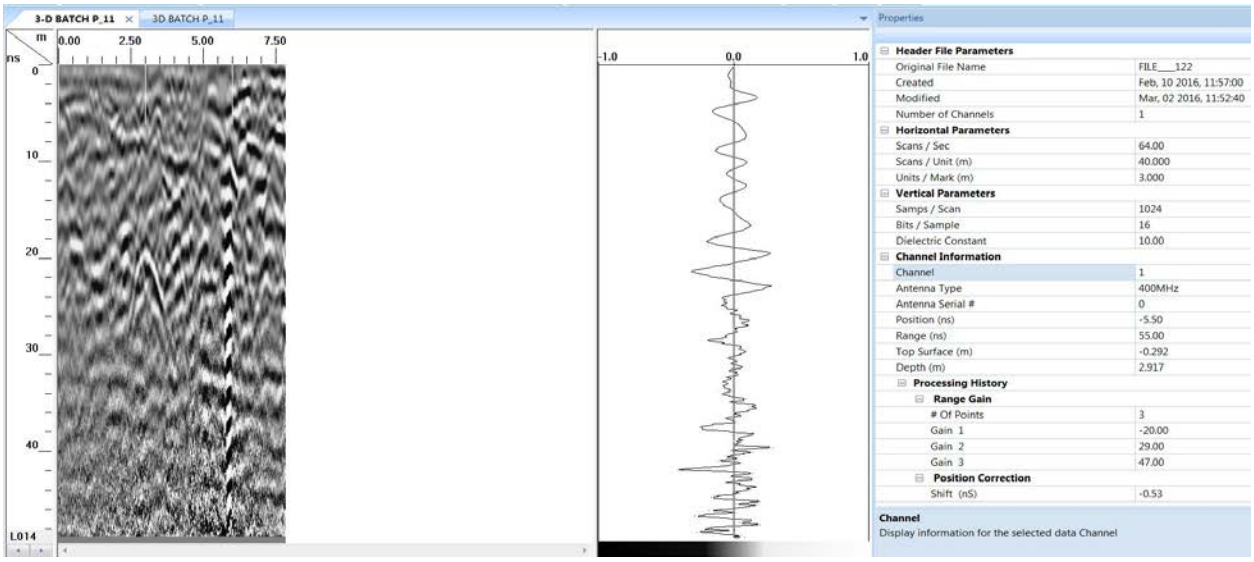

Figure 4.1.12: Radargram, single scan, and parameters (left to right respectively) of profile L014 collected during winter 2016.

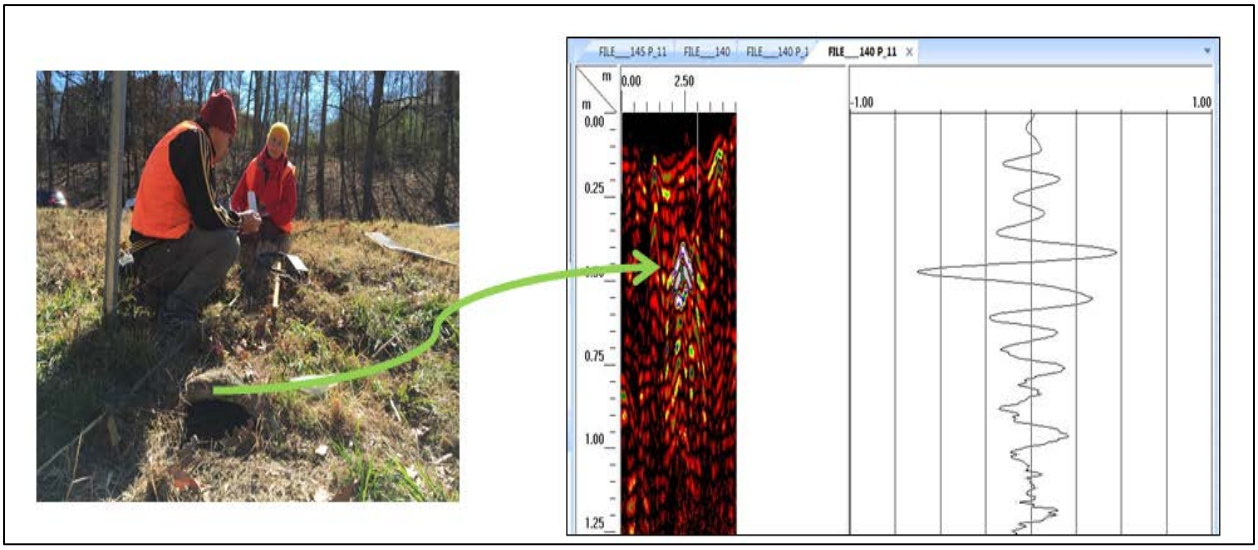

Figure 4.1.13 shows the GPR profile and a single scan (right panel) across the visible drainage pipe shown in the photograph to the left.

4.1.2 Site-2

Site-2 is located on HWY 10 near 12915 Cantrell Rd and the layout map provided by the AHTD shows the prospective location of the utility pipes (Figure 4.1.14). Due to the changes in surface ground forms, this site is divided into two sections for GPR surveying; Section A and B. The zoomed-in portion of the map shows these sections in red rectangles. The total size of the survey area was 16 m by 46 m (52.5 ft by 150.9 ft), where Section A covers a relatively smaller portion (16 m by 10 m - 52.5 ft by 33.2 ft) than Section B (11 m by 30 m - 98.4 ft by 36.1 ft).

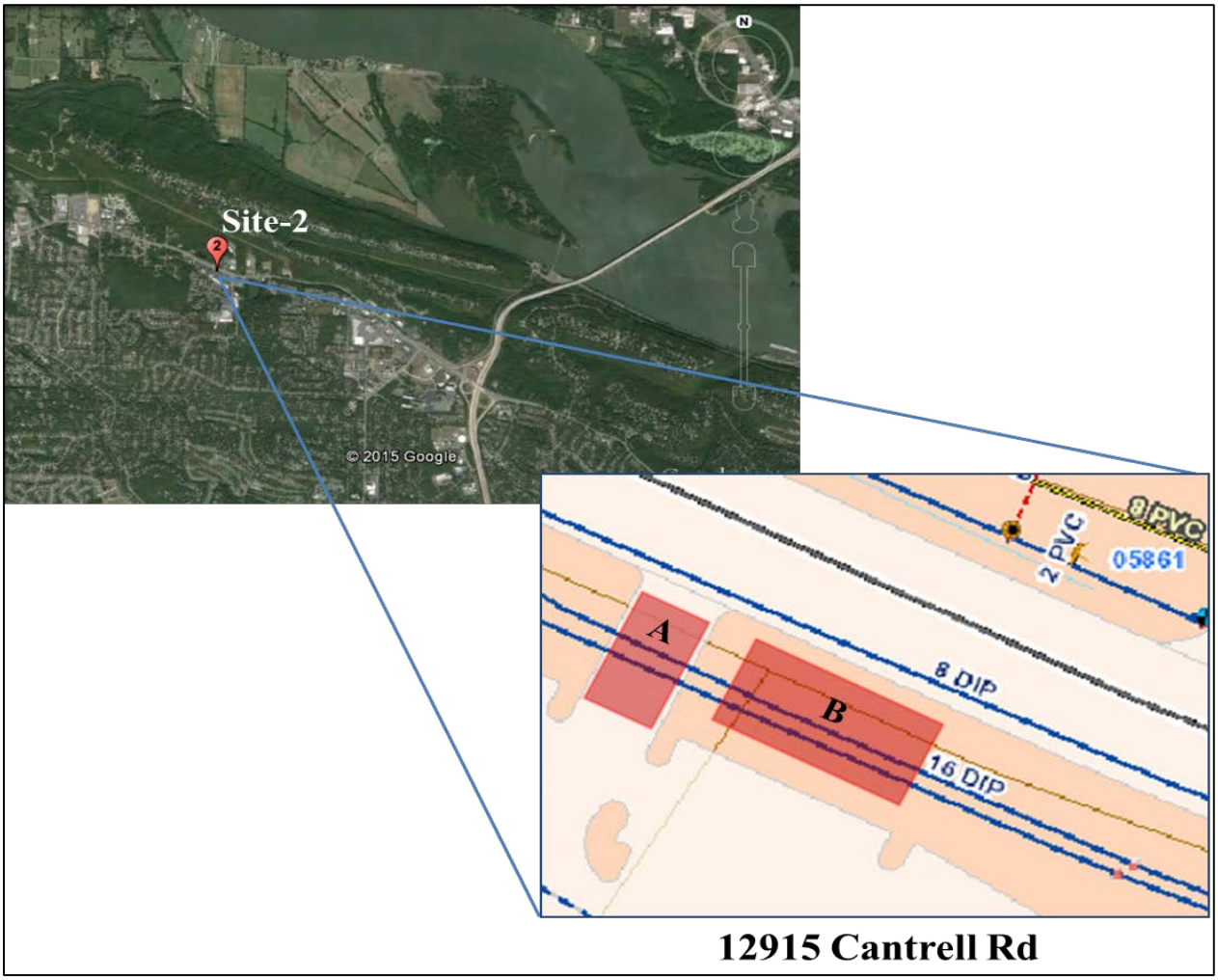

Figure 4.1.14 – The Google satellite image of Site-2 (upper left) and the layout map provided by the AHTD showing the locations of the utility pipes and the surveyed areas in red rectangle (bottom right).

According to the layout map, two (16 and 36 DIP) prospective pipes buried parallel to the road, therefore, the GPR profiles were collected perpendicular to the direction of the pipe(s). Figure 4.1.14 shows the locations of the profiles in a satellite image and a more detailed survey scheme provided in the zoomed-in portion. In total 29 profiles were collected. Fifteen profiles collected using the 200 MHz and fourteen profiles using the 400 MHz antenna in Section A and B. Only six of the total collected profiles were in Section A, which were 16 m (52.5 ft) long and 4.5 m (14.8 ft) apart from each other. The rest of the profiles collected in Section B were 3 m (9.8 ft) apart from each other. Twenty-two profiles that were approximately 11 m (36 ft) long collected in NS orientation. A single profile (#12), 28 m (91.8 ft) long, was collected parallel to the pipes in W-E orientation using 200 MHz antenna. The total length of all profiles for Site-2 was 197 m (646.3 ft).

Figure 4.1.15 - Google Earth satellite image showing the locations of the profiles in Site-2. A more detailed survey plan showing the names and the directions of the profiles (top right).

For Site-2, GSSI SIR-3000 control unit with 200 MHz and 400 MHz mono-static antennas were used. A several different values of time-ranges were applied for both antennas, which are 80 and 100 ns for 400 MHz and 150 ns for 200 MHz The soil has extremely high moisture content because of the presence of drain pipe and the continuously watered grass in section B. Although, section A was in the paved area, the presence of shallow water table in that area also masked the signal. The topography of the area was also not ideal for electromagnetic signal to penetrate since the water flows to the bottom of the trough, which causes the area immediately above the pipes to be wet all the time due to continuous watering. The conjectural representation of the water flow in the trough is provided in figure 4.1.16. The red flags shown in the figure indicate the start and end points of some of the profiles numbered from 1 through 11 and 13 through 23, for 200 MHz and 400 MHz antennas respectively. The zoomed-in image shows the drain cap located at the bottom of the trough oriented in EW direction.

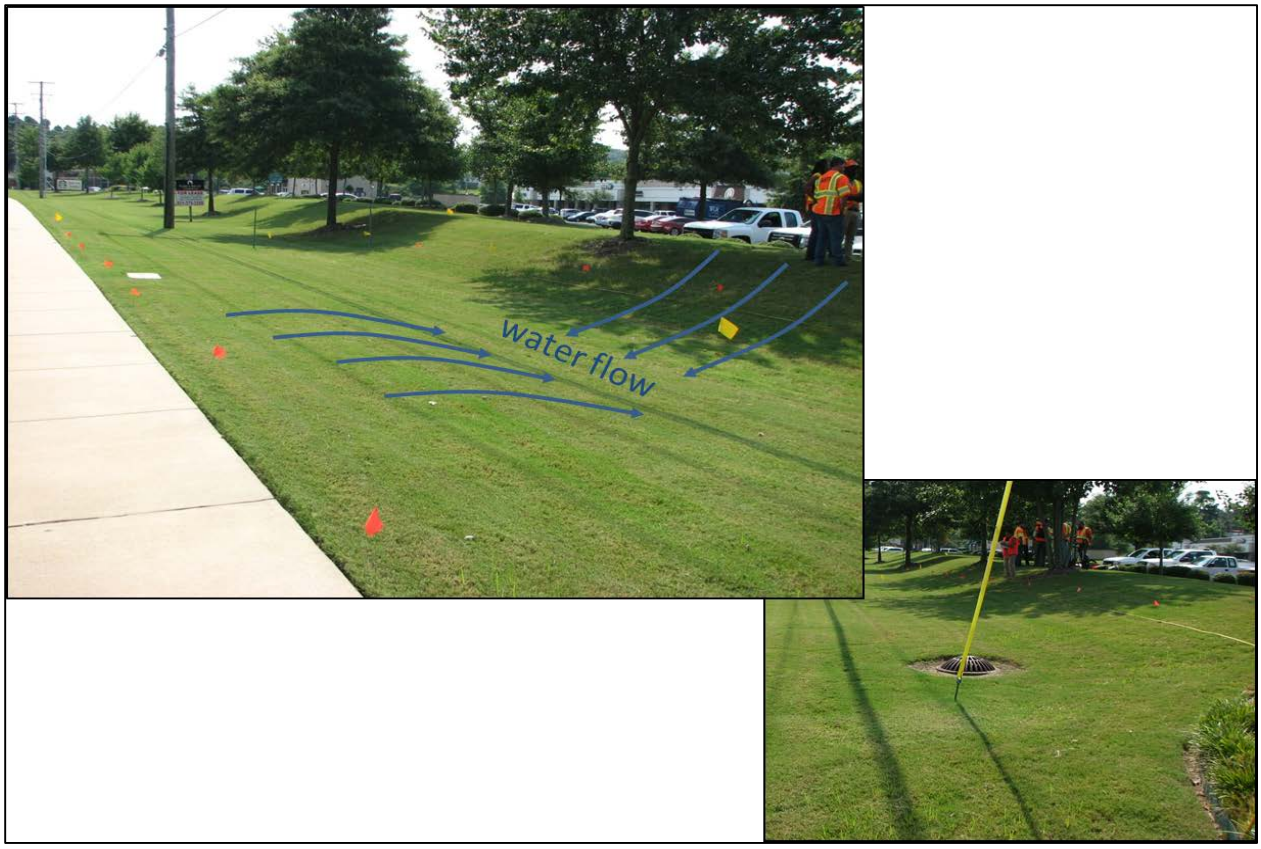

Figure 4.1.16 – Section B of Site-2. The red flags indicate the start and end points of some of the profiles from 1 through 11 and 13 through 23. The blue curved lines represent the conjectural direction of water flow towards the bottom of the trough. The zoomed-in image shows the drain cap located at the bottom of the trough oriented in EW direction.

As mentioned earlier, the presence of water in the immediate vicinity of the survey area is not desired since it reduces the signal to noise ratio (SNR) and a shallow water table reflects most of the electromagnetic signal masking the anomalies below this level. Nevertheless, after processing the 200 MHz data, the research team was able to discern two weak broad hyperbolae, around 45 ns and 75 ns time-range. These time-ranges correspond to 2.25 m (7.4 ft) and 3.75 m (12.2 ft) depth, respectively, using a dielectric constant value of 10.

Figure 4.1.17 shows the radargram of the profile #2 after applying Time Zero correction, Background Removal (left panel) and FIR filter (right panel).

Figure 4.1.18 shows the radargram of the profile #7 after applying Time Zero correction, Background Removal (left panel) and FIR filter (right panel). The same hyperbolic reflections are seen in these two figures.

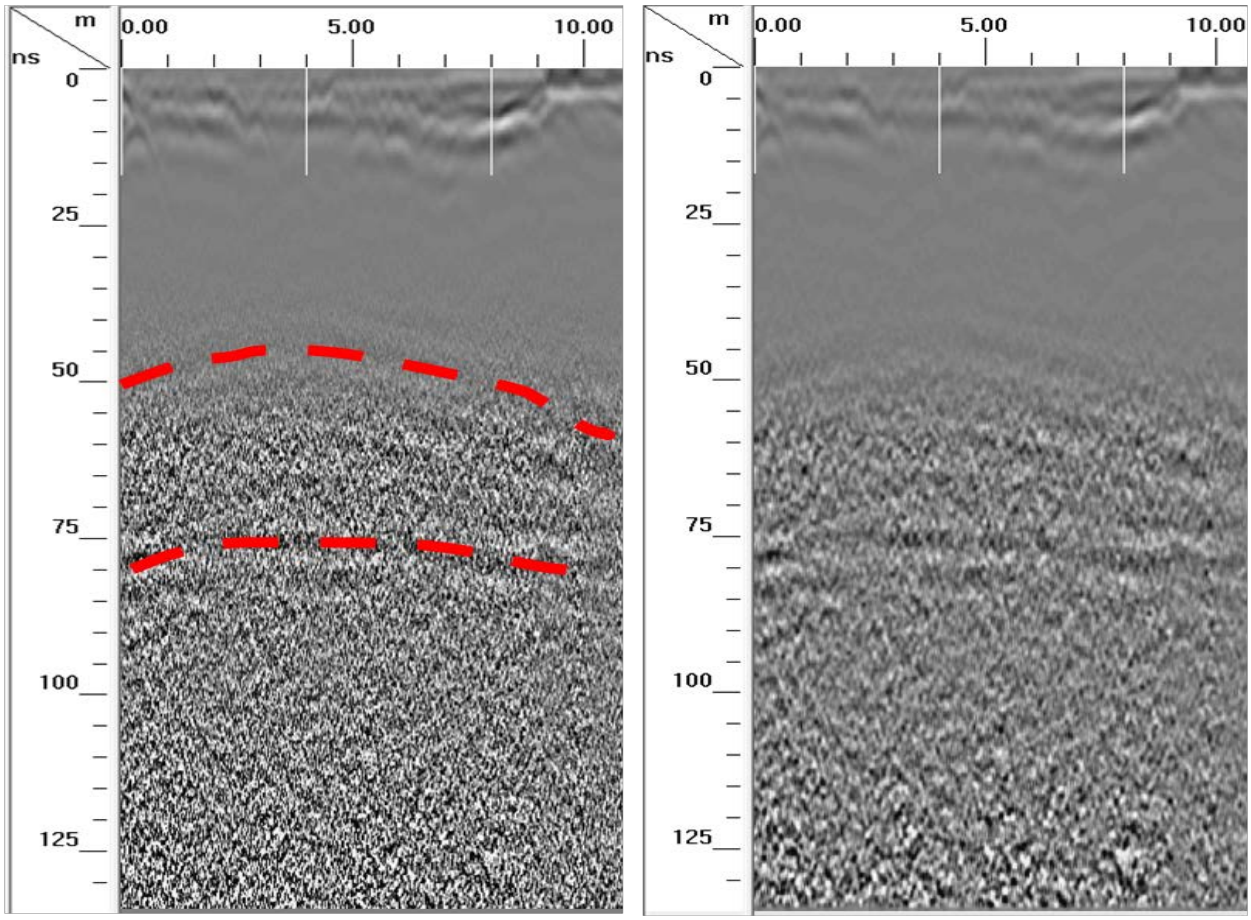

Figure 4.1.17 - Radargram of the profile #2 after applying Time Zero correction, Background Removal (left panel) and FIR filter (right panel). Red dotted lines represent the weak hyperbolic reflections.

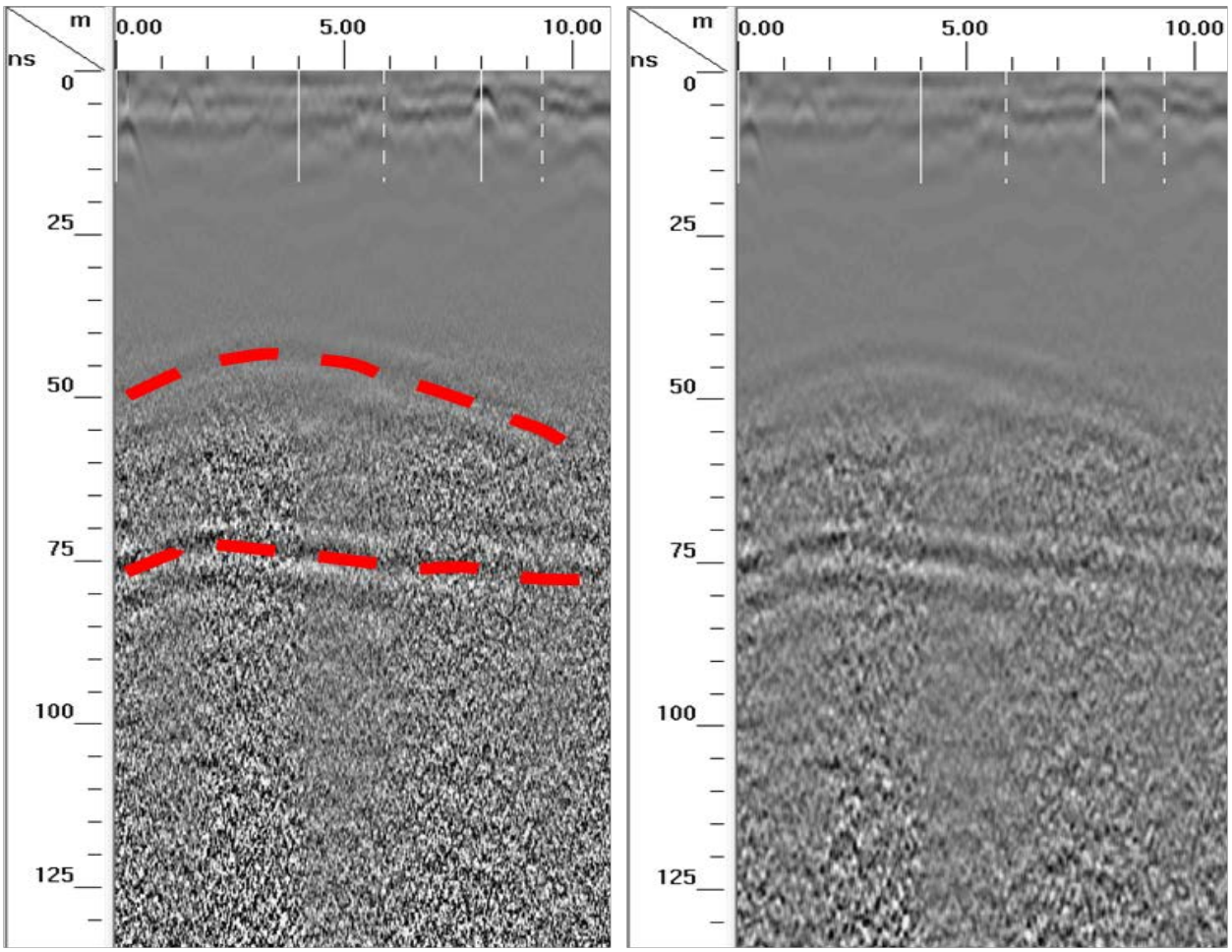

Figure 4.1.18 - Radargram of the profile #7 after applying Time Zero correction, Background Removal (left panel) and FIR filter (right panel). Red dotted lines represent the weak hyperbolic reflections.

At this point, we do not have substantial evidence to believe these anomalous features are related to the two expected DIPs. This requires future modification to the survey setup and further adjustment of the survey parameters such as time-range and manual gain control. In addition, there might be a need to run more surveys along different sections of the pipes during different weather and soil conditions. This issue will be discussed during winter survey section.

Figure 4.1.19 shows profile 12, collected with 200 MHz antenna in E-W direction, along the DIP at the bottom of the trough. The shallow water table is marked with the light green line, which is around 25 ns time-range. The SNR decreases well below the acceptable limits to do any type of interpretations almost immediately below the water table. This can be observed from the increased noise level below the light green line. Under ideal condition, the expected anomaly should resemble continuous horizontal anomaly. However, a faint anomaly was observed below this level further to the east, which is circled in white. Although, this is a hyperbolic reflection resembling a pipe, the sheer size of this hyperbola is around 12.5 m (41 ft), which is unlikely a pipe but more probably from a further object that is at a distance from the profile or the antenna.

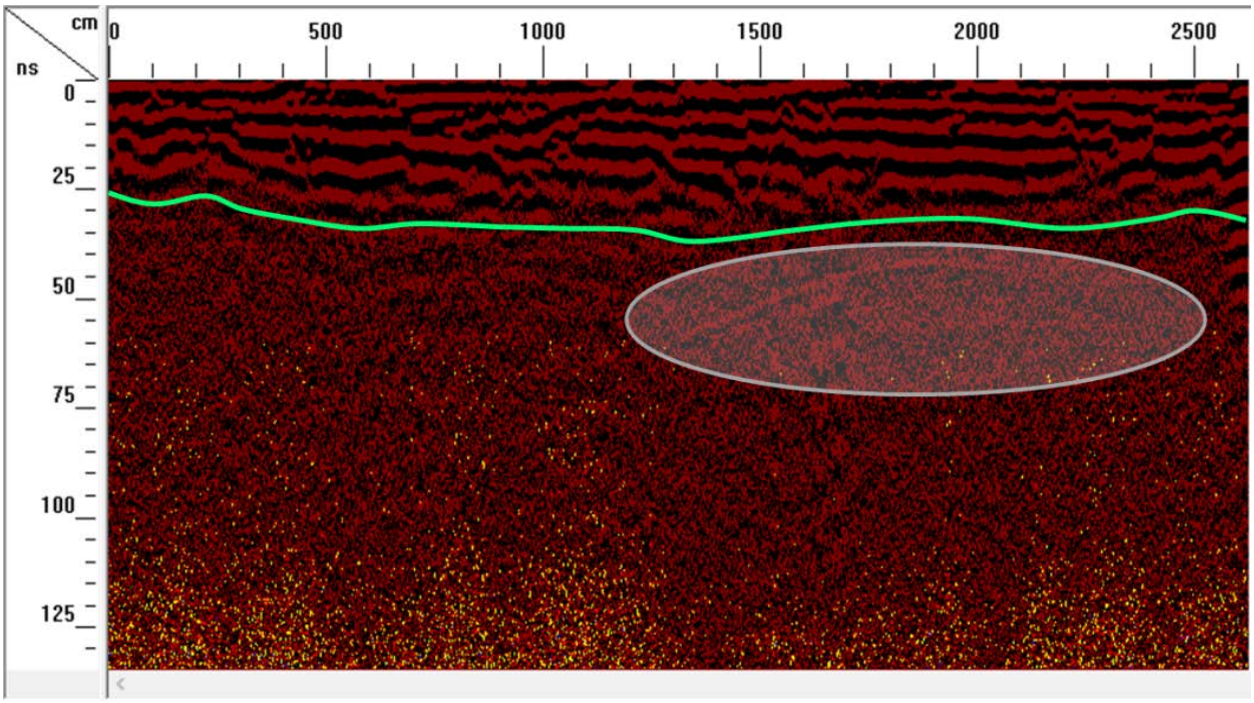

Figure 4.1.19 - Profile 12 collected in EW direction along the drainpipe at the bottom of the trough. The shallow water table is masking the anomalies below the 25 ns range.

Figure 4.1.20 shows the profile 27 (Section A) and profile 17 (Section B) collected in NS direction with 200 MHz and 400 MHz antenna, respectively. The light green line in (Figure A) shows the water table boundary, where the SNR decreases below the acceptable level of 25 ns. Similar to the profile 12, this can be observed from the increased noise level below the light green line. The research team also collected data in Section A with the intent of avoiding the water in the trough however, a similar scenario was observed with all collected profiles.

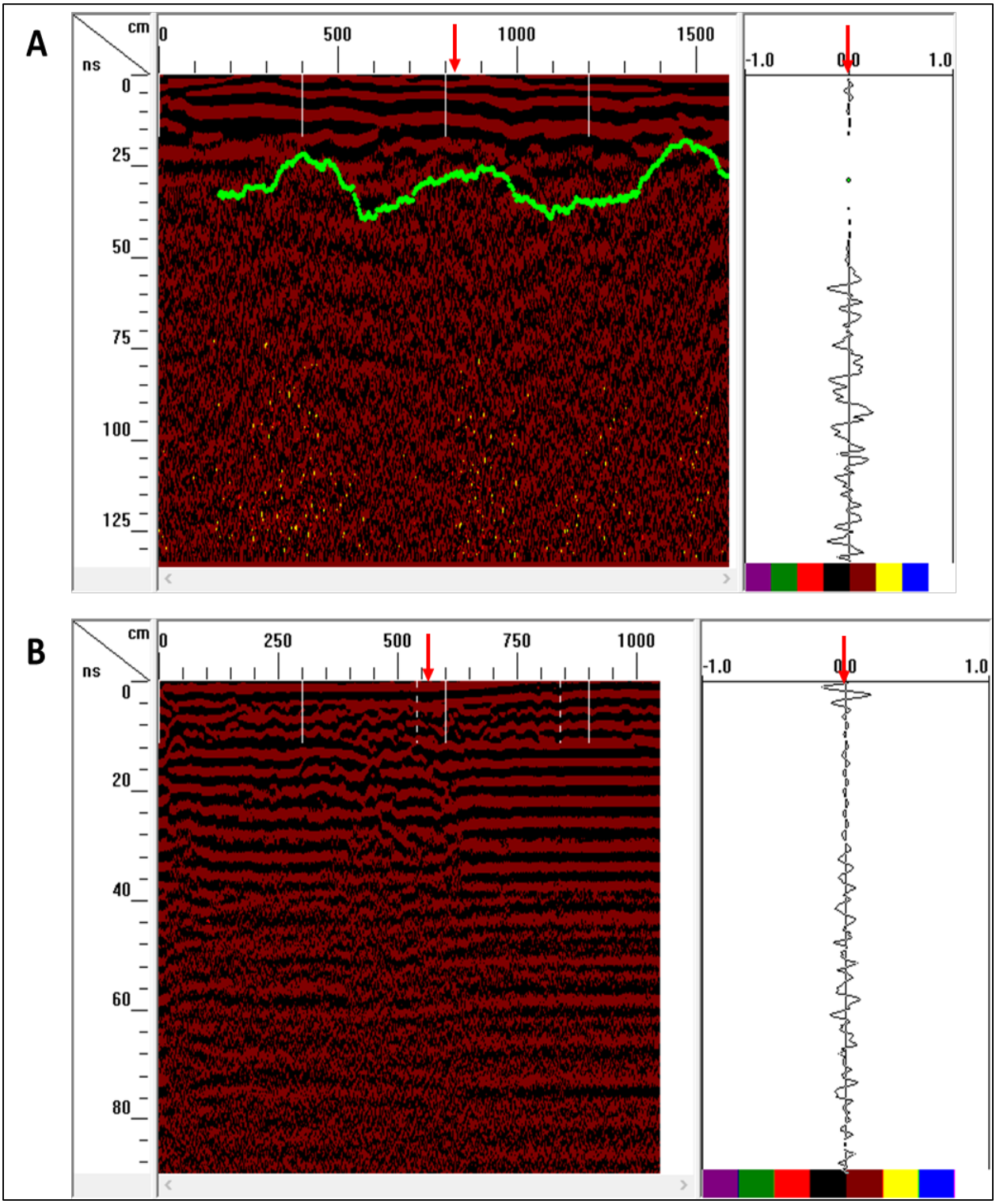

Figure 4.1.20 – (A) Profile 27 in Section A and (B) Profile 17 in Section B collected in NS direction with 200 MHz and 400 MHz antenna, respectively. Light green line shows the water table boundary, where the SNR decreases below the acceptable levels (A).

Figure 4.1.20A shows the radargram image for the subsurface under the asphalt in Section A (using 200 MHz antenna). No hyperbolic reflection was detected as an indicative of the DIP even after necessary processing of the data. However, profiles 24, 25 and 26, collected using 400 MHz data over the asphalt in Section A, exhibit faint hyperbolic anomalies at approximately 26 ns time-range and 10 m (33.2 ft) from the beginning of the profiles (concrete driveway) as seen in Figure 4.1.21 . The location, the depth calculated from ε_r=10 and the shape of the anomalies (hyperbolae) suggest that, there lies a pipe parallel to the road at the depth of 1.2 m (4 ft) under the ground.

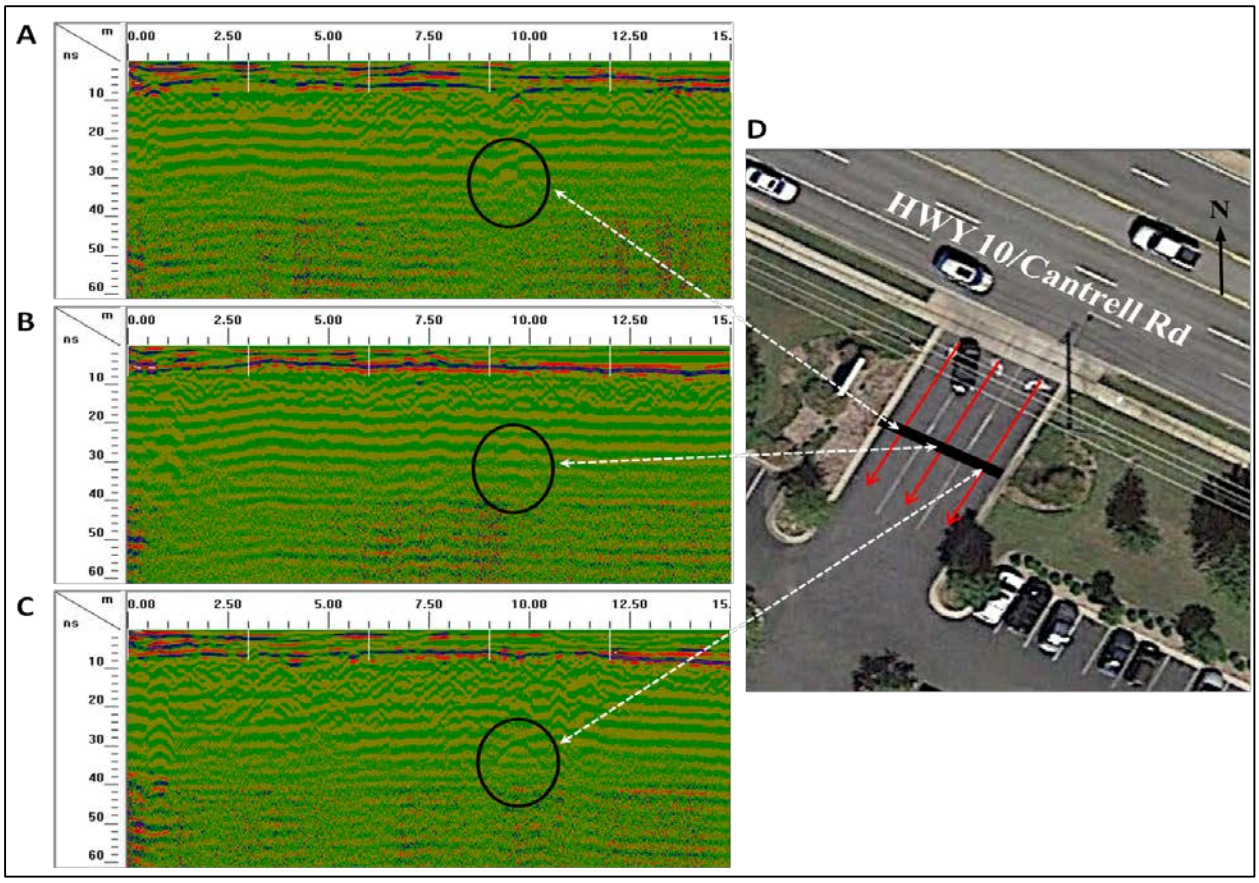

Figure 4.1.21 - The profiles 24 (A), 25(B) and 26 (C), collected using 400 MHz data over the asphalt in Section A exhibiting faint hyperbolic anomalies (circled in black). The Google satellite image (D) shows the projected locations of the anomalies on the ground (white dashed arrows), the profiles (red arrows) and the possible conduit (black line).

The Google satellite image (Figure 4.1.21D) shows the projected locations of the anomalies on the ground (white dashed arrows), the profiles (red arrows) and the projection of the possible conduit on the ground (black line). These results confirm the GPR system capability in locating utility pipes, however the water content of the soil influence the overall performance of the system dramatically.

Site-2-Winter Survey

The second fieldwork of data collection was done on Feb 9, 2016 using SIR-3000 GSSI equipment with both 200 MHz and 400 MHz antennas. We repeated the data collection on section B collecting 11 lines with 3.0 m (9.8 ft) spacing between them. This time we increased the length of the lines to 16.0 meters to cover the entire area. In addition, we collected more data in different locations other than the summer field profiles, in order to constraint and gather more GPR data to help with the final interpretation. Figure 4.1.22 is a google map showing the layout map of the winter survey and Figure 4.1.23 is a map showing the GPR profiles relative to the underground utility lines.

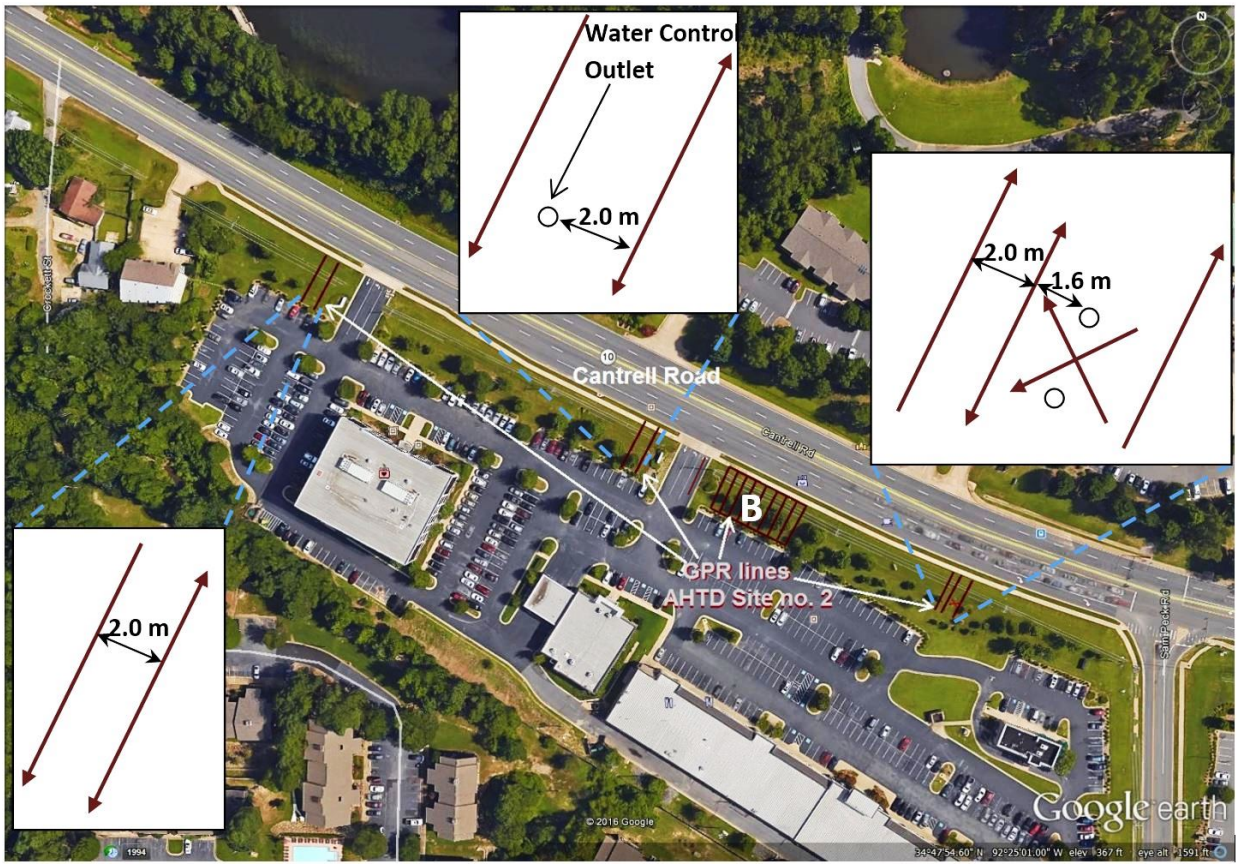

Figure 4.1.22: Location map of the GPR survey conducted February 2016 in AHTD Site no. 2. White rectangles show the additional GPR lines that were collected during winter survey.

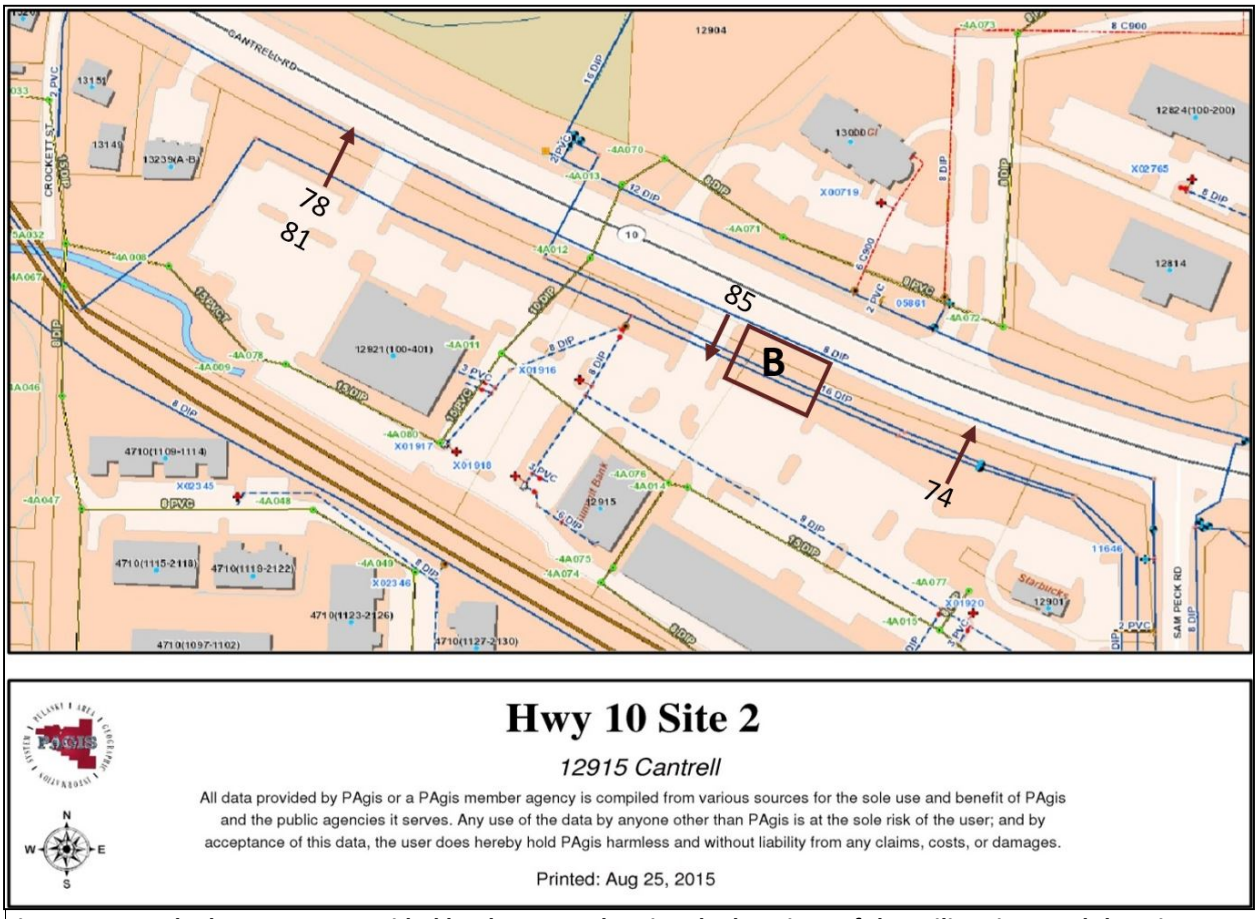

Figure 4.1.23: The layout map provided by the AHTD showing the locations of the utility pipes and the winter surveyed areas in maroon-colored rectangle and lines

Figure 4.1.24 shows two GPR profiles on grassy area after applying Time Zero correction and Background Removal. Left panel represent the radargram of GPR profile File 81 (see figure 4.1.23 for location) using 400 MHz antenna collected from S to N. The right panel represents the GPR data of file 78 collected on the same profile as file 81 using 200 MHz antenna. We decided to take GPR measurement further west of the summer survey area in anticipation of constraining the result of the summer field data. Under this area, we expect to find one underground utility pipe. Figure 4.1.25 shows two GPR profiles on grassy area after applying Time Zero correction, Background Removal and FIR filter. Both profiles collected using 200 MHz antenna. File 78 (left panel) crosses the area that contain just one utility pipe, while file 74 (right panel) located east of the B survey area in front of Larry's Pizza on Cantrell that has two underground pipes.

All Radargrams show broad hyperbolic multiple reflections. These reflections do not hold the signature of underground pipes. There are electrical high-tension cables run along the surveyed area (see figure 4.1.26). Most likely, the two broad hyperbolic anomalies that are shown in the radargrams are not the pipes anomalies but rather are the effect of the high tension cables on the GPR signal in addition to the effect of the many parked cars in the nearby parking lots. The radar energy travels in the air (dielectric constant of 1.0) 12 inch/ns. For the top of the hyperbola around 50ns two-way-travel time, this equals 600 inches two-ways travel distance (300 inches one way). 300 inches (7.6m) is about the height of the high tension cables. If these two anomalies

are due to the pipes that we are trying to locate then we would expect to see just one in file 78 (see figure 4.1.25) because it runs across an area that contains just one pipe according to the provided layout map of figure 4.1.23. GPR was not successful in detecting the two pipes (or the one pipe to the west) in this area partly because of the effect of the high-tension cables and other external noise sources on the GPR signal and also the wetness of the surface layer which absorb most of the GPR signal.

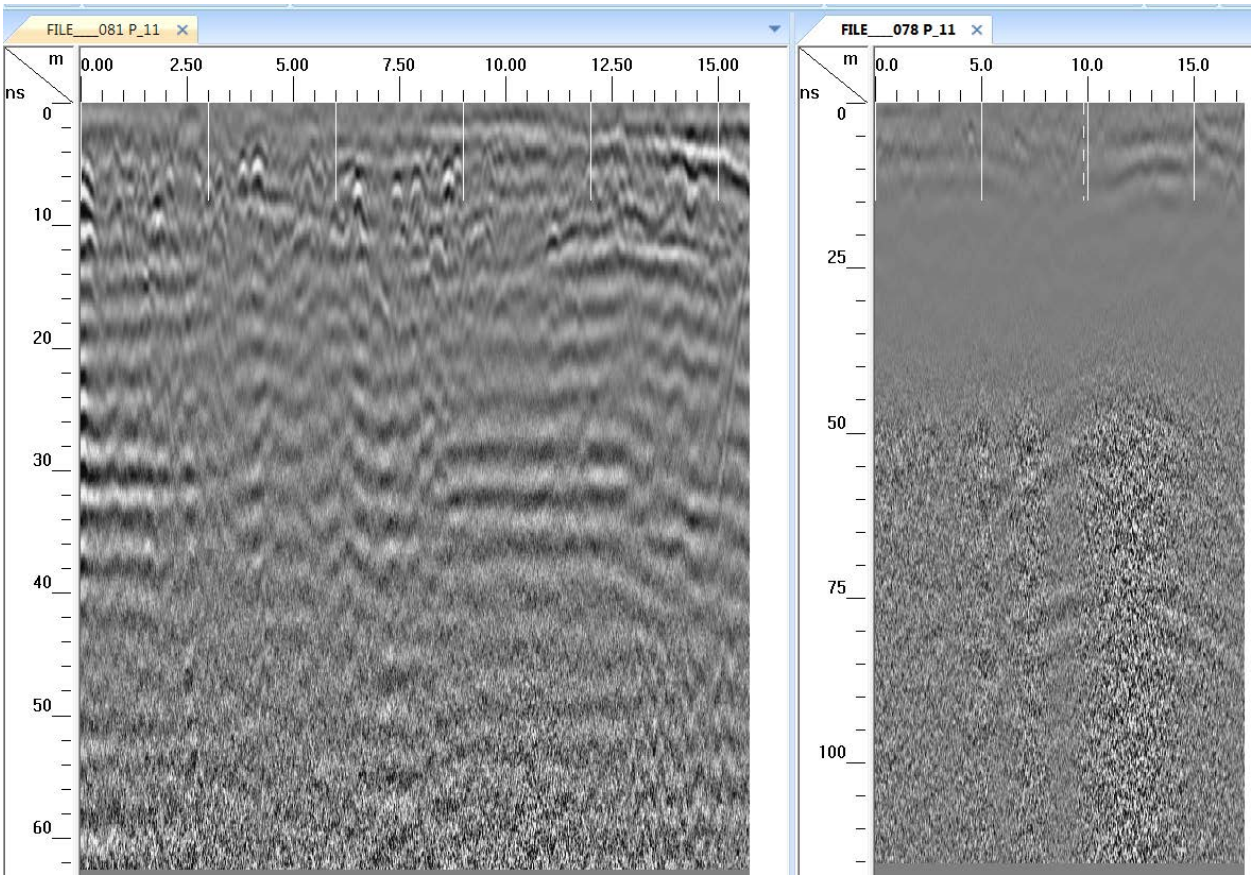

Figure 4.1.24: Two GPR profiles collected in winter of 2016 to the west of the summer 2015 survey area after applying Time Zero Correction and Background Removal. Left panel represents the radargram of GPR profile File 81 using 400 MHz antenna. The right panel represents the GPR data of file 78 collected on the same profile as file 81 using 200 MHz antenna.

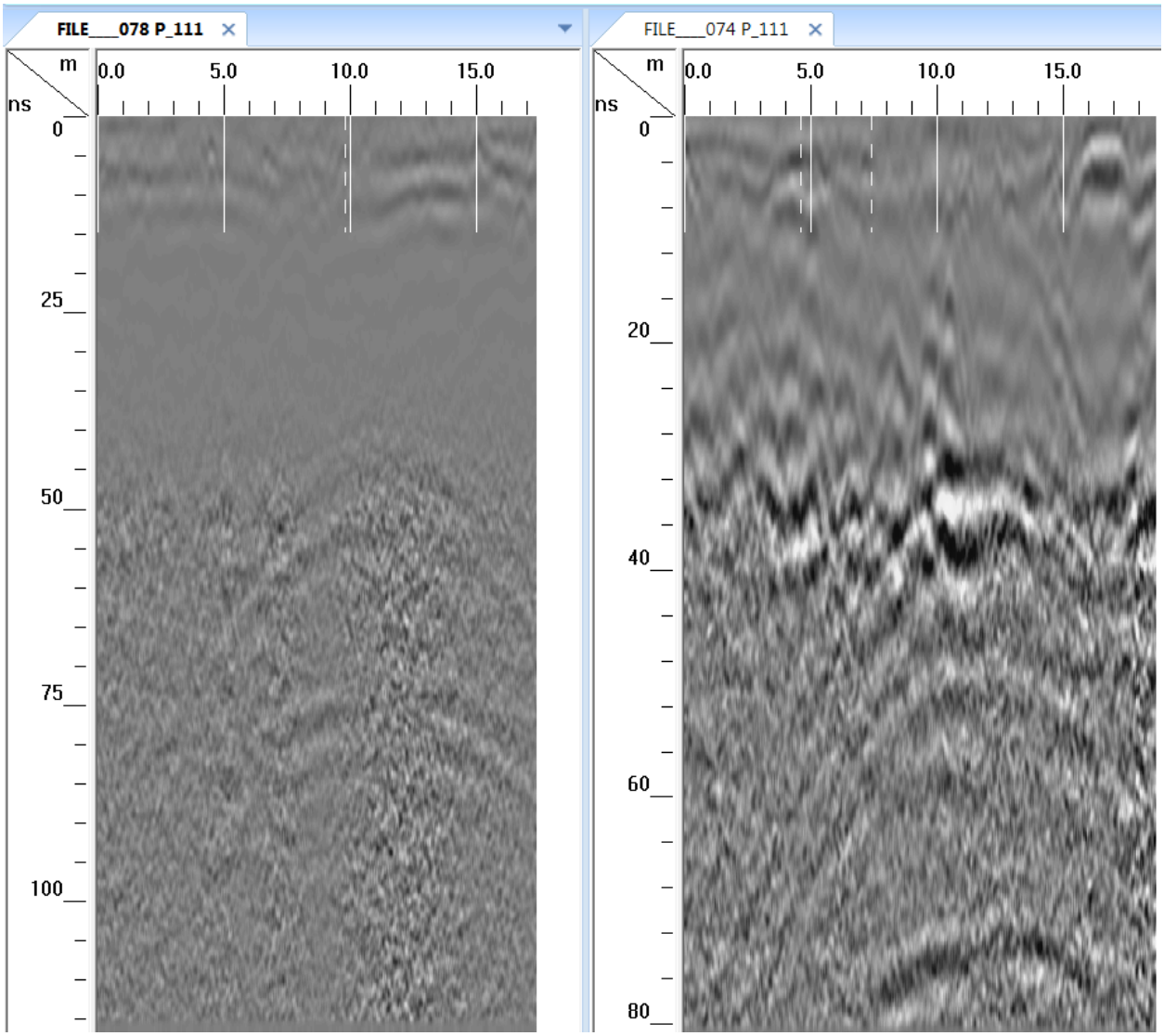

Figure 4.1.25: Two GPR profiles collected in winter of 2016 after applying Time Zero Correction, Background Removal and FIR filter. Both profiles collected using 200 MHz antenna. File 78 (left panel) crosses the area that contain just one utility pipe, while file 74 (right panel) located in front of Larry's Pizza on Cantrell that has two underground pipes.

Figure 4.1.26: A photograph near the survey area of Site-2 on Cantrell showing the high-tension cables present in the area.

Figure 4.1.27 represents a comparison between file 26 which was collected in summer 2015 using 400 MHz antenna and run along the paved entrance of the Plaza with file 85 which was collected in winter of 2016 at the same spot as file 26 and also using same antenna but different gain level (higher). See figure 4.1.23 for location. We detected two pipes around 30 ns and 40 ns (red circled). Using a dielectric constant value of 15.0 the depth to the first pipe is around 1.13 m (3.7 ft) while the second one is around 1.55 m (5.1 ft). These two pipes appeared to be on top of each other and separated by about 0.5 m (1.6 ft). This example shows that the surface moisture and the gain control are more important in locating the target than temperature variation. Under the grassy wet area, it was difficult to detect any pipe during both summer and winter at this site. Figure 4.1.28 shows the radargram of file 85 (left panel) along with the single scan across the first pipe. It is obvious that this pipe is a DIP from the phase of the signal, which is white-black-white or positive-negative-positive. The right panel of the figure shows the GPR parameters that were used to collect this profile.

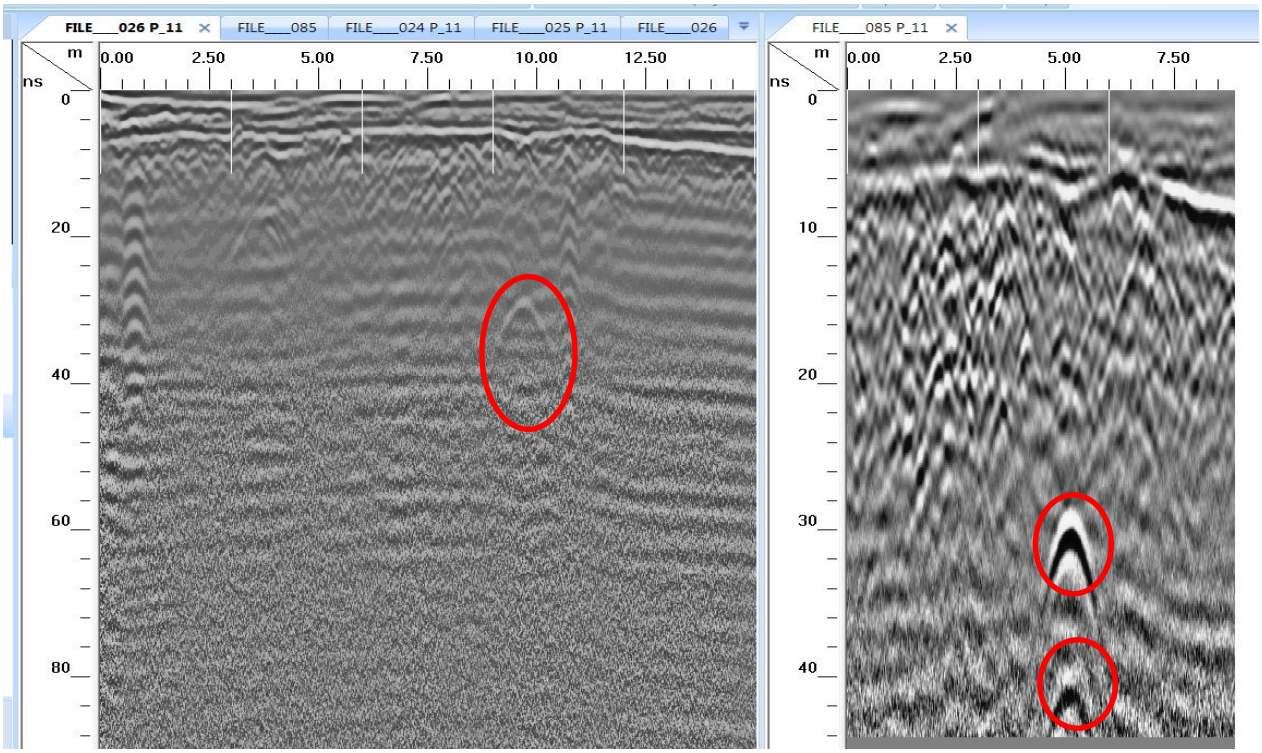

Figure 4.1.27: A comparison between file 26 (left panel) collected in summer 2015 with file 85 (right panel) collected in winter of 2016. Both GPR files collected at the same location, using 400 MHz antenna and corrected for Time Zero and Background Removal. Red circled anomalies represent underground utility pipes.

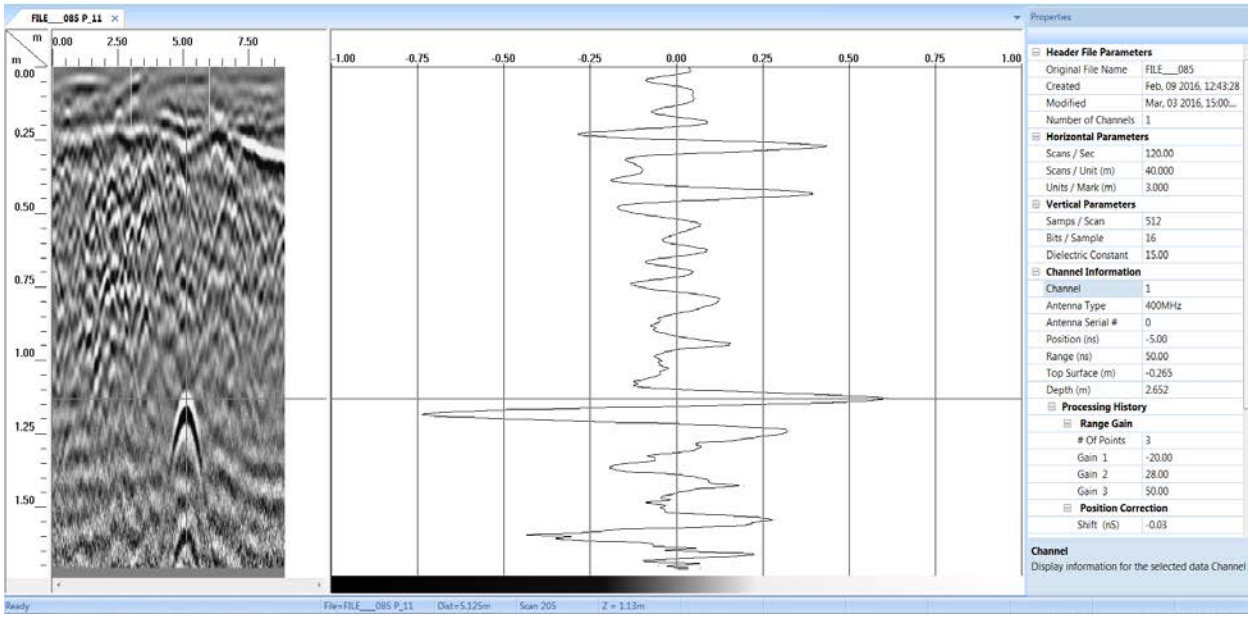

Figure 4.1.28: Radargram of file 85 (left panel) collected in winter of 2016. Middle panel is a single scan across the first pipe. The right panel shows the GPR parameters used to collect this profile.

4.1.3 Site-3

Site-3 is located on the east of the River Bridge near the I-30.

Figure 4.1.29 shows the layout map provided by the AHTD with the prospective location of the utility pipe(s). In addition, the figure shows google map with summer GPR survey profiles (yellow arrows).

For this site, GSSI SIR-3000 control unit with 200 MHz mono-static antenna was used to insure deeper penetration of the signals. In order to measure the depth of the buried pipes, the GPR profiles were collected perpendicular to the direction of the pipe(s). For this survey setup, the pipe's signature will be a hyperbolic reflection, which makes its identification much easier. A close up Google Satellite image showing the locations of the profiles is provided in Figure 4.1.30.

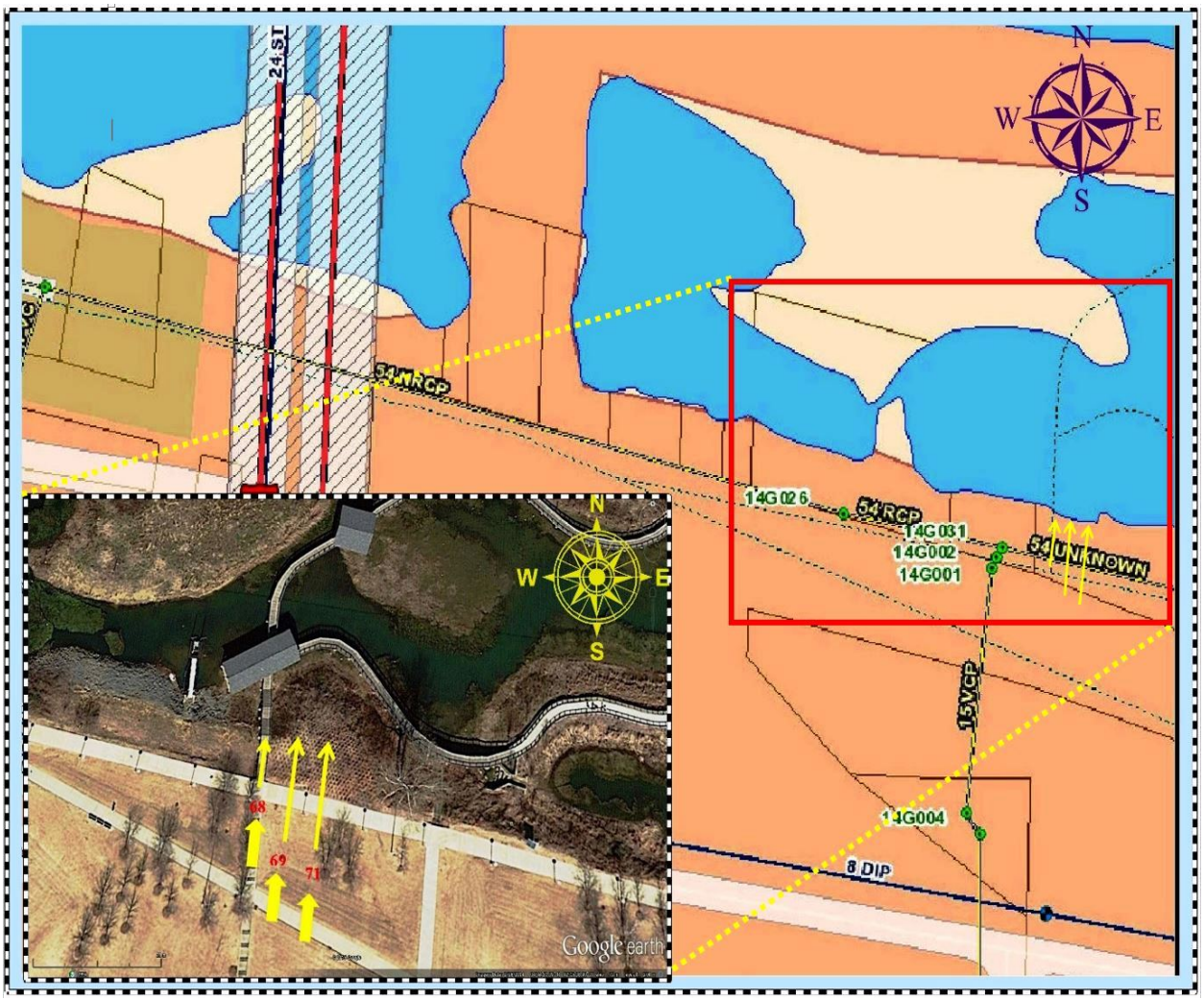

Figure 4.1.29 - Area layout provided by the AHTD shows the location of the utility pipes and the GPR profiles in the zoomed-in satellite image.

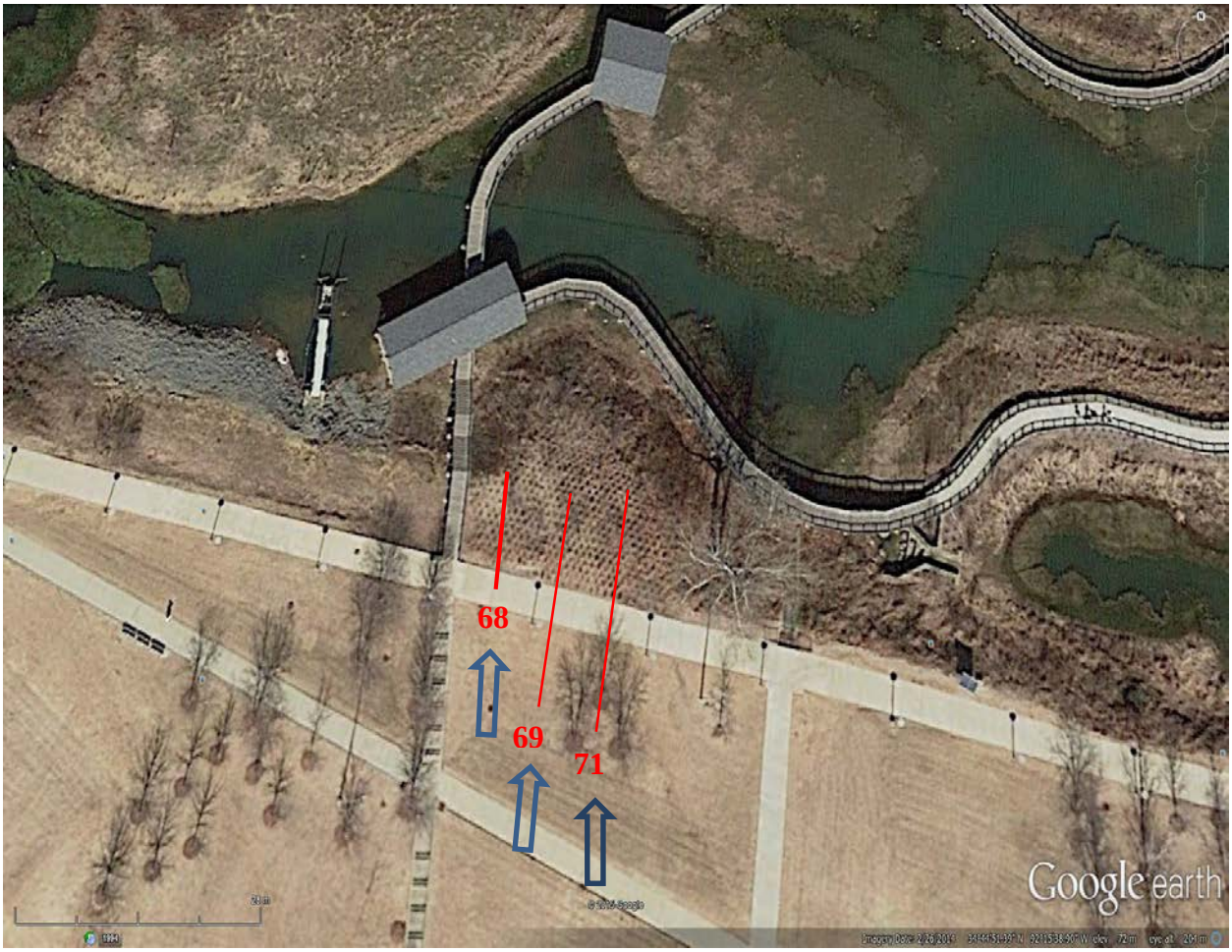

Figure 4.1.30 - Google Earth satellite image showing the locations and the directions of the summer survey profiles near the I-30 River Bridge.

In total, five profiles were collected three in SN and two in NS orientation having a total length of 128 m (420 ft). Red lines show the locations of the three profiles in S to N direction. Some of the profiles were collected with different antenna parameters in order to enhance the SNR. The selected time-ranges for the survey were between 150 ns and 300 ns due to the deep nature of the expected pipe. However, the dense bushes forced the research team to cover an area smaller than initially planned. In addition to obstructions due the thick bushes and weeds, the soil had relatively high moisture content because of the wide spread roots of the weeds. This produce GPR profiles with undesired high-noise content.

Figure 4.1.31 shows the thick/dense bushes in the survey area, which limited the extent of the profiles and the signal strength.

Figure 4.1.31 - Thick bushes/weeds made the survey extremely difficult due to the large size of the 200 MHz antenna.

In addition to the standard data reduction methods such as Background Removal and zero-time correction, a high pass Infinite Impulse Response (IIR) filter was applied to the data to minimize the noise. Although, SIR-3000 allows the operator to select additional Finite Impulse Response FIR filter during data collection, research team most often prefers to further process the data in the laboratory depending on the type of noise content.

Figure 4.1.32 shows raw data collected over the wooden bridge. The cross patterns of the refracted waves from the bridge boards are visible after 3.5 m (11.4 ft) from the start of the profile below the time-range of 48 ns (Figure 4.1.33). Although the strength of the reflections below 48 ns level seems to increase, the noise becomes the dominant factor in the signal (Figure 4.1.32) due to the continuously increase of gain with depth. A single scan shown in Figure 4.1.32 highlights the artificial noise masking the subsurface anomalies. The red down arrow in the profile shows the location of this scan.

The processed GPR profile and the corresponding single scan shows that the noise is significantly reduced after the necessary signal processing steps (Figure 4.1.33). However, the signal diminishes due to the presence of the water table, which is also around 48 ns.

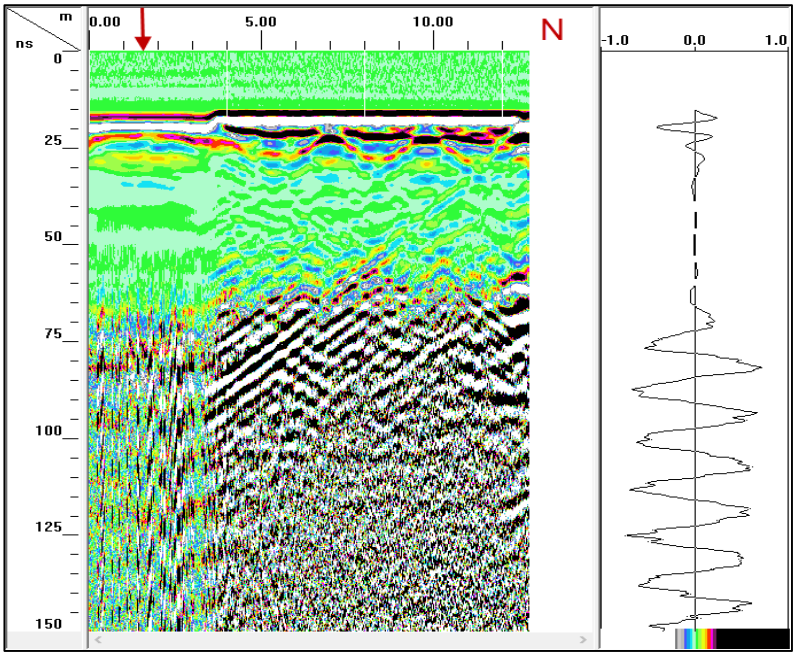

Figure 4.1.32 - 200 MHz data collected towards and over the bridge. The red arrow shows the location of the single scan on the right. The single scan shows an increase in the signal with depth indicating artificial noise.

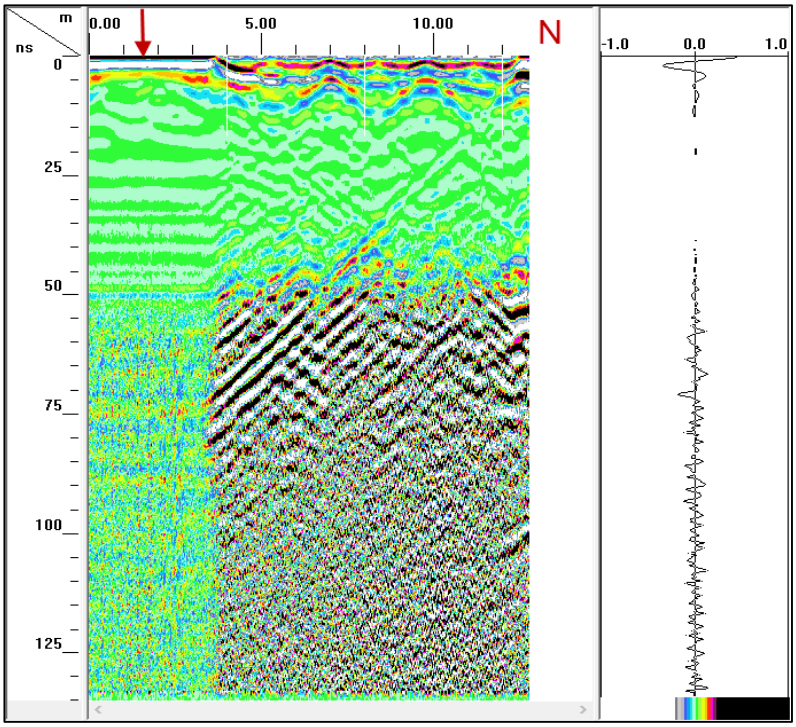

Figure 4.1.33 - The processed data shows that the artificial noise was minimized after Background Removal, Time Zero Correction and IIR filters.

Site-3 Winter Survey:

The second fieldwork of data collection conducted on Feb 12, 2016 using SIR-3000 GSSI equipped with both 200MHz and 400 MHz antennas. This time we collected data along four GPR lines trending S-N, two of them on the same previous lines as the first survey in Aug 2015. These are Line no. 1; with 13 m (42.7 ft) length and Line no. 2; with 15 m (49.2 ft) length. The other two lines were laid out further east close to the bridge near Clinton Library. The length of line 3 is 14 m (45.9 ft), while line 4 is 11 m (36.1 ft) length and the spacing between them is 15.6 m (51.2 ft) (Fig. 4.1.34). The research team tried to repeat the survey by choosing an optimal weather condition hoping they might obtain better results than summer survey. The weather was crisp, sunny, and dry for many days. The grass and the bushes that cover the survey area were dry too. The main target in this area is a 54" of unknown type (NRCP or RCP) (see figure 4.1.30). A big pipe with a metal reinforcement like this one should be easy to locate with GPR, as the metal reinforcement will reflect the GPR signal. If the pipe is a concrete pipe, it will be challenging and hard to locate since the difference in dielectric constant between the concrete and the soil is minimal. Figure 4.1.35 shows the radargrams of two GPR profiles collected on the same location at different time. Left panel is GPR file 156 (profile 1 in figure 4.1.34) collected during winter survey. Right panel is GPR file 68 (figure 4.1.30 and 4.1.31) collected during summer survey. Both profiles collected in S to N direction using 200 MHz antenna and processed for Time Zero correction and Background Removal. Comparing these two profiles reveals the absence of any clear hyperbolic anomaly that is indicative of any underground utility pipe. Also noted was the effect of the high level noise on the GPR signal due to subsurface water saturation. Figure 4.1.36 shows three radargrams. The left and middle panels are from the summer survey (69 and 71 in figure 4.1.30 and 4.1.31) and the right panel (file 157) is from the winter survey (number 2 in figure 4.1.34). Locations of these profiles are very close to each other. All profiles collected in S to N direction using 200 MHz antenna and processed for Time Zero correction and Background Removal. Comparing all profiles indicates the nonexistence of a typical pipe anomaly. In addition, it was noticed that the water table is deeper in summer (around 50 ns) than in winter (around 30 ns). This shows that water saturation effect on GPR signal starts at shallower depths in winter. The only difference was that in winter (profile 157) there was shallow digging or a wet spot close to the ground surface next to the sidewalk as indicated from the disturbance in the radargram. More GPR profiles collected further east hoping to obtain better results in locating the target. Figure 4.1.37 shows two GPR profiles. In the left panel is GPR file 148 (profile 3 in Google map) collected in S to N direction using 400 MHz antenna and to the right is file 158 collected along same path using 200 MHz antenna. Both profiles corrected for Time Zero and Background Removal. No well-defined hyperbola was observed. Neither the 400 MHz nor the 200 MHz antenna could detect a major underground utility pipe.

Figure 4.1.34: Google map showing the layout of the winter GPR survey lines (red) at AHTD Site no. 3 in Feb 2016.

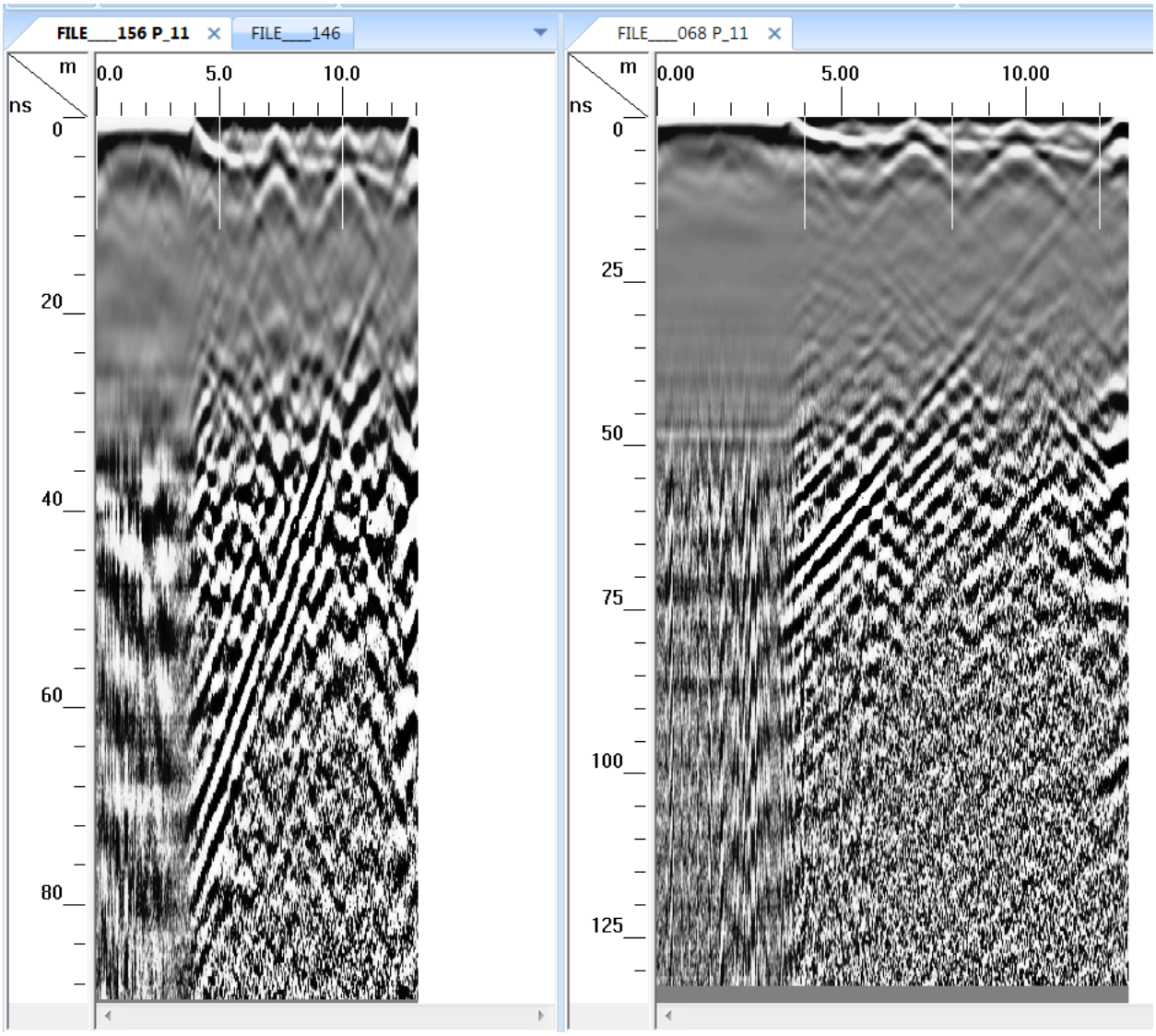

Figure 4.1.35: left panel is GPR file 156 (profile 1 in Google map) collected during winter survey. Right panel is GPR file 68 (see google map) collected during summer survey. Both profiles collected in S to N direction using 200 MHz antenna and processed for Time Zero correction and Background Removal.

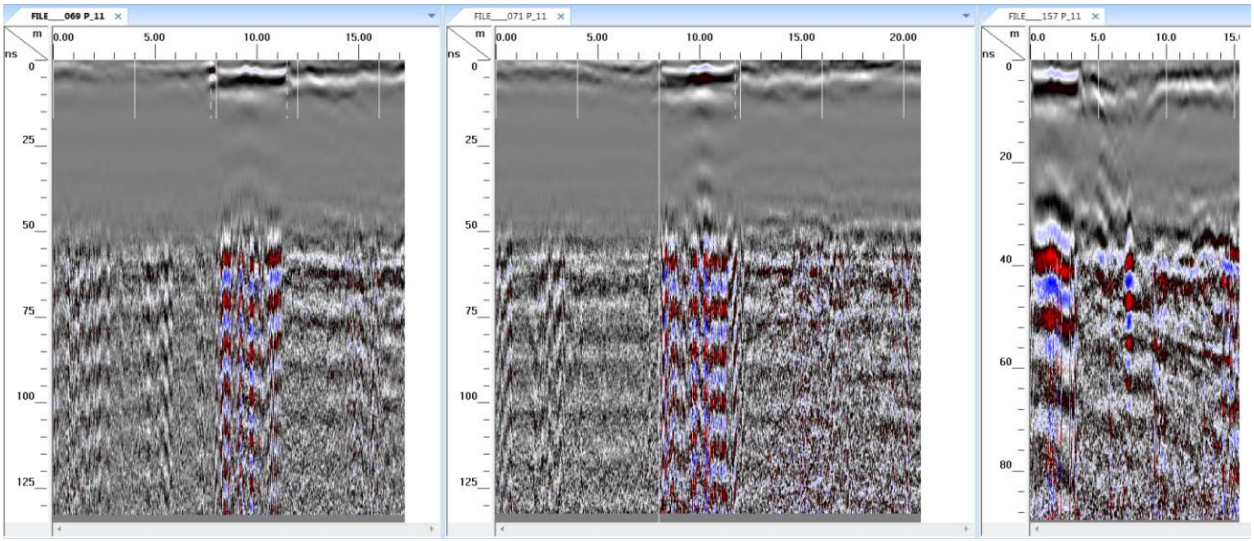

Figure 4.1.36: left panel (file 69) and middle panel (file 71) represent the GPR profiles collected during summer survey. Right panel represents the radargram of GPR profile 157 collected along profile 2 in Google map during winter survey. All profiles collected in S to N direction using 200 MHz antenna and processed for Time Zero correction and Background Removal.

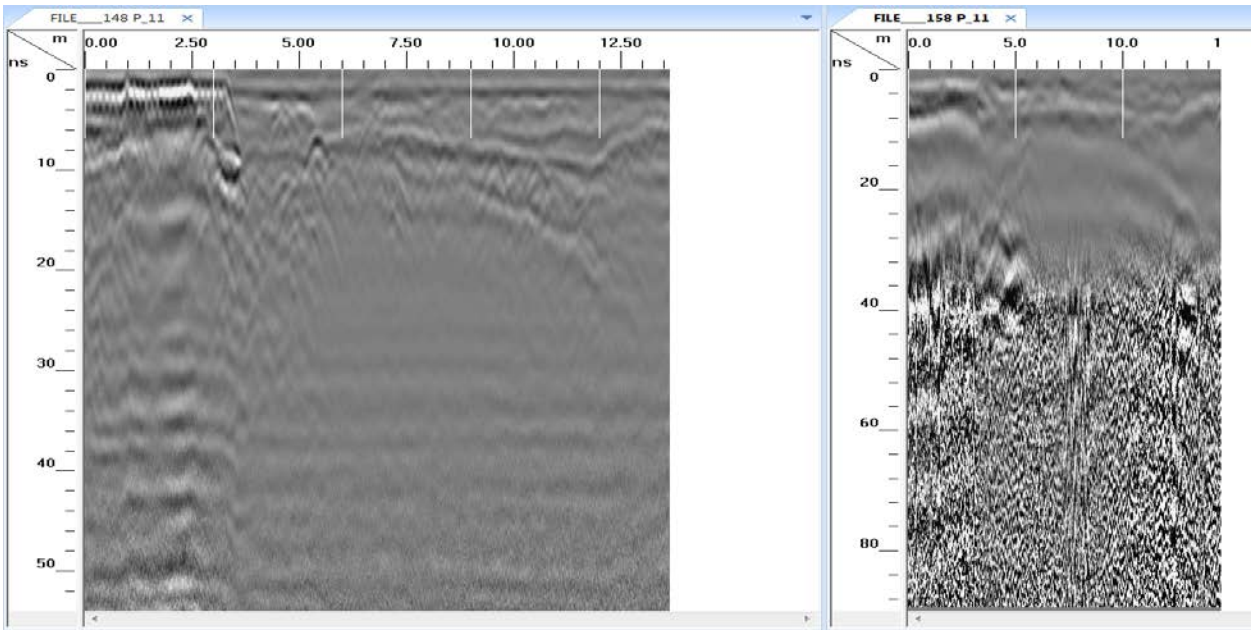

Figure 4.1.37: left panel is GPR file 148 (profile 3 in Google map) collected in S to N direction using 400 MHz antenna and file 158 collected along same path using 200 MHz antenna during winter survey of 2016. Both profiles corrected for Time Zero and Background Removal.

4.1.4 Concluding Remarks:

The intention of the surveys was to use GPR equipment to locate relatively large utility pipe(s) possibly buried at varied depths and to verify the applicability of the different frequency antenna under different survey conditions. The outcome of the surveys was compromised by the following challenges:

I. The heavy vegetation, surface roughness and aerial extension were major obstacles to conduct a viable survey and collect credible data. The heavy vegetation also prevented the signal penetration, which seems to have been dissipated at the surface. In addition to that, surface roughness introduces artificial noise that cannot be removed by signal processing. The horizontal extension of the profile is an important factor relative to the target size. The bigger the target, the longer the profile should be. This influence was observed in Site-3.
II. The high moisture content in the soil and the shallow water table sharply attenuated the signal, which rendered pipe detection practically impossible.
III. Concrete (non-metallic) pipes are usually more difficult to detect than DIPs.
IV. So far, our estimation of the target depths is based on known values of dielectric constant due to the lack of collecting "ground-truth" data.

4.2: Using Ground Penetrating Radar to Detect Unmarked Burial Sites

Comprehensive Ground Penetrating Radar (GPR) surveys were conducted at the Old Carlisle Cemetery, east of Little Rock, Arkansas, to investigate the locations of historic burial sites and to identify unmarked graves. The Old Carlisle Cemetery has been in use since 1872 and a potential expansion will be planned with the help of the geophysics data to identify unused areas. GPR survey was conducted at the cemetery using GSSI SIR-3000 with 400 MHz and 900 MHz antennas. A total of 310.4 m (1018.4 ft) profiles of GPR data were acquired from three areas within the old and new sections of the cemetery. In addition, supper 3-D survey was conducted on small area for detailed analysis.

4.2.1 Introduction:

For over 40 years, geophysical methods played a great role in archeological applications and cemetery works. GPR method is the most suitable geophysical method for detecting unmarked graves due to its non-destructive nature and fast real time results. One of the first applications of GPR in cemetery studies for the discovery of unmarked graves was reported in the work of Bevan and Keynon (1975). This work found that burials with substantial coffins were easier to detect, while those containing only reburied bones were not detectable. Several works (Vaughn,

1986; Doolittle and Bellantoni, 2010; Bladon et. al., 2011; Damiata et. al., 2013; Manenti et. al. 2015) reported successful implementation of GPR survey to identify and locate burial sites. Others (Bevan, 1991; Jones, 2008; Dionne et. al., 2010) used GPR and electric methods to study burial sites.

Schultz, J. J. (2012) investigated different models of burials in 6 graves to monitor the ability of GPR to detect burials over a period of 30 months in Florida. The result suggests that the 500 MHz antenna may be a better option for detecting shallow features (less than 0.50 m), while the 250 MHz antenna is a better option for detecting deeper features (greater than 0.50 m). Thieme (2013) used MALA 250 MHz shielded antenna to show large rectangular anomalies appear at depths from (1.6 - 2.24 m) interpreted to be probable unmarked graves. Also using MALA 500 MHz antenna the GPR profiles recorded anomalies to a depth of at least three meters and identified approximately 20 possible grave shafts.

Bigman (2013) used Electromagnetic Induction (Conductivity), Electrical resistivity and GPR for a family cemetery reservation in Georgia. Two potential anomalies for burial status lying outside of the fence perimeter were determined to be questionable features. Bigman (2014) used three geophysical techniques including GPR to image the subsurface and locate unmarked graves at a cemetery. The results indicate that up to 21 possible unmarked graves exist. Nine possible unmarked graves were tested with a metal probe. Every tested anomaly revealed less compact soils indicative of an unmarked grave.

The Old Carlisle Cemetery Association Inc., a nonprofit organization that manages the Old Carlisle Cemetery at Carlisle, AR 72024, requested GPR surveys at few locations in the cemetery to help plan for future expansion. The main reason for the GPR survey was to locate possibly unmarked graves on the east end of the mapped area, and also find empty lots that could be added to the mapped area and extend the cemetery. GPR surveys were conducted at three locations. At Area 1, GPR data collected along 6 parallel profiles. Data reveals four unmarked graves at a depth of about 0.5 to 1.0 m (1.6 to 3.3 ft) and one misplaced headstone or collapsed grave were detected. Other marked graves with headstones were also verified by their typical reflection hyperbolas around 1.0 m (3.3 ft) depth. A super 3-D survey was conducted at the northeast corner of this location. Results indicate the existence of unmarked grave outside the cemetery border.

At Area 2, the data collection was performed along 4 parallel profiles to locate potential areas that were not used for burial in the past. GPR data showed that there were no graves in the area below at least two of the profiles. Three marked graves, which were verified by their headstones, might have metal caskets due to their strong reflection hyperbolas around a depth of about 1.2 m. Three other graves were either collapsed or decomposed due to their very weak reflections within a subsided surface area. Animal burrows and a rusted old key were found and verified by near surface digging.

At Area 3, the data was collected along 3 parallel profiles. GPR was able to detect one unmarked grave and two marked graves, each with two coffins, by displaying strong reflection hyperbolas at about 0.75 m (2.5 ft) depth. A grave with a headstone to the north of the two graves did not

show strong reflection hyperbola although the burial date was in 1987, which is younger than the other two. This might reflect different type of burial practice than the other two graves or signal attenuation due to moisture. GPR did not detect any additional burial site at the studied locations. The following section discusses analysis and results in detail.

4.2.2 Geophysical Fieldwork:

The fieldwork started on July 21, 2015, using the SIR-3000 GSSI Inc. equipment with a 400 MHz antenna and a 623-model cart. System's parameters were set for 512 samples, 16 bit, 40ns range, and 40 scans per unit. According to the request of Carlisle Cemetery Personnel, arrangement was made to collect GPR data on three prospect areas. These areas are designated as Area 1, Area 2, and Area 3 (Fig. 4.2.1).

Area 1

In this area, data collected along six parallel GPR profiles (Fig. 4.2.1) trending North-South. The eastern two profiles (1 and 2) extended to the north by 3.0 meters depending on the possibility of existence of unmarked graves in that area. The lengths of these profiles (1 and 2) were 20.8 meters while the length of each of the remaining four profiles (3, 4, 5 and 6) was 17.7 (58.1 ft) meters. 2.0 meters (6.6 ft) separate the first two profiles, while the spacing between the other profiles was 1.5 m (4.9 ft) (Fig. 4.2.2).

Area 2

The data collected along four profiles (Fig. 4.2.1) trending North-South. The length of these profiles was 17.0 meters. The spacing could not be kept equal due to the location of headstones; therefore, the distance between profiles no. 7, 8, 9 and 10 was 1.0 m (3.3 ft), 1.5 m (4.9 ft), and 2.0 m (6.6 ft) respectively.

Area 3

In this area, the data collected along three profiles (Fig. 4.2.1) trending North-South and having 17.9 m (58.7 ft) of length. The spacing was 4.4 m (14.4 ft) and 3.4 m (11.2 ft) between profiles no. 11, 12, and 13 respectively.

Table 4.2.1 shows a summary of all GPR profiles acquired in the three surveyed areas.

Table (4.2.1): GPR profiles acquired in the three areas of Old Carlisle Cemetery.

	Area 1			Area 2			Area 3		
Used Frequency	GPR Profiles	Length		GPR Profiles	Length		GPR Profiles	Length	
		m	ft		m	ft		m	ft
400 MHz	1	20.8	68.2	7	17.0	55.7	11	17.9	58.7
	2	20.8	68.2	8	17.0	55.7	12	17.5	57.4
	3	17.7	58.1	9	17.0	55.7	13	17.5	57.4
	4	17.7	58.1	10	17.0	55.7			
	5	17.7	58.1						
	6	17.7	58.1						
900 MHz	14	20.8	68.2	18	17.0	55.7	17	18.5	60.7
	15	20.8	68.2						
	16	17.7	58.1						
	Total length	**154**	**505.2**	Total length	**85**	**278.9**	Total length	**71.4**	**234.3**
Total Length of all the profiles in the three areas				**310.4 m (1018.4 ft)**					

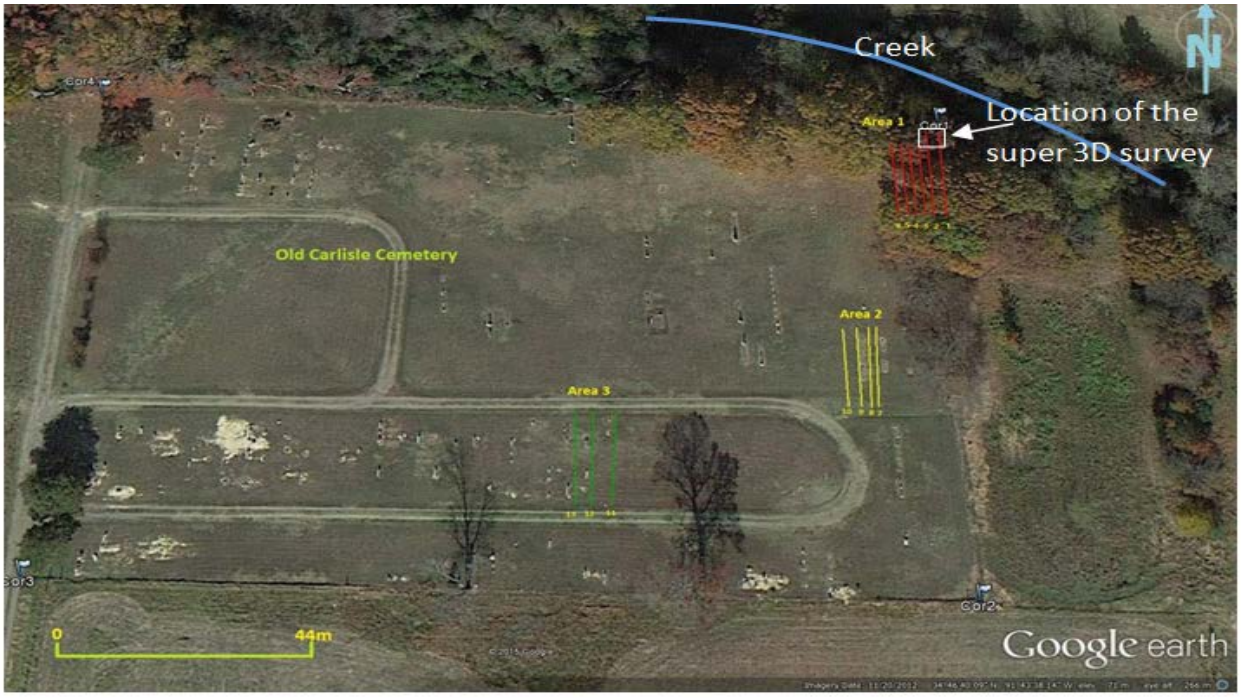

Figure. 4.2.1. Survey layout map of the GPR profiles in Old Carlisle Cemetery showing the locations of Area 1 (red), 2 (yellow), and 3 (green) profiles. Location of the super 3-D survey is shown as white rectangle.

Figure. 4.2.2. Photograph at Area 1 showing location of profiles 1 – 6 and the GPR cart.

4.2.3 Interpretation and Results:

The raw GPR data was processed using GSSI RADAN 7 software with the application of the following procedures (see section 3.2 for details):

1- Time Zero Correction
2- Background Removal
3- Migration Procedure
4- Low and High pass filters

4.2.4 Measuring Dielectric Constant for the Areas

From GPR reflection data and the time-distance relationship, depth to different anomalies can be calculated if the dielectric constant of the medium is known. Likewise, if the depth to a target is known, the dielectric constant for the medium can be calculated (Morey, 1998). In addition, if the depth to the target is unknown, then signal migration may be used to measure the electromagnetic propagation velocity and dielectric constant for the medium. The average propagation velocity can be measured from the simple relationship as shown in equation 1 (Persico, 2014) where v is the propagation velocity of the electromagnetic waves, *D* is the depth of the target, and *t* is the two-way travel time.

$$v = \frac{2.D}{t} \tag{1}$$

The velocity of the electromagnetic waves (v (m/ns)) in a medium can be represented as (Daniels, 2004; Davis and Annan, 1989):

$$v = \frac{C}{\sqrt{\varepsilon}} \tag{2}$$

Where *C* is the speed of light in vacuum (≈ 0.299 m/ns), and $\boldsymbol{\varepsilon}$ is the dielectric constant of the medium. This allows the calculation of the dielectric constant:

$$\varepsilon = \left(\frac{C}{V}\right)^2 \tag{3}$$

Dielectric constant varies from one media to another depending mainly on the soil chemistry, moisture content, and electric conductivity.

Old Carlisle cemetery was classified into three areas according to their dielectric constant. The more the water contents the higher conductivity and dielectric constant and vice versa. Water content in Area 1 is more than Area 2 and Area 3 because it is closer to the creek and covered by trees (Fig. 4.2.1), which possibly resulted in higher dielectric constant for this area. A clear hyperbola was chosen from profile no. 1 of Area 1 to measure the dielectric constant. Data were migrated with RADAN 7 using a value of 12.04 for dielectric constant. Fig. 4.2.3a shows the radargram before migration and Fig. 4.2.3b shows the migrated data.

Area 2 is farther away from the creek, so the soil is drier than Area 1. A clear hyperbola was chosen from profile no. 7 for measuring dielectric constant in area 2 as shown in Fig 4.2.4a and b. The value of 6.7 was calculated for the dielectric constant in Area 2.
In Area 3, there was a very clear reflection on the data collected along profile no. 11 as shown in Fig. 4.2.5. The type and depth of the interface that caused the reflection was confirmed by digging a 1 x 1 m (3.3 x 3.3 ft) trench. The digging revealed that there was a wet clay layer at a depth of 51 cm (Fig. 4.2.6). The two-way travel time was measured from the radargram as 7 ns (Fig. 4.2.5). The propagation velocity of the electromagnetic waves was measured by the following equations:

$$v = \frac{2.D}{t}$$

v = $\frac{102\ cm}{7\ ns}$ = 14.5 cm/ns = 0.145 m/ns $\Rightarrow$

$$v = \frac{C}{\sqrt{\varepsilon}}$$

0.145 = $\frac{0.299 m/ns}{\sqrt{\varepsilon}}$ $\Rightarrow$

$$\varepsilon = \left(\frac{C}{V}\right)^2$$

ε = $\left(\frac{0.299\ m/ns}{0.145\ m/ns}\right)^2$ $\Rightarrow$ ε = 4.25

The final number represents the measured dielectric constant for the dry soil layer (the upper layer) in Area 3.

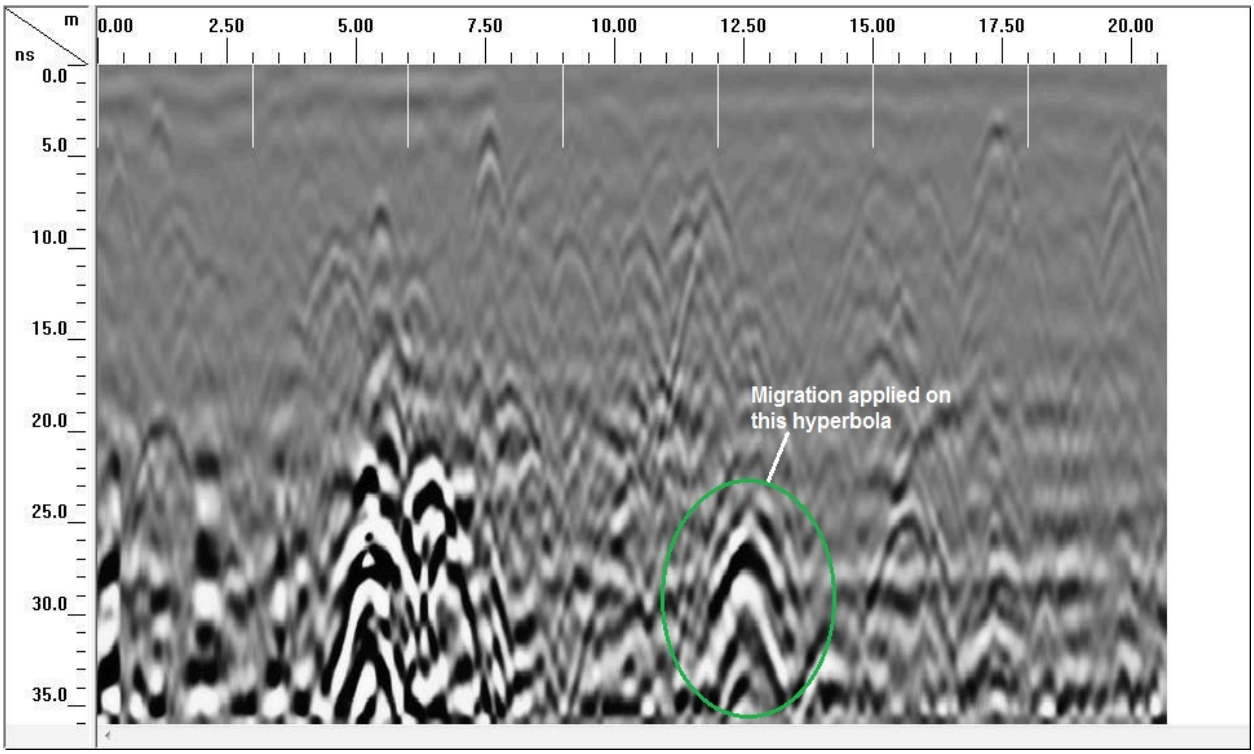

Fig. 4.2.3a. Data before migration profile no. 1, Area 1

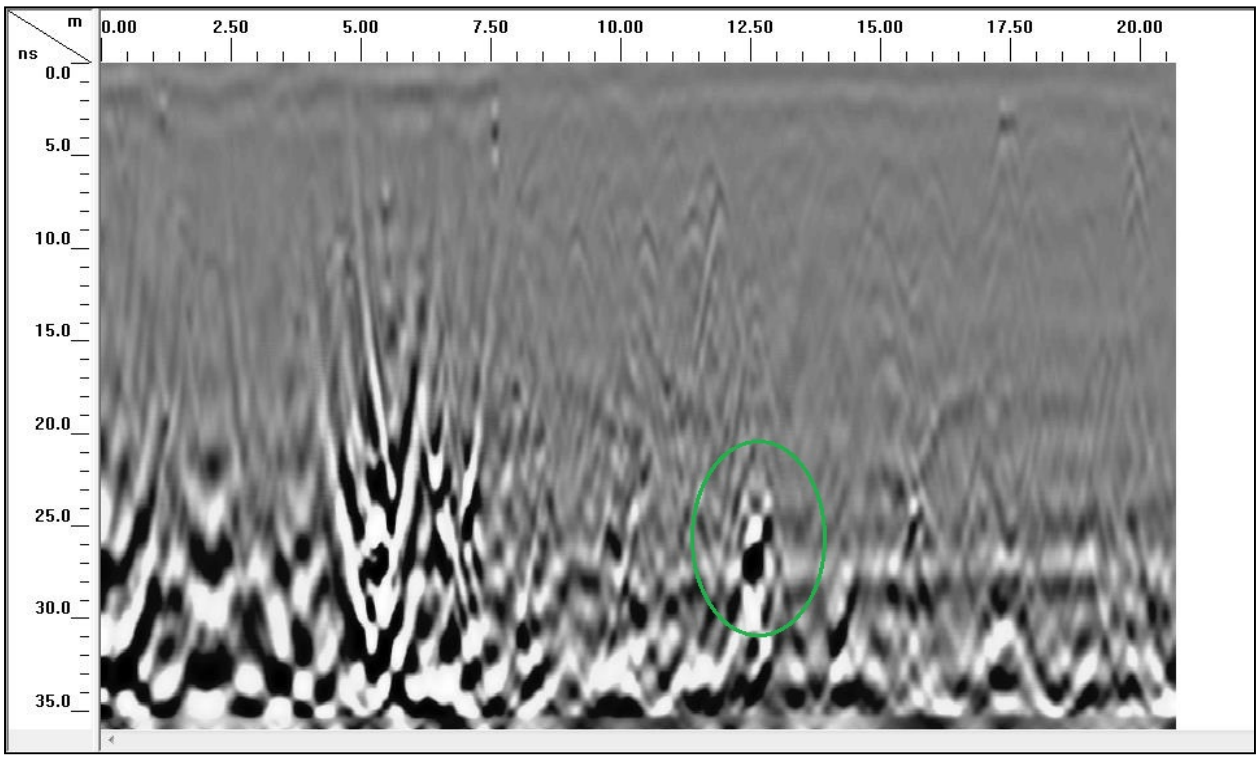

Fig. 4.2.3b. Data after migration profile no. 1, Area 1.

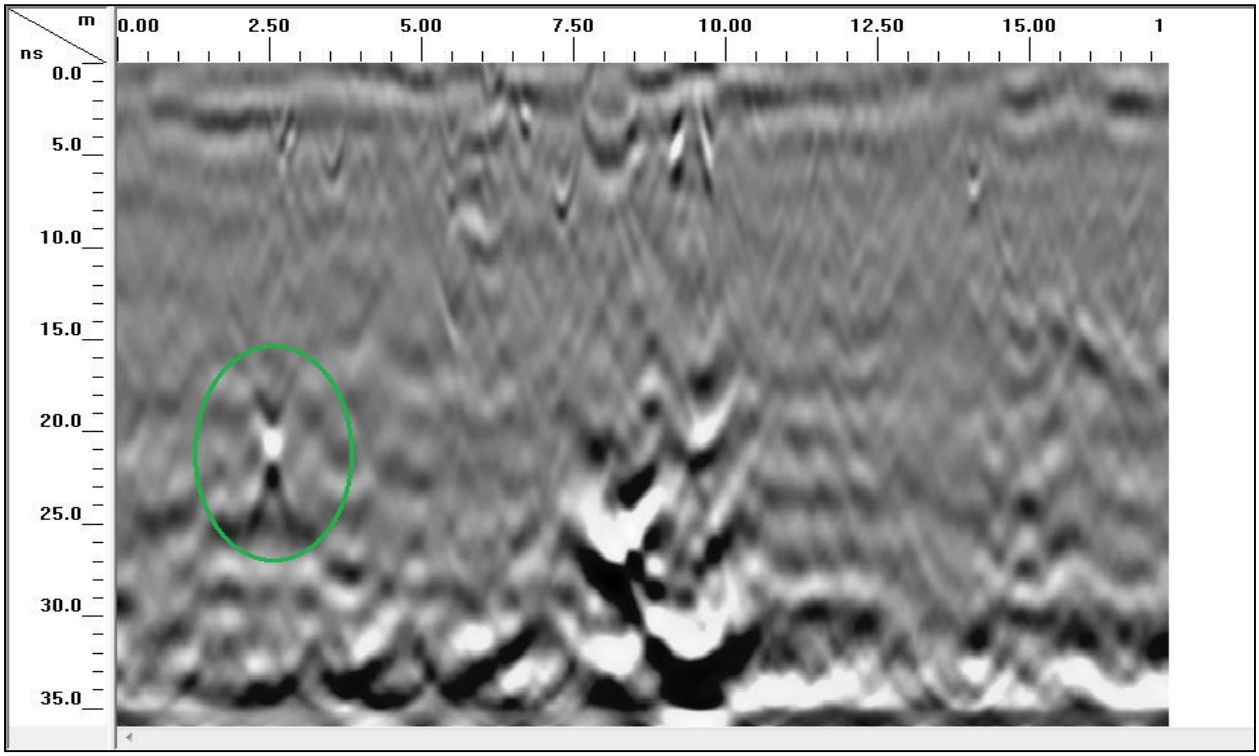

Fig. 4.2.4a. Data before migration profile no. 7, Area 2

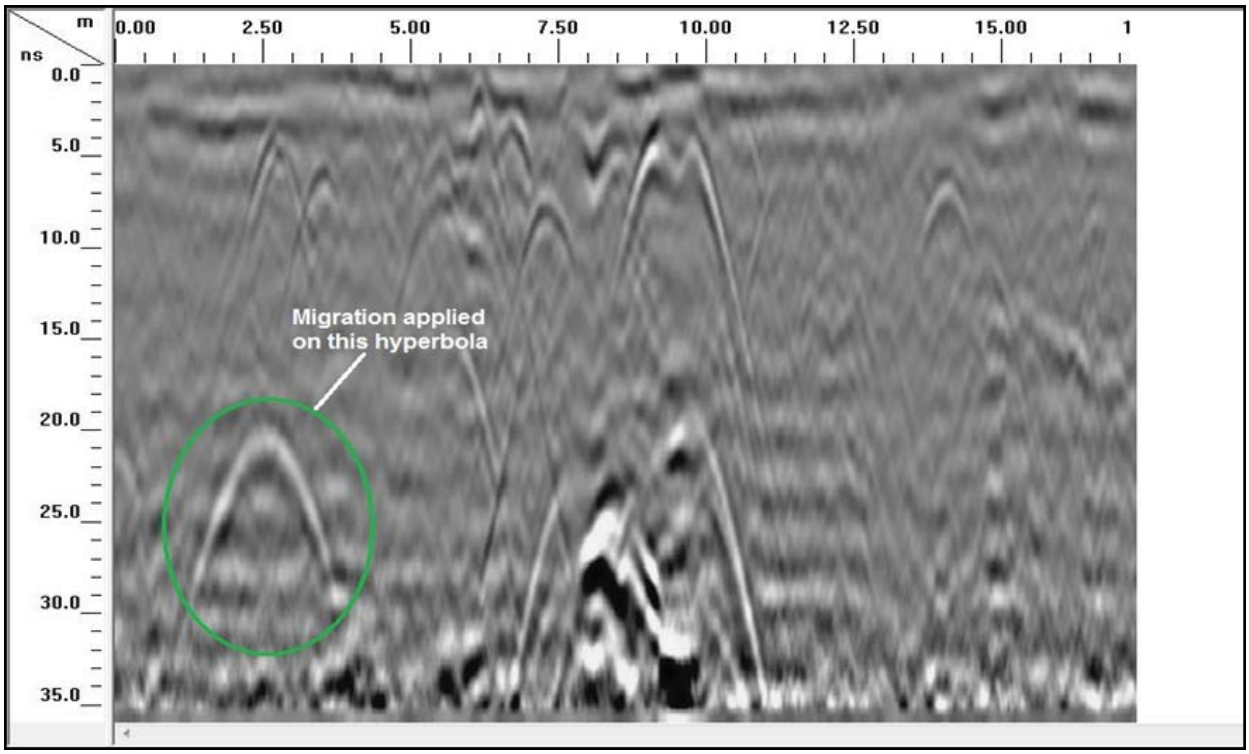

Fig. 4.2.4b. Data after migration profile no. 7, Area 2

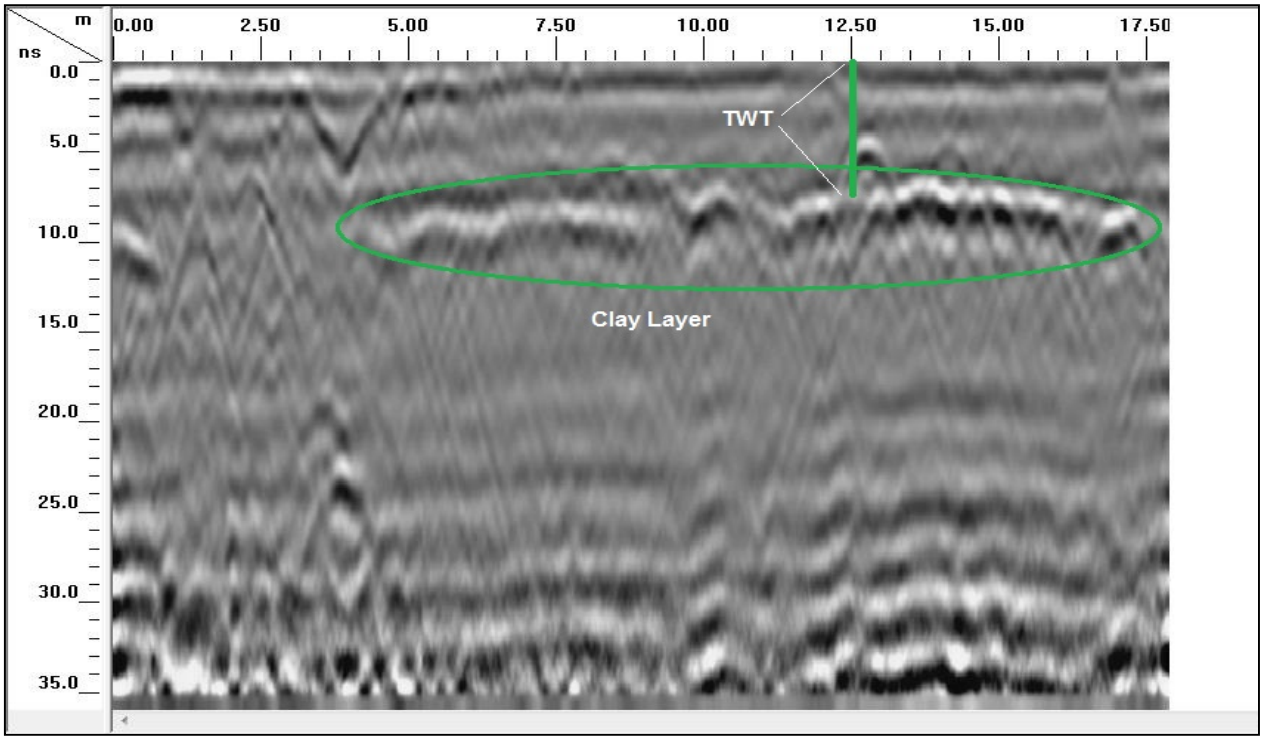

Fig. 4.2.5. Radargram of profile no. 11 in Area 3 showing the two-way travel time from the wet clay layer.

Fig. 4.2.6. A photo showing the trenching along profile no. 11 in Area 3 and the contact between the dry upper layer and the wet clay lower layer at depth of 0.51 m.

4.2.5 Interpretation of Data:

Area 1:

This area located at the northeastern corner of the cemetery and it is heavily covered by trees (Fig. 4.2.1 & 4.2.2). Result of the migration procedure on clear hyperbolic reflections of this area, a value of 12.04 was calculated to for the dielectric constant. This slightly elevated value is due to its closeness to the creek, which runs at the northern boundary of the cemetery. Below are representative examples of GPR profiles and their interpretations.

Profile No.1:

The length of this profile is 20.8 m (68.2 ft) and runs from North to South (Fig. 4.2.1 & 4.2.7). Fig. 4.2.8 shows the processed radargram of this profile:

- The first anomalously high amplitude reflection located at distance 5.0 – 5.8 m (16.4 – 19 ft) from the start of the profile and depth of about 0.90 m (3 ft) (21 ns). This is consistent with the location of headstone of burial no. 1 (1904-1972). The high amplitude reflection indicates that this burial site might contain casket or vault made of metallic or reinforced concrete.
- There is a large headstone for two coffins, burials 2a (1882 - unknown) and 2b (1881-1956) at distance of 7.0 – 8.3 m (23 – 27.2 ft) from the start of the profile. This is confirmed by the two reflection hyperbolas at depth around 1.0 m (3.3 ft) (23ns), considering that their headstone was shifted by 0.5 m (1.6 ft) to the South.
- A grave headstone at distance of 10.0 – 10.30 m (32.8 – 33.8 ft) belongs to burial no. 3 (1907-1936). GPR data shows a very weak reflection from this grave, which might indicate collapsed or decomposed burial. Caskets or void spaces in partially collapsed caskets are still visible in profiles as distinct hyperbolic reflections (Conyers, 2006).
- The other four headstones (for burial 4, 5, 6, and 7) were confirmed with the GPR data. Headstone belongs to burials 6a (1836-1914) and 6b (1852-1929) at distance of 16.0 – 17.2 m (52.5 – 56.4 ft) is shifted to the south by less than 1.0 m (3.3 ft).
- There are shallow reflections along this profile, which are expected to be the effect of the tree roots that are relatively close to the profile location.

Fig. 4.2.7. A photo (viewing south) shows the location of profile no.1 (yellow line) in Area 1.

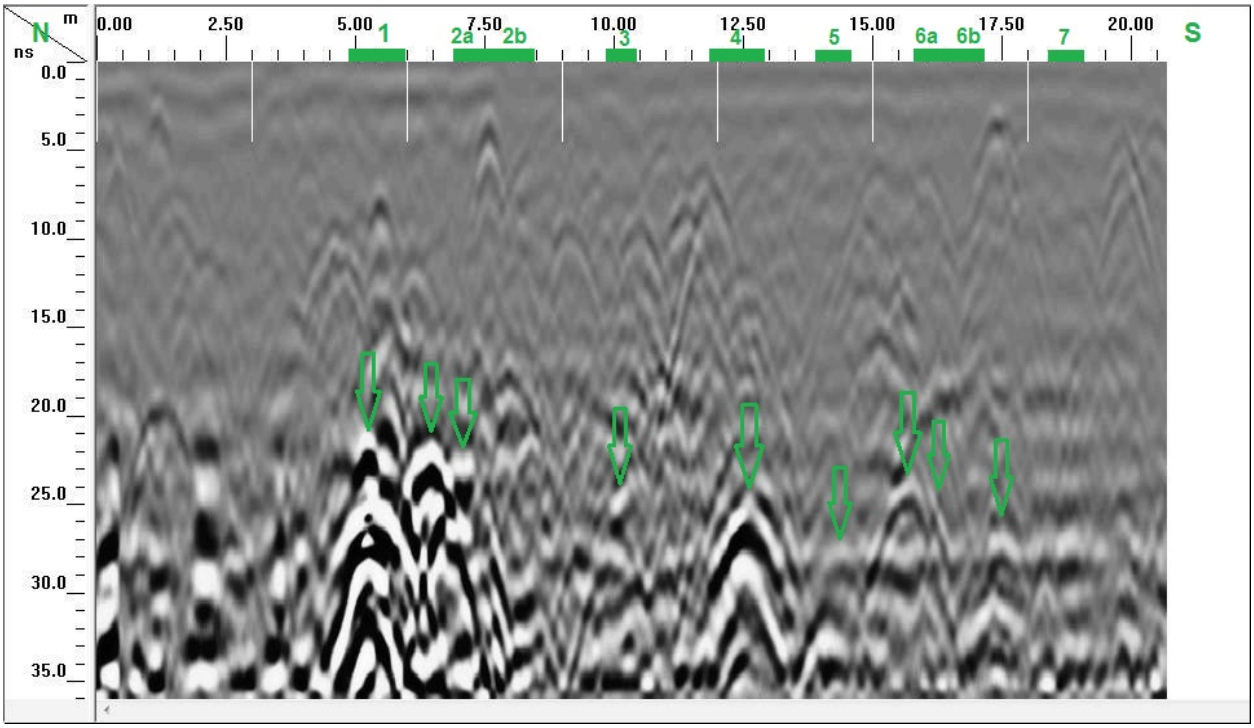

Fig. 4.2.8. Interpreted GPR data along profile no.1 showing the location of burials relative to current headstones.

Profile No.4:

This profile runs from north to south with a length of 17.2 meters. Fig. 4.2.9 shows the radargram of the GPR profile:

- At distance of (4.5 – 5.0) m (14.7- 16.4 ft), a possible unmarked grave detected at a depth about 0.80 m (2.6 ft) (18.5ns).
- A headstone at distance of (6.0 – 6.5) m (19.7 – 21.3 ft) belong to burial no. 8 (Nov, 1907 – Feb, 1908) is confirmed by a clear hyperbolic reflection at a depth about 0.85 m (2.8 ft) (20ns).
- At the distance of (7.2 – 7.7 m) (23.6 – 25.3 ft); a headstone belongs to burial no. 9 (Feb. 2, 1936 – Feb. 8, 1936) could not be identified with a clear reflection. Given the fact that this burial site is belong to a baby six days old, most likely the coffin was buried at a much shallower than regular depth of burial and within the disturbed (grave shaft) area around 0.4 m (1.3 ft) depth (10ns).
- There is no evidence of other burials along this profile, as the subsurface layers seem undisturbed until the end of the profile.

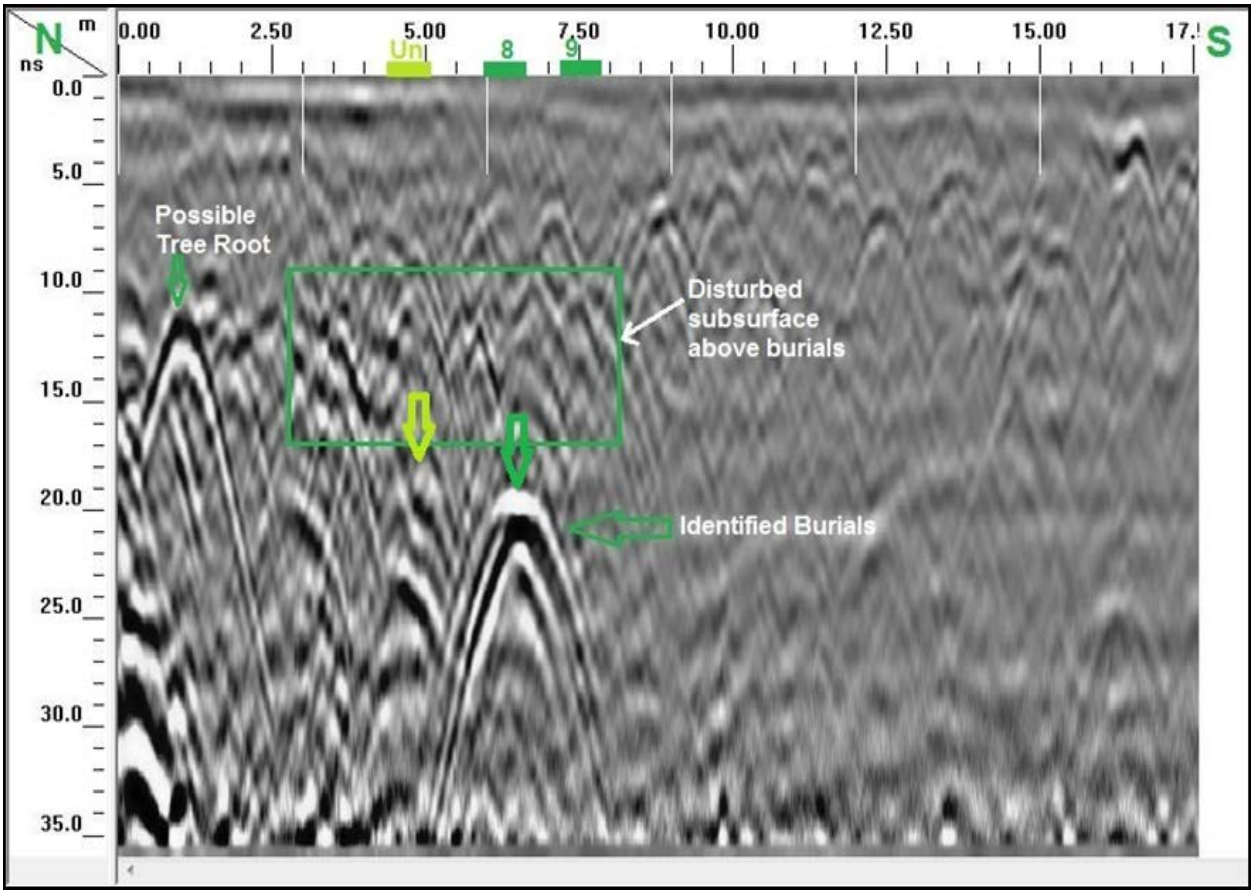

Fig. 4.2.9. Interpreted GPR data along profile no.4

Profile No.6:

This profile also runs from north to south with a length of 17.2 meters. Fig. 4.2.10 shows the GPR radargram of the profile:

- A headstone located at distance of 2.6 – 3.5 m (8.5 – 11.5 ft) belongs to burial no.10 (1854-1917). According to family members, they expect instead of one but three burials at this site. Two adults and one baby. From the GPR data, it is possible to identify one hyperbolic reflection at a distance of 1.25 m (4.1 ft) around a depth of 0.85 m (2.8 ft) (20ns). There are two more hyperbolic reflections around the same location, but at a shallower depth (around 0.5 m (1.6 ft) (12ns)). This possibly represents the unmarked graves of the other two burials. This interpretation is feasible since those two were buried during wintertime when the temperature was sub-freezing and they were buried at a shallower depth because of the harsh weather condition. The headstone of this burial site was shifted at least 1m to the south.

- Another distinct hyperbolic reflection at distance of 6.0 m (19.7 ft) is consistent with a headstone of burial no. 11 (1911 – 1930).

- A headstone belongs to burial no. 12 (1888 – 1976) at distance of 6.6 – 7.2 m (21.7 – 23.6 ft) is confirmed with a very high amplitude hyperbolic reflection at depth of about 1.0 m (3.3 ft) (23ns). This is relatively a new grave and possibly has a metal coffin or reinforced concrete vault.
- An unmarked grave at distance of 8.0 – 8.5 m (26.2 – 27.9 ft) detected at depth of about 0.92 m (3 ft) (21.5ns).

- There is an old headstone at distance of 10.1 – 10.4 m (33.1 – 34.1 ft) belongs to burial no. 13 (1865 – 1894). GPR data shows no clear reflections for this burial site. This may be due to the possibility of deteriorated coffin. Burial without caskets or with deteriorated wooden caskets results little remains from the primary interment. This produces no or limited radar energy reflection back to the surface and no distinctive hyperbolas (Conyers, 2006).

On the other hand, there is a possibility that this headstone may be misplaced from the previous location having a hyperbolic reflection at distance of 8.0 m (26.2 ft), which was interpreted as unmarked grave. This scenario is more acceptable by the cemetery personnel since this cemetery experienced a strong tornado that caused many head stones to be misplaced.

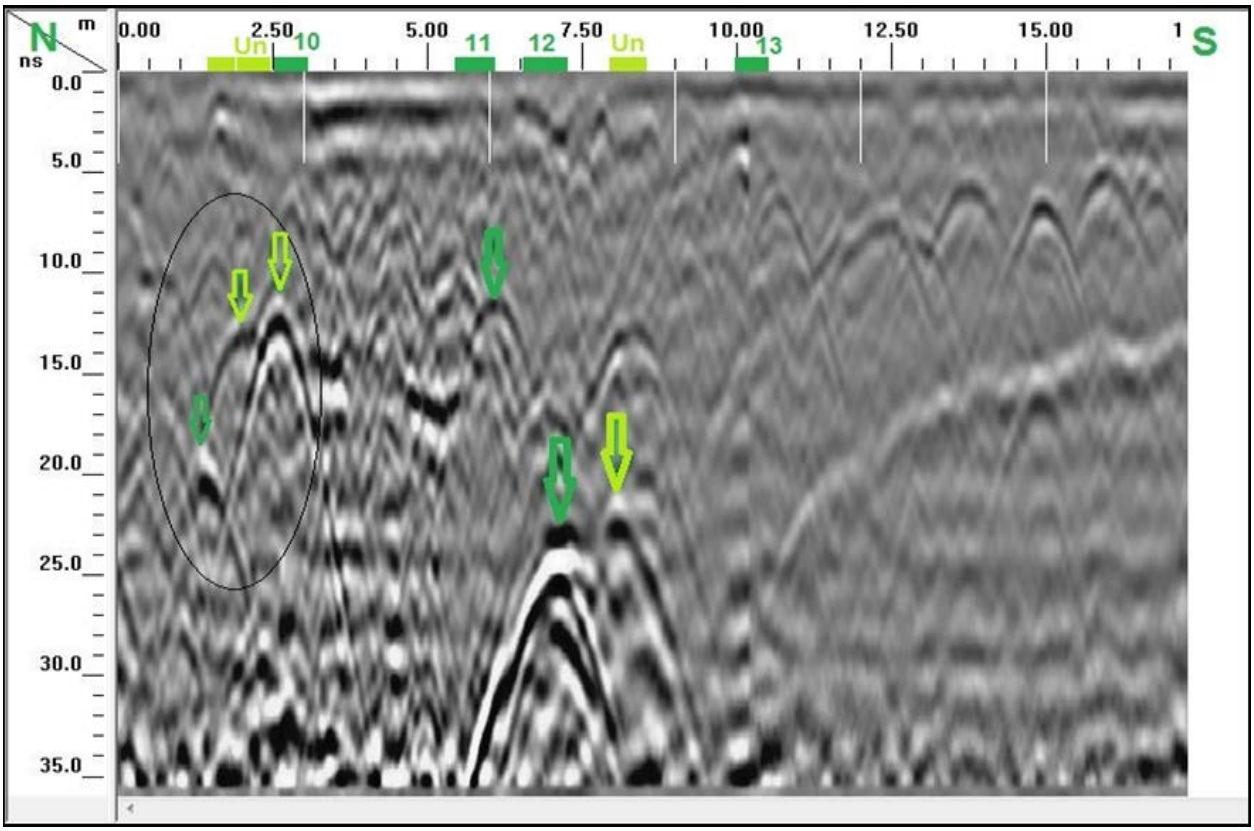

Fig. 4.2.10. Interpreted GPR data along profile no.6

Area 2:

This area located in the eastern part of the cemetery (Fig. 4.2.1) where the cemetery caretakers are interested in finding empty lots. They were also interested to know if there are two adjoining graves close to site no. 17. The dielectric constant value of 6.7 was calculated for this area, which was verified by the depth of an old buried key found along one of the profiles (profile no. 9) and the migration procedure for the best hyperbolas.

Profile No.7:

Figure 4.2.11 shows the radargram of GPR profile no. 7. Results include:

- A grave marked with a headstone at distance of 2.1 – 2.7 m (6.9 – 8.9 ft) belongs to burial no. 14 (1916 – 1942) was confirmed using the strong hyperbolic reflection at depth of about 1.1 m (3.6 ft) (20ns) of the GPR data.
- A headstone at distance of 4.0 – 4.6 m (13.1 – 15.1 ft) belongs to burial no. 15 (1917 – 1937) and another at distance of 5.9 – 6.50 m (19.4 – 21.3 ft) belongs to burial no. 16 (1914 – 1936). There are ground depressions visible on the surface at both graves. GPR data shows no clear hyperbolic reflections for these sites. In cases where bodies were placed in coffins or other containers that might be deteriorated over time and partially or totally collapsed, most likely produce subsurface and surface slump features. These surface depressions will often slowly

have filled with sediment resulting in a leveled ground making surface identification of these graves difficult (Conyers, 2006).

- Two clear reflections at distances of 8.0 m (26.2 ft) and 9.0 m (29.5 ft) at depth of about 1.30 m (4.3 ft) (22.5ns) and 1.10 m (3.6 ft) (20ns) respectively are consistent with a large headstone at distance of 8.0 – 9.6 m (26.2 – 31.5) belongs to burial 17a (1904 – 1967) and 17b (1914 – 1974).
- A headstone at distance of 10.5 – 11.2 m (34.4 – 36.7 ft) belongs to a baby burial no. 18 (Feb – Nov. 1936). No obvious reflections confirmed to be associated with this headstone.
- Data shows several shallow reflections at about 0.1 m (0.33 ft) depth interpreted to be animal burrows as was confirmed from the surface observations.

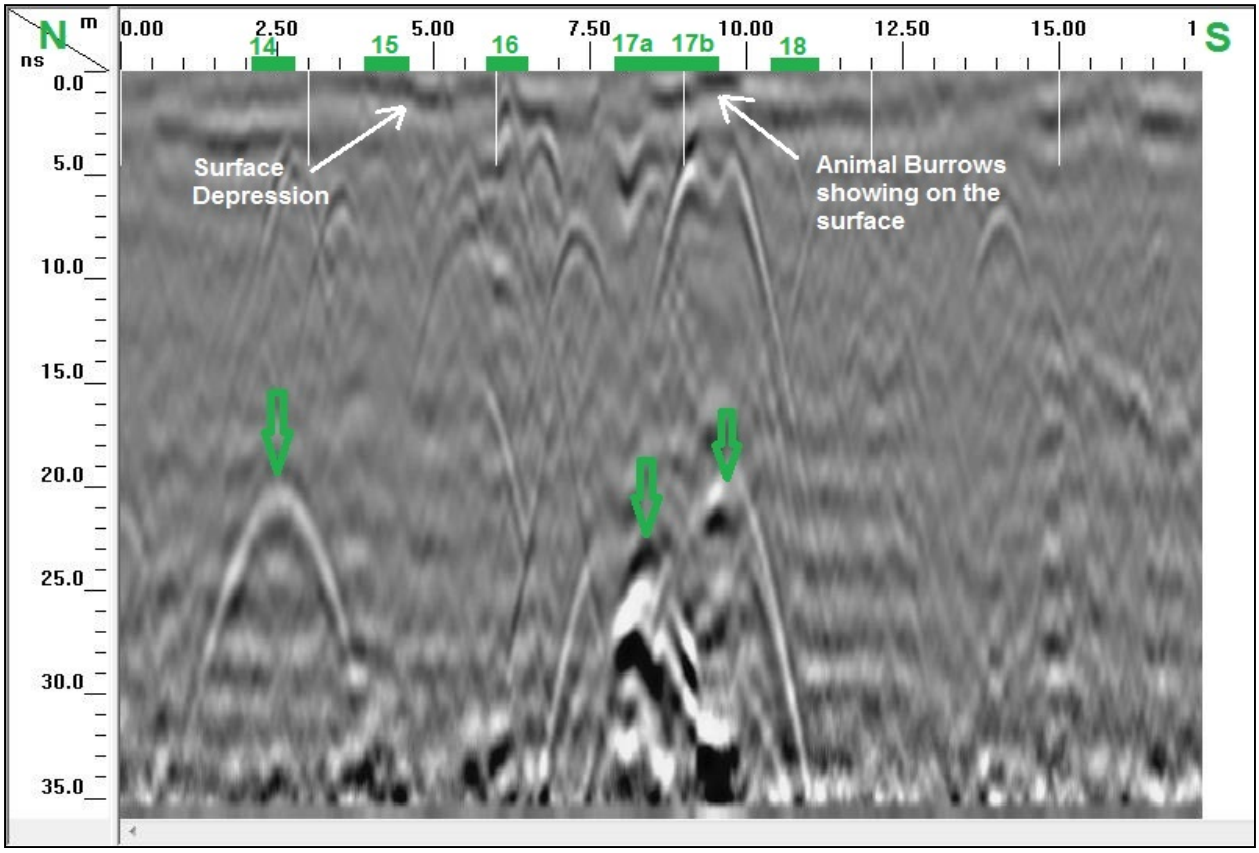

Fig. 4.2.11. Interpreted GPR data along profile no.7

Profile No.8

Fig. 4.2.13 shows the radargram of GPR profile no. 8. This profile runs 1.0 m (3.3 ft) to the west of profile no.7. It was closer to the same row of headstones (Fig. 4.2.12). All reflections shown in profile 7 were also shown in this profile; however, with clearer and higher amplitudes since the GPR profile runs closer to the burial sites than profile no.7. The shallow reflections related to animal burrows were also shown in this profile.

Fig. 4.2.12. A photo viewing NW showing Area 2 with location of the profiles 7 – 10.

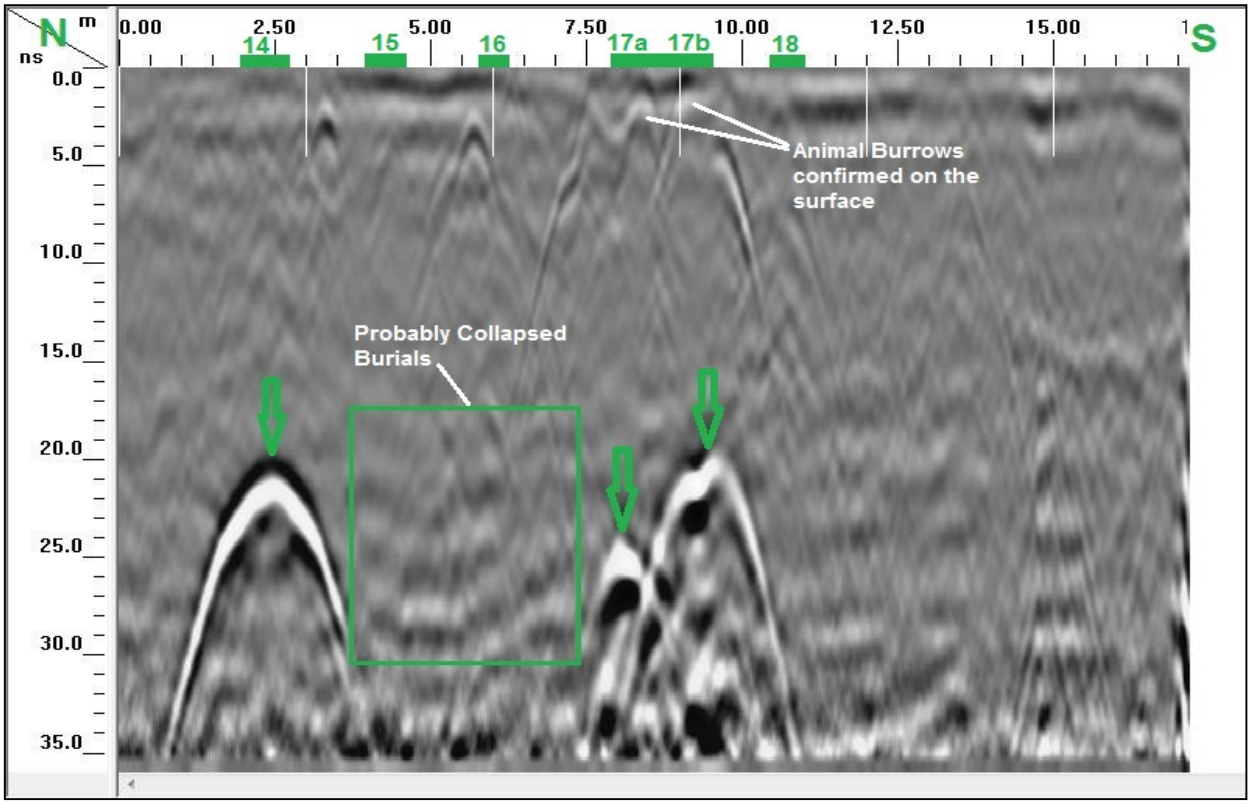

Fig. 4.2.13. Interpreted GPR data along profile no.8

Profile No.9:

Fig. 4.2.14 shows the radargram of the GPR profile no. 9. One of the main objectives of the GPR survey in this area was to confirm of no burials along this profile. The data does not show any disturbance of the subsurface soil and no clear hyperbolic reflections. The following results have been interpreted from the radargram:

- Animal burrows detected between the distances of 4.0 m (13.1 ft) and about 12.0 m (39.4 ft) and were confirmed by the surface observations.
- A small repetitive hyperbolic reflection with high amplitude at distance of 15.0 m (49.2 ft) and depth of about 0.09 m (0.3 ft) (1.5ns) was verified by digging to be related to an old rusted key (Fig. 4.2.14 &4.2.15).

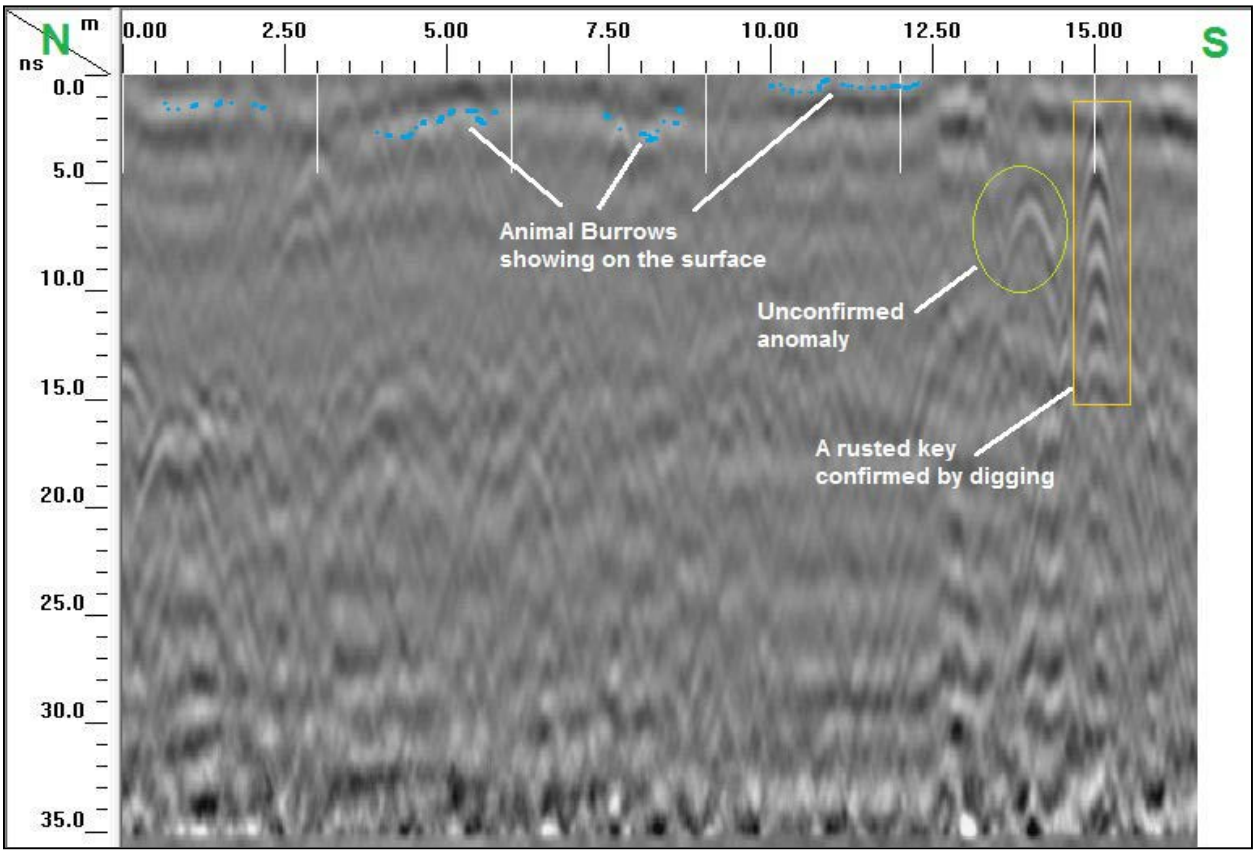

Fig. 4.2.14. Interpreted GPR data along profile no.9

Fig. 4.2.15. An old rusted key was found and verified by digging along profile no.9

Area 3:

This area located in the south part of the cemetery close to the empty lots. GPR survey conducted along three parallel profiles (see Fig.4.2.1 & Fig. 4.2.16).

Fig. 4.2.16. A photo viewing N showing Area 3 with location of the profiles 11 – 13.

Profile No. 11:

Fig. 4.2.17 shows the radargram of profile no. 11. The following observations were made:

- A marked gravesite no. 19 is at a distance of 1.10 to 1.40 m (3.6 to 4.6 ft), confirmed by the hyperbolic reflection at depth of about 0.60 m (2 ft) (8ns).
- A possible unmarked grave at distance of 2.5 m (8.2 ft) and depth of about 0.50 m (1.6 ft) (6.5ns) between two marked graves with headstones.
- A metal headstone of burial no. 20 at distance of 3.60 to 3.90 m (11.8 to 12.8 ft) confirmed with a hyperbolic reflection at depth of about 1.30 m (4.3 ft) (18ns). All of the three burial sites are located within the same trenched area, which appears in the radargram as a discontinuity in the subsurface layer.
- There are no additional burials along this profile, as indicated by a reflection of the undisturbed horizontal clay (soil) layer at a depth of about 0.50 m (1.6 ft). To verify this, a small trench was dug at distance of 12.5 to 13.0 m (41 to 42.7 ft) for a depth 0.65 m (2.1 ft). The trench showed a hard, wet clay layer at a depth of 0.51 m (1.7 ft) (Fig. 4.2.6).

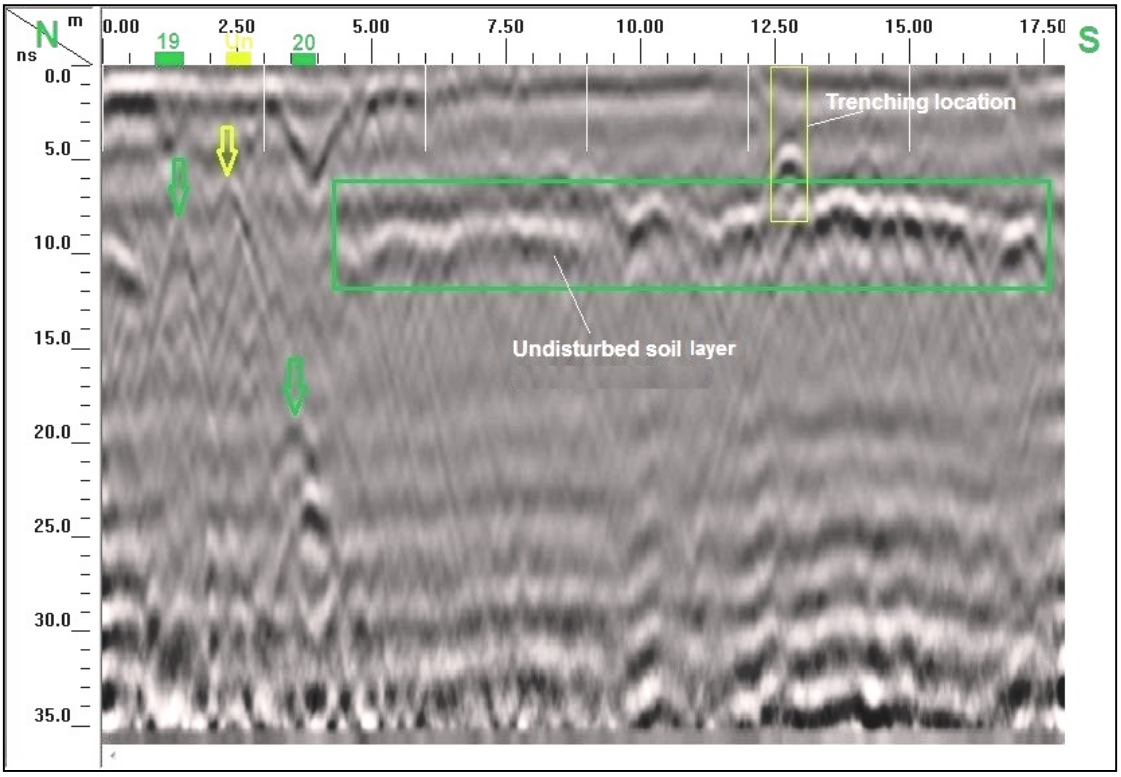

Fig.4.2.17. Interpreted GPR data along profile no.11

Profile No.12

Along this profile (Radargram is not shown) there are two headstones and one footstone placed for future burials by their owners; the first headstone at distance of (5.25 – 6.75 m) (17.2 – 22.1 ft), the second headstone at distance of (11.4 – 12.5 m) (37.4 – 41 ft), a footstone at distance of (15.2 – 15.7 m) (49.9 – 51.5 ft). GPR data revealed a continuous unbreached horizontal layer, which represents the boundary between the dry upper soil layer and the wet clay lower layer, verified by trenching. This implies that the area along this profile contains no burial sites.

Profile No.13

Fig. 4.2.18 shows the GPR data for this profile. The following interpretation was made for this data:

- A repeated reflection possibly from wet saturated ditch areas observed on the ground surface at 0.5 m (1.6 ft), 11.0 m (36.1 ft), and at the end of the profile.
- At distance of 1.7 – 3.5 m (5.6 – 11.5 ft), there is a large headstone belongs to burials no. 21a (1899 – 1993) and 21b (1895 – 1961). These burials were confirmed with a relatively wide hyperbolic reflection with a positive peak at distance of 2.5 m (8.2 ft) and depth about 0.85 m (2.8 ft) (11.5ns). This wide hyperbola contains two small hyperbolic reflections at distance of 2.0 m (6.6 ft) and 3.0 m (9.8 ft). The left one is deeper by about 0.05 m (0.16 ft) and higher amplitude. It is expected that these two small hyperbolas are reflections from the two coffins that might be vaulted.

- Immediately after this feature, there is a relatively horizontal stratigraphic layer at a depth ranging from 0.50 m (16.4 ft) (7ns) to 0.70 m (2.3 ft) (9.5ns), which is at about the same boundary that was confirmed by digging along the profile no. 11 (Fig. 4.2.6). This horizontal soil layer is interrupted in the area where grave shafts have been excavated, and it is undisturbed where there are no graves.
- There are two relatively long headstones; the first at distance of 5.0 – 6.3 m (16.4 – 20.7 ft) site burial no.22) and distance of 8.2 – 9.7 m (26.9 – 31.8 ft) (site burial no.23). These are lots assigned for future burials. Despite the presence of these headstones, GPR survey indicated no graves due to the undisturbed horizontal subsurface layer and the lack of any hyperbolic reflections.
- Two marked graves with one headstone belong to burial no.24a (1890 – 1960) and 24b (1909 – 1989), at distance of 12.0 – 13.0 m (39.4 – 42.7 ft) and a depth of about 0.8 m (2.6 ft) (11ns). The GPR data confirmed these two graves with strong reflection hyperbolas at the same distance and they are enclosed within a wider hyperbolic reflection.
- A headstone at distance of 14.3 – 15.2 m (46.9 – 49.9 ft) belongs to burial no.25 (1937 – 1987), can be identified with a weak hyperbolic reflection at distance of 14.5 m (47.6 ft). Although it is not a very clear anomaly, this might be due to signal attenuation caused by the wetness of the area close to the nearby ditch.

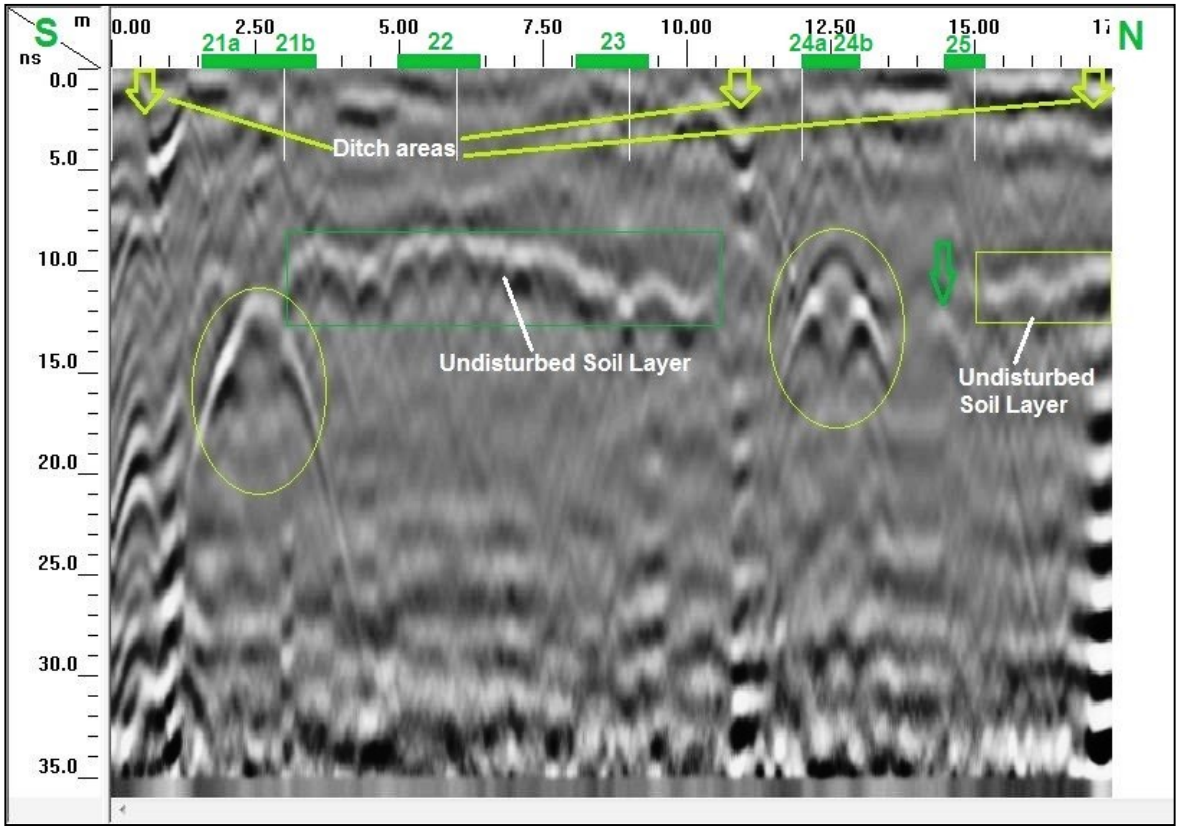

Fig. 4.2.18. Interpreted GPR data along profile no.13.

The 900 MHz antenna was also used for the same profile hoping for more resolution of the shallow reflections, but the results was not as impressive as the 400 MHz antenna. Fig. 4.2.19 shows the GPR data using the 900 MHz antenna. The figure shows the same anomalies as profile no. 13 but with less resolution. We attributed this observation to the increased attenuation of the high-frequency signal.

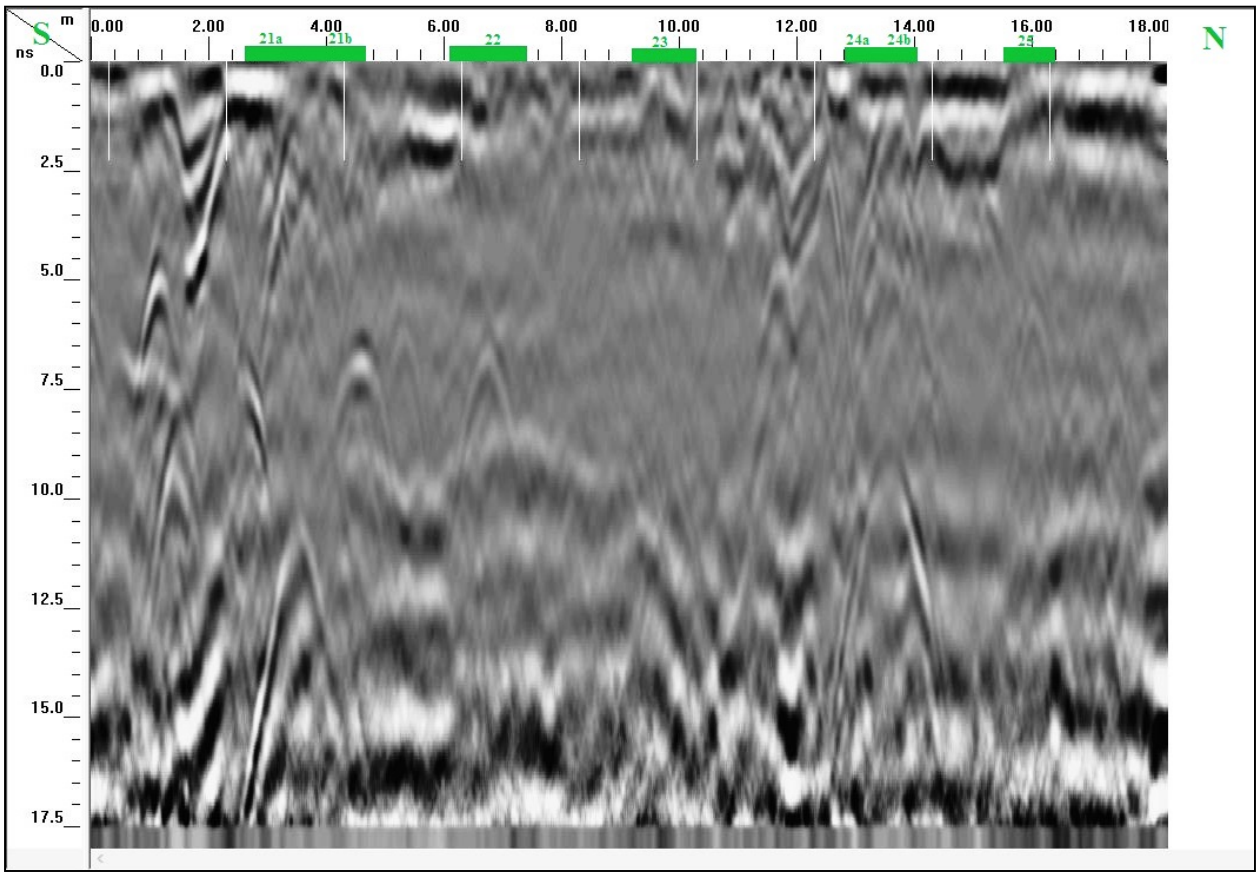

Fig. 4.2.19. GPR data collected with 900MHz antenna along profile no. 13.

4.2.6 Super 3D GPR Survey at Old Carlisle Cemetery:

In order to verify the possibility of the existence of unmarked grave in the northeastern corner of Area 1, where GPR profiles 1 & 2 overlapped (Fig. 4.2.1), a high resolution super 3D survey was conducted. The survey layout was designed using the results of these two profiles separated by 2 meters (6.6 ft).

4.2.7 Data Acquisition:

Prior to data collection, the area under consideration was cleared of heavy bushes and leveled. Due to the restriction of moving the headstones, we were unable to extend the area further than what was surveyed. The super 3D survey was conducted over a grid of 4 x 5 m (13.1 x 16.4 ft) with a line spacing of 0.5 m (1.6 ft) in both X and Y directions resulting in 20 GPR lines (Fig. 4.2.1 & 4.2.20). The data was collected using 400MHz antenna and the tricycle cart. The survey parameters were set as; 512 samples, 16 bit, 40ns range, 50 scans per unit and manual gain control with 3 points.

Fig. 4.2.20. Photo showing the area of the super 3D survey with the grid lines.

4.2.8 Data Interpretation:

The data was processed with RADAN 7 software using the same processing procedure used for the single profiles. Fig. 4.2.21 shows an example of a profile processed with these procedures.

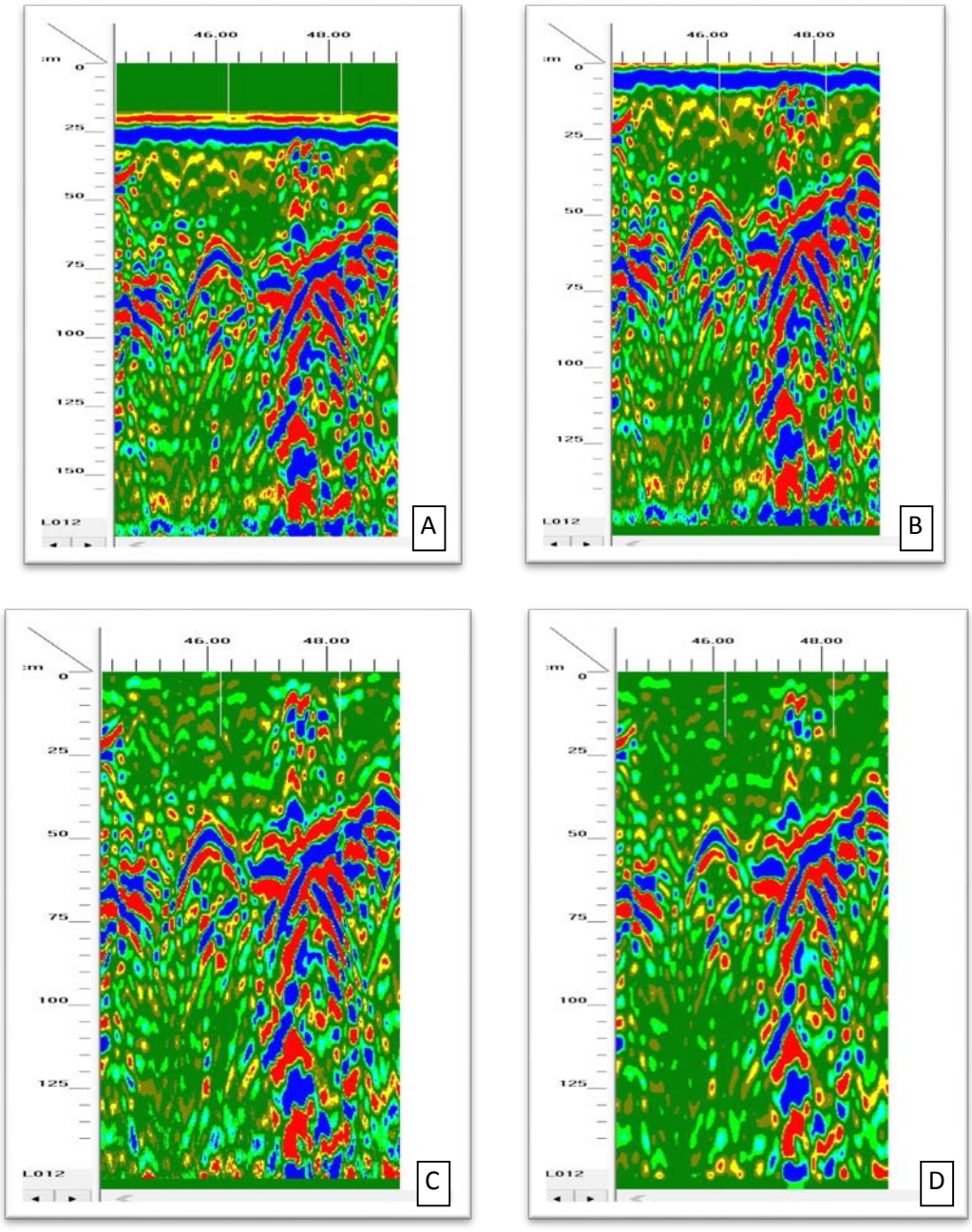

Fig. 4.2.21. Processing procedures applied on file-12; raw data (A), Time Zero corrected (B), Background removed (C) and high & low pass filters applied (D).

4.2.9 Results:

Several iterations of migration procedure on clearly visible hyperbolic reflections resulted the value of 12.04 dielectric constant for this location. Fig. 4.2.22 represents a depth slice of the 3D image of the survey grid at 0.68 m (2.2 ft).

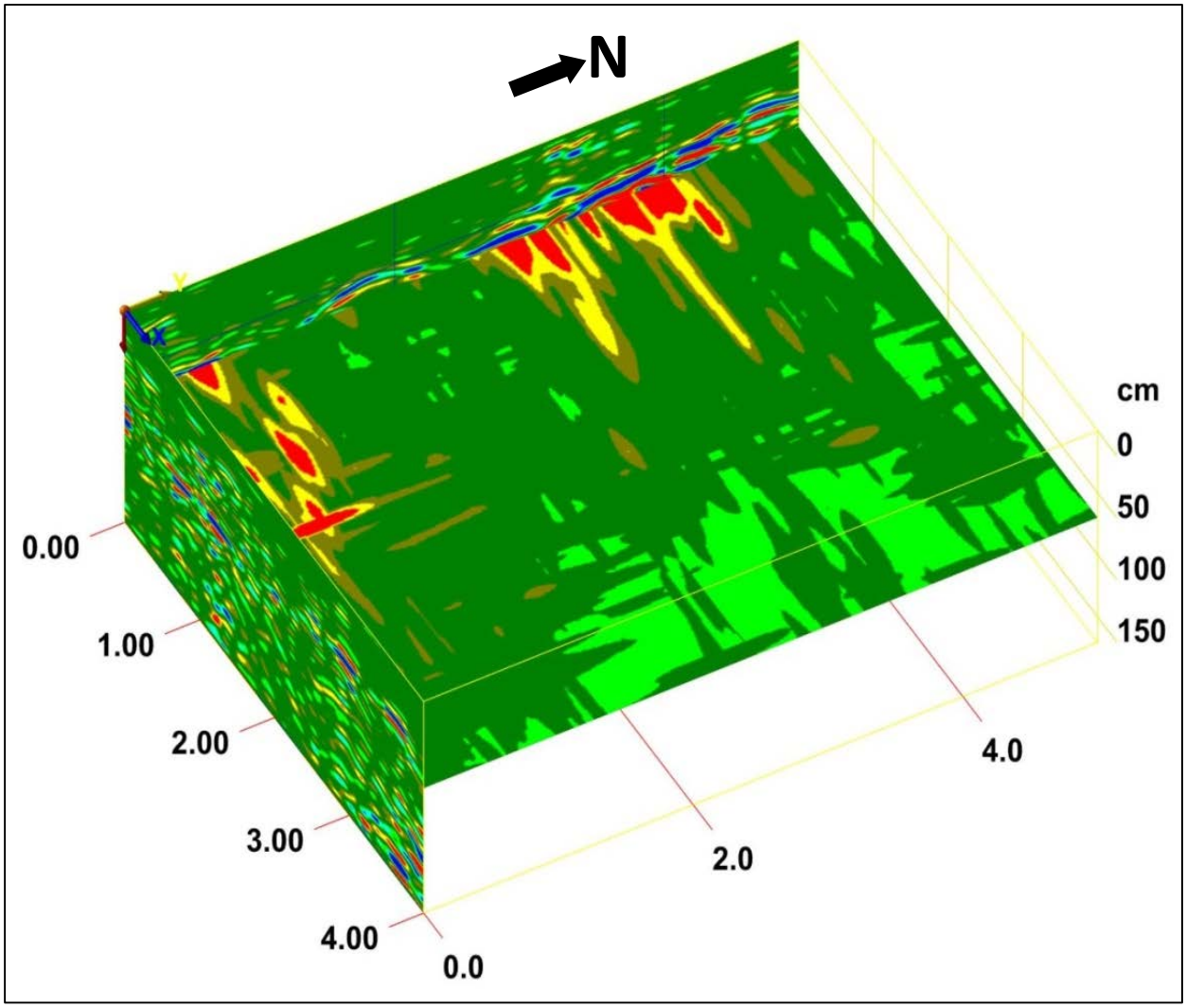

Fig. 4.2.22. 3D image of the grid area 4m X 5m (13.1 X 16.4 ft). Section taken at 68 cm (2.2 ft) depth.

- The 3D image shows a very high energy anomaly at the northwestern part of the surveyed area. A possible cause for this anomaly is the roots of the large tree, which is about 1 meter (3.3 ft) from the grid. Nevertheless, the possibility of having an old grave that may be overrun by tree roots is feasible. Butnor et. al. (2001) used GPR to study tree roots in southeastern USA. They found that orientation and geometry of the reflective surface seemed to have a greater influence on parabola dimensions than did root size. In addition, the multiple reflections of the tree roots are clear on their radar profiles. A similar situation observed in our 2D profile (example file 12 used for Fig. 4.2.21). Other results include:
- In the southwestern part of the 3D area (Fig. 4.2.22), there is another elongated, high energy anomaly, extends from 0.0 to more than 1.0 m (3.3 ft) in the X direction and consistent with the East-West orientation of the graves. This reflection most likely from an unmarked grave.
- Between the two high-energy reflections areas, a well distinguished hyperbolic reflection can be seen along the first two profiles only. This reflection probably from a large buried stone. Individual rocks will usually be visible in only one reflection profile and not on other parallel profiles, unless they are very large (Conyers, 2006).
- Further to the east (along the X direction) between the distances of 2.0 and 3.0 m (6.6 and 9.8 ft), another anomaly is observed and is related to a confirmed grave located immediately next to the GPR profile outside the surveyed area (Fig. 4.2.23).

Fig. 4.2.23 represents an integration of the super 3-D survey interpretation into a photo showing the 3D grid area and indicating the unmarked grave location.

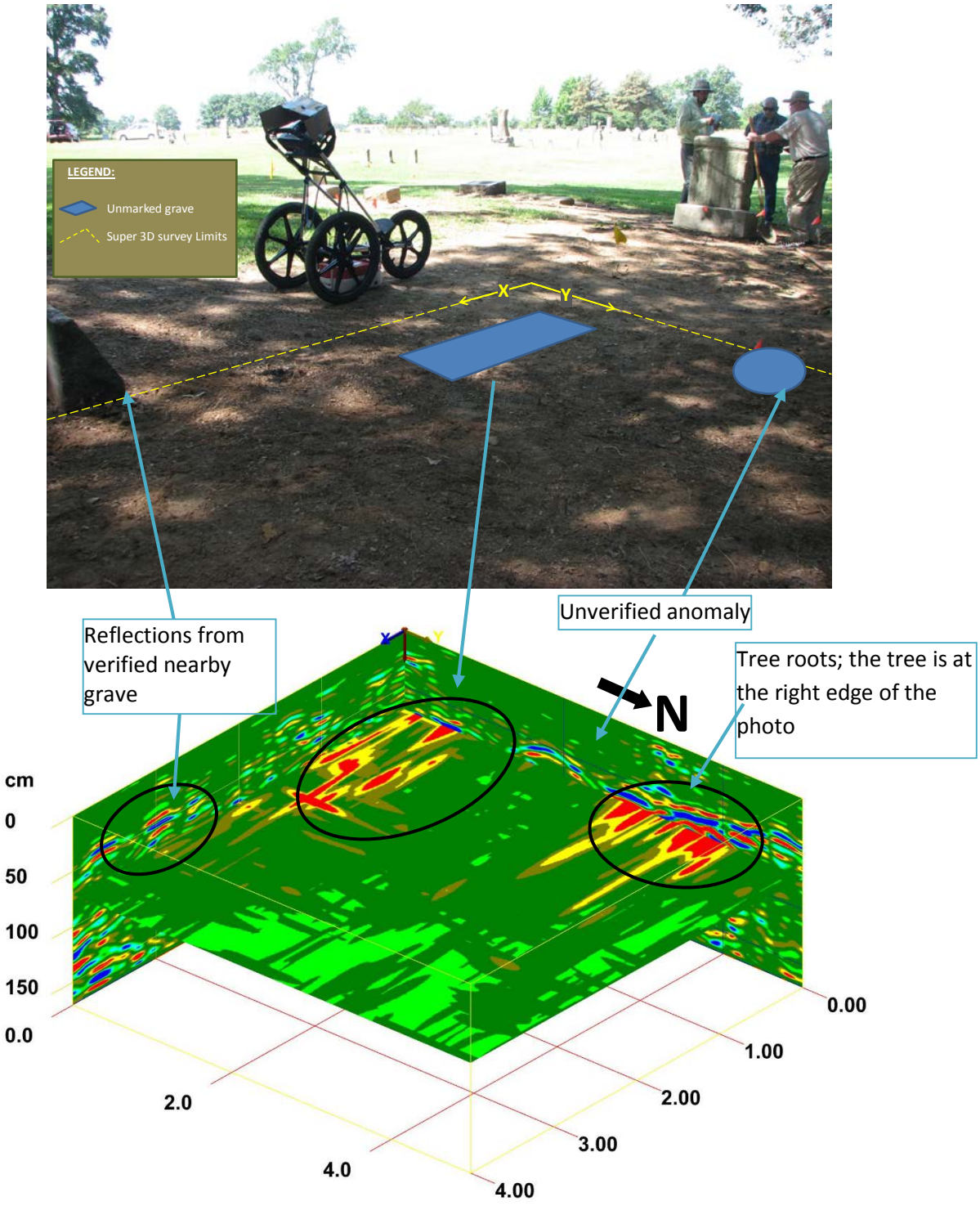

Fig. 4.2.23. Integration of the super 3-D survey interpretation into a photo (viewing SW), showing the 3D grid area and the unmarked grave location.

4.2.10 Summary

GPR is an ideal method for cemetery investigation especially if the clay content of the soil is low. The successful use of GPR to identify burials will depend mainly on the burial nature, the choice of a suitable radar antenna, signal processing techniques, and the subsurface condition of the site. Even under ideal site conditions, some graves will be misidentified, while other features, like tree roots and large rocks within the soil, will be misinterpreted as burials.

GPR survey using the 400 MHz antenna was successful in locating many verified burial sites in addition to locate few unmarked graves and misplaced headstones. The association, in particular, requested to know if there are two adjoining graves that are close to burial site no. 17 (in Area 2) near the east edge of the cemetery. GPR data revealed two clear reflections at depth of about 1.30 m (4.3 ft) and 1.10 m (3.6 ft) and were found to be consistent with the location of a large headstone belongs to burial 17a and 17b. In addition, the northeast corner of the cemetery has been encroached by large trees and private hedge. It is believed that a grave may be outside the cemetery boundary. The association believes there may be unmarked graves in line with burial site no. 10 in Area 1. Family members expect, instead of one, at least three burials at this site; two adults and one baby. GPR data shows one hyperbolic reflection around a depth of 0.85 m (2.8 ft). There are two more hyperbolic reflections around the same location but at a shallower depth of around 0.5 m (1.6 ft). This possibly represent the unmarked graves of the two other burials. According to the family member, this interpretation is feasible since those two were buried during wintertime when the temperature was sub-freezing and they were buried at a shallower depth because of the harsh weather condition then. The head stone of this burial site seems to have shifted at least 1.0 m (3.3 ft) to the south. In addition to these two unmarked graves, the super 3-D survey revealed the existence of two major anomalies, one was interpreted as a possible existence of another unmarked grave in the same area and the other anomaly might represent the large tree roots that were located immediately outside the 3-D survey area.

4.2.11 Acknowledgment

We thank Mr. Melvin Raborn, representative of the Old Carlisle Cemetery Association Inc., his brother Jerry, and Mr. Bob Elder for contacting us with their need of such study. Their help is greatly appreciated.

4.3- Rebar Studies Using the 1.5/1.6 GHz Antenna

4.3.1- Detecting Transvers and Longitudinal Rebar Mesh:

GPR is capable of precisely detect rebar net within concrete. The objective of this lab experiment was to show the ability and accuracy of the 1.5/1.6 GHz GPR antenna to locate complex rebar net under ceramic tiles and concrete for quality assurance. In addition, this antenna can be used in many highway related problems such as in bridge deck assessment process and in studying the reinforcement of bridge decks and bridge columns.

A 1.2 by 1.5 m (3.9 by 4.9 ft) area was exploited in the old earthquake center at UALR (Figure 4.3.1). Eleven lines were delineated in both x and y directions with a 0.3 m (1 ft)-line spacing. SIR-3000 GPR system with 1500 MHz antenna was used to collect data in this area. The following are the parameters that were set up during the survey: For the horizontal parameters; 120 scans per second, 60 scans per foot, and 2 units per mark. For the vertical parameters; 512 samples per scan, 16 bits per sample, and 6 was set as the dielectric constant for concrete. For channel information; 8 ns was set as range. Eleven profiles equivalent to 12.2 m (40 ft)-distance of data were collected; five of them along the x direction and the other six along the y direction. Radan 7 was used to process the collected data. Super 3D data was assembled from profiles collected in both, X and Y directions (Figure 4.3.2). Raw data was processed by applying Time Zero correction and Background Removal. Stacking filter was applied to remove the horizontal-high frequency noise. Moreover, vertical-low and high pass filters were applied to the data. In addition, diffraction was removed by applying migration on the data and dielectric constant for the medium was recalculated as (10) and consequently depth of the rebar was recalculated using this value instead of the default one (8). The 3-D GPR grid can be presented as a number of depth slices or 3-D block diagram. The depth of the displayed block is 0.07 m (0.25 ft). The rebar spacing was 15.8 cm (0.52 ft) along the X direction and 15.2 cm (0.5 ft) along the Y direction. The 3-D grid shows that the rebar net is not horizontal but rather it tilts left towards the manhole.

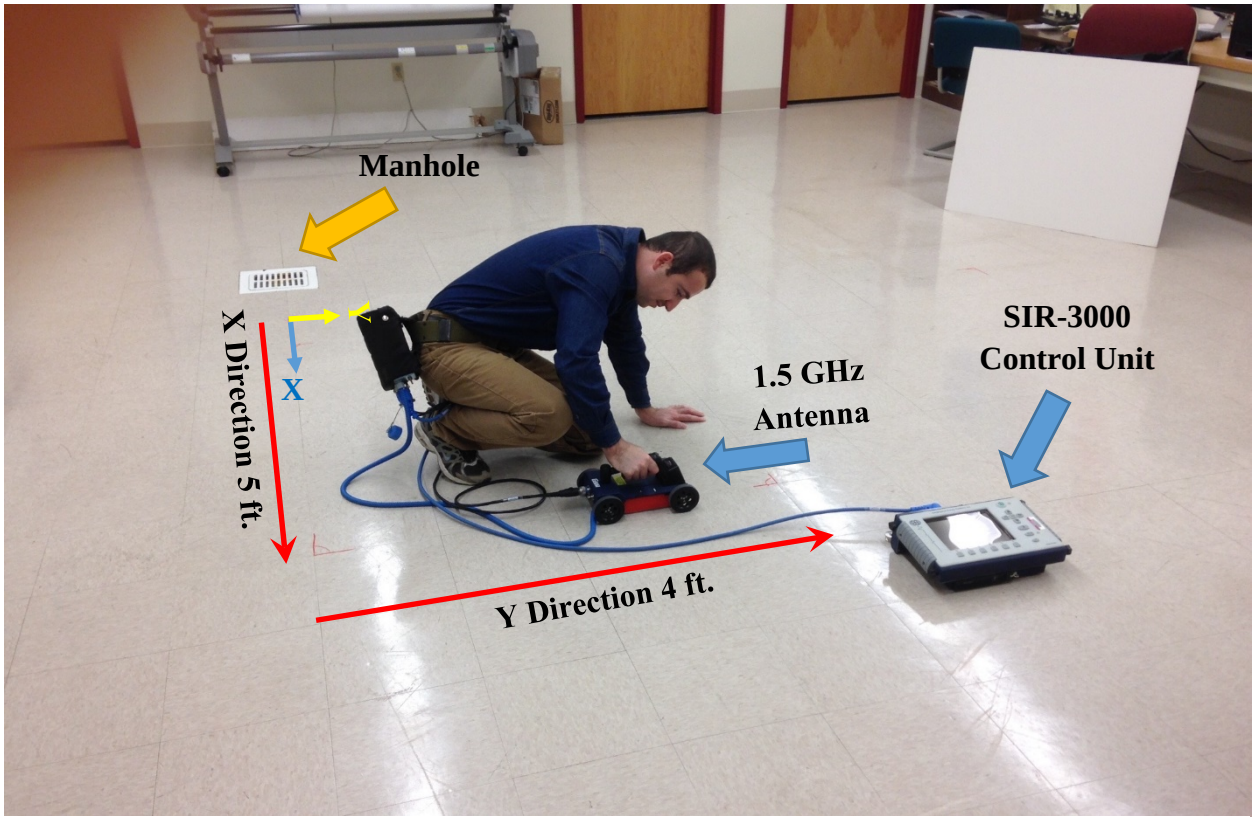

Figure 4.3.1. Picture showing a layout set for 3-D survey

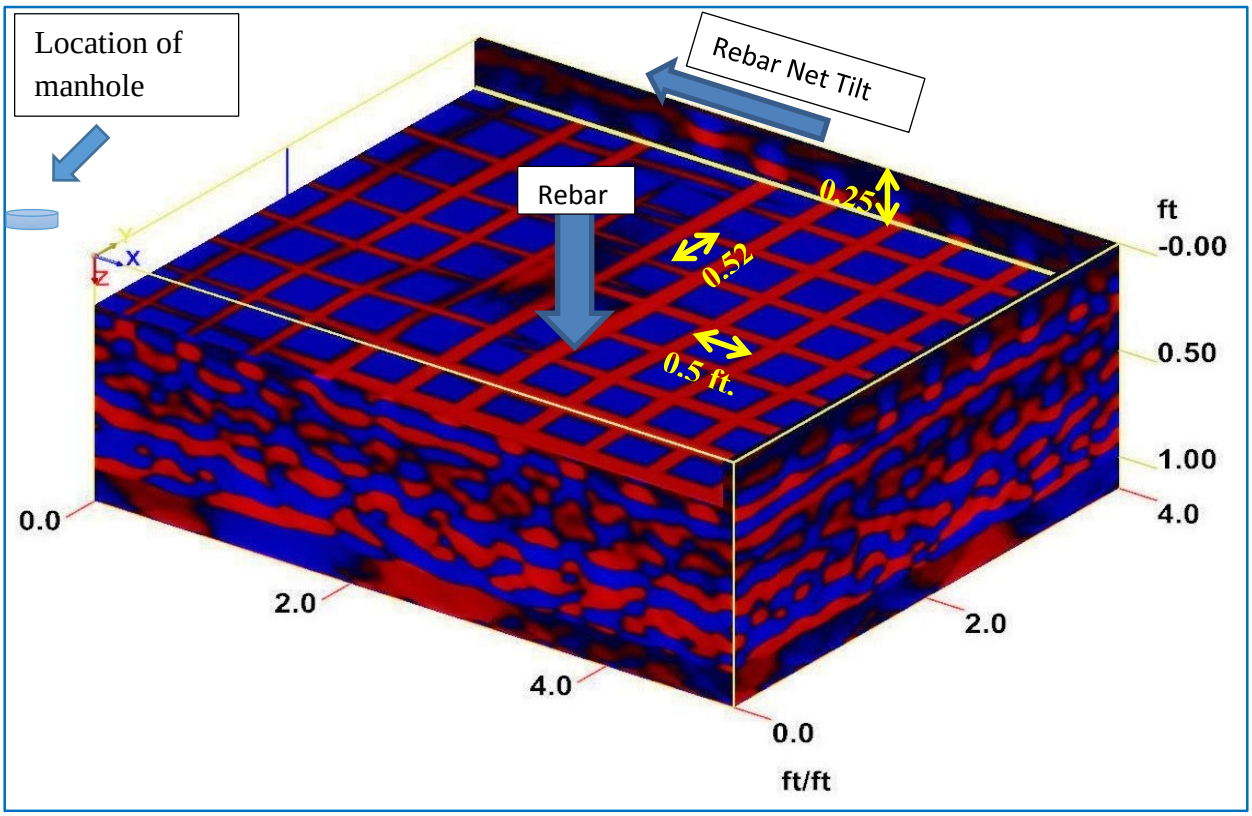

Figure 4.3.2.: 3D-GPR data presentation of rebar net structure

Chapter 5: GPR Equipment Purchase and Training

Based on the results of different fieldwork conducted throughout the course of this project, and our expertise in this field, the P.I. made her recommendation about the needed GPR system to cover a wide spectrum of applications for alternative uses for highway needs. With the approval of the AHTD personnel, UALR purchased the agreed upon system. The decision to purchase GSSI equipment was because the company is one of the top manufacturers of GPR equipment all over the world, if not the largest. In addition, the majority of the U.S. States' DOTs use GSSI equipment for their needs in different highway applications. The geophysics team at UALR has been testing, evaluating, and using GSSI products for more than 15 years. The standard testing and calibration performed before the equipment was delivered to AHTD verified that all system components were functioning according to the manufacturer specifications. Also purchased with the GPR system was the most advanced and up to date version of Radan 7 software, which includes StructureScan, RoadScan, and BridgeScan modules. A workshop at AHTD facilities held on July 7, 2016, provided the required training for the AHTD personnel on the purchased GPR system. Table 5.1 lists all the purchased GSSI GPR equipment that was delivered to the AHTD. **Appendix -2** is a summarized training manual on setting and using the GPR equipment including the GSSI SIR 4000 control unit and the different type of antennas. It also contains a list of dielectric constant values for some of the most common materials. These values range from 1 (for air-high electromagnetic velocity) to 81 (for water- low electromagnetic velocity).

Table 5.1- List of the AHTD GPR equipment items

#	Product	Line Item Description
1	UtilityScan System, SIR 4000, 50400S (400MHz) antenna, 624 cart (3 wheeled cart).	Complete subsurface Locater System, includes: SIR-4000 Advanced Data acquisition System w/ Sunshade, 2 Batteries, Dual Bay Charger, AC Adapter & Transit case; 400 MHz Antenna; 3 wheel survey cart; 2m Antenna Control Cable.
2	200 MHz antenna	200 MHz center frequency antenna. Includes two straps.
3	Survey wheel encoder	Survey wheel encoder assembly with 16” wheel that attaches directly to antenna, for use with 400, 270, and 200 MHz antennas.
4	Antenna Control Cable, 7m	Recommended longer length cable for use with 200 MHz antenna.
5	1.6 GHz Antenna, w/ Smart ID	
6	Handcart	Handcart with built-in encoder for use with 1600 & 2600 antennas. Includes extension handle.
7	Cable for using Model 5100B/5101/52600 antenna in 614/615 cart	Handcart to antenna connection cable. For use with 1600 & 2600 antennas.
8	Antenna Control Cable, 2m, for BridgeScan.	For use with 1600 & 2600 antennas.
9	Cable for using Model 5100B/5101/52600 antenna in 623 cart	Adapter cable to connect 1600 & 2600 MHz antennas to the encoder of 3-wheel and 4-wheel survey cart.
10	SIR 4000 carry harness	Backpack style carry harness for use with SIR-4000 control unit. Allows for hands-free operation during data collection.
11	SIR 4000 stand	Floor stand with adjustable tilt.
12	SMART Li-ION Battery 10.8 V 8265 mAH.	Recommended spare SIR-4000 batteries.

Chapter 6: Conclusion and Recommendation

6.1 Concluding Remarks

GPR is a non-invasive, remote sensing, and easy to use method with the capability of on-site data interpretation. The system can be used as a handheld device, on a survey wheels, or on a vehicle operated with traffic speed. The general rules for a successful GPR outcome depend mainly upon the nature of the target as a reflector to the GPR signal, the choice of suitable radar subsystems (e.g. antenna frequency, data acquisition), and signal processing techniques. Despite these general rules and due to the complexity of near surface earth, it becomes very difficult to guarantee an effective survey but rather each survey is unique in its outcome. To plan for a successful GPR survey one needs to consider the depth of the target relative to the saturation zone of the area and the nature of the surrounding material. A water-saturated soil attenuates GPR signal at a much faster rate than the dry soil. This provides explanation to the inability to detect a target if it is located within the saturation zone. Under such condition, utilities and pipes detection becomes harder to achieve. The contrast in the dielectric properties between the target and the surroundings is another critical factor to any successful results. The survey of Area 3, close to the Clinton Library, reflected the inability of the GPR equipment to detect the buried concrete pipe even with the use of the suitable antenna and survey layout. The moisture content of the ground upper layer also has a crucial role to play in the successful detection of the pipes. In Area 2 on Cantrell, we were unable to detect the two pipes that we were looking for under the grassy unpaved area. However, we were able to detect them under the paved area, as the soil underneath was dryer.

Other findings that worth addressing are:

1- Detection of metal pipes was more successful than concrete or PVC pipes. This was true even when the metal pipe was significantly smaller in diameters than the concrete or PVC pipe. In addition, metal pipe might be detected in a saturated soil while it becomes increasingly difficult to detect PVC or concrete pipes in such conditions.
2- Significant tradeoff observed between antenna frequency, depth of penetration, and target resolution. Higher frequency antenna provides high resolution at shallow depths. GPR signals from such antennas attenuate near the surface and do not penetrate deep. On the contrary, low frequency antenna has low resolution, especially for relatively small target; however, their signals penetrate deeper.
3- It is desirable to collect field data in a raw format and not extensively processed. This will allow operator to reprocess the data in easily interpreted format. Collecting processed data might not allow the operator to reprocess with the desired outcome.

4- It is important that operators follow standard fieldwork procedures by taking detail notes, examining the collected data, checking equipment setup parameters, accurate distance measurement, etc. This will prevent returning to the field to repeat the survey and save money and resources.
5- It is desirable that operators complete the survey of an area within a relatively short period to avoid changes in the soil conditions (e.g. water saturation). Integrating data for the same site at different soil condition is not an easy process in many cases for a feasible interpretation process.

6.2 Recommendation for Future Research

The research project sponsored by the Arkansas Highway and Transportation Department allowed the research team at the University of Arkansas at Little Rock to study the effect of different parameters on GPR readings. In addition, the research team was able to study the possibility of using different devices/antennas on different applications that help AHTD personnel in future project. Additional research is required to cover different engineering/structural applications for future highway construction projects, as listed in the following section:

- Bridge deck evaluation

The bridge deck condition in the State of Arkansas, and on a national level, needs to be evaluated for possible deterioration. Bridge decks in the State of Arkansas are susceptible to damage due to the multiple freeze-thaw cycles acting on bridge decks, and the higher traffic volumes resulting in abrasion of surface layers of bridge decks. Major bridge deterioration was noticed on the bottom fibers of bridge decks poured using stay-in-place metal forms (SIPMF) due to the inaccessibility of bridge inspectors to the slab bottom fibers. GPR technology is required to be used, in addition to other non-destructive testing techniques, to evaluate the bridge deck conditions and decide on further maintenance.

- Alkali-Silica reactivity

The alkali-silica reactivity represents a major problem resulting in concrete projects deterioration without the application of any external stresses. Alkali-silica reactivity results in a white gel-like expansive material within the concrete that presents an internal pressure that leads to concrete cracking. In today's application, ASR is confirmed through destructive petrographic testing of suspected concrete specimens. GPR, as a non-destructive technique, may be used in detecting ASR through the detection of the expansive gel-like material that has different properties than concrete. GPR can be a fast, non-laborious, and user-friendly technique in ASR detection.

- **Conditions of reinforcing steel**

Reinforcing steel corrosion is a major factor in deteriorating infrastructure projects in the United States. Corrosion of steel can be initiated by minor corrosion within steel bars prior to their incorporation in the project, and increases under the chloride and sulfate attacks acting on reinforced concrete section from the surrounding environment. Environmental attacks may be attributed to the presence of salty sea or oceans in the neighborhood of the project; In addition to the potential attacks from the chlorides in the underground water table. In the northern states, chlorides attacks the concrete as a result of the use of deicing salts. The steel rebars, upon corrosion, has a smaller diameter that structurally support the concrete section, which results in a minimized strength for the section, and may lead to structural sudden failure during the service life of the structure.

Currently, destructive test methods are mainly used in detection of corrosion through core drilling and visual inspection of steel reinforcing bars. The core drilling process is laborious, and costly. GPR may be used in detecting corrosion, and its amplitude, and location by interpreting the GPR signal and evaluating the difference in signal when corrosion is encountered as compared to regular steel bars. The use of GPR technique may allow the concrete inspectors to locate the places where corrosion exists, and the extent of the corrosion, hence, determine the appropriate maintenance required to reduce the deterioration of the structural member, hence increase the life span of the structure.

Acknowledgments

This work was sponsored by the Arkansas Highway and Transportation Department to identify the best GPR equipment required to perform construction projects funded by the AHTD. The authors would like to thank the AHTD research division for their generous financial and technical support. The authors would like to acknowledge graduate students Rauf Hussein and Taher H. Ameen who presented a significant support and help to the work during the course of this project. Thanks also go to Dr. Mert Su who worked on the project as a Post-Doctoral Fellow for four and a half months.

References and Bibliography

Al-Qaser, G. N. (1991). *Progressive Failure of an Overtopped Embankment* (Unpublished doctoral dissertation). Colorado State University, Colorado.

Al-Shukri, H., Mahdi H., & Al Kadi O. (2006). *Application of Ground Penetrating Radar for near surface geology*. Geophysics, Highway Transportation Meeting, St. Louis, MO.

Anderson, N.L., and S. Cardimona. (2000). Evaluating the Utility of Geophysical Surveying Methods. Federal Highway Administration and Missouri Department of Transportation special publication. MoDOT web site.

Anderson, R. C., Buehler, M. G., Seshardri, S., & Schaap, M. G. (2004). *Dielectric Constant Measurements on Lunar Soils and Terrestrial Minerals*. Space Resources Roundtable VI (p. 7). Colorado USA: Colorado school of mines.

Annan, A. P. (2001). *Ground Penetrating Radar*. Workshop Notes. Canada: Sensors & Software Inc.

Annan, A. P., Cosway, S. W. (1992). Ground penetrating radar survey design. *Proceedings of the Symposium on the Application of Geophysics to Engineering and Environmental Problems, SAGEEP'92* (pp. 329–351). Illinois: Oakboro.

Asch, T. H., Deszcz-Pan, M., Burton, B. L., and Ball, L. B. (2008). *Geophysical characterization of American River levees, Sacramento, California, using electromagnetic, Capacitively coupled resistivity, and dc resistivity* (Open-File Report 2008–1109). U.S. Geological Survey.

Belesky, R. M., Hardy, H. R. Jr., Dr. (1986). Seismic and microseismic methods for cavity detection and stability monitoring of near-surface voids. *Proceedings of the 27th US Symposium on Rock Mechanics: Key to Energy Production* (pp. 248-258). Alabama: University of Alabama.

Benedetto, A., & Pensa, S. (2007). Indirect diagnosis of pavement structural damages using surface GPR reflection techniques. *Journal of Applied Geophysics*, *62*(2), 107–123. doi: 10.1016/j.jappgeo.2006.09.001

Bevan B., Kenyon, J. (1975). Ground-Penetrating Radar for Historical Archaeology. MASCA Newsletter, 11(2), 2-17.

Bevan, B. W. (1991). The search for graves. Geophysics, 56(9), 1310-1319.

Bigma, D. P. (2014). Mapping social relationships: geophysical survey of a nineteenth-century American slave cemetery. Archaeological and Anthropological Sciences, 6(1), 17-30.

Bladon P., Moffat, I., Guilfoyle, D., Beale, A., Milani, J. (2011). Mapping anthropogenic fill with GPR for unmarked grave detection: a case study from a possible location of Mokare's grave, Albany, Western Australia. Exploration Geophysics, 42(4), 249-257.

Boryssenko, A. (1999). In M. Meng (Ed.) Subsurface radar imaging of underground archeological objects in Kyiv Petcherskaja Lavra, Kyiv, Ukraine. *Engineering Solutions for the Next Millennium- Proceedings of the 1999 IEEE Canadian conference on electrical and computer engineering* (vol. 2, pp.855-860). Edmonton, Alberta, Canada. doi: 10.1109/CCECE.1999.808090

Brenton, A. L., Drale, C. S., Craw, R. (2005). *Down by the riverside where vital public goals converge.* A report by the College of Professional Studies and the Center for Public Conflict Solutions. Arkansas: University of Arkansas at Little Rock.

Bristow, C.S. & Jol, H.M. (Eds). (2003). *Ground penetrating radar in sediments*. The Geological Society, London.

Burger, H. R., Sheehan, A. F., and Jones C. H. (2006). *Introduction to Applied geophysics: Exploring the Shallow Subsurface*. New York: W. W. Norton & Company, Inc.

Butler, D. K. (1984). Microgravimetric and gravity gradient techniques for detection of subsurface cavities. *Geophysics*, *49*(7), 1084-1096. doi: 10.1190/1.1441723

Butler, J., Roper, T. J., & Clark, A. J. (1994). Investigation of badger (Meles meles) setts using soil resistivity measurements. *Journal of Zoology*, *232*(3), 409–418. doi: 10.1111/j.1469-7998.1994.tb01582.x

Butnor J. R., Doolittle, J. A., Kress, L., Cohen, S., Johnsen, K. H. (2001). Use of ground-penetrating radar to study tree roots in the southeastern United States. Tree Physiology, 21(17), 1269-1278.

Cardarelli, E., Cercato, M., Cerreto, A., & Di Filippo, G. (2010). Electrical resistivity and seismic refraction tomography to detect buried cavities. *Geophysical prospecting*, *58*(5), 685-695. doi: 10.1111/j.1365-2478.2009.00854.x

Cardimona, S. (2002) *Electrical resistivity techniques for subsurface investigation*. Paper presents at the 2nd Annual Conference on the Application of Geophysical and NDT Methodologies to Transportation Facilities and Infrastructure. Los Angeles, CA.

Carrol, P. H. (1949). *Soil piping in south-east Arizona*. U.S.D.A. Soil Conserv. Serv., Region 5, Bull. 110, Soil Ser. 13.

Chamberlain, A. T., Sellers, W., Proctor, C., Coard, R. (2000). Cave Detection in Limestone using Ground Penetrating Radar. *Journal of Archaeological Science*, *27*, 957–964. doi:10.1006/jasc.1999.0525

Chen, D. H., Wimsatt, A. (2010). Inspection and condition assessment using ground penetrating radar. *Journal of Geotechnical and Geoenvironmental Engineering*, *136*(1), 207-214. doi: 10.1061/_ASCE_GT.1943-5606.0000190

Chlaib, H. K., Mahdi, H., Al-Shukri, H., Su, M. M., Catakli, A. & Abd, N. (2013). Levee evaluation with ground-penetrating radar. *Changing times-the challenges and risks of managing aging infrastructure under a new financial reality*, *The 33th USSD conference, Phoenix Arizona, USA*, 30-45.

Chlaib, H. K., Mahdi, H., Al-Shukri, H., Su, M. M., Catakli, A., & Abd, N. (2014). Using ground penetrating radar in levee assessment to detect small scale animal burrows. Journal of Applied Geophysics, 103, 121-131.

Chlaib, H. K., Su, M., Abd, N., Catakli, A., Mahdi, H., Al-Shukri H. (2014). Detection of weakness zones in Helena levee using Ground Penetrating Radar, 34th United States Society on Dams (USSD) Annual Meeting and Conference, San Francisco, CA, pp. 1015-1029.

Conyers, L. B. (2004). Moisture and soil differences as related to the spatial accuracy of GPR amplitude maps at two archaeological test sites. *Tenth International Conference on Ground Penetrating Radar* (1-5). Delfa, The Netherlands.

Conyers, L. B. (2006). Ground-penetrating radar techniques to discover and map historic graves. Historical Archaeology 40, 64-73.

Damiata, B. N., Steinberg, J. M., Bolender, D. J., Zoëga, G. (2013). Imaging skeletal remains with ground-penetrating radar: comparative results over two graves from Viking Age and Medieval churchyards on the Stóra-Seyla farm, northern Iceland. Journal of Archaeological Science, 40(1), 268-278.

Daniels, D. J. (2004). *Ground Penetrating Radar* (2nd ed.). Institution of Engineering and Technology.

Daniels, D. J. (2004). Ground penetrating radar-2nd ed. IEE, UK, 734 P.

Daniels, J. J. (2000). *Ground Penetrating Radar Fundamentals*. The U.S.EPA, Region V. 21.

Daniels, J. J., Roberts, R., & Vendl, M. (1995). Ground Penetrating Radar for the detection of liquid contaminants. *Journal of Applied Geophysics*, *33*(1–3), 195–207. doi: 10.1016/0926-9851(95)90041-1

Davis, J. L. & Annan, A. B. (1989). Ground penetrating radar for high-resolution mapping of soil and rock stratigraphy. *Geophysical prospecting*, *37*, 531-551. doi: 10.1111/j.1365-2478.1989.tb02221.x

Davis, J. L., Annan, A. P. (1989). Ground-penetrating radar for high-resolution mapping of soil and rock stratigraphy. Geophysical prospecting, 37(5), 531-551.

Department of Water Resources. (2008)... *Levee evaluation program, Levee analysis methods* [Brochure]. Sacramento, CA: Scott, E.

Di Prinzio, M., Bittellib, M., Castellarin, A., & Pisa, P. R. (2010). Application of GPR to the monitoring of river embankments. *Journal of Applied Geophysics*, *71*(2–3), 53–61. doi:10.1016/j.jappgeo.2010.04.002

Dionne, C. A., Wardlaw, D. k., Schultz, J. J. (2010). Delineation and resolution of cemetery graves using a conductivity meter and ground-penetrating radar. Technical Briefs in historical archaeology, 5: 20-30.

Do, J. (2003). *Ground penetrating radar*. Villanova University, Villanova, USA.

Dodge, R. A. (1988). *Overtopping flow on low embankment dams*. (Report No. REC-ERC-88-3) USA: U.S. Bureau of Reclamation.

Doolittle, J. A., Bellantoni, N. F. (2010). The search for graves with ground-penetrating radar in Connecticut. Journal of Archaeological Science, 37(5), 941-949.

El Fouly, A. (2000). Voids investigation at Gabbari Tombs, Alexandria, Egypt using ground penetrating radar technique. *ICEHM,* 84- 90.

Eyuboglu, S. (2005). *Ground Penetrating Radar: A Tool for Environmental and Geotechnical Applications* (Unpublished doctoral dissertation). University of Arkansas at Little Rock, Arkansas.

Fish, M., Richard, L. (2002). *Enhancing geotechnical information with Ground Penetrating Radar*. USA: New Hampshire Department of Transportation Bureau of Materials and Research.

Francke, J., Utsi, V. (2009). Advances in long-range GPR systems and their applications to mineral exploration, geotechnical and static correction problems. *First break*, *27*(7), 85-93.

Fullagar, P. K., Livelybrooks, D. (1994). Trial of tunnel radar for cavity and ore detection in the Sudbury mining camp, Ontario. *Proceedings of the fifth International Conference on Ground Penetrating Radar*. Canada, *3*, 883-894.

Geometrics. (2001). *OhmMapper TR1 operation manual*. USA.

Geophysical Survey Systems, Inc. (2009). *RADAN 6.6 User's manual*. USA.

Geophysical Survey Systems, Inc. (2011). *RADAN 7 User's manual*. USA.

Geophysical Survey Systems, Inc. (2011). *SIR System-30 User's manual*. USA.

Geophysical Survey Systems, Inc. (2011). *SIR System-3000 User's manual*. USA.

Gillip, J. A., Payne, J. D. (2011). *Geophysical characterization of the Lollie Levee near Conway, Arkansas, using capacitively coupled resistivity, coring, and direct push logging*. USA: U.S. Geological Survey.

Gizzi, F. T., Loperte, A., Satriani, A., Lapenna, V., Masini, N., & Proto, M. (2010). Georadar investigations to detect cavities in a historical town damaged by an earthquake of the past. *Advances in geosciences*, *24*, 15–21.

Golebiowski, T. (2010). Velocity analysis in the GPR method for loose-zones detection in the river embankments. *13th International Conference on Ground Penetrating Radar (GPR). Poland*, 1-6. doi: 10.1109/ICGPR.2010.5550220

Goodwin, B.T. (2014). Bridge Deck Condition Assessment using Destructive and Non-Destructive Methods. A Thesis, submitted to Missouri Science and Technology University, Rolla, Missouri.

Grandjean, G., Gourry J.C., & Bitri, A. (2000). Evaluation of GPR techniques for civil-engineering applications: study on a test site. *Journal of Applied Geophysics*, *45*(3), 141–156.

Gunn, D., Hirnyck, R., Shewmaker, G., Takatori, S., Ellis, L. (2011). *Meadow Voles and Pocket Gophers: Management in Lawns, Gardens, and Cropland*. (PNW 627). USA: Idaho Commission for libraries.

Hickin, A. S., Kerr, B., Barchyn, T. E., Paulen, R. C. (2009). Using ground-penetrating radar and capacitively coupled resistivity to investigate 3-D fluvial architecture and grain-size distribution of a gravel floodplain in northeast British Columbia, Canada. *Journal of Sedimentary Research*, *79*(6), 457–477. doi: 10.2110/jsr.2009.044

Hyndman, D. & Tronicke J. (2005). Hydrogeophysical Case Studies at the Local Scale: The Saturated Zone. In Y. Rubin, S. Hubbard (Eds), *Hydrogeophysics* (pp. 391-412). New York, NY, Springer. doi: 10.1007/1-4020-3102-5.

Inazaki, T. (2007). Integrated geophysical investigation for the vulnerability assessment of earthen levee, *Proceedings of the 20th Annual Symposium on the Application of Geophysics to Engineering and Environmental Problems (SAGEEP2007)*, *USA*, *1*, 90-97.

Iowa State University (2009). *Managing Iowa Wildlife Pocket Gophers*. PM 1302A. USA.

Johnson, W. J. (2003). Geophysical Detection of Graves–Basic Background and Case Histories from Historic Cemeteries. Council for West Virginia Archaeology Spring Workshop Charleston, West Virginia June 7, 2003.

Jol, H. M. (2009). *Ground Penetrating Radar: Theory and Applications*, Elsevier.

Jones, G. (2008). Geophysical mapping of historic cemeteries. Technical Briefs in Historical Archaeology, 3, 25-38.

Kinlaw, A., Conyers, L. B., & Zajac, W. (2007). Use of ground penetrating radar to image burrows of the gopher tortoise (Gopherus Polyphemus). *Herpetological Review*, *38*(1), 50-56.

Kirsch, R. (2006). *Groundwater Geophysics A Tool for Hydrogeology*. Springer Berlin, Heidelberg, New York.

Knight J. E. (2000). *Guide to Pocket Gopher Control in Montana*. USA: Montana State University-Bozeman.

Knight, J. E. (2005). *Controlling Pocket Gophers in New Mexico*. Guide L-109. USA: New Mexico State University.

Kowalsky, M. B., Finsterle S., Rubin Y. (2004). Estimating flow parameter distributions using ground-penetrating radar and hydrological measurements during transient flow in the vadose zone. *Advances in Water Resources*, *27*, 583–599. doi: 10.1016/j.advwatres.2004.03.003

Lambot, S., Bosch, I. V. D., Slob, E. C. (2004). Frequency domain GPR signal forward and inverse modelling for identifying the subsurface dielectric properties. *European Association of Remote Sensing Laboratories (EARSeL) eProceedings*, France, *3*(3), 398-404.

Llopis, J. L. and Simms, J. E. (2007). *Geophysical Surveys for Assessing Levee Foundation Conditions, Feather River Levees, Marysville/Yuba City, California*. ERDC/GSL TR-07-25. USA: U.S. Army Corps of Engineers.

Loeffler, O. and Bano M. (2004). Ground Penetrating Radar Measurements in a Controlled Vadose Zone: Influence of the Water Content. *Vadose Zone Journal*, *3*(4), 1082-1092. doi:10.2113/3.4.1082

Loke, M. H. (2004). *Tutorial: 2-D and 3-D electrical imaging surveys*.

Loken, M. (2007). *Use of Ground Penetrating Radar to evaluate Minnesota roads*. USA: Minnesota Department of Transportation.

Lu, Q. and Sato, M. (2007). Estimation of Hydraulic Property of an Unconfined Aquifer by GPR. *Sensing and Imaging*, *8*(2), 83-99. doi: 10.1007/s11220-007-0035-x

Maerz , N. H., Kim, W. (2000). Potential use of Ground Penetrating Radar in highway rock cut stability. *Geophysics*, 1-9.

Maharaj, A. and Leyland, R. (2010). The dielectric constant as a means of assessing the properties of road construction materials. *Proceedings of the 29th southern African transport conference (SATC)*, South Africa, 487-498.

Manenti, R. R., Williams, K. K. (2015). Using Ground Penetrating Radar to Locate Historical Graves in Western New York. SBGf - Sociedade Brasileira de Geofísica. This paper was prepared for presentation during the 14th International Congress of the Brazilian Geophysical Society held in Rio de Janeiro, Brazil, August 3-6, 2015. http://www.researchgate.net/publication/277195392

Masannat, Y. M. (1980). Development of piping erosion conditions in the Benson area, Arizona, U.S.A. *Quarterly Journal of Engineering Geology and Hydrogeology*, *13*, 53-61.

Mellett, J. S. (1995). Ground Penetrating Radar applications in engineering, environmental management, and geology. *Journal of Applied Geophysics*, *33*(1–3), 157–166.

Miele, M., Flemmer, J., Dobecki, T., and Lightner, M. (2009). Synergistic geophysical techniques for assessing seepage pathways in earthen levees. *Proceedings of the 22th Annual Symposium on the Application of Geophysics to Engineering and Environmental* Problems (SAGEEP 22), *USA*, *22*(1), 135-143.

Milsom, J. (2003). *Field geophysics* (3rd ed.). Chichester: John Wiley and Sons.

Mochales, T., Casas, A. M, Pueyo, E. L., Pueyo, O., Roman, M. T., Pocove, A., Soriano, M. A., Anson, D. (2008). Detection of underground cavities by combining gravity, magnetic and ground penetrating radar surveys: a case study from the Zaragoza area, NE Spain. *Environmental Geology*, *53*, 1067–1077. doi: 10.1007/s00254-007-0733-7

Morey, R. M. (1998). Ground Penetrating Radar for Evaluating Subsurface Conditions for Transportation Facilities. Washington, D. C: Transportation Research Board, 1998. Print.

Nichol, D., Lenham, J. W., and Reynola, J. M. (2003). Application of ground –penetrating radar to investigate the effects of badger setts on slope stability at St Asaph Bypass, North Wales. Quarterly Journal of Engineering Geology and Hydrogeology, *36*, 143–153. doi: 10.1144/1470-9236/2002-42

Nuzzo, L. (2004). The contribution of GPR to investigate damages in the crypt of the cathedral of otranto (Apulia, Italy). *Proceedings of the Tenth International Conference on Ground Penetrating Radar*; The Netherlands, *1*, 479-482.

O'Brien J. M. (1994). Voles. In S. E. Hygnstrom, R. M. Timm, G. E. Larson (Eds), *The Handbook: Prevention and Control of Wildlife Damage* (pp. B-177-B-182).

O'Conner, J. E. and Costa, J. E. (2004). *The World's Largest Floods, past and present – Their causes and magnitudes*. US Geological Survey Circular 1254.

Olhoeft, G. R. (1998). Electrical, magnetic, and geometric properties that determine ground penetratingn radar performance. *Proceedings of the Seventh International Conference on Ground- Penetrating Radar, USA*, 177–182.

Olhoeft, G. R. (2003). Electromagnetic field and material properties in ground penetrating radar. *Proceedings of the 2nd international workshop on advanced GPR, The Netherlands*, 144-147. doi: 10.1109/AGPR.2003.1207309nubjn

Olhofet, G. R. and Strangway, D. W. (1975). Dielectric properties of the first 100 meters of the Moon. Earth and Planetary Science Letters, *24*, 394-404. doi: 10.1016/0012-821X(75)90146-6

Parkhomenko, E. I. (1967). *Electrical Properties of Rocks*. Plenum, New York.

Persico, R. (2014). Introduction to GPR Prospecting. Introduction to Ground Penetrating Radar: Inverse Scattering and Data Processing. First ed. Hobcken: Wiley, 2014. 392. Print.

Peters, L., Jr., L. P., Daniels J. J., Young, J. D. (1994). Ground Penetrating Radar as a Subsurface Environmental Sensing Tool. *Proceedings of the IEEE*, *82*(12), 1802-1822. doi: 10.1109/5.338072

Pîrnău, R. G., Mihu-Pintilie, A., Bodi, G., Asăndulesei, A., Niacșu, L. (2014). Ground Penetrating Radar as noninvasive method used in Soil Science and Archaeology. Journal of Soil Forming Factors and Processes from the Temperate Zone, 13(1), 15-32.

Prinzio, M. D., Bittellib M., Castellarin A., Pisa, P. R. (2010). Application of GPR to the monitoring of river embankments. *Journal of Applied Geophysics*, *71*, (2–3), 53–61. doi: 10.1016/j.jappgeo.2010.04.002

Rao, D. S. P., Kumar, V. S. S., Kishore, R., & Bhikshma, V. (2007). Ground penetrating radar and its applications in civil engineering. *The Indian Concrete Journal*, 35-40.

RDADN 7 Manual (2015). Geophysical Survey Systems, INC. MN43-199 rev F, 02.20.2015.

Reynolds, J.M. (1998). *An introduction to applied and environmental geophysics*. Wiley, New York.

Richards, K. S., & Reddy, K. R. (2010). New Approach to Assess Piping Potential in Earth Dams and Levees. *ASCE NEWS*, 51(6), pp.A1, A4, A5, andA10.

Riley, P. and William Johnson, B. J. (2004). Historic hill cemetery – does it contain remains of general Anthony Wayne's Cantonment at Legion Ville?. *Proceeding of The Society for Pennsylvania Archaeology, 75th Annual Meeting, USA*, 9 pages.

Risk Management Solutions. (2007). *The 1927 Great Mississippi Flood: An 80 Year Retrospective*. Available from www.rms.com/Publications/1927_MississippiFlood.pdf.Internet; accessed 28 September 2012.

Rister, B., Graves, C., & Creech, J. (2008*). Investigation of the extended use of ground penetrating radar (GPR) for measuring in-situ material quality characteristics*. (KTC-08-31/SPR307-05-1F). Kentucky Transportation Center. University of Kentucky.

Saintenoy, A., Schneider, S., & and Tucholka, P. (2008). Evaluating ground penetrating radar use for water infiltration monitoring. *Vadose Zone Journal*, *7*(1), 208-214. doi: 10.2136/vzj2007.0132

Salmon, T. P and Baldwin, R. A. (2009). *Pocket Gophers Integrated Pest Management for Home Gardeners and Landscape Professionals*. PEST NOTES Publication 7433University of California Statewide Integrated Pest Management Program Agriculture and Natural Resources.

Sato, M. (2001). GPR and its application to environmental study, center for Northeast Asian studies (CNEAS) Tohoku University, Japan.17 pages. In http://cobalt.cneas.tohoku.ac.jp/users/sato/.

Schneider, J. B. (2013). *Understanding the Finite-Difference Time-Domain Method*.

Schultz, J. J., Martin, M. M. (2012). Monitoring controlled graves representing common burial scenarios with ground penetrating radar. Journal of Applied Geophysics, 83, 74-89.

Schultz, J.J. (2012). Detecting Buried Remains Using Ground-Penetrating Radar. Report, Submitted to the National Institute of Justice, Office of Justice Programs, U.S. Department of Justice.

Scullion, T., & Timo S. (1998). Applications of Ground Penetrating Radar technology for network and project level pavement management systems. *Proceedings of the 4th International Conference on Managing Pavements 17th-21th May 1998, Durban, South Africa*, 18 pages.

Shao, W. (2013). Radar Signal Representation and Classification. Thesis, submitted to University of Wollongong.

Stevens® Water Monitoring System, Inc. (2007). *POGO quick start instructions*. StevensS Water Monitoring.

Stott, P. (1996). Ground-penetrating radar: a technique for investigating the burrow structure of fossorial vertebrates. *Wildlife Research*, *23*(5), 519–530. doi: 10.1071/WR9960519

Strangway, D. W., & Olhoeft, G. R. (1977). The Moon; Electrical Properties of Planetary Surfaces, A new appraisal from space missions and laboratory analysis. *Philosophical Transactions of the Royal Society of London*, 285(Series A), 441-450.

Strangway, D. W., Pearce, G. W., & Olhoeft, G.R. (1977). Magnetic and dielectric properties of lunar samples. In Pometory, J. H., & Hubbard, N. J. (Eds.), *The Soviet-American Conference on Cosmochemistry of the Moon and planets* (pp. 417-433). NASA SP-370, Washington.

Su, M. M. (2013). *Identification and estimation of concentration of metal bearing minerals in lunar soil using ground penetrating radar* (Unpublished doctoral dissertation). University of Arkansas at Little Rock, Arkansas.

Sutinen, R. (1992). Glacial deposits, their electrical properties and surveying by image interpretation and ground penetrating radar. *Bulletin of the Geological Survey of Finland, 359*, 1-123.

Szymczyk, M., & Szymczyk, P. (2013). Preprocessing of GPR data. Image Processing & Communications, 18(2-3), 83-90.

Tarver, G., Bigman, D. P. (2013). Preservation of McVicker Family Cemetery, Jonesboro, Georgia. Early Georgia, 41(2): 211–242.

The Federal Emergency Management Agency (FEMA), Department of Homeland Security. (2006). *Emergency Management and Assistance*, Title 44, V. 1.

Thieme, D. M. (2013). Identification of unmarked graves at two historic cemeteries in Georgia. Early Georgia, 41(2), 257-274.

Travassos, J. d. M. & Menezes P. D. T. L. (2004). GPR exploration for groundwater in a crystalline rock terrain. *Journal of Applied Geophysics*, *55*, 239-248. doi:10.1016/j.jappgeo.2004.01.001

Trigwell, S., Starnes, J., Brown, C., White, C., White, T., Su, M.; Mahdi, H. H., Al-Shukri, H. J., Biris, A. (2010). Measurement of the dielectric constant of lunar minerals and regolith. *American Geophysical Union, fall meeting*, abstract #P53A-1504. Abstract retrieved from The Smithsonian/NASA Astrophysics Data System.

Tsoflias, G. P., & Matthew, W. B. (2008). Ground-penetrating-radar response to fracture-fluid salinity: Why lower frequencies are favorable for resolving salinity changes. *Geophysics*, *73*(5), J25–J30. doi: 10.1190/1.2957893

U.S. Department of Commerce, National Oceanic & Atmospheric Adminstration (NOAA), NOAA Central Library. (2012). http://www.photolib.noaa.gov/htmls/wea00733.htm.

Ulugergerli, E. U., & Akca, I. (2006). Detection of cavities in gypsum. *Journal of the Balkan geophysical society*, *9*(1), 8-19.

URL 1: www.iwr.usace.army.mil/docs/MMDL/FLD/Feature.cfm?ID=5

US Army Corps of Engineers. (1995). *Geophysical Exploration for Engineering and Environmental Investigations, Design Manual.* (Report No. EM1110-1-1802).

US Army Corps of Engineers. (2000). *Design and construction of levees.* Engineer Manual. No. 1110-2-1913.

Vaughan, C. J. (1986). Ground-penetrating radar surveys used in archaeological investigations. Geophysics, 51(3), 595-604.

Vilbig, R.A. (2014). Air-Coupled and Ground Coupled Ground Penetrating Radar Technique. A Thesis, Submitted to Northwestern University, Boston, MA.

Wadhwa, R. S., Ghosh, N., Chaudhari, M. S., Chandrashekhar, V., & Sinharay, R. K. (2008). Delineation of cavities in a canal bed by geophysical survey in Navargaon Project Area, Maharashtra. *Journal of Indian Geophysical Union*, *12*(1), 55-62.

Waite, A. H., & Schmidt, S. J. (1962). Gross errors in height indication from pulsed radar altimeters operating over thick ice or snow. *Proceedings of the IRE*, *50*(6), 1515-1520. doi: 10.1109/JRPROC.1962.288195

Wiscomb, G. W. and Messmer, T. A. (2010). *Pocket Gophers*, Utah State University.

Wu, R., Li, X., Li, J. (2002). Continuous pavement profiling with ground-penetrating radar. *IEE proceeding- Radar, Sonar, and Navigation*, *149*(4), 183-193. doi:10.1049/ip-rsn:20020276

Yang, X., Henderson, G. Lixin Mao, L., & Evans, A. (2009). Application of Ground Penetrating Radar in detecting the hazards and risks of termites and ants in soil levees. *Environmental Entomology*, *38*(4), 1241-1249. doi: http://dx.doi.org/10.1603/022.038.0435

Yee, K. S. (1966). Numerical solution of initial boundary value problems involving Maxwell's equations in isotropic media. *IEEE Transactions on Antennas Propagation*, *14*(3), 302-307. doi: 10.1109/TAP.1966.1138693

Yoshino, T. (1967). *The reflection properties of radio waves on the ice cap*. IEEE transactions on antennas and propagation, AP-15(4), 541-551.

Yu, W., Mittra, R., Su, T., Liu, Y., & Yang, X. (2006). *Parallel Finite-Difference Time-Domain Method*. Artech House electromagnetic analysis series.

Appendix 1: Literature Search Related to Highway Studies

No.	Agency	Date of Study	Title and Intended application	Key findings and limitations
1	MnDOT	2016	**Pavement Design Manual**: This manual contains standards and guidelines used for pavement design and related subjects. A list of topics that are within the scope of this manual is shown in chapter one Section 100 -Scope. http://www.dot.state.mn.us/materials/pvmtdesign/manual.html	Chapter two contains standards and recommendations for performing an investigation to assess the condition of an existing roadway to determine the project design parameters. One of devices used to evaluate pavement is GPR. Section 240 discusses the use of GPR technology. It is recommended to use GPR to determine the HMA pavement thickness for different projects (see **Table 230.1**). For these types of projects, the thickness of the existing pavement is critical and unlike coring, GPR images the pavement thickness continuously and can produce thickness data of the pavement (and potentially the base layer) as needed - up to the GPR's maximum sampling density. The minimum recommended coring interval and the recommended use of GPR for different project types is shown in table 230.1.
2	NMDOT NM12SP-01	2015 Research in Progress	**Use of Falling Weight Deflectometer and Ground Penetrating Radar in Pavement Design, Maintenance and Management**: The purpose of this research is to determine the benefits of non-destructive pavement testing technology, such as Falling Weight Deflectometer (FWD) and Ground Penetrating Radar (GPR), for pavement design, maintenance and management rather than destructive coring. And to perform a needs assessment and market survey of available GPR technology and to purchase appropriate GPR equipment in accordance with recommendations from the Technical Panel.	**Anticipated Benefits** These technologies will enable the Department to determine the life of a pavement from a mechanistic standpoint. Refining pavement design according to actual field condition is expected to significantly reduce maintenance costs and extend pavement life.
3	Transportation Research Board Annual Meeting 2015 Paper #15-2324	2015	**Using Ground-Penetrating Radar to Detect Indicators of Premature Joint Deterioration in Concrete Pavements:** This paper examined the potential use of ground penetrating radar (GPR) as one technique to rapidly and non-destructively assess whether fluid may be accumulating in the saw-cut joint behind the joint sealant.	An experimental campaign was performed using a large number of slabs with differing fluid concentrations. It is recognized that the typical GPR response (wiggle trace or scan) is complex and may be hard to interpret accurately, especially in the field. To overcome this challenge the researchers propose the use of CID signal processing to obtain a single number that reflects the potential for fluid in the joint. It is proposed that the CID can be used with other simple features of the wave (e.g., the derivate) to estimate which joints may contain fluid thereby providing insights into which joint sealant sections may need to be repaired or which joints may require a larger maintenance effort.

4	AHTD	2014	**Geophysical Survey of Unmarked Graves at the Unity Baptist Church on Highway 82, Ashley County, Arkansas:** Panamerican Consultants, Inc. conducted a geophysical survey and archival research on unmarked graves reported by a local informant on a pimple mound behind the Unity Baptist Church on Highway 82 east of Crossett in Ashley County, Arkansas. All information gathered through the study was designed to assist the Arkansas State Highway and Transportation Department in assessing the impact of the proposed Highway 82 widening on the cemetery (AHTD Job No. 020534). The primary goals of the project were to: (1) use geophysical methods to predict the probable locations of burials; and (2) determine the location and boundary of the cemetery relative to the proposed alignment.	The geophysical survey of the project area was conducted using two types of remote sensing equipment: Gradiometer and Ground Penetrating Radar. The Ground Penetrating Radar survey successfully located two unmarked graves and one possible unmarked grave on the pimple mound. The Gradiometer was unsuccessful in locating burials. The two unmarked graves are located approximately at 1.2 m below the summit of the pimple mound behind the Unity Baptist Church. The GPR data had a Dielectric of 16 and a velocity of 0.075 m/ns and achieved a maximum penetration depth of 1.75 m below ground surface. A 400 MHz ground coupled antenna was used for the survey.
5	Federal Highway Administration in cooperation with the American Association of State Highway and Transportation Officials **SHRP2 R01B**	2014	**Utility Locating Technology Development Using Multisensor Platforms:** Develop prototypes of geophysical techniques capable of detecting and locating underground utilities under all geologic conditions. The project also researched an innovative seismic detection technology with an intended similar detection capability to GPR but for use in those soils that are not compatible with GPR.	The project resulted in the development of two functional prototypes, a multi-channel GPR system (TerraVision II™) and a new advanced multi-sensor TDEMI system. It was determined that these advanced geophysical tools offer their greatest value if they are used as an enhancement, not a replacement, to traditional utility mapping methods. On certain projects the cost benefits of using these advanced tools can be significant if utilized early enough within construction phases. Further testing and verification measures are required to more completely assess these systems' capabilities in providing reliable utility depth estimates, to resolve unknown, small, and deep utility targets, and to accurately identify the cost benefits directly associated with their use.
6	Federal Highway Administration in cooperation with the American Association of State Highway and Transportation Officials **SHRP 2 R01C**	2014	**Innovations to Locate Stacked or Deep Utilities:** The project proposed research into developing five technologies to locate stacked or deep utilities. These were: Pipe mapping, electromagnetic locator, Seismic reflection, Active acoustic, RFID smart tags. These five technologies were reduced to two for prototype development; Smart Tags and Active Acoustic	One of the findings was that in dry, sandy soils, GPR works well for finding buried utilities. However, for wet and clay soils, the waves attenuate very rapidly. At the frequencies required to detect a 6-inch pipe with GPR, depth of detection is less than 4 feet. Research in improved signal processing, antenna design and greater power in the pulse signal is extending the depth range; however, the exponential nature of attenuation and the high attenuation constants in clay/high moisture soils is too strong to overcome for deeply buried pipe. An additional technique is needed for such soils. The project developed information for future researchers on the three technologies that did not reach the prototype stage.

7	**LOWE, et.al. Archaeology in Oceania, Vol. 49 (2014): 148–157 DOI: 10.1002/arco.5039**	**2014**	**Ground-penetrating radar and burial practices in western Arnhem Land, Australia:** GPR survey was carried out in advance of archaeological excavations at Madjedbebe (formerly known as Malakunanja II), a sandstone rock shelter in western Arnhem Land (Australia) containing numerous Aboriginal burials. This study was an opportunity to test a way to identify unmarked burials using GPR in sandstone rock shelters and to document a marker for burial identification in this region. Application of the methodology developed through this case study provides a useful management tool for Indigenous communities and other heritage practitioners.	GPR data were collected with a Geophysical Survey Systems, Inc. (GSSI) SIR-3000, 400 MHz antenna and a model 620 survey wheel. Sixteen-bit data were collected with an 80 ns time window, 512 samples per scan and with 25 scans per meter. The GPR results provided, first, information on subsurface material associated with geological features such as bedrock and roof-fall and, second, cultural material, in the form of deliberately positioned rocks associated with human burials.
8	MoDOT Report No. cmr14-010	2014	**Nondestructive Evaluation of Modot bridge decks – pilot study**: The primary objective was to demonstrate the utility of the GPR tool in evaluating the condition of MoDOT bridge decks and confirms that this noninvasive method can be implemented as a part of a long term program that enables faster, better, and more cost-effective bridge deck assessments. The GPR data were acquired using a GSSI SIR-3000 system and a 1.5 GHz ground coupled antenna mounted to a push-cart. The GPR data were acquired on the top surface of the bridge deck along parallel traverses variably spaced at 0.75 to 2 ft. The GPR data were processed using GSSI RADAN 6.6 and RADAN 7 processing software. Eleven bridge decks were investigated.	GPR interpretations of the top reinforcement reflection amplitude showed a strong correlation with visual assessment results in areas where visual deterioration was noted. A fair to good correlation was observed between the GPR data and the visual core evaluation results. A higher degree of correlation can be anticipated in areas where the concrete cores are visibly deteriorated; a lower degree of correlation can be expected in areas where the concrete cores do not exhibit signs of deterioration. GPR interpretations presented in this study were based on the reflection amplitude from the top transverse layer of reinforcement and do not represent the condition of the concrete below the top transverse reinforcement.

9	**S W Jaw and Hashim M**	**2014**	Urban Underground Pipelines Mapping Using Ground Penetrating Radar: This study was conducted to extract locational information of the urban underground utility pipeline using trenchless measuring tool, namely ground penetrating radar (GPR). The focus of this study was to conduct underground utility pipeline mapping for retrieval of geometry properties of the pipelines, using GPR.	A series of tests were first conducted at the preferred test site and real-life experiment, followed by modeling of field-based model using Finite-Difference Time-Domain (FDTD). Results provide the locational information of underground utility pipelines associated with its mapping accuracy. GPR system with 250 MHz and 700 MHz frequencies was used to acquire data at the selected sites, and numerical modelling analysis was used to validate the locational information of the buried pipelines, without requiring much effort to explore the nearest manhole for accuracy assessment as is commonly done in the conventional way of underground utility mapping. Data that was acquired were subjected for pre-processing in order to enhance image quality and remove unnecessary echoes caused by background noise. The selection of pre-processing steps to be undertaken in the study was based on the researcher's personal preferences and data processing experience. Different routines of pre-processing steps can be adopted as well according to user's preferences and experiences relating to types of GPR system being used. The urban underground utility pipeline mapping using GPR yielded detection accuracy within 10cm, equivalent to the quality level A utility data.
10	SHRP 2 R01B So-Deep, Inc.	2014	**Field Evaluation of Tools Developed in the SHRP 2 R01B and R01C Projects:** So-Deep, Inc. was selected as the subsurface utility engineering observation firm for the geophysical tools produced by the Second Strategic Highway Research Program (SHRP 2) project on Utility Locating Technology Development Utilizing Multi-Sensor Platforms (R01B) and the project on Innovations to Improve the Extent of the Locatable Zone (R01C). Virginia DOT (VDOT) and Georgia DOT (GDOT) projects were selected as test sites.	1. The SHRP R01B GPR tool (TerraVision IITM) was ineffective in the Virginia clay soils and was unable to image utilities and therefore no depth readings were obtained. 2. Due to terrain issues only about 50% of the total project area would have been capable of utilizing the SHRP R01B tools, given their size and towing restrictions. 3. Both tools found a majority of the metallic water and metallic gas lines in the areas covered. TerraVision II had some success on the non-metallic sewer lines. Neither tool had great success on the communication systems. 4. In addition to increased mapping costs and time of processing and correlating results, using these tools will also have an impact on the traveling public. 5. The final report listed numerous challenges that make the use of these tools impractical and unbeneficial to the DOTs at this stage of development.

11	**SHRP 2 R06D**	2014	**Nondestructive testing to identify delamination between HMA layers phase III –** develop user guidelines for use of ground penetrating radar and mechanical wave (spectral analysis of surface waves and impact echo) nondestructive technologies to detect delamination between asphalt pavement layers	The guidelines identify the hardware and software requirements necessary to achieve measurement of a pavement lane width in a single pass. Stand-alone user guidelines for both technologies are included as appendices. The guidelines include general theory, equipment specifications, data output and display requirements, equipment calibration and verification, testing conditions, data format and quality control, data analysis, and test reporting. Both technologies can be used to detect discontinuities in asphalt pavements; however, they cannot be used to conclusively distinguish between types of pavement discontinuities.
12	SHRP 2 Renewal Project R06C	2014	**Pre-Implementation of Infrared and Ground-Penetrating Radar Technologies for Improving Asphalt Mixture Quality:** In this project, researchers performed pre-implementation of infrared (IR) and ground-penetrating radar (GPR) technologies for measuring uniformity and promoting quality of asphalt mixture paving. The project team coordinated with industry to streamline the processes required for using GPR in this application, developed draft procedures for both IR and GPR technologies, and conducted pilot projects with the Virginia and Pennsylvania Departments of Transportation.	The pilot projects demonstrated that both IR and GPR provide a useful full-coverage view of the paving operation. Each pilot project employed a warm-mix asphalt (WMA) technology as a compaction aid. These pilot project results suggested that the significance and acceptance criteria of thermal segregation may need more reevaluation with WMA. The utility of GPR was realized on all pilot projects, where the radar results provided quantitative assessment of density and uniformity. A new radar system developed specifically for uniformity assessment of asphalt mixtures achieved significant advances in the state of the practice with radar. This report presents the pilot project results, draft standard specifications for both IR and GPR, and conclusions on how these technologies could be used in construction specifications. The team worked with the Virginia DOT (VDOT) and Pennsylvania DOT (PennDOT) to pilot the thermal profile and radar technologies on three construction projects. This SHRP 2 project achieved significant advances in the state of the practice with GPR. All pilot projects were evaluated with both a 1 GHz and a new 2.5 GHz air-coupled radar system. While the first-generation prototype GPR system tailored for asphalt mixture evaluation encountered some stability and overheating issues, the second generation 2.5 GHz system did not exhibit those problems and provided stable readings, rapid results, and easy operation as compared to the 1 GHz system.

13	SHRP 2 Report S2-R06G-RR-1	2014	**Mapping Voids, Debonding, Delaminations, Moisture, and Other Defects Behind or Within Tunnel Linings**: This report documents the work conducted under Phase 2 of Strategic Highway Research Pro-gram (SHRP 2) Renewal Project R06G. Renewal Project R06G seeks dependable nondestructive testing (NDT) techniques that minimize disruption to traffic. One of the objectives of the proposed research was toIdentify NDT technologies for evaluating the condition (e.g., moisture, voids, and corrosion) of various types of tunnel linings (e.g., unreinforced concrete, reinforced concrete, shotcrete, and steel) and tunnel lining finishes such as tile. The techniques must be capable of analyzing conditions within the tunnel lining and the surrounding substrate.	Air-coupled GPR: Locates defect within 1 ft. of its actual Location. Does not measure depth, but indicates areas of high moisture or low density (high air voids). Such areas may represent problems within or behind the tunnel lining. Detected Tile debonding, delaminations, air-filled voids, water-filled voids, moisture intrusion. Tunnel lining type were Concrete, tile lined concrete, and shotcrete . Ground-coupled GPR: Can determine defect depth within 10% of the actual depth without reference cores— 5% if cores are available. Can possibly detect defects at any depth within or immediately behind tunnel linings. However, specimen testing indicates it cannot locate 1-sq-ft voids in steel plates behind tunnel linings. Detected delamination, air-filled voids, water-filled voids, moisture intrusion. Tunnel lining type, concrete, tile lined concrete, and shotcrete.
14	AHTD	2013	**Geophysical survey of the Goforth Cemetery (3IN1262) on us highway 167, Independence County, Arkansas:** Panamerican Consultants, Inc. conducted a geophysical survey and archival research for the Goforth Cemetery (3IN1262) located along US Highway 167/Arkansas Highway 394 (Antioch Road) in Independence County, Arkansas. All information gathered through this survey was designed to assist Arkansas State Highway and Transportation Department in assessing the impact of the proposed US Highway 167/Arkansas Highway 394 realignment on the cemetery. The primary goals of the project were to: (1) use geophysical methods to predict the probable locations of burials; and (2) determine the location and boundary of the cemetery relative to the proposed alignment.	The geophysical survey of the project area was conducted using two types of remote sensing equipment: gradiometer and GPR. The GPR survey of the study area was conducted using a GSSI SIR3000 GPR with a 400 Mhz antenna. The entire project area was subjected to a GPR survey at 1-m traverse intervals with equipment settings of: 512 samples per trace; 16 bit data format; 30 nano second (ns) range; 120 scan rate; and 32 scans per m. The GPR data was collected using the RTK GPS system to position the readings. A 20-x-10 m high-probability area was subjected to a “high resolution” GPR survey using 50-cm transverse intervals. This resulted in the identification of three fairly well defined anomalies that are interpreted as possible unmarked graves.
15	AHTD	2013	**Geophysical Survey of the Stout Cemetery near Highway 7, South of Dover, Pope County, Arkansas:** Panamerican Consultants, Inc. conducted a geophysical survey and archival research on a historic cemetery located near Highway 7 south of Dover in Pope County, Arkansas. All information gathered through the study was designed to assist Arkansas State Highway and Transportation Department in assessing the impact of the proposed Highway 7 realignment on the cemetery. The primary goals of the project were to: (1) use geophysical methods to predict the probable locations of burials; and (2) determine the location and boundary of the cemetery relative to the proposed alignment.	A geophysical survey of a 120-x-140-m (4.2-ac.) project area was conducted using two types of remote sensing equipment: gradiometer and ground penetrating radar. The project area was surveyed using 1-m traverse intervals by both types of equipment. A 20-x-20-m high-probability area- was subjected to a high-resolution ground penetrating radar survey using 50-cm transverse intervals resulted in the identification of two fairly well defined anomalies that were interpreted as possible unmarked graves. The GPR survey was conducted using a GSSI SIR3000 GPR with a 400 Mhz antenna. The entire project area (less the pond and collapsed shed areas) was subjected to a GPR survey at 1-m traverse intervals with equipment settings of: 512 samples per trace; 16 bit data format; 30 nano second (ns) range; 120 scan rate; and 32 scans per m. The GPR data was collected using the RTK GPS system to position the readings.

16	AHTD	2013	**Changes in Pavement Section for BB 0613:** A survey using pavement management's ground penetrating radar (GPR) was performed on January 7, 2013. The project site was 8.5 miles in length and was located on Interstate 530 in Pulaski County. The purpose of the survey was to determine in the project site where the pavement structure changes.	Knowing where the pavement structure changes, sections of the site can be created. The analysis that was performed determines that there were five areas where there was a structure change. Six sections were determined. No mention in the report about type of equipment or antennas that was used for this survey.
17	**Arab J Geosci (Saudi Society for Geosciences)**	**2013**	**On the application of GPR for locating underground utilities in urban areas:** Conducting GPR surveys for locating underground utilities in three cities along the coast of the Red Sea using SIR-3000 GSSI system equipped with a single 100-MHz and 400-MHz antennas	The GPR survey succeeded in detecting three upright cylindrical reinforced concrete tanks with a network of steel pipes connecting them and a metallic pipe at depths ranging between 1 and 2 m below the surface. The survey was successful also in detecting concrete water pipes, PVC pipe housing communication cable, and power cable but it failed to detect a fiber optic cable buried directly in the ground. The GPR survey was used successfully to track and to detect another fiber optic cable inside a 10-cm diameter PVC tube buried at depth of 0.5 m in the study area. The cable itself was not detected but the PVC pipe can be easily detected.
18	**Cheng, et.al.**	**2013**	**Identification and positioning of underground utilities using ground penetrating radar (GPR):** Little researches had been investigated about the significances of measuring pipes and cables in Hong Kong. In this research, general procedures on how to design the grids and to conduct the radar surveys were reviewed. The main objective was to compare the radar results for different types of utilities, site conditions, and frequency antenna with the conventional survey methods in three trial sites. Also to evaluate the use of antenna frequency and the accuracy of the obtained data.	Equipment used in the study was the hand-pulled SIR-20 GPR unit with two ground coupled center frequency antennas - 270 and 400 MHz (GSSI, USA). Survey transects were spaced 1 m for Sites 1 and 2, and 0.5 m for Site 3 apart. The study found that both 270 and 400 MHz antennas were calibrated well on site with adoption of K of 8. Post-processing techniques including time-zero correction, IIR and FIR filters, and deconvolution were performed to enhance the interpretability of original radar signals. It was found that under ideal conditions the 400 MHz antenna was good at distinguishing underlying objects with less than 2-m depth, whereas 270 MHz one was good for more than 2-m.

19	IHRB Project TR-638	2013	**Western Iowa Missouri River Flooding— Geo-Infrastructure Damage Assessment, Repair, and Mitigation Strategies:** The main goals of this research project were to assist county and city engineers by deploying and using advanced technologies to rapidly assess the damage to geo-infrastructure and develop effective repair and mitigation strategies and solutions for use during future flood events in Iowa. Used technologies included falling weight deflectometer, dynamic cone penetrometer, three-dimensional (3D) laser scanning, ground penetrating radar, and hand auger soil sampling.	The GSSI SIR-20 multi-channel data acquisition unit along with 200 MHz, 400 MHz, and 900 MHz antennas was used in this study. The data was analyzed using GSSI's RADAN version 7.0.4.5 software For Gravel Roads and Culvert Crossings: GPR scanning using 200 and 400 MHz antennas identified changes in gravel layer thicknesses, culvert locations, and weep holes. For Bridge Abutments: GPR scans detected areas of potential voids and backfill erosion beneath the gravel surface after about 8 months after flooding in spite of reconstruction. For Paved Roadways: Isolated voids at shallow depths (< 0.5 ft.) and deeper depths (>0.5 ft.) were located.
20	**Ismail et.al, Caspian Journal of Applied Sciences Research**	**2013**	**Predictive Mapping of Underground Utilities Using Ground Penetrating Radar:** This study was conducted to detect and map utilities of the study area.	The study implemented MALA 250MHz shielded antenna to detect and map utilities at different depths. In this study, GPR method successfully detected and mapped three underground utilities with different depth. First anomaly possibly underground pipe detected at depth about 0.97m while second anomaly which suggested as manhole trench detected at depth of 2.07m. Third anomaly detected at depth of 1.55m may due to metal pipe or underground cable.
21	MDOT FHWA/MS-DOT-RD-13-255	2013	**A Synthesis Study of Noncontact Nondestructive Evaluation of Top-down Cracking in Asphalt Pavements**: The primary objective of this research study was to conduct an extensive literature review on top-down cracking evaluation studies, prepare a synthesis of findings, and recommend a follow up phase for a pilot study in Mississippi with a candidate technology.	A procedure is needed to expedite field survey of top-down cracking without depending on cores. The most promising nondestructive noncontact technology operating at highway speed is the ground penetrating radar. The data interpretation must yield top-down cracking presence on the surface and penetration depth in asphalt pavements. Unfortunately, at this stage of knowledge a follow up phase is not recommended for a pilot study in Mississippi with a candidate technology. Because a viable noncontact highway speed technology is not found; therefore, a problem statement for research need will be prepared and submitted for a national study through NCHRP.

22	MIDOT RC-1597	2013	**Research on Non-Destructive Evaluation – Workshop** The workshop held on March 28 at the MIDOT Aeronautics Auditorium in Lansing, Michigan, was organized with the goal of providing an overview of readily available and proven NDE technologies and the process of integrating these technologies into the bridge management program	Base on the information presented during the workshop and the subsequently held panel discussion, the following conclusions and associated recommendations are developed: 1. GPR is recommended to evaluate the existence of deteriorated concrete which may provide a corrosive environment for reinforcing steel, the potential for delamination due to corrosion of embedded steel, and to map concrete delamination exposed by the presence of a moisture layer. This GPR data will be useful for developing deck deterioration models. 2. GPR combined with IR and laser based imaging systems, is recommended for acquiring deck condition data. 3. GPR, combined with ultrasonic echo, is recommended for locating steel post-tensioning ducts (GPR) and to identify grout voids (ultrasound).
23	MN/RC 2013-29	2013	**Implementation of Pavement Evaluation Tools**: The objective of this project was to render the Falling Weight Deflectometer (FWD) and Ground Penetrating Radar (GPR) road assessment methods accessible to field engineers through a software package that is menu driven.	The software implements both methods more effectively by integrating the complementary nature of GPR and FWD information. For instance, the use of FWD requires prior knowledge of pavement thickness, which is obtained independently from GPR. The software was programmed in MATLAB and includes two separate graphical user interfaces for FWD and GPR. The users can easily switch back and forth between the two. The GPR part provides the ability to plot the waveforms and each scan for air, metal, and pavement. Users go through steps of plotting, preprocessing, and calculating to obtain the thicknesses of the layer. Currently, the software works with a 1 GHz antenna only. Then the FWD section extracts the static response from the FWD data. The algorithm also calculates modulus and structural number for the pavement.
24	**Shawn M. Patch, submitted to Federal Highway Administration, Eastern Federal Lands Highway Division**	**2013**	**Grave Marker Assessment and Ground Penetrating Radar Survey of the Woodlawn Baptist Church Cemetery, Fairfax County, Virginia:** New South Associates conducted a detailed grave marker assessment and ground penetrating radar (GPR) survey of the Woodlawn Baptist Church cemetery in Fairfax County, Virginia. The study was funded by the Federal Highway Administration, Eastern Federal Lands Highway Division. The scope of work for this survey required detailed mapping and inventory of all grave markers and associated cemetery features, as well as a GPR survey to identify the extent and distributions of possible unmarked graves. Archival research was conducted to develop a history of the cemetery.	The GPR results correlate very well with the number of graves as documented from the marker inventory and suggest there are few unmarked graves present. The survey was conducted with a Geophysical Survey Systems, Inc. (GSSI) SIR 3000 control unit with an attached 400MHz antenna. The first step was to calibrate the antenna to local conditions by walking the survey area and adjusting the instrument's gain settings. Field calibration was repeated as necessary to account for changes in soil and/or moisture conditions. Effective depth penetration was approximately 1.75 meters. Slight signal attenuation (degradation) was noted in the field, which was due to the presence of clay soils. However, signal attenuation was not severe enough to limit detection of graves.

25	**SHRP 2** **S2-R06D-RR-1**	2013	**Nondestructive Testing to Identify Delaminations Between HMA Layers Volume 1-Summary:** The focus of the study was to find NDT technologies that could detect the two most common causes of delamination: loss of bond and stripping. The criteria for evaluating each technology focused heavily on the ability to detect delamination, but also emphasized depth of detection, equipment availability, speed of data collection, and simplicity of data analysis. The three technologies were: GPR (antenna array, frequency sweep, GPR single antenna, single frequency was dropped from this study), impact echo (IE), and spectral analysis of surface waves (SASW)	GPR technology is the only NDT technology that is capable of testing full lane width and at moderate testing speed. Advances in mechanical wave NDT equipment significantly reduce the testing time but are limited to testing at speeds of less than 5 mph. None of the NDT technologies can conclusively distinguish between types of pavement discontinuities. The measurement identifies a discontinuity, or change, in the pavement condition, but cannot determine from the measurement why the change occurred. GPR can identify variations in the pavement, isolate the depth of a discontinuity in the pavement, and provide a relative degree of severity. IE can identify variations in the pavement below a depth of 4 in., but confident analysis requires the HMA to be cool and stiff. The measurement has limited ability to provide the degree of severity and cannot measure pavement condition below the top of the discontinuity. SASW can identify variations in the top 7 in. of the pavement provided that the analysis uses a reasonable value for the stiffness of the pavement. Like IE, the SASW measurement has a limited ability to provide the degree of severity and cannot measure pavement condition below the top of the discontinuity. One of the recommendations for this study was :GPR equipment should have an array of antennae and frequency sweep pattern ranging up to 3 GHz.
26	SHRP 2 **S2-R06A-RR-1**	2013	**Nondestructive testing to identify concrete bridge deck deterioration:** The ultimate goal of this research was to identify and describe the effective use of NDT technologies that can detect and characterize deterioration in bridge decks. This included identifying and characterizing NDT technologies for the rapid condition assessment of concrete bridge decks; Validating the strengths and limitations of applicable NDT technologies from the perspectives of accuracy, precision, ease of use, speed, and cost; Recommending test procedures and protocols for the most effective application of the promising technologies; and Synthesizing the information regarding the recommended technologies needed in an electronic repository for practitioners.	There is not a single technology that has shown potential for evaluating all deterioration types. The top technologies, based on their overall value in detecting and characterizing deterioration in concrete decks, include ground penetrating radar, impact echo, and ultrasonic surface waves. However, the ultimate decision on which equipment to acquire and which technology to use will primarily depend on (1) the type of deterioration that is of the highest concern to the agency and (2) whether the evaluation is being done for network-level condition monitoring or for project-level maintenance or rehabilitation.

27	**Sutton and Conyers Int J Histor Archaeol DOI 10.1007/s10761-013-0242-1**	**2013**	**Understanding Cultural History Using Ground-Penetrating Radar Mapping of Unmarked Graves in the Mapoon Mission Cemetery, Western Cape York, Queensland, Australia:** The Mapoon Mission Cemetery in Cape York, Queensland contains unmarked pre-contact burials with potential national heritage values, despite a lack of formal recognition and protection through State and National heritage listings. GPR survey at the Mapoon Mission Cemetery was carried out in December 2010with involvement of Mapoon Elders and assistance from Mapoon Land and Sea Rangers. The aims of the survey were to comply with the aspirations of Mapoon Elders to delineate burials and define cemetery boundaries in hopes of subsequently fencing the area so as to ensure preservation, protection and as an aid for managing the Cemetery.	The GSSI (Geophysical Survey Systems Inc.) Subsurface Interface Radar Model3000 with a 400 MHz center-frequency antenna was used to collect radar reflection in the Mapoon Mission Cemetery. A survey wheel was used for encoding distance into the reflection data string. Reflections were recorded in a 60 ns time window and all reflections were filtered prior to recording, removing all received frequencies lower than 200 MHz and higher than 800 MHz A total of 70 reflection profiles were recorded in a grid that was 69x50m in maximum extent. Profile length varied through this grid in order to avoid large trees and other surface obstructions. The GPR results show that the Cemetery contains evidence of a minimum of 120 burials, including potential pre-contact and early mission time Aboriginal burials with all buried at approximately the same depth (1.5 m or so to the top of the casket or remains).
28	**Thieme, Early Georgia, volume 41, number 2**	**2013**	**Identification of Unmarked Graves at two Historic Cemeteries in Georgia:** The two field investigations summarized in this paper both involve detection of unmarked graves in historic cemeteries using ground-penetrating radar (GPR).	The author used MALÅ 250 and 500 MHz shielded antenna to collect the GPR data. The two field investigations demonstrate that significant results can be obtained on historic cemetery sites by using ground-penetrating radar in ways that have been developed for archaeological applications. Neither the Sunset Hill Cemetery nor the Dixon-Rainey Burial Ground site investigations represents an ideal case in terms of the available equipment, time available, or opportunities to obtain “ground truth” through excavation of the anomalies identified.
29	**Wahab, et.al, 2013 IEEE International Conference on Control System, Computing and Engineering, 29 Nov. - 1 Dec. 2013, Penang, Malaysia**	**2013**	**Interpretation of Ground Penetrating Radar (GPR) Image for Detecting and Estimating Buried Pipes and Cables:** Interpretation of Ground Penetrating Radar (GPR) dataset towards detecting underground utility is a challenging task. The underground utility information such as location, depth and type serves as a reference prior to any construction project in order to avoid damage to the utility during excavation. However, the interpretation of GPR images is a tedious and timely process which requires human intervention. This study proposed a new hyperbola fitting technique to estimate the radius of buried utility (pipes and cables).	The method was applied to nine (9) different sizes of buried pipes for radius estimation purposes. The result indicates that the technique is capable of estimating the radius of buried pipes with acceptable result; approximately 97.7% to 99.2% for cable/pipe type with a radius between 45mm to 150mm are detected accurately.

30	WisDOT 0092-11-01	2013	**Investigation and Development of a Non-Destructive System to Evaluate Critical Properties of Asphalt Pavements during the Compaction Process** : The purpose of this report is to present findings from a two-stage investigation to develop a non-destructive system to evaluate critical properties and characteristics of asphalt pavements during the compaction process	The first stage aligned critical properties and characteristics with available non-destructive testing (NDT) technologies. The three higher-ranked NDTs for the evaluation and selected for a field evaluation were: Infrared Thermography (IR), Ground Penetrating Radar (GPR), and Portable Seismic Pavement Analyzer (PSPA). The nuclear density gauge was also used in the evaluation. The second stage of the investigation collected and analyzed field data from three projects, The average nuclear density on the three projects was nearly identical, ranging from 92.4% to 92.6%, and standard deviations of 2.21%, 1.66%, and 1.40%. The GPR density standard deviation was about half that of nuclear density. GPR thickness among the projects had a standard deviation ranging from 0.1 to 0.2 inches. Data from the three projects found no definitive relationship between continuous thermal temperatures behind the paver and final density measured by GPR and nuclear density gauge. Placement temperature did not appear to affect modulus; this finding is limited to the three projects in this study and may not be true for all mixes placed in Wisconsin or other states. GSSI air-coupled antenna with a central frequency of 2 GHz was used in this study.
31	**Woodward and Fuselier,** **64th HGS 2013**	**2013**	**Cooperative Geotechnical Designs to Build on Liquefiable and Compressible Soil in Salem, Massachusetts:** The Massachusetts Bay Transit Authority (MBTA) is addressing accessibility throughout their facilities. The Commuter Rail station in Salem, Massachusetts is upgrading their facility to improve site accessibility and increase parking capacity. Historical records, a geophysical survey, and an archaeological survey indicate structural remains from a historic train depot are largely intact beneath the surface of the existing lot.	During the site history review process it was suspected that foundations of the roundhouse, turntable, and other appurtenant structures may have been abandoned in place and if so, they would have archeological significance. A geophysical exploration was performed using precision utility locating methods (PUL), time domain electromagnetics (EM), and ground penetrating radar (GPR) techniques to explore their presence. Results of the EM and GPR together provided good indications that the features identified in the geophysical surveys correspond well with the locations of the historical structures and would require historical cataloging to meet site permitting and historical commission requirements in addition to extra consideration for construction methods and sequencing. No mention in the report about the type of GPR equipment or the frequency of the antenna used for the survey.

32	WSDOT	2013	**Prediction of scour depth in gravel bed rivers using radio frequency IDs:** application to the Skagit river: The objective of this project is to develop the technology for permitting the determination of the maximum scour depths near proposed flow deflection structures such as ELJs to be installed at MP 100.7 on the Skagit River using the IIHR Radio Frequency Identification (RFID) system. For the purposes of this study, a Low Frequency (LF) (134.2 kHz), passive RFID system developed by Texas Instruments (TI) was employed	The research offers a new innovative approach for detecting scour in natural environments and/or around hydraulic structures. The main results of this study were: 1. The material casing used to encapsulate the transponder plays a role to the system overall performance and should be taken into consideration at the designing phase of the project. 2. A key finding of this study is that the orientation of the transponder with respect to the excitation antenna plane plays a significant role in terms of the detection efficiency of the RF signal strength An RFID system fitted with data telemetry equipment can provide the ability to collect and transmit data to a maintenance office. Remote monitoring could mitigate the inefficiencies and dangers inherent in the current practices, as well as provide early warning of impending bridge failure and the ability to track long-term degradation as a result of scouring.
33	**John J. Schultz**	**2012**	**Detecting Buried Remains Using Ground-Penetrating Radar:** The purpose of this study was to determine the applicability of GPR for detecting controlled graves. Objectives for this project included determining how different burial scenarios (e.g., wrapping the carcass and placing items over the carcass) are factors in producing a distinctive anomalous response, determining how different GPR imagery options can provide increased visibility of the burials, and comparing GPR imagery between the 500 MHz and 250 MHz antennae. An electromagnetic induction (EMI) meter was also employed to determine the applicability of this technology to locate unmarked graves. Finally, the last objective was to provide basic guidelines for forensic investigators to utilize when conducting buried body searches involving these geophysical tools.	The research design included constructing a grid on secured land in a field area that contained a total of eight graves representing common burial scenarios in Spodosol, a common soil type of Florida. Six burial scenarios contained a pig carcass at a deep (1.00 m) or a shallow (.50 m) depth: a shallow unwrapped pig carcass, a deep unwrapped pig carcass, a deep pig carcass wrapped in a tarp, a deep pig carcass wrapped in a cotton blanket, a deep pig carcass covered with a layer of rocks, and a deep pig carcass covered with a layer of lime. Two blank control graves, one shallow and one deep were also constructed. Graves were monitored with EMI (24 months) and GPR (30 months) using both the 500 and 250 MHz antennae. GPR was shown to be a favorable tool for monitoring controlled graves for a 30 month period as many scenarios were still detected at the end of the monitoring period. Overall, the 250 MHz antenna results were more favorable than the results of the more commonly used 500 MHz, as the 250 MHz antenna provided increased visibility for large cadavers buried in deep graves while the 500 MHz results were more favorable for the shallow pig scenario. The probability of detecting a grave for a longer postmortem interval differs with the soil type, the moister, and the materials added to the grave with the body.

34	WYDOT FHWA-WY-10/07F	2012	**Bridge Deck Evaluation using Non-destructive Test Methods**: The goal is to develop a practical solution that WYDOT can implement. In particular, the solution should capitalize on safety, efficiency and accuracy. The author evaluated each bridge using standard WYDOT practices for chain dragging and half-cell potentials, along with newer technologies of impact echo, thermal imaging, and ground penetrating radar (GPR), which provides a comprehensive assessment of the NDE evaluation techniques.	Cores removed from the bridges were compared to the results from the evaluation methods and generally correlated well and factors are presented in this report. The ground penetrating radar systems provide a detailed analysis of the bridge decks. GSSI 1500 MHz ground-coupled antenna and 1000 and 2000 MHz air horn antennas were used. The GSSI BridgeScan System was recommended. The research team recommends a combination of impact echo scanning and GPR for more accurate bridge deck evaluations. This provides the most accurate predictions of delamination, debonding, and active corrosion on bridge decks. Currently, a full lane dual-polarization system is still in the developmental stage and is very expensive. If a full lane GPR scanner becomes commercially available, the authors recommend considering this type of system.
35	CDOT	2011	**Evaluative test excavation of eleven historic sites for the Colorado department of transportation interstate 25 new pueblo freeway improvement project, pueblo county, Colorado**	In this project, a 400 MHz antenna was used, which generally produced data of good resolution at depths to just under 2 m (about 5 ft). This was sufficient to map below the majority of buried features in these areas. Below this depth, energy was attenuated and only extraneous noise from radio and cell-phone transmissions was recorded. In the current project, the ground surface was generally flat, and overall, the antenna was able to maintain good contact with the ground, and good data resolution was achieved to depth.
36	FL/DOT/SMO/11-542	2011	**US 27/SR 25 Pavement Evaluation: The Central Pavement Management Office requested that the State Materials Office perform a pavement evaluation of a one mile long section of US 27/SR 25 in Palm Beach County**. The primary objective of the evaluation was to assess whether pavement cracks initiated from the top or bottom of the asphalt. Performance was also evaluated in terms of pavement stiffness, rut depth, and roughness.	FDOT's GPR system consists of a Geophysical Survey Systems, Incorporated (GSSI) SIR 20 and two 2.0 GHz air-launched antennas. The GPR was used to estimate the thickness of the hot-mix asphalt (HMA) along the section of interest. Data was collected at 55 mph, using a 1ft sampling interval with the antennas positioned along the inside and outside wheel-paths. HMA thickness was estimated by averaging the six GPR readings closest to each core location and was then compared to actual core thickness. On average, the GPR estimated HMA thickness deviated by 1.0 inch from core thickness. A previous FDOT study on the accuracy of the GPR system showed that on average the system can predict asphalt thickness within approximately 8%. The GPR estimated thickness for US 27 is a relatively good match considering the GPR system was not calibrated against a core value, in addition to compensating error due to data averaging.
37	IDOT ICT Report No. 11-096	2011	**In-place hot mix asphalt density estimation using ground penetrating radar** : To overcome the limitations of the traditional methods, this study proposes to develop a nondestructive method of using ground penetrating radar (GPR) to measure in-situ asphalt mixture density accurately, continuously, and rapidly	Traditionally, two methods have been commonly used for in-situ asphalt mixture density measurement: laboratory testing on field-extracted cores and in-situ nuclear gauge testing. However, both these methods have limitations. It was found that the prediction accuracy of the GPR was comparable to, or better than, that of the traditional nuclear gauge. For the asphalt mixtures without slags, the average density prediction errors of GPR were between 0.5% and 1.1% with two calibration cores, while those of the nuclear gauge were between 1.2% and 3.1%. 1 GHz air-coupled antennas were used in this study.

38	Iowa DOT SPR-NDEB(90)--8H-00	2011	**Comprehensive Bridge Deck Deterioration Mapping of Nine Bridges by Nondestructive Evaluation Technologies**: The primary objective of this research was to demonstrate the benefits of NDT technologies for effectively detecting and characterizing deterioration in bridge decks. In particular, the objectives were to demonstrate the capabilities of ground-penetrating radar (GPR) and impact echo (IE), and to evaluate and describe the condition of nine bridge decks proposed by Iowa DOT.	Results from this study confirm that the used technologies can provide detailed and accurate information about a certain type of deterioration, electrochemical environment, or defect. However, they also show that a comprehensive condition assessment of bridge decks can be achieved only through a complementary use of multiple technologies at this stage. All of the bridge decks were surveyed using both ground-coupled GPR antennas (1.5GHz and 2.6GHz), but some of them were also surveyed using air-coupled (horn) 1.0GHz GPR antennae
39	MDT	2011	**Ground Penetrating Radar (GPR) Analysis: Phase II Field Evaluation**: The objective of this work was to evaluate the feasibility and value of expanding the MDT's Ground Penetrating Radar (GPR) program to pavement design and rehabilitation, and to network level evaluation. Phase I of this project concluded that in order to investigate the feasibility and value of these program expansions, a Phase II field evaluation project be designed and implemented to evaluate the accuracy of GPR pavement thickness data on Montana pavements, and to correlate these findings with the accuracy requirements of the individual applications	The field evaluation for this project began with identifying 26 pavement test section of different composition and structure located throughout the diverse climatic regions of Montana. At each site, FWD and GPR (2 GHZ horn and 900 MHZ) data was collected, followed by coring and augering to determine the thickness of the pavement layer structure and base moisture content. This testing was carried out both in the spring of 2010 and in the fall of 2010 to capture seasonal variations. The GPR data was analyzed for thickness, and the GPR thickness data was evaluated for seasonal changes, and compared to core and plan data to investigate thickness accuracy and the effectiveness of calibration methods. Compared to cores, the average GPR bound layer thickness error was 10.3% vs. 15.2% using plan data. A GPR data checking method was developed using FWD and plan data to identify potential analysis layer analysis inconsistencies and suggest alternative interpretation. Implementation of this method reduced the GPR error to 7.6%. A sensitivity study was carried out to investigate the impact of having the more accurate GPR data. This study showed that, on average, the use of GPR reduced the pavement life prediction error by 62% when compared to using as-built plan data.
40	NHDOT FHWA-NH-RD-14282N	2011	**Pilot study – rolling wheel deflectometer, falling weight deflectometer, and ground penetrating radar on New Hampshire roadways**: This project evaluated non-destructive testing methods to evaluate pavement thickness and deflection information by means of ground penetrating radar (GPR) and rolling wheel deflectometer (RWD) testing respectively. One of the objectives was to Compare pavement thicknesses estimated from vehicle-mounted ground penetrating radar testing to pavement core samples collected at select highway locations.	The GPR testing covered 115 miles and resulted with substantial variations in pavement thicknesses ranging from 4.0 to 12.0 inches. These predictions, when correlated with data from 35 ground cores, show an average accuracy of 6.5%. Although an initial purchase of a GPR system is costly, once in place, this testing is expected to cost $140 per lane mile compared to the cost of pavement core sampling at $10,000 per lane mile. The project utilized a SIR-20 GPR system attached to a 1 GHz horn antenna mounted to the rear bumper of sport/utility vehicle over the right wheel path.

41	NJDOT FHWA-NJ-2011-001	2011	**Innovative and Effective Techniques for Locating Underground Conduits:** The purpose of this research was to find an effective means for locating these conduits. The solution must meet requirements for accuracy and depth sensitivity, be practical to implement, cost effective, work with both metallic and plastic conduits, and be reliable.	Innovative means for locating underground conduits were investigated, evaluated and compared. Possible solutions are identified and documented and the most effective discussed in detail. Approaches included Acoustic Transmission (AT), Ground Penetrating Radar (GPR), Ground Penetrating Sonar (GPSon), and the Measurement of Electro-Magnetic Impedance (EMI). The project established the ability of GPR (using 400MHZ) to identify multiple buried utilities, but there was concern regarding its ability to distinction between such utilities in cluttered areas. The difficulty in distinguishing between co-located multiple objects could be a problem in applying GPR technology. It was also clear that GPR technology would not function properly under severe flooding or high water table conditions. In favorable conditions it can locate conduits buried up to 12' deep.
42	SHRP 2 **S2-R01-RW-2**	2011	**Development of the Selection Assistant for Utility Locating Technologies**; This report outlines the software development tasks associated with SHRP 2 Renewal Project R01 (2009), "Encouraging Innovation in Locating and Characterizing Underground Utilities".	The software (SAULT) has been implemented in a web-based application that includes a decision-support system to assist users with limited expertise in understanding the types of utility locating equipment that are most appropriate to different utility-locating problems. The website for this software is: http://138.47.78.37/sault/home.asp
43	AHTD	2010	**Thickness Estimation of Existing Pavements Using Nondestructive Techniques: Matching Accuracy to Application:** It was proposed that the required accuracy of an NDT-based system be considered from the perspective of the application in which thickness data will be used. Four typical applications, including construction quality control/quality assurance (QC/QA), layer moduli estimation (using an elastic layered approach), estimation of remaining service life (using procedures contained in the 1993 AASHTO Guide), and overlay design (using one AASHTO-based empirical procedure and the mechanistic-empirical procedures in the new MEPDG), were examined to assess the relative sensitivity to variations in surface layer thickness.	It was demonstrated that the required accuracy of layer thickness estimates varies by application. Specifically, it is suggested that construction QC/QA requires highly accurate thickness estimates (±2.5-5%); layer moduli determination requires moderate accuracy (±5%); overlay design – considering both empirical and mechanistic-empirical procedures – requires lower accuracy (±10%); and remaining life determination requires the lowest accuracy (>±10%). Agencies seeking to implement NDT-based techniques for estimating layer thickness of existing pavements should carefully consider the uses for which the data will be used, and develop their measurement systems accordingly.
44	CADOT CA10-1895	2010	**Preliminary Project Study Report for Shasta 299, PM 51.8 – 60**: The objective of this project was to provide assistance to the staff of Caltrans District 2 with determining whether full-depth reclamation using foamed asphalt and cement is an appropriate rehabilitation option for Shasta 299.	This project investigation has found that FDR-FA (Full Depth Reclamation with Foamed Asphalt) is a viable rehabilitation option for the Shasta 299 project between PM 51.8 and PM 60.0. The stiffness of the subgrade, determined from FWD testing was found to be adequate for FDR-FA projects. The thickness of the HMA, based on GPR and core measurements was found to be thicker than that typically appropriate for FDR-FA over approximately 60 percent of the project. There was not much detail about what kind of GPR equipment used to conduct this research.

45	**Charles A. Dionne, Dennis K. Wardlaw, and John J. Schultz**	**2010**	**Delineation and Resolution of Cemetery Graves Using a Conductivity Meter and Ground-Penetrating Radar:** This study was designed to compare the applicability of two geophysical instruments, a conductivity meter and ground-penetrating radar (GPR), to detect historical land modern-period graves at Greenwood Cemetery in Orlando, Florida. A modern-period grid was set up in a section containing primarily shallow, vaulted, and marked burials. Conversely, a historical-period grid was constructed in an older section containing only five headstones that was believed to include multiple deep, non-vaulted, and unmarked graves	Both instruments detected multiple vaulted burials in the modern-period grid, while only the GPR detected the older non-vaulted burials in the historical-period grid. Neither instrument detected the backfill of the vertical grave shafts that consisted of homogenous sands. The use of various processing techniques allowed for determination of the best data collection procedures for maximum resolution of GPR grave anomalies when using horizontal slices. A transect interval spacing of 0.25 m was preferable to 0.5 m, and is recommended when performing surveys of cemeteries containing unmarked graves. When collecting data in one direction only, transects should be oriented perpendicular to the burials, if this orientation is known. Otherwise, maximum delineation and resolution of graves is obtained using a composite grid containing transects oriented in both X and Y directions. The GPR unit used for this project was a MALA RAMAC X3M with a 500 MHz antenna mounted on a cart containing a survey wheel.
46	**Doolittle and Bellantoni**	**2010**	**The search for graves with ground-penetrating radar in Connecticut:** The search for unmarked and clandestine graves is a labor-intensive, time-consuming, and often frustrating task. Ground penetrating radar (GPR) is often considered the most useful tool to delineate possible graves. This paper is the result of many years of GPR testing for unmarked graves in Connecticut. Natural and cultural conditions are considered in the failure and/or success of detection, and the use of GPR in archaeological studies.	A Subsurface Interface Radar (SIR) System 3000 with a 400 MHz antenna of Geophysical Survey Systems Inc. (GSSI) was used in the investigations reported in this paper. Radar records were processed with RADAN for Windows version 6.5 (GSSI). In the search for unmarked graves, success is never guaranteed with GPR. Most soils in Connecticut are considered quite favorable for deep penetration with GPR. The successful use of GPR to identify burials will depend upon the distinctiveness of the burial as a reflector of electromagnetic energy, the amount of clutter and background noise present in the soil, the availability of suitable radar antennas and signal processing techniques, and the amount of uncertainty or omission that is acceptable. Even under ideal site and soil conditions, some burials will be overlooked with GPR, while other features within the soil will be misidentified as burials. The use of 3D-GPR has improved the identification of some unmarked graves in Connecticut. With the passage of time, burials become increasingly more difficult to detect with GPR. Because of the inviolability of cemeteries, confirmation of GPR interpretations in the context of unmarked graves is difficult.
47	FHWA/VTRC 11-R2VDOT	2010	**Field Trials of High-Modulus High-Binder-Content Base Layer Hot-Mix Asphalt Mixtures**: The purpose of this study was to document the field experience of the Virginia Department of Transportation (VDOT) in the use of high-modulus high-binder-content (HMHB) base layer hot-mix asphalt (HMA) mixtures. Information was gathered with regard to the construction of HMHB base mixtures at three field trial sites in Virginia, and laboratory tests were conducted on samples that were gathered before and during construction.	GPR was used to assess the layer thickness of the BM-25.0 layers placed on the SR 207/652 project. The GPR system used in this study consisted of a 2.0 GHz air-launched horn antenna and a SIR-20 controller unit, both manufactured by Geophysical Survey Systems, Inc. All data were processed by the software RADAN (version 6.6) developed by Geophysical Survey Systems, Inc. Information from GPR testing can be used in the FWD analysis and can also be used to identify differences in planned versus as-built conditions.

48	MN/RC 2010-37	2010	**Incorporating GPS and Mapping Capability into Ground Penetrating Radar (GPR) Operations for Pavement Thickness Evaluations**: The objectives of this project were; first to develop a more robust system for GPR surveying using dual air coupled antennas to provide redundancy in data collection and to improve accuracy and completeness of the survey results. Secondly; the addition of Global Positioning System (GPS) location data, acquired in coordination with the GPR data, for improved project location and ArcGIS mapping capability. Thirdly; the development of a standard format for GPR data reporting in a more user-friendly, exportable format.	Ground Penetrating Radar (GPR) investigations performed by Mn/DOT of pavements and other subsurface features have been limited by an inefficient and poorly documented GPR survey process and underdeveloped project mapping and reporting process. After completing the project objectives, a GPR Manual was developed, describing GPR vehicle and survey operations, GPS with GPR data collection, mapping using ArcGIS, and the new standardized reporting format. The result was an improved and better documented subsurface data collection and reporting process that incorporates GPS and improves the effectiveness of Mn/DOT's GPR program.
49	VDOT VTRC 10-R13	2010	**Condition Assessment and Determination of Methods for Evaluating Corrosion Damage in Piles Encapsulated in Protective Jackets on the Hampton Roads Bridge- Tunnel**: The primary purpose of this study was to assess the condition of piles that had been encapsulated in fiberglass and mortar jackets on four bridges that are part of the Hampton Roads Bridge-Tunnel (HRBT). A necessary objective of the study was to consider visual, non-destructive, and destructive techniques and recommend those that were most effective and efficient in assessing pile condition under the fiberglass jacket systems. A secondary purpose of this study was to assess the effectiveness of the fiberglass jacket and mortar system in resisting corrosion and to make specific recommendations about application of these or similar systems on Virginia bridges in the future. To accomplish the purposes of this study, 52 HRBT piles were systematically selected for study. These piles represented a variety of conditions, ages, types, and locations.	Destructive and non-destructive methods were used to evaluate the piles. Destructive methods included chloride analysis and jacket autopsy. Non-destructive methods included cross-hole sonic logging, ground-penetrating radar, sonic echo, impulse response, half-cell potential, electrical resistivity, ultrasonic pulse velocity, and visual assessment. No single test method was able to assess completely the condition of the jacketed piles. However, a combination of half-cell measurements, sonic echo, impulse response, and chloride analysis was useful in evaluating the condition of jacketed piles. Ground-penetrating radar was ineffective in determining the condition of the underlying pile while the jacket was intact because of signal reflection and attenuation caused by steel mesh reinforcement in the mortar.

50	MDT	2009	**Ground Penetrating Radar (GPR) Analysis: Phase 1** The objective of this work is to evaluate the feasibility of expanding the MDT's Ground Penetrating Radar (GPR) program to a broader range of pavement evaluation activities. MDT uses GPR in conjunction with its Falling Weight Deflectometer (FWD) data collection program to provide layer thickness data for backcalculation. This project has included a review of literature and software dealing with pavement applications of GPR, a survey of state highway agency (SHA) use of GPR for pavement applications, a review of MDT's GPR program, and a review of MDT's pavement structures, environment, and pavement management and rehabilitation practices.	1. A detailed review of 47 documented studies shows that GPR pavement thickness measurements typically fall within 2-10% of core values for the bound layers. Most of these studies have used a 1.0 GHz horn antenna (vs. the 2.0 GHz antenna currently used by MDT). Accuracy of the unbound material is less precisely documented. 2.The survey of SHA GPR practice supports the application of GPR for pavement thickness measurements—some agencies use GPR on a regular basis, while other use GPR on a project-specific basis 3.GPR program can be expanded to provide useful information for the following applications: (a) calculation of structural number for pavement reconstruction and rehabilitation design; (b) insuring proper depth control for mill and fill rehabilitation, and cold in-place recycling; (c) improved structural capacity calculation for network level evaluation; and (d) quality assurance of new pavement thickness and density 4. In order to investigate the feasibility and value of these program expansions, it is recommended that a field evaluation project (phase II)be designed and implemented to evaluate the accuracy of GPR pavement thickness (and density) data on Montana pavements, and to correlate these findings with the accuracy requirements of the individual applications.
51	ODOT-FHWA-OR-RD-10-02	2009	**Investigating Premature Pavement Failure Due to Moisture:** This report details the forensic investigations conducted to identify the causes of pavement failures shortly after a rehabilitation activity on five interstate highway projects in Oregon. One of the principal objectives of this research effort was to identify sources of moisture and other conditions that led to the early rutting problems observed along the five projects.	GPR surveys were shown to provide valuable information regarding the thickness of pavement layers and locations of non-uniform pavement that could be indicative of moisture damage. Although conclusive validation of the use of a GPR survey for detecting moisture-damaged pavement was not obtained in this study, the technique should be further investigated for routine use during pre-construction site investigations. There was not much detail about what kind of GPR equipment used to conduct this research
52	**Shawn Patch**	**2009**	**Identification of Unmarked Graves at B.F. Randolph Cemetery Using Ground Penetrating Radar (GPR):** New South Associates conducted a ground penetrating radar (GPR) survey of selected portions of B.F. Randolph Cemetery, in Richland County, South Carolina. This project was completed under a contract with Historic Columbia Foundation. The purpose of the survey was to investigate the possibility for unmarked graves within property owned by the cemetery. GPR data were collected in nine separate grids spread over various parts of the cemetery.	The GPR data suggested that most open areas in the cemetery likely contain unmarked graves. New South Associates recommends that cemetery authorities carefully evaluate the possibility of closing the cemetery to future burials because of the high probability of disturbing earlier graves. Alternately, GPR survey should be completed for any locations selected for future interments. The survey was conducted with a Geophysical Survey Systems, Inc. (GSSI) SIR 3000 control unit with an attached 400mhz antenna. program, RADAN, was used for analyzing and processing the data.

53	SHRP 2 **S2-R01-RW**	2009	**Encouraging innovation in locating and characterizing underground utilities**: Encouraging Innovation in Locating and Characterizing Underground Utilities project explores underground utility locating practices, examines current and emerging technologies, and identifies potential areas for improvement and for subsequent research.	There is no prospect that a tool will be developed in the foreseeable future that can simply and quickly locate and characterize all of the buried utilities at a site, However, there are many technological improvements that would improve our ability to cost-effectively detect utilities. Technological advances in utility locating and characterization must be accompanied by complementary improvements in management and procedures to allow this technology to be used effectively.
54	VDOT FHWA/VTRC 10-R3	2009	**Evaluation of Jointed Reinforced Concrete Pavement Rehabilitation on I-64 in the Richmond and Hampton Roads Districts of Virginia:** The purpose of this study was to document the initial condition and performance to date of the I-64 project and to summarize similar work performed by state departments of transportation other than VDOT.	Ground-penetrating radar (GPR) was used to assess the layer thickness of the HMA overlay. The GPR system used in this study consisted of a 2.0 GHz air-launched horn antenna and a SIR-20 controller unit, both manufactured by Geophysical Survey Systems, Inc. All data were processed by the software RADAN (version 6.5.3.0) developed by Geophysical Survey Systems, Inc. GPR testing showed that the thickness of the HMA overlay in the majority of the pavement was equal to or slightly greater than the as-designed thickness. However, areas exist where the thickness of the HMA overlay appears to be less than the as-designed thickness. Coring was not performed to confirm the GPR survey results.
55	MnDOT MN/RC 2008-10	2008	**Pavement Evaluation using Ground Penetrating Radar**: The objective of this project was to develop an efficient and accurate algorithm for the back analysis of pavement conditions measured by ground penetrating radar (GPR). In particular, more reliable information about the thickness of the asphalt concrete (AC) layer and the dielectric constants of the AC and base layers were obtained from the electromagnetic field measurements performed on roads using GPR.	A brief introduction to the existing methodology for interpreting GPR images is reviewed, and the theory associated with electromagnetic wave propagation in layered structures is described. Utilizing the full waveform solution, algorithms for back analysis of pavement conditions were developed based on the artificial neural network approach and the frequency response function concept. Software called "GopherGPR" uses the GPR signal from one antenna to interpret the characteristics of the AC layer with no assumptions on material properties. Thus, the new technique has the capability of providing information not previously available.

56	VTrans 2008-7	2008	**Detection and mitigation of subsidence and voids on Vermont roadways: I-89 Hartford and US 7 Manchester, Vermont**: The objective was to assess the performance of three non-destructive geophysical methods (GPR, CCR, and FWD) for characterizing the causes of subsidence as well as determine the effectiveness and feasibility of employing these methods for characterizing the subsidence conditions.	GSSI radar antennas with 200, 400, and 900 MHz and a GSSI SIR 3000 controller were used. This range of frequencies provided varying compromises between depth of penetration and range/object resolution. The 400 and 900 MHz antennas were cart-mounted, enabling spatial triggering from the road wheel with resolutions to 0.1-0.2 ft over 100 feet with depth penetrations of roughly 12 ft and 7 ft. respectively. The larger 200-MHz antenna was dragged on a radar-transparent sled with an approximate resolution of 0.5 ft within 100 ft with a depth penetration of roughly 15 ft. GPR data revealed the remediation history of the site. The 400-MHz antenna surveys yielded the best results, with sufficient penetration of the patch to resolve small features beneath the overlay.
57	WisDOT SPR# 0092-07-07	2008	**Evaluation of Fiberglass Wrapped Concrete Bridge Columns**: The main purpose of this project is to assess the effectiveness of the fiberglass wrapping in reducing the corrosion degradation rate of the columns. The research team tested a total of eight different bridge columns to evaluate the integrity of the reinforced concrete in fiberglass-wrapped and non-wrapped columns. These tests include: P wave velocity measurements, P-wave and ground penetrating radar tomographic imaging, half-cell potential, and determination of chloride ion content.	A Sensors & Software pulseEKKO 100 Ground Penetrating Radar (GPR) system was used to collect data for the evaluation of electromagnetic properties (permittivity and conductivity) of the concrete columns. The goal of this test was to evaluate distribution of volumetric water content (related to the measured electromagnetic wave velocity) and chlorine ion content (related to the attenuation of the collected signal). These results could be then related to potential corrosion activity in the columns. That is, lower velocities indicate greater volumetric water content, while larger signal attenuations indicate greater electrical conductivity (i.e., Cl and water content in the columns). The test setup consisted of two 200 MHz antennae connected through fiber optic cables to a driver and data acquisition consoled and driven by a laptop computer. The collected data were post processing, reduced and interpreted using the pulseEKKO View software. P-wave and electromagnetic wave (GPR) travel-time data and tomographic images were used to evaluate the integrity of concrete column. Not much discussion about the advantage or disadvantage of using the GPR.
58	WSDOT Project DTFH61-05-C-00008, Task No. 8	2008	**Detection of voids in prestressed concrete bridges using Thermal imaging and ground-penetrating radar**: The objective was to detect simulated air voids within grouted post-tensioning ducts, thus locating areas where the post tensioning steel strands are vulnerable to corrosion	Ground-penetrating radar (GPR) inspection was conducted on fourteen concrete specimens between August and October 2007. Based on the GPR surveys conducted in this study, it was apparent that the detection of post-tensioning strands and simulated voids within grouted ducts embedded in concrete is possible with a 1.5 GHz GPR system. The layout of the top layer of steel reinforcement in each concrete specimen was evident in the GPR images, but the bottom layer of reinforcement was not clearly detected since it was effectively “hidden” beneath the top layer of rebar. Although none of the post-tensioning strands and simulated air voids within the grouted steel ducts was detectable, simulated voids within plastic ducts were generally detectable in GPR images. The high dielectric constant of the steel ducts did not allow the microwaves to transmit through the surface of the duct and reach the simulated voids. However, the general location of the duct, its orientation and its depth in the concrete were accurately determined using GPR. Thus it can be inferred that the void orientation is critical for detection in GPR images

59	FL/DOT/SMO/07-505	2007	**Accuracy and repeatability of ground penetrating radar for surface layer thickness estimation of Florida roadways**: The primary objective of this study is to evaluate the accuracy and repeatability of FDOT's 2.0 GHz air-launched GPR system for measuring the bound surface layer thickness of typical Florida pavements. A total of 9 in service pavements have been selected and studied.	The results showed that the GPR system is reliable in terms of both accuracy and repeatability. The pavement thicknesses estimated from stationary GPR data resulted in overall average absolute deviations of 0.4 inches for HMA and 0.6 inches for PCC without the aid of calibration cores. These results were further improved to be 0.3 inches and 0.4 inches for HMA and PCC, respectively, when the cores were used to calibrate the velocities.
60	**Lawrence B. Conyers**	**2006**	**Ground-Penetrating Radar** **Techniques to Discover and Map Historic Graves:** GPR devices can measure physical and chemical changes in the ground. These changes may be related to grave shafts, coffins, void spaces, and even the human remains themselves**.** This paper provides a very nice summarization of literature search that is related to the use of the GPR technology in archeology.	GPR can often determine grave attributes such as depth of burial, grave size, type of caskets and their orientation; numbers of graves in certain locations; and the spatial distribution of graves within certain areas of a cemetery. The success of GPR surveys in historical archaeology is largely dependent on soil and sediment mineralogy, clay content, ground moisture, depth of burial and surface topography, and the type of surface soils present. Most GPR surveys used to detect and map historic graves use antennas that range in frequency between 900 and 300 MHz, which produces good resolution data at depths between about 1 m and 3 m, respectively.
61	NYSDOT **C-04-04**	2006	**Applications of Ground Penetrating Radar for Highway Pavements:** The research project objective was to develop an implementation strategy for the use of Ground Penetrating Radar (GPR) technology to address pavement systems and underground utilities. The project was divided into three tasks. Task 1 dealt with a review in the state-of-the-art in technology, relevant applications, and regulations in the use of GPR. Task 2 discussed the effort and results of GPR survey projects on pavements systems and underground utilities that were performed as part of this project in selected locations. Task 3 developed an implementation strategy for NYSDOT for defining and procuring GPR services in addressing problems in pavement systems and mapping & locating underground utilities.	For Underground Utilities: The subsurface utility imaging systems should be composed of an integrated system consisting of: · A multi-channel GPR system with associated software capable of producing three dimensional subsurface images. · An available EMI system including capability for inversion of the EMI data to independently obtain depth to utilities · An infield integration system capable of handling GPS or laser positioning, GPR, and EMI · Software for 3-D processing, visualization, and interpretation · Final output in the Department's CAD and data formats While a single GPR antenna can be used to collect information for locating subsurface utilities at the project level, it is very effort-intensive and the collected information can normally be portrayed in only two dimensions (X and Z). It is possible to produce three dimensional data with single channel system but with significant limits in both accuracy and cost-effectiveness. The most useful approach, from the perspectives of both productivity rates and obtaining the most effective final product, is the use of a multi-channel array of antennas.

62	SDDoT	2006	**Feasibility of Using Ground Penetrating Radar (GPR) for Pavements, Utilities, and Bridges**: The evaluation was carried out through a literature review, a survey of SDDOT personnel, a survey of the use of GPR by other state agencies, a series of demonstration projects, a cost/benefit analysis, and a utilization plan.	1. The literature review and surveys indicated that GPR are for pavement thickness and bridge deck condition evaluations. 2.The demonstration projects focused on these two applications, and on geotechnical applications for fault detection and evaluation of subgrade moisture content 3. The bridge deck evaluation showed that the GPR technology worked well for determining corrosion-induced delamination in overlaid decks with slab-on-girder construction, but was less effective on one-way slab bridges. 4. The pavement evaluations, conducted on two AC and one PCC section, demonstrated the ability to accurately measure and plot pavement layer thickness. 5. The subgrade moisture evaluation showed good correlation between GPR and boring data, and demonstrated the ability of GPR to map out variations of subgrade moisture content. 6. The fault evaluation did not produce positive results, due to the attenuation caused by the high clay content in South Dakota soil. 7. A cost-benefit analysis was conducted for different scenarios shows benefit/cost ratios range from 1.98 for the bare deck delamination evaluation (GPR vs. sounding) to 113 for thickness quality assurance of new pavement 8. The analysis also showed the tradeoffs between using outside consultants vs. doing the work in-house. A utilization and equipment plan recommended that SDDOT initially use consultants for the lower volumes of startup work, and then move into owning and operating equipment and analyzing data when then volume increase warrants the additional investment.
63	TxDOT, 0-4495-S	2006	**Integrating Deflection and Ground Penetrating Radar Data for Pavement Evaluation:** TxDOT has used both falling weight deflectometers (FWD) and ground penetrating radar (GPR) technology for more than 10 years to provide structural information about its pavements. GPR data used to be processed independently of FWD analysis.	TxDOT developed the PAVECHECK program to integrate both data processing and reporting. The complete system provides TxDOT pavement engineers with a tool for diagnosing pavement problems and for assisting in selecting the optimal pavement repair strategy. TxDOT recommended that the PAVECHECK program should be thoroughly evaluated on several forensic and a rehabilitation projects and that was beyond the scope of this research effort.

64	VDOT VTRC 06-R37	2006	**Use of Nondestructive Evaluation to Detect Moisture in Flexible Pavements**: The purpose of this study was to identify the currently available nondestructive evaluation technology that holds the greatest potential to detect moisture in flexible pavements and then apply the technology in multiple locations throughout Virginia. Ground-penetrating radar (GPR) was chosen for use in a field investigation because of its ability to measure large areal extents and reports of successful implementation by other researchers. This technology was used to determine the moisture content of the subgrade beneath five flexible pavement sections in Virginia.	This study showed that GPR can identify areas of varying dielectric constant attributed to variations in the moisture content of the subgrade of various pavement sections. The GPR survey was conducted at normal driving speeds, and data were collected at a sampling rate of 1 scan per foot. For each site, three scans were collected in the travel lane (in the right wheel path, the center of the lane, and in the left wheel path). Existing passing lanes were also scanned. Initial data processing subdivided each pavement section into a three-layer system composed of the hot-mix asphalt layers, the aggregate base layers, and the subgrade. The processing also included calculating the dielectric constant of each layer. These raw data were used to conduct further analyses considering data from only the subgrade. The data were normalized to highlight those areas with the highest dielectric constants since it is known that moisture will have the greatest influence on the dielectric properties of the material. The testing was performed during a dry period in the summer. The GPR system employed was manufactured by Geophysical Survey Systems, Inc. (GSSI), and consisted of a 1.0 GHz air coupled horn antenna controlled by a SIR-20 system that collected and recorded the data. Recommendations: VTRC should revisit the sites tested in this study after a precipitation event to determine the change in subgrade moisture condition and quality of pavement drainage in accordance with the 1993 AASHTO Guide for the Design of Pavement Structures (AASHTO, 1993). Also, should investigate whether the statistical methodology for evaluating the GPR results could be correlated to quantitative subgrade moisture content across a variety of subgrade and pavement conditions through the use of soil borings in a future study.
65	AHTD	2005	**Use of ground penetrating radar in a Pavement management system:** The Arkansas State Highway and Transportation Department (AHTD) contracted with Infrasense, Inc. of Arlington, Massachusetts to provide pavement layer thickness data utilizing Ground Penetrating Radar (GPR) technology. The focus of the research was to determine if GPR could provide relatively fast and reliable thickness data on a network level survey for use in a Pavement Management System (PMS) without the benefit of calibration cores. Secondary data was also provided to determine if GPR could be used to locate voids in certain pavement structures, excessive moisture levels in the base and subgrade, and to determine if GPR could provide accurate characteristic information on bridge decks.	The results of the data analysis indicated that on asphalt pavements GPR can provide reliable thickness data for use at the network level. Concrete pavements did not provide the same results. Known differences in pavement thickness were evident but GPR measured thickness did not compare well to measures of core samples taken from the pavements. However, based on previous research studies by other agencies this was not unexpected. A 1.0 GHz dual horn antenna GPR system manufactured by (GSSI) was used to collect the data on approximately fifty miles of pavements in the central Arkansas area. Eight pavement sections of varying lengths and cross-sections were chosen for the analysis of pavement layer thickness. Analysis of the secondary data was outside of the scope of this report and findings were not discussed.

66	INDOT FHWA/IN/JTRP-2003/12	2003	**Imaging and Locating Buried Utilities**: imaging technologies that have potential for being applied in locating underground utilities were identified through literature review and case studies and the conditions under which use of these technologies are most appropriate were analyzed.	Based on the characterizations of imaging technologies, a decision tool named IMAGTECH was developed in order to provide site engineers/technicians with a user-friendly tool in selecting appropriate imaging technologies. Ten criteria were chosen to assist in the selection of the most appropriate imaging technology. The criteria include type of utility, material of utility, joint type of metallic pipe, special material for detection, access point to utility, surface condition, inner state of utility, soil type, the depth of utility and the diameter of utility. One of the findings in this report is that the detectable range of GPR depends on the frequency range used in the GPR instrument, the type and the moisture content of soil. In practice, the GPR is difficult to detect pipes of any size buried beyond six feet from the surface according to the following: Diameter (in) / Depth (ft) > 1 ----- applicable to GPR Diameter (in) / Depth (ft) < 1 ----- inapplicable to GPR
67	**William J. Johnson, Council for West Virginia Archaeology Spring Workshop Charleston, West Virginia**	**2003**	**Geophysical detection of graves – Basic background and case histories from historic cemeteries:** This paper reviews the three most commonly applied geophysical techniques and presents several case histories documenting the detection of graves. The main physical basis for grave detection is that grave shafts represent a disruption to the natural layering of the ground. Disruptions to soil layers can often be detected with GPR. Grave shafts represent a mixing of the soil types excavated, so there is usually a physical contrast of the grave fill with natural soil. Graves are often manifested by magnetic lows because they disrupt the natural fabric of soil magnetization and are also often delineated by resistivity lows, primarily because grave fill is not as dense as natural soil and can therefore retain higher moisture content.	In most cases, the best technique for mapping graves is ground penetrating radar (GPR), but electrical and magnetic measurements can also be effective. Nevertheless, the identification of graves can be a complicated problem, depending on the age of the graves and soil conditions. Surface conditions, soil conditions, type and age of burial and condition of the coffins are all important factors in determining the effectiveness and costs of geophysical surveying. The most effective surveys will be multidisciplinary, where the geophysicist and archaeologist are teamed together to interpret the data. The scope of the report was general in discussing the applications of the geophysical methods. No specific details about the surveys.
68	**Lewis, Owen, and Narwold**	**2002**	**GPR as a tool for detecting problems in highway-related construction and maintenance:** Three case studies utilizing GPR in highway related projects are presented. The first case involves the use of GPR for void detection and delineation caused by washout from an old brick-lined sewer beneath pavement showing varying signs of subsidence. A secondary purpose of this study was also the delineation of the sewer itself. The second case involves GPR evaluation of possible construction deficiencies related to cracking observed of a newly The third case involves GPR evaluation of possible construction deficiencies in a concrete bridge approach slab constructed soundwall. The third case involves GPR evaluation of possible construction deficiencies in a concrete bridge approach slab.	In the first case the GPR was able to delineate the void/washout/ loose soil zone and the location of the sewer. In the second case, Efforts at void location within the soundwall and adjacent to rebar were mostly unsuccessful due to antennae resolution, although two potential voids were imaged. Although rebar posed difficulties in allowing the GPR signal to penetrate the wall, the rebar imaging itself gave indications of construction weaknesses. Correct antenna orientation allowed the location of soundwall bond beams and vertical rebar. Zones of excess concrete, missing bond beams, and vertical rebar were detected. In the third case, Variations in the concrete and rebar mat (relative to baseline data collected nearby), and other radar anomalies indicate poor construction. All investigations involved a Sensors and Software PulseEKKO 1000 acquisition system with different frequency antennas. A software package accompanying the acquisition system was used in collecting, processing, analyzing and displaying the radar data. Both the 900 MHz and 1200 MHz antennas were employed.

69	**Brady, T., S. Cardimona and N. Anderson**	**2000**	**Detection and Delineation of Underground Fuel Storage Tanks and Associated Utility Lines Using Electromagnetic Induction and Ground Penetrating Radar Methods:** The proposed expansion of selected highways in Missouri required several gas stations to be demolished. During demolition of a gas station property, damage can occur to the underground fuel storage tanks and associated utility lines. Noninvasive mapping of these features prior to excavation can greatly reduce problems associated with unexpected tank discovery. In this study, nonintrusive geophysical methods were used to map the underground fuel storage tanks and associated utility lines	Ground penetrating radar proved important for the accurate delineation of these tanks. The integrated use of ground penetrating radar and electromagnetic induction methods allowed them to create a map of exact tank locations at each site in this study. A 400 MHz ground coupled antenna was used to detect the tanks which were approximately 1.5 meters deep.
70	WSDOT	2015-2016	**Ground Penetrating Radar (GPR) to Determine In-Place Asphalt Density** : The goal of the "GPR to Determine In-Place Asphalt Density" project is to purchase a GPR device that uses dielectric contents of the asphalt mix to determine the asphalt density and whether this type of device works as well as the methods they currently use (nuclear density gauge and cores).	Depending on the timing of the purchase, they expect to be in the field testing in either 2015 or 2016. No further information on this project is available.
71	KDOT	2014-2016	**Bridge Deck Reinforcing Steel Cover Verification by Utilizing Ground Penetrating Radar:** This project will investigate the use of Ground Penetrating Radar (GPR) as an alternative to the pachometer testing of reinforcing steel concrete cover thicknesses for bridge deck quality assurance/quality control (QA/QC). The objective of this project is to provide a new method for evaluating the concrete cover over the steel reinforcement on both new bridge construction and bridge deck rehabilitation projects. GPR technology can be more accurate, more thorough, more cost efficient, and safer than the current standard of practice of utilizing the older pachometer technology.	Still active

72	MoDoT	2013-2015	**Air-Launched GPR Evaluation for Rapid Assessment of MoDOT Bridge Decks:** The objectives of this study are to demonstrate the utility of the air-launched ground penetrating radar (GPR) tool in rapidly evaluating the general condition of Missouri Department of Transportation (MoDOT) bridge decks and confirm that it can be implemented as part of a long-term program that enables faster, better, and more cost-effective bridge deck assessments. The results of the deck evaluation conducted using air-launched GPR will enable better, more cost-effective decisions regarding different repair or treatment options. Results will also enable more cost-effective decisions regarding whether a more comprehensive bridge deck investigation should be conducted on a given bridge.	Still active
73	UDOT	2011-Present	http://www.udot.utah.gov/main/f?p=100:pg:0::::V,T:,2131 **Ground Penetrating Radar (GPR)** This is fairly new data collected to gather information about the pavement thickness. Several hundred miles were collected in 2003, 2004 & 2005. It is expected that additional miles will continue to be collected.	There are two maps available and a report showing the data collected using GPR. The first GPR map shows the (HMA) thickness ranges for the routes with data available The second GPR map shows the years the data was collected. The data report shows the mile by mile thickness interpretations for the pavement and base. Detailed files are available with the raw scanned interfaces graphed. These are useful to investigate consistency in thickness and locate questionable areas to assist with selecting coring locations. These are on DVD or CD in several formats in each Region -- contact the Region Pavement Management Engineer or Gary Kuhl at gkuhl@utah.gov

References

1- Minnesota Pavement Design Manual. (2016). Minnesota Department of Transportation. Retrieved September 20, 2016, from http://www.dot.state.mn.us/materials/pvmtdesign/manual.html

2- Tarefder, R. (2015). Use of Falling Weight Deflectometer and Ground Penetrating Radar in pavement design, maintenance and management (Project. No. NM12SP-01). New Mexico Department of Transportation Research Bureau, New Mexico.

3- Harris, D., Imbrock, P., & Weiss, J. (2015). Using ground penetrating radar to detect indicators of premature joint deterioration in concrete pavements.

4- Buchner, C. A., Walker, C., & Clifton, A. (2014). Geophysical survey of unmarked graves at the Unity Baptist Church on highway 82, Ashley County, Arkansas (Draft Report, Project No. 34055). Panamerican Consultants, Inc., Memphis, Tennessee. A draft report prepared for the Arkansas Highway and Transportation Department (AHTD Job NO. 020534).

5- Young, G. N., & Kennedy, C. M. (2014). Utility Locating Technology Development Using Multisensor Platforms (No. SHRP 2 Renewal Project R01B). Transportation Research Board of the National Academies, Washington, D.C.

6- Hammerschmidt, A., Ziolkowski, C., Huebler, J., Givens, M., & McCarty, J. (2014). Innovations to Locate Stacked or Deep Utilities (No. SHRP 2 Renewal Project R01C). Transportation Research Board of The National Academies.

7- Lowe, K. M., Wallis, L. A., Pardoe, C., Marwick, B., Clarkson, C., Manne, T., ... & Fullagar, R. (2014). Ground-penetrating radar and burial practices in western Arnhem Land, Australia. Archaeology in Oceania, 49(3): 148-157.

8- Sneed, L.H., Anderson, N., and Torgashov, E. (2014). “Non-Destructive Evaluation of MoDOT Bridge Decks – Pilot Study (CMR14-010). Missouri Department of Transportation, Jefferson City, MO.

9- Jaw, S. W., & Hashim, M. (2014). Urban underground pipelines mapping using ground penetrating radar. In IOP Conference Series: Earth and Environmental Science (Vol. 18, No. 1, p. 012167). IOP Publishing.

10- So-Deep, Incorporation. (2014). Field evaluation of tools developed in the SHRP 2 R01B and R01C Projects (No. SHRP 2 Renewal Project R01B and R01C). Transportation Research Board of the National Academies, Washington, D.C.

11- Heitzman, M, Tran, N. H., & Maser, K. (2014). Nondestructive Testing to Identify Delaminations Between HMA Layers: Phase III (Final Report. No. R06(D). Transportation Research Board of The National Academies.

12- Sebesta, S., & Scullion, T. (2014). Pre-Implementation of Infrared and Ground-Penetrating Radar Technologies for Improving Asphalt Mixture Quality (No. SHRP 2 Renewal Project R06C). Texas A&M Transportation Institute, The Texas A&M University System, College Station, Texas. Transportation Research Board of the National Academies, Washington, D.C.

13- Wimsatt, A. J., et al., (2014). Mapping voids, debonding, delaminations, moisture, and other defects behind or within tunnel linings (No. SHRP 2 Report S2 R06G-RR-1). Transportation Research Board of the National Academies, Washington, D.C.

14- Buchner, C. A., Walker, C., & Clifton, A. (2013). Geophysical survey of the GoForth cemetery (31N1262) on US highway 167, Independence County, Arkansas (Final Report, Project No. 33076). Panamerican Consultants, Inc., Memphis, Tennessee. A final report prepared for the Arkansas Highway and Transportation Department (AHTD Job NO. 050213).

15- Buchner, C. A. (2013). Geophysical survey of the Stout cemetery near highway 7, south of Dover, Pope County, Arkansas (Draft Rep. No. 33078). Panamerican Consultants, Memphis, Tennessee. A draft report prepared for the Arkansas Highway and Transportation Department (AHTD Job NO. 080164).

16- Nguyen, A. (2013). Changes in Pavement Section for BB 0613. Arkansas Highway and Transportation Department, Little Rock, Arkansas.

17- Rashed, M. A., & Al-Garni, M. A. (2013). On the application of GPR for locating underground utilities in urban areas. Arabian Journal of Geosciences, 6(9): 3505-3511.

18- Cheng, N. F., Conrad Tang, H. W., & Chan, C. T. (2013). Identification and positioning of underground utilities using ground penetrating radar (GPR). Sustainable Environ Res, 23(2), 141-152.

19- Vennapusa, P., White, D. J., & Miller, D. K. (2013). Western Iowa Missouri River Flooding--Geo-Infrastructure Damage Assessment, Repair and Mitigation Strategies (No. IHRB Project TR-638). Center for Earthworks Engineering Research, Iowa State University, Ames, Iowa.

20- Ismail, N. A., Saad, R., Muztaza, N. M., & Ali, N. (2013). Predictive mapping of underground utilities using ground penetrating radar. Caspian Journal of Applied Sciences Research, 2, pp. 104-108.

21- Uddin, W. (2013). A Synthesis Study of Noncontact Nondestructive Evaluation of Top-down Cracking in Asphalt Pavements (Final Report No. FHWA/MS-DOT-RD-13-255). Center for

Advanced Infrastructure Technology, The University of Mississippi, Carrier 203B University, Mississippi.

22- Aktan, H., Attanayake, U., Mohammed, A. W., & Wiggenhauser, H. (2013). Research on Non-Destructive Evaluation-Workshop (Final Report No. RC-1597). Western Michigan University, Kalamazoo, Michigan.

23- Tang, S., Guzina, B., & Labuz, J. (2013). Implementation of Pavement Evaluation Tools (Final Report No. MN/RC 2013-29). Department of Civil Engineering, University of Minnesota, Minneapolis, Minnesota.

24- Patch, S. M., Lowry, S., Botwick, B., & Davis, V. (2013). Grave marker assessment and ground penetrating radar survey of the Woodlawn Baptist Church Cemetery (Rep. No. 2152). Fairfax County, Virginia: Federal Highway Administration.

25- Heitzman, M., Maser, K., Tran, N. H., Brown, R., Bell, H., Holland, S. D., ... & Hiltunen, D. (2013). Nondestructive Testing to Identify Delaminations Between HMA Layers Volume 1-Summary. (No. SHRP 2 Report S2-R06D-RR-1). Transportation Research Board of the National Academies.

26- Gucunski, N., Imani, A., Romero, F., Nazarian, S., Yuan, D., Wiggenhauser, H., et al. (2013). Nondestructive testing to identify concrete bridge deck deterioration (No. SHRP 2 Report S2-R06A-RR-1). Transportation Research Board, Washington, D.C.

27- Sutton, M. J., & Conyers, L. B. (2013). Understanding cultural history using ground-penetrating radar mapping of unmarked graves in the Mapoon Mission Cemetery, Western Cape York, Queensland, Australia. International Journal of Historical Archaeology, 17(4), 782-805.

28- Thieme, Donald M., (2013). Identification of unmarked graves at two historic cemeteries in Georgia. Early Georgia 41(2):257–274.

29- Wahab, W. A., Jaafar, J., Yassin, I. M., & Ibrahim, M. R. (2013). Interpretation of Ground Penetrating Radar (GPR) image for detecting and estimating buried pipes and cables. In Control System, Computing and Engineering (ICCSCE), 2013 IEEE International Conference on (pp. 361-364). IEEE.

30- Schmitt, R. L., Faheem, A., & Al-Qadi, I. L. (2013). Investigation and Development of a Non-Destructive System to Evaluate Critical Properties of Asphalt Pavements during the Compaction Process (No. 0092-11-01).

31- Woodward, N., & Fuselier, T. (2013). Cooperative Geotechnical Designs to Build on Liquefiable and Compressible Soil in Salem, Massachusetts. The 64th Highway Geology Symposium (HGS).

32- Papanicolaou, A. N., Moustakidis, I., Tsakiris, A., Wilson, C., & Abban, B. (2013). Prediction of Scour Depth in Gravel Bed Rivers using Radio Frequency IDs: Application to the Skagit River (Final Report No. WA-RD 821.1). The Washington State Department of Transportation Research Program.

33- Schultz, J. J. (2012). Detecting buried remains using ground penetrating radar. Department of Anthropology, University of Central Florida.

34- Robison, T. W., & Tanner, J. E. (2012). Bridge deck evaluation using non-destructive test methods (Report No. FHWA-WY-10/07F). Department of Civil and Architectural Engineering, University of Wyoming, Laramie, Wyoming.

35- Zier, C. J., Kineer, C. C., Bryant, J. E., & Sturm, J. O. (2011). Evaluative test excavation of eleven historic sites for the Colorado Department of Transportation Interstate 25 New Pueblo Freeway Improvement Project, Pueblo County, Colorado. Centennial Archaeology, Inc. and TEC, Inc.

36- Nazef, A. (2011). US 27/SR 25 Pavement Evaluation (FL/DOT/SMO/11-542). Florida Department of Transportation.

37- Al-Qadhi, I. L., Leng, Z., & Larkin, A. (2011). In-Place Hot Mix Asphalt Density Estimation Using Ground Penetrating Radar. (Final Report No. 11-096). Department of Civil and Environment Engineering, University of Illinois at Urbana-Champaign Urbana, Illinois.

38- Gucunski, N., Romero, F., Kruschwitz, S., Feldmann, R., & Parvardeh, H. (2011). Comprehensive bridge deck deterioration mapping of nine bridges by nondestructive evaluation technologies (Final Report No. Project SPR-NDEB (90)--8H-00). Rutgers, The State University of New Jersey, Center for Advanced Infrastructure and Transportation, Piscataway, New Jersey.

39- Maser, K. R., Puccinelli, J., Punnackal, T., & Carmichael, A. (2011). Ground penetrating radar (GPR) analysis: Phase II field evaluation (Final Report No. FHWA/MT-11-002/8201-001). A report prepared for Montana Department of Transportation. Infrasense, Inc., Arlington, Massachusetts.

40- Smart, A. L. (2011). Pilot Study-Rolling Wheel Deflectometer, Falling Weigh Deflectometer, And Ground Penetrating Radar on New Hampshire Roadways (Final Report No. FHWA-NH-RD-14282N). New Hampshire Department of Transportation, Arlington, Massachusetts.

41- Katz, A., Karaa, F., & Niver, E. (2011). Innovative and effective techniques for locating underground conduits (Final Report No. FHWA/NJ-2011-001). The College of New Jersey, Ewing, New Jersey.

42- Sterling, R. L., Allouche, E. N., Anspach, J., Matthews, J., Berchmans, J., & Simicevic, J. (2011). Development of the Selection Assistant for Utility Locating Technologies (No. SHRP 2 Report S2-R01-RW-2). Transportation Research Board of The National Academies, Washington, D.C.

43- Hall, K. D., Xiao, X., & Wang, K. C. (2010). Thickness estimation of existing pavements using nondestructive techniques: matching accuracy to application. In Transportation Research Board 89th Annual Meeting (No. 10-2480).

44- Guada, I., Wu, R., Signore, J., Lea, J., Harvey, J., & Jones, D. (2010). Preliminary Project Study Report for Shasta 299, PM 51.8–60 (Technical Report No. CA10-1895). University of California Pavement Research Center, Civil and Environmental Engineering, University of California, Davis, Davis California.

45- Dionne, C. A., Wardlaw, D. K., & Schultz, J. J. (2010). Delineation and resolution of cemetery graves using a conductivity meter and ground-penetrating radar. Technical Briefs in Historical Archaeology, 5, 20-30.

46- Doolittle, J. A., & Bellantoni, N. F. (2010). The search for graves with ground-penetrating radar in Connecticut. Journal of Archaeological Science, 37(5), 941-949.

47- Diefenderfer, B. K., & Maupin Jr, G. W. (2010). Field trials of high-modulus high-binder-content base layer hot-mix asphalt mixtures (Final Report No. FHWA/VTRC 11-R2). Virginia Transportation Research Council, Charlottesville, Virginia.

48- Lebens, M. A. (2010). Incorporating GPS and Mapping Capability into Ground Penetrating Radar (GPR) Operations for Pavement Thickness Evaluations (Final Report No. MN/RC 2010-37). Minnesota Department of Transportation, Office of Materials and Road, Maplewood, Minnesota.

49- Pailes, B. M., Brown, M. C., & Sharp, S. R. (2010). Condition assessment and determination of methods for evaluating corrosion damage in piles encapsulated in protective jackets on the Hampton Roads bridge-tunnel (Final Report No. VTRC 10-R13). Virginia Transportation Research Council, Charlottesville, Virginia.

50- Maser, K. R., & Puccinelli, J. (2009). Ground Penetrating Radar (GPR) Analysis: Phase 1 (Final Report No. FHWA/MT-09-005/8201). A report prepared for Montana Department of Transportation. Infrasense, Inc., Arlington, Massachusetts.

51- Scholz, T. V., & Rajendran, S. (2009). Investigating premature pavement failure due to moisture (Final Report No. FHWA-OR-RD-10-02). Kiewit Center for Infrastructure and Transportation, Oregon State University, Corvallis, Oregon.

52- Patch, S. (2009). Identification of unmarked graves at B.F. Randolph Cemetery using ground penetrating radar (GPR) (Rep. No. 1748). Richland County, South Carolina: Historic Columbia Foundation.

53- Sterling, R. L., Anspach, J. H., Allouche, E. N., Simicevic, J., Rogers, C. D., Weston, K. E., & Hayes, K. (2009). Encouraging innovation in locating and characterizing underground utilities (No. SHRP 2 Report S2-R01-RW). Transportation Research Board of The National Academies, Washington, D.C.

54- Diefenderer, B. K., & Mokarem, D. W. (2009). Evaluation of jointed reinforced concrete pavement rehabilitation on I-64 in the Richmond and Hampton roads districts of Virginia (Final Report No. FHWA/VTRC 10-R3). Virginia Transportation Research Council, Charlottesville, Virginia.

55- CAO, Y., GUZINA, B. B. & LABUZ, J. F. (2008). Pavement evaluation using ground penetrating radar (MN/RC 2008-10). Department of Civil Engineering, University of Minnesota, Minneapolis, Minnesota.

56- Applied Research Associates, Inc. (2008). Detection and mitigation of subsidence and voids on Vermont roadways: I-89 Hartford and US 7 Manchester (Rep. No. 2008-7). Applied Research Associates, Inc. South Royalton, Vermont.

57- Fratta, D., Pincheira, J. A., & Kim, K. S. (2008). Evaluation of Fiberglass Wrapped Concrete Bridge Columns (No. WHRP 08-06). Department of Civil and Environmental Engineering, University of Wisconsin-Madison.

58- Pollock, D. G., Dupuis, K. J., Lacour, B., & Olsen, K. R. (2008). Detection of voids in prestressed concrete bridges using thermal imaging and ground-penetrating radar (Report No. WA-RD 717.1). Washington State Transportation Center, Pullman, Washington.

59- Holzschuher, C., Lee, H., & Greene, J. (2007). Accuracy and Repeatability of Ground Penetrating Radar For Surface Layer Thickness Estimation of Florida Roadways (FL/DOT/SMO/07-505). Florida Department of Transportation.

60- Conyers, L. B. (2006). Ground-penetrating radar techniques to discover and map historic graves. Historical Archaeology, 40(3): 64-73.

61- Grivas, D. A. (2006). Applications of Ground Penetrating Radar for Highway Pavements (Final Report No. C-04-04). Institute for Infrastructure Asset Management, Latham, New York.

62- Maser, K. R. (2006). Feasibility of using Ground Penetrating Radar (GPR) for pavements, utilities, and bridges (Final Report No.SD2005-05-F). A report prepared for the South Dakota Department of Transportation. Infrasense, Inc., Arlington, Massachusetts.

63- LIU, W., & SCULLION, T. (2006). Integrating Deflection and Ground Penetrating Radar Data for Pavement Evaluation.

64- Diefenderfer, B. K., Mokarem, D. W., & Sharp, S. R. (2006). Use of nondestructive evaluation to detect moisture in flexible pavements (Final Report No. VTRC 06-R37). Virginia Transportation Research Council, Charlottesville, Virginia.

65- Evans, M. A. (2005). Use of Ground Penetrating Radar in a Pavement Management System (Final Report No. TRC-0102).

66- Jeong, H. S., Arboleda, C. A., Abraham D. M., Halpin D. W., & Bernold L. E. (2003). Imaging and locating buried utilities (Final Report No. FHWA/IN/JTRP-2003/12). Joint Transportation Research Program, Purdue University, West Lafayette, Indiana.

67- Johnson, W. J. (2003). Geophysical detection of graves-basic background and case histories from historic cemeteries. Council for West Virginia Archaeology Spring Workshop, Charleston, West Virginia.

68- Lewis, J. S., Owen, W. P., & Narwold, C. (2002). GPR as a tool for detecting problems in highway-related construction and maintenance. In Proceedings of 2nd Annual Conference on the Application of Geophysics and NDT Methodologies to Transportation Facilities and Infrastructure (Geophysics2002), 11p.

69- Brady, T., Cardimona, S., & Anderson, N. (2000). Detection and delineation of underground fuel storage tanks and associated utility lines using electromagnetic induction and ground penetrating radar methods. Proceedings of Geophysics, 4-32.

70- Washington State Department of Transportation. (2015-2016). Ground Penetrating Radar (GPR) to Determine In-Place Asphalt Density.

71- Rister, B. (2014-2016). Bridge Deck Reinforcing Steel Cover Verification by Utilizing Ground Penetrating Radar. College of Engineering, University of Kentucky, Lexington, Kentucky.

72- Sneed, L., Anderson, N., & Torgashov, E. (2013-2015). Air-Launched GPR Evaluation for Rapid Assessment of MoDOT Bridge Decks (Final Report No. NUTC R369). Center for Transportation Infrastructure and Safety, NUTC Program, Missouri University of Science and Technology, Rolla, Missouri.

73- Kuhl, G. (Ed.). (2011-present). Ground Penetrating Radar. State of Utah Retrieved September 20, 2016, from http://www.udot.utah.gov/main/f?p=100:pg:0::::V,T:,2131

Appendix 2: Training Manual

Ground Penetrating Radar SIR-4000 System

Training Manual

Reference

Geophysical Survey Systems, Inc. (2016). UtilityScan with SIR 4000, Training Manual.

Outline

SIR-4000 Control Unit

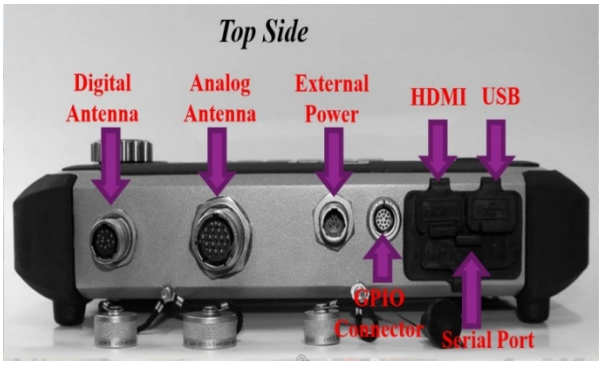

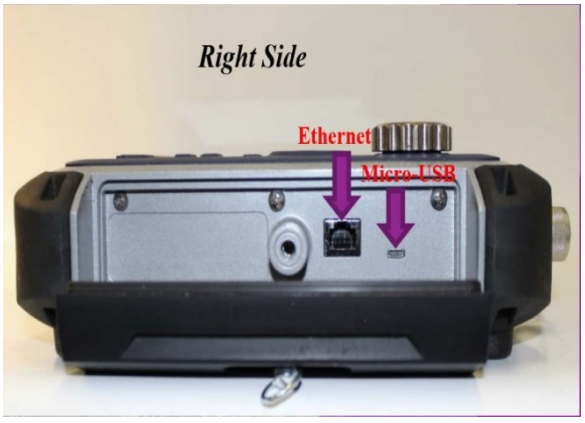

Antennas

1- 1600 MHz - General Purpose Concrete Antenna

The 1600 MHz is a high-resolution, all-purpose antenna used to inspect concrete structures to locate embedded rebar, post tension cables and conduits. It is also a popular choice for bridge deck condition assessment and to determine concrete cover

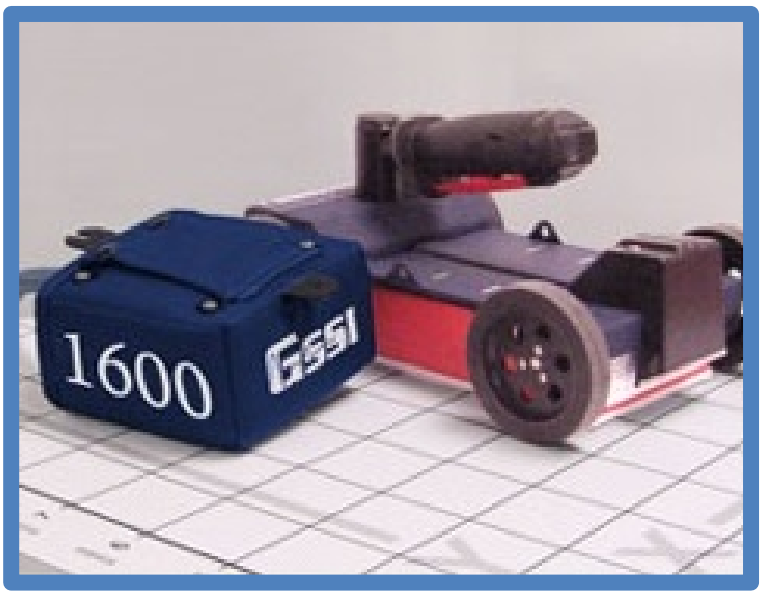

Center Frequency	1600 MHz
Depth Range	0-18 inches (0.5m)
Antenna Weight	4 lbs (1.8 kg)
Dimensions	1.5*4*6.5 in (3.8*10*16.5 cm)
Model	51600S

2- 400 MHz - Utility Detection and Mapping

The 400 MHz is ideally suited for detection and mapping of utility pipes, as well as shallow engineering and environmental applications.

Center Frequency	400 MHz
Depth Range	0-12 ft (0-4 m)
Antenna Weight	11 lbs (5 kg)
Dimensions	12x12x6.5 in (30x30x17 cm)
Model	50400S

3- 200 MHz - Geotechnical and Environmental

The 200 MHz can penetrate to a depth of 9 meters (30 feet), making it ideally suited for geotechnical and environmental applications, as well as archaeological investigations.

Center Frequency	200 MHz
Depth Range	0-30 ft (0-9 m)
Antenna Weight	45 lbs (20.5 kg)
Dimensions	24x24x12 in (60x60x30 cm)
Model	5106 (U.S./Canada), 5106A (International)

Section 1: Startup System

1- Assemble your cart as shown in the assembly instructions in the manual.

2- Attach the SIR® 4000 to the bracket on the cart, connect the antenna control cable, and insert a battery. Push the green power button to turn the system on.

3- After the system boots-up you will see the Introduction screen. The top row of icons allows the user to select among various operation modes. Using either the control knob or the directional keypad, highlight Expert Mode and push enter to select. Note: upon the initial release of the SIR 4000 Expert Mode will automatically be selected.

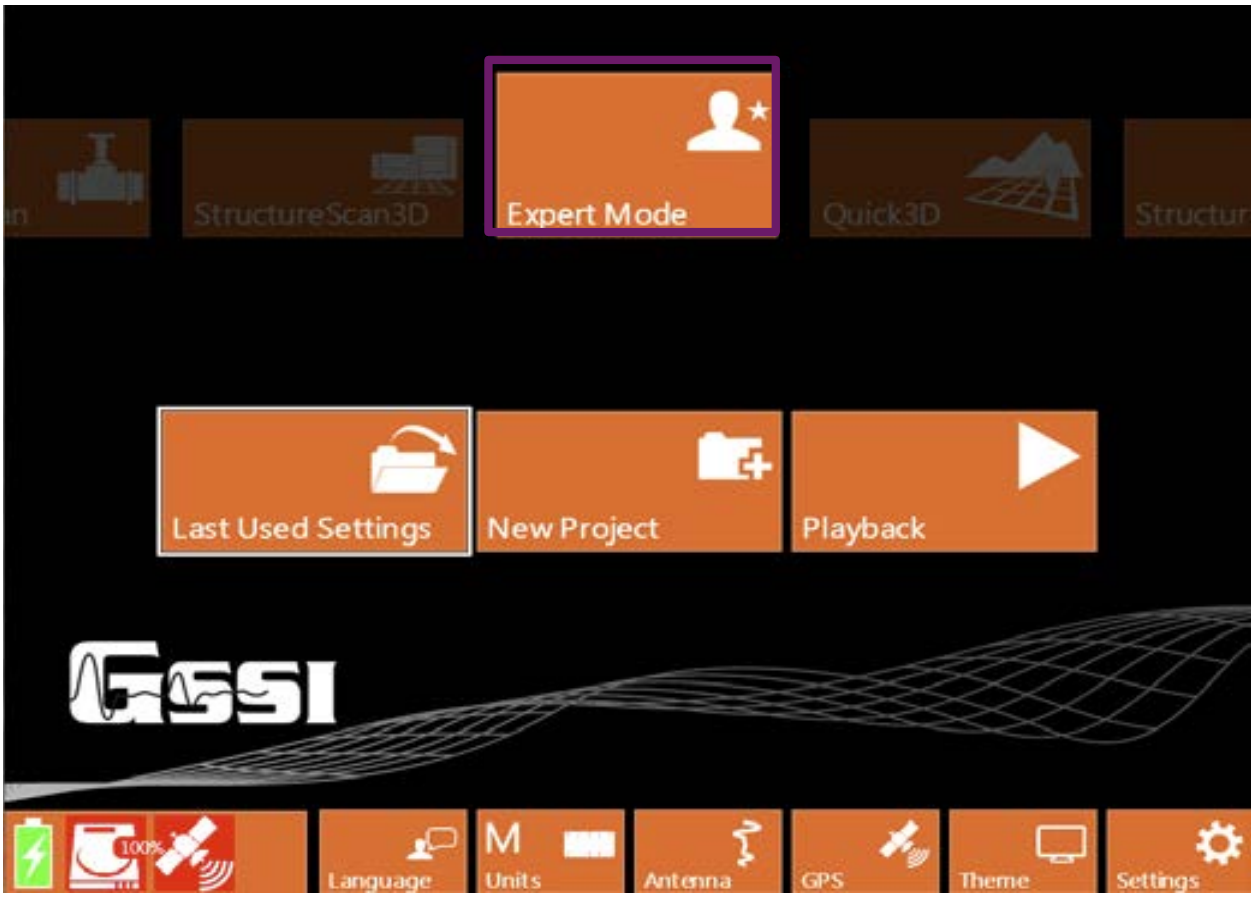

4- Along the bottom of the screen is a toolbar allowing access to change general system settings and universal setup options. Push the Units button to change units between English and Metric. The units displayed in bold are the ones currently selected.

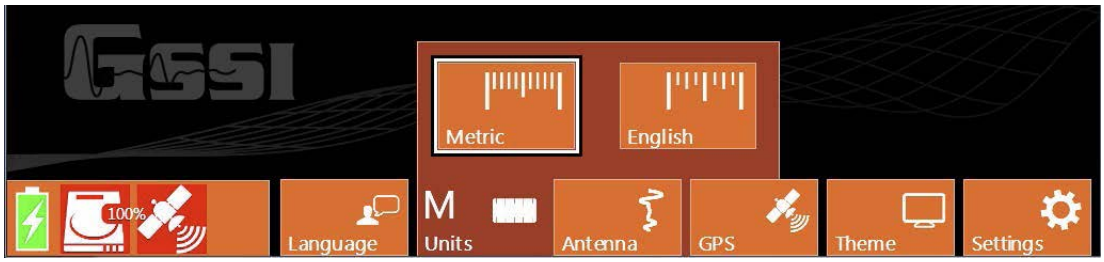

5- Next to the Units is the Antenna button. If the antenna connected has a "Smart ID" the SIR 4000 will automatically recognize and display the antenna model (Ex: 50400S). If the antenna connected is an older analog model without "Smart ID" push the Antenna button. Highlight the Antenna Type box and select from the list the type of antenna you have connected. Select done when finished.

6- The last toolbar button is Settings; push this to access additional universal setup options such as date and time.

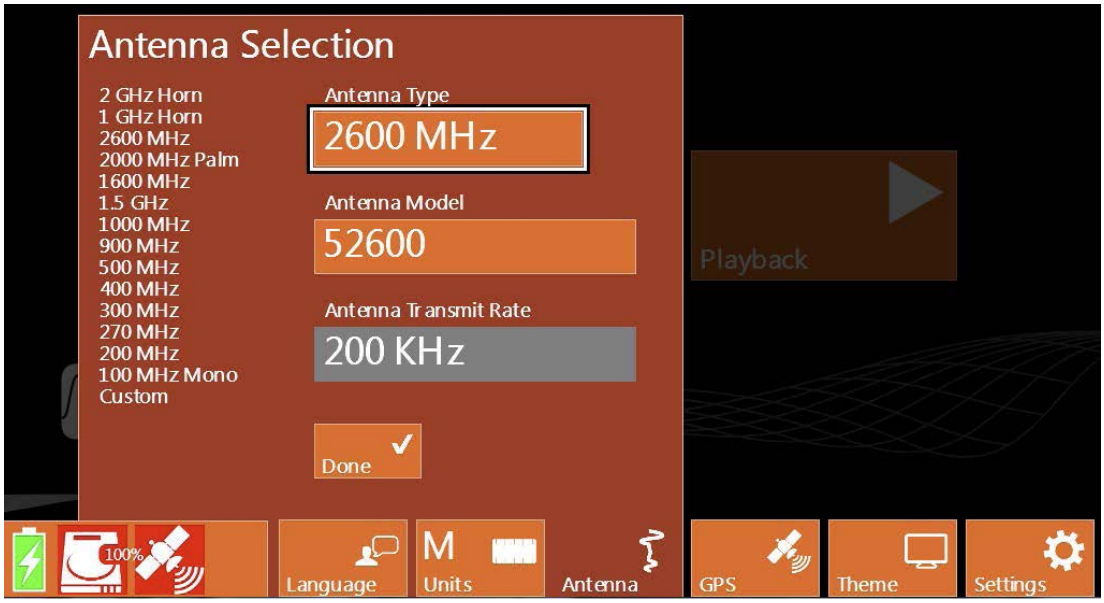

Section 2: Data Collection Setup

After setting the universal setup parameters on the Introduction screen, select either Last Used Settings or New Project and create a project name. After accepting a project name you will enter the Setup screen. The Setup screen is split into three windows. You will see the main data display at the left, a single scan in the O-scope display in the center, and the setup menu. The six function keys will be displayed in a bar at the bottom.

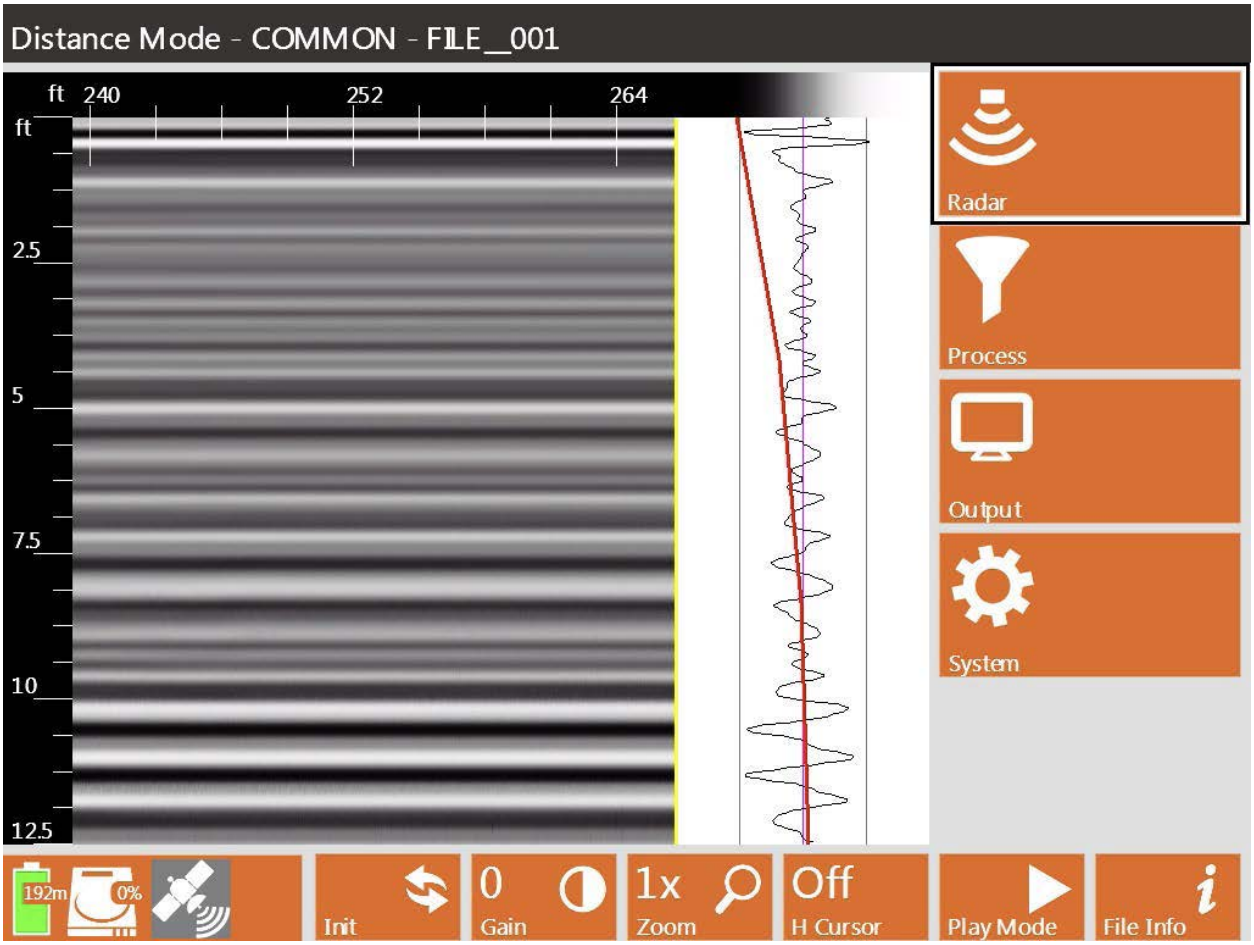

1- Press the Up-Down arrows on the keypad or rotate the scroll wheel to navigate the setup menu. To activate the submenus, press the center Enter key of the keypad or press the scroll wheel. The keypad and the scroll wheel have the same functionality so any step performed with one method has a corresponding step on the other.

2- Select Setup: Go to System ➡ Recall Setup and click the Enter button. Choose the appropriate antenna and cart combination from the list and press Enter. This will cause the antenna to re-initialize and data will begin to move across the screen.

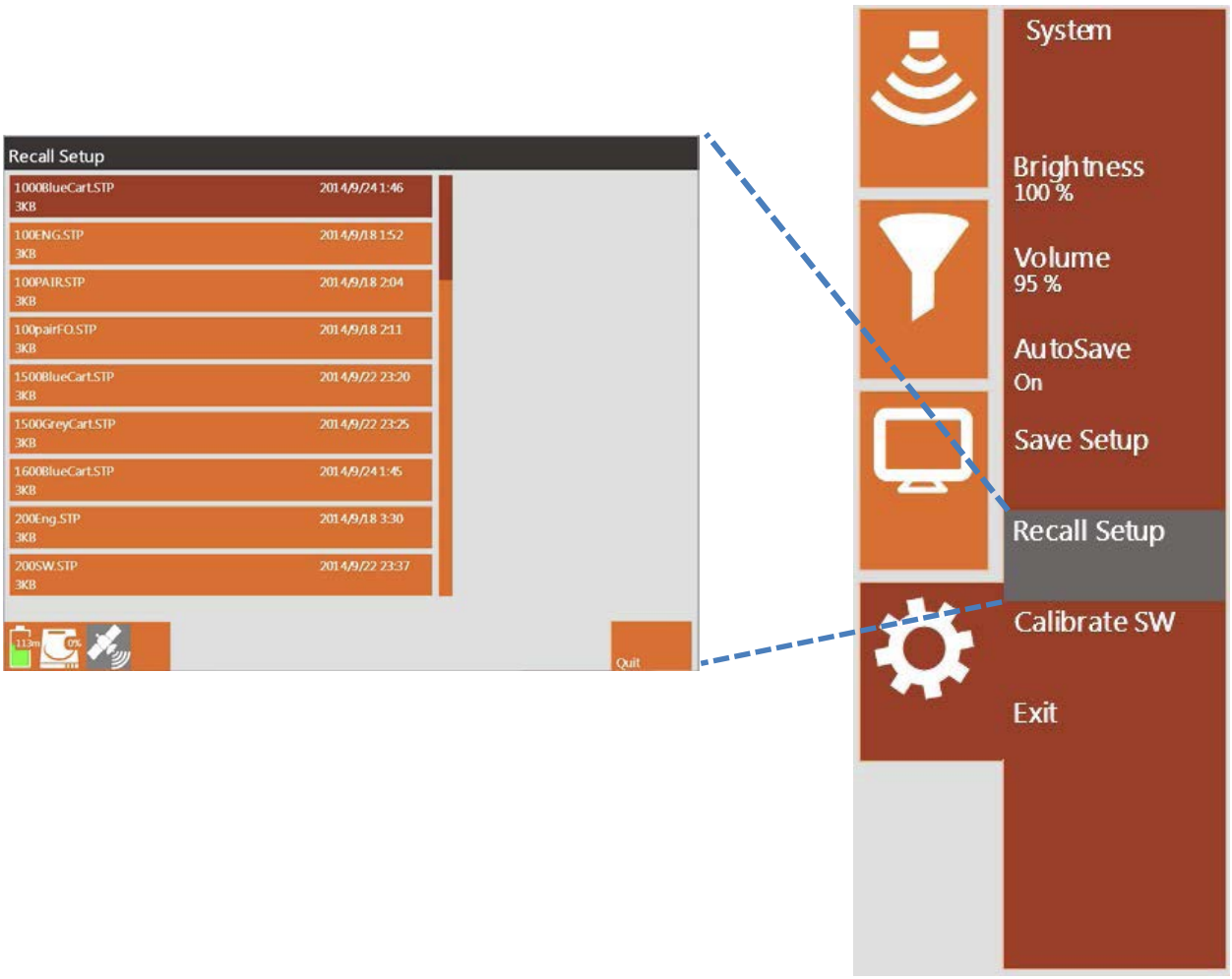

3- Calibrate Survey Wheel: Go to System ➡ Calibrate SW and press Enter. This will bring up the survey wheel calibration window.

- Lay out a measured distance on the survey surface and position the cart at the beginning of that distance.

- Highlight the calibration distance box, press Enter and enter in the distance that you have laid out on the ground as your calibration distance. Then press the green Start button.

- Move the UtilityScan to the end of that distance and then press the red Stop button. Highlight the Apply tab and press Enter.

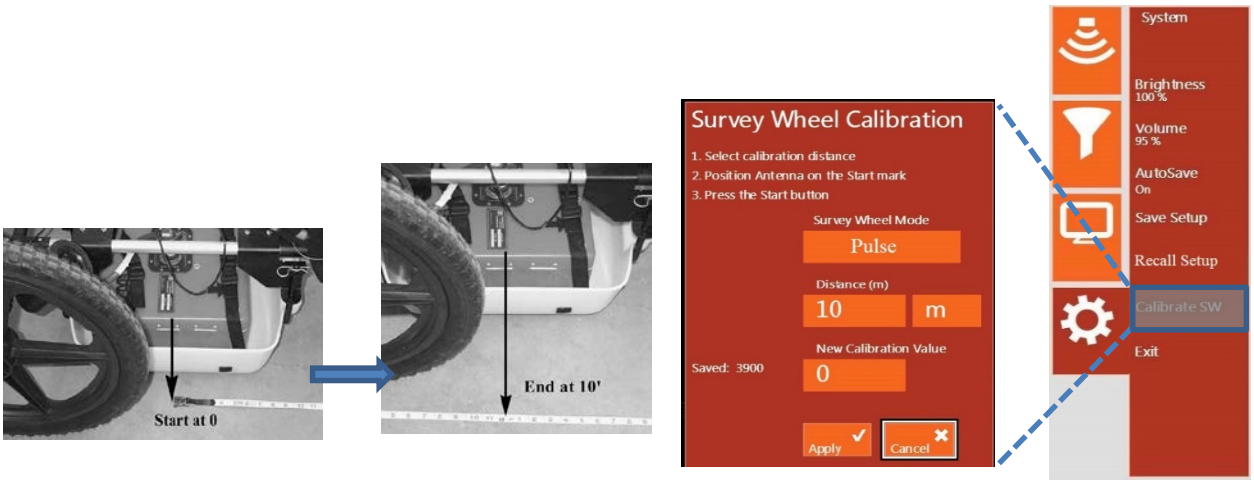

4- Set Depth Range: Under the Radar submenu, highlight Depth Range and press Enter. Use the scroll wheel or the Up-Down arrows to select your maximum depth of interest, and then press enter to accept. Always choose a depth that is deeper than the targets you are trying to image. Note that Depth Range and Time Range are interrelated menu options and a change in one will affect the value in the other.

5- Set Soil Type: This parameter is important for an accurate depth calculation. Under the Radar submenu, highlight Soil Type and press enter. Scroll through the options and highlight the choice that best reflects the local conditions. After making your choice, click Enter to accept the selection. Changes to the Soil Type or Dielectric will have an effect on the Time Range and/or Depth Range values.

Material	Dielectric Constant
Snow/Ice	3.0
Dry Sand	4.0
Pavement	6.0
Rock	8.0
Dry Soil	9.0
Ave. Soil	14.0
Wet Soil	20.0
Wet Sand	25.0
Water	80
Custom	

6- Set Scans/Unit: This sets the resolution along your survey line. Under the Radar submenu, highlight Scans/ft (Scans/m if units are set to Metric) and press enter. Use the scroll wheel or the Up-Down arrows to change this value, and then press Enter to accept. In Expert Mode the user has complete control over this value. For utility locating purposes values of 18 or 24 scans per foot are commonly used. If you are working in Metric, those values equate to 60 or 75 scans per meter.

7- Gains: If you believe the gains are set too low and the contrast of the linescan is too low to see targets, press the Init(ialize) button at the bottom left of the display. This will cause the system to re-initialize the gains and may help visibility. This will typically need to be done if the surface of your survey area changes. For example, if you are scanning a paved area and then move onto a grassy field, then the gains will likely need readjustment.

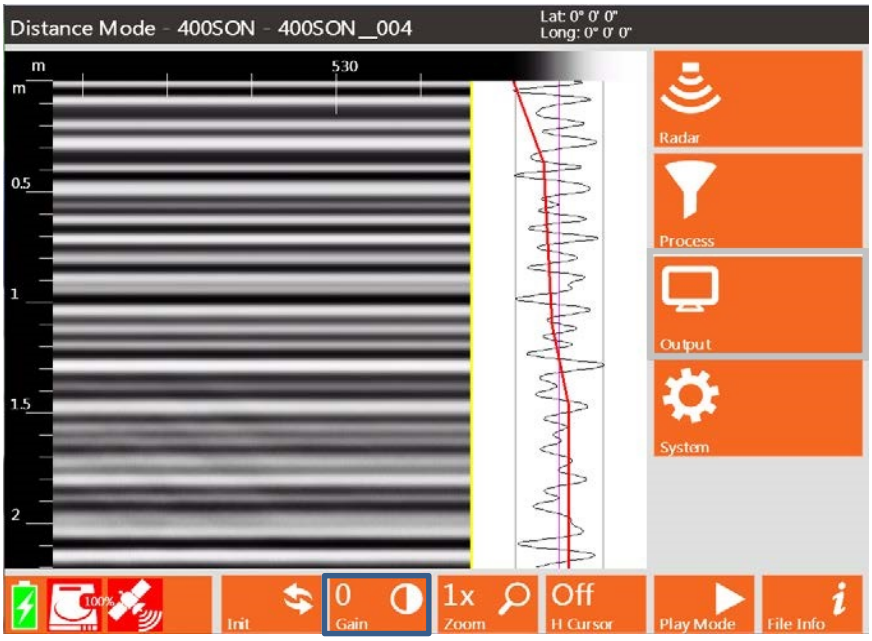

In addition, Expert Mode allows the user to manually adjust the gain values applied to the GPR signal. Under the Process submenu highlight Gain Mode and press Enter to toggle from Auto to Manual, then highlight Edit Gain Curve and press enter. The number of gain points can be increased or decreased, and the values for each individual point can be changed.

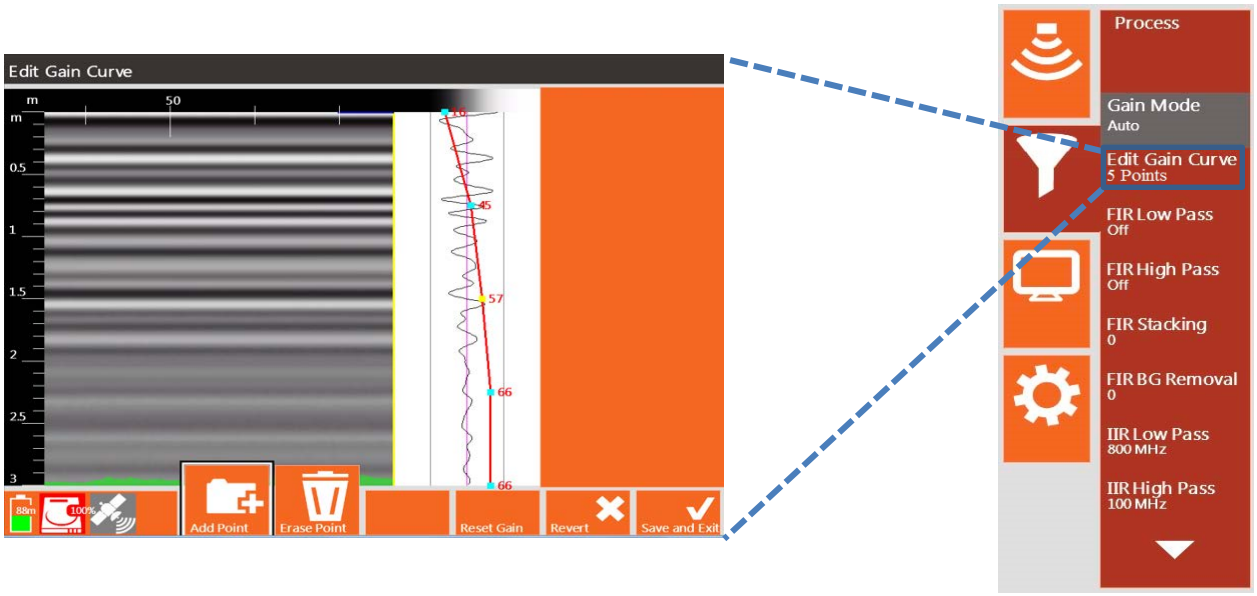

Section 3: Collecting Data

1- Start Collection: **Click the green Start button to begin collecting a data file. The data file's name will appear in the top left corner of the screen. Data only gets collected when you move the cart forward.**

2- Locating Targets: After you see a hyperbola on the screen, pull the system straight back along your survey line. You will see a yellow vertical line (the backup cursor) scroll along your data. When that vertical line is right over the apex of the hyperbola, the center of the antenna is over that target. The center of the antenna is directly under the connector panel. After marking the location on the ground, push the cart straight forward. No data will be collected until you have passed the spot where you started to reverse.

3- Calibrating Depth: (Optional) Match the target location in the data to its location in your survey area. Dig down to that target and measure the depth. Press the H Cursor button on the bottom toolbar to turn the horizontal cursor on. Use the scroll wheel to position the cursor to the top of the target in the data and form a crosshair. Press Set Depth to bring up the depth input window and enter in the measured depth, then press Enter. The vertical scale will adjust and the dielectric will be updated. Please note that this is only an approximation of the true depth because dielectrics can change with depth and across the site.

4- Go to Next File: When you have finished calibrating, press the red Stop button to finish collecting the open file. Press the green Start button to collect more data or press and hold the Stop button for > 2 seconds to return to the Setup screen

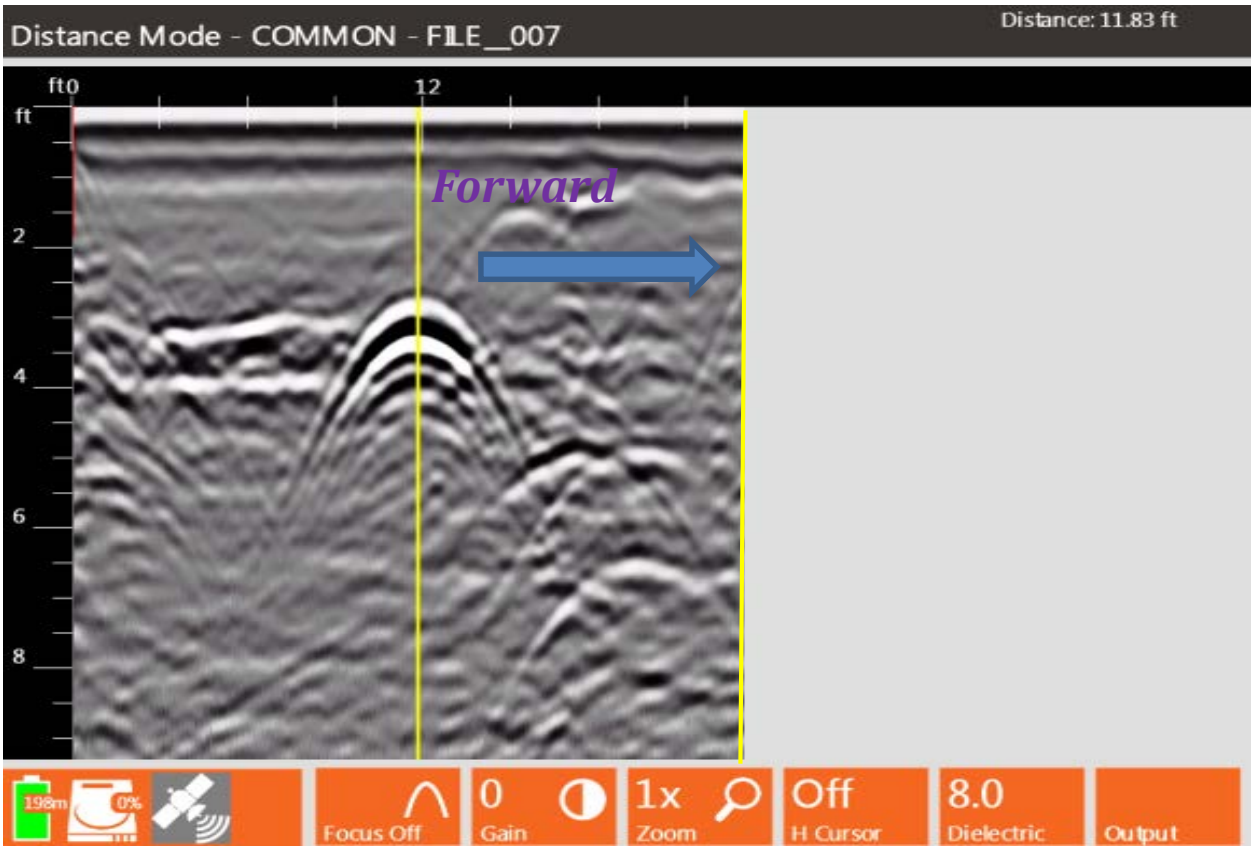

Section 4: Data Playback and Review

1- Recall Data: From the Collect Setup screen, press the Play Mode button on the bottom toolbar to bring up the list of saved files. Highlight the file you want to view and depress the scroll wheel to put a 'check' next to it. Press the Enter key to load the file.

2- Review Data: The file will scroll repeatedly on the Playback Setup screen. Press Start to replay the file once. Press Pause on the bottom toolbar to pause playback of a file and Resume to continue the playback. While playback is paused the horizontal and distance cursors can be moved by activating the appropriate cursor on the bottom toolbar. These can be moved with the Arrow keys or the scroll wheel to get the coordinates of any target. Also check to see if you can easily interpret your data or if it needs any processing.

3- Background Removal: **Apply this filter to check whether targets near the surface are being hidden by the direct coupling, or if you have strong horizontal banding (ringing) that you believe is making it difficult to see targets. The input here is in scans. Find the length of the band that you want to remove in feet, then multiply that number by the SCAN/UNIT that you collected the data at. If you want to remove the surface reflection, then set this at 1023.**

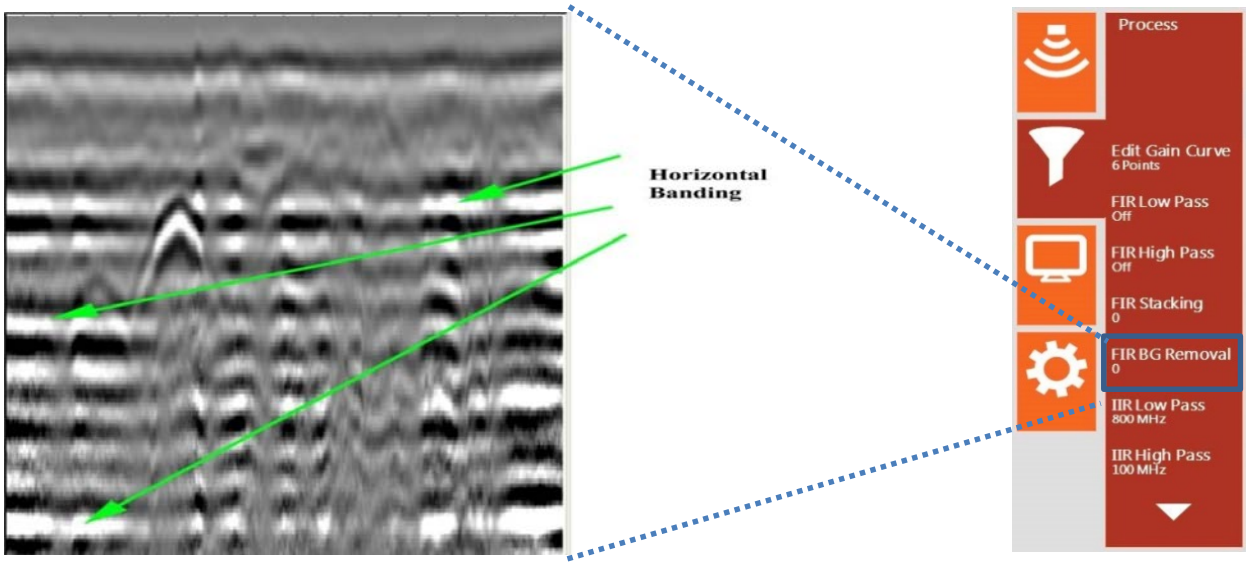

4- Collect More Data: **To return to data collection mode, press the Collect button along the bottom toolbar.**

Section 5: Saving a Screen-Capture Image

- **The SIR 4000 operating system includes a feature called Screen Capture. Screen Capture allows you to save a screenshot of the SIR 4000 screen being viewed and save that image automatically to the SIR 4000 memory as a Portable Network Graphics (.PNG) file.**

1- Button Sequence: Press and hold the down arrow, then press the Up arrow once. Screen Capture works in either Collect or Playback mode.

2- Screen Capture Image: The SIR 4000 screen capture feature will save the entirety of the image that is currently on the screen. This means that for longer data files, you must scroll left or right to capture images of an entire file. You will hear an aural indication that the SIR 4000 has saved the screen capture. It is now stored as the file name with a letter designator. For example, an image from FILE___036.DZT will be saved as FILE___036A.PNG. Multiple .PNG files can be captured from a single .DZT file.

3- Transfer the File: Transfer the data file (DZT) file to your computer following the steps in the next section. The .PNG file(s) will transfer automatically. There is no way to transfer the image without transferring the data.

- **The data that you collect with SIR 4000 can easily be transferred to a PC for either intensive processing in RADAN, or permanent archiving. Follow the steps below:**

1- Turn on the SIR 4000: Insert a battery or connect to AC power and push the green power button to turn on the system. You do not need to have an antenna connected.

2- Plug in USB jump drive: Uncover the USB port on the back left of the SIR 4000 and insert the USB jump drive card. There is only one right way for it to go in, so do not force it.

3- Playback Mode: All file management on the SIR 4000 occurs in Playback Mode. Select Playback Mode from the Introductory Screen. Once selected you enter the Select File menu where all data files within a project folder are listed, along with their size and the date they were collected.

4- Select Files and Transfer: Highlight each file you want to transfer and depress the scroll wheel to select a file and put a checkmark next to the file name. Alternatively press Select All on the bottom toolbar to select and checkmark all files within a project folder. Once the files are selected you have two options to transfer files to the USB thumb drive. On the bottom toolbar press Copy to USB save a copy of the GPR files to the USB while keeping the files on the SIR 4000 or Move to USB to move each file from the internal memory to the USB thumb drive.

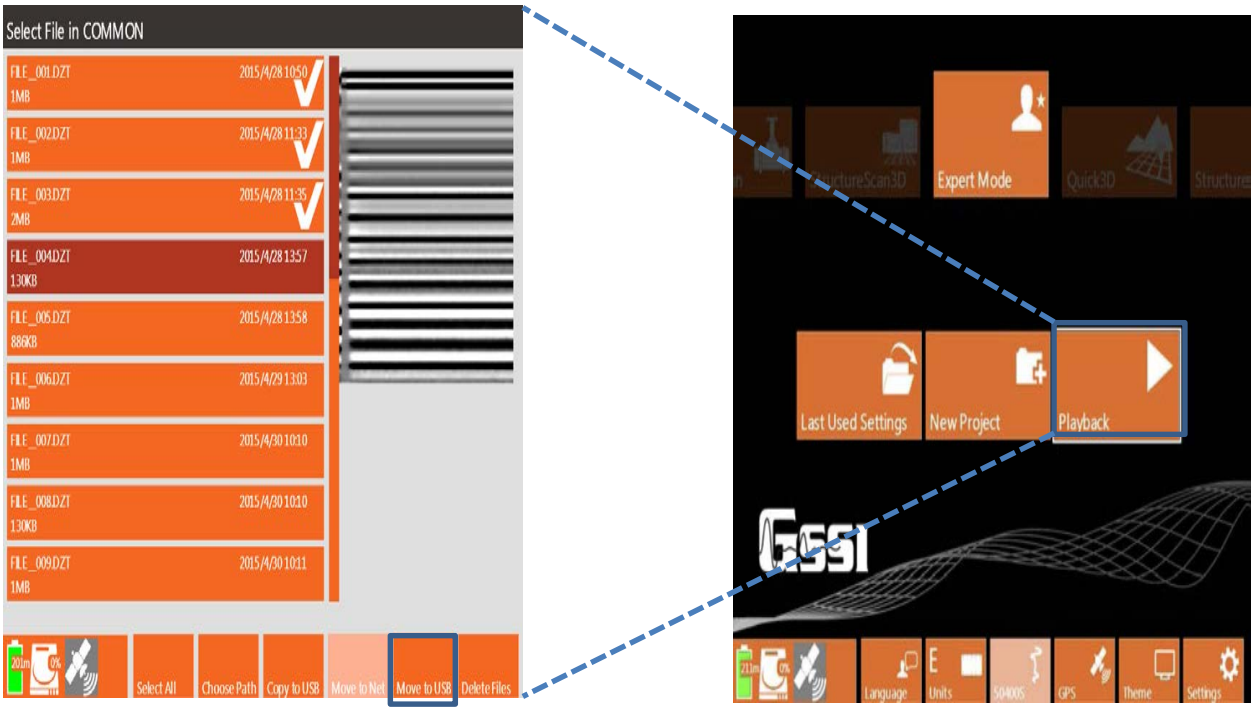

5- Plug USB thumb drive into PC: **Remove the USB thumb drive from the SIR 4000 and insert it into a USB port on your PC. Your PC should automatically find it, or click the "My Computer" icon and then "USB Disk (D:)". You will now see all of the contents of the USB thumb drive.**

6- Copy Data to PC: **You will see a folder on the thumb drive which matches the project name on the SIR 4000 you collected the data to. This folder contains your data, including .DZT radar files, .DZX header files, and any .PNG screen captures you may have collected. Copy this entire folder to you**

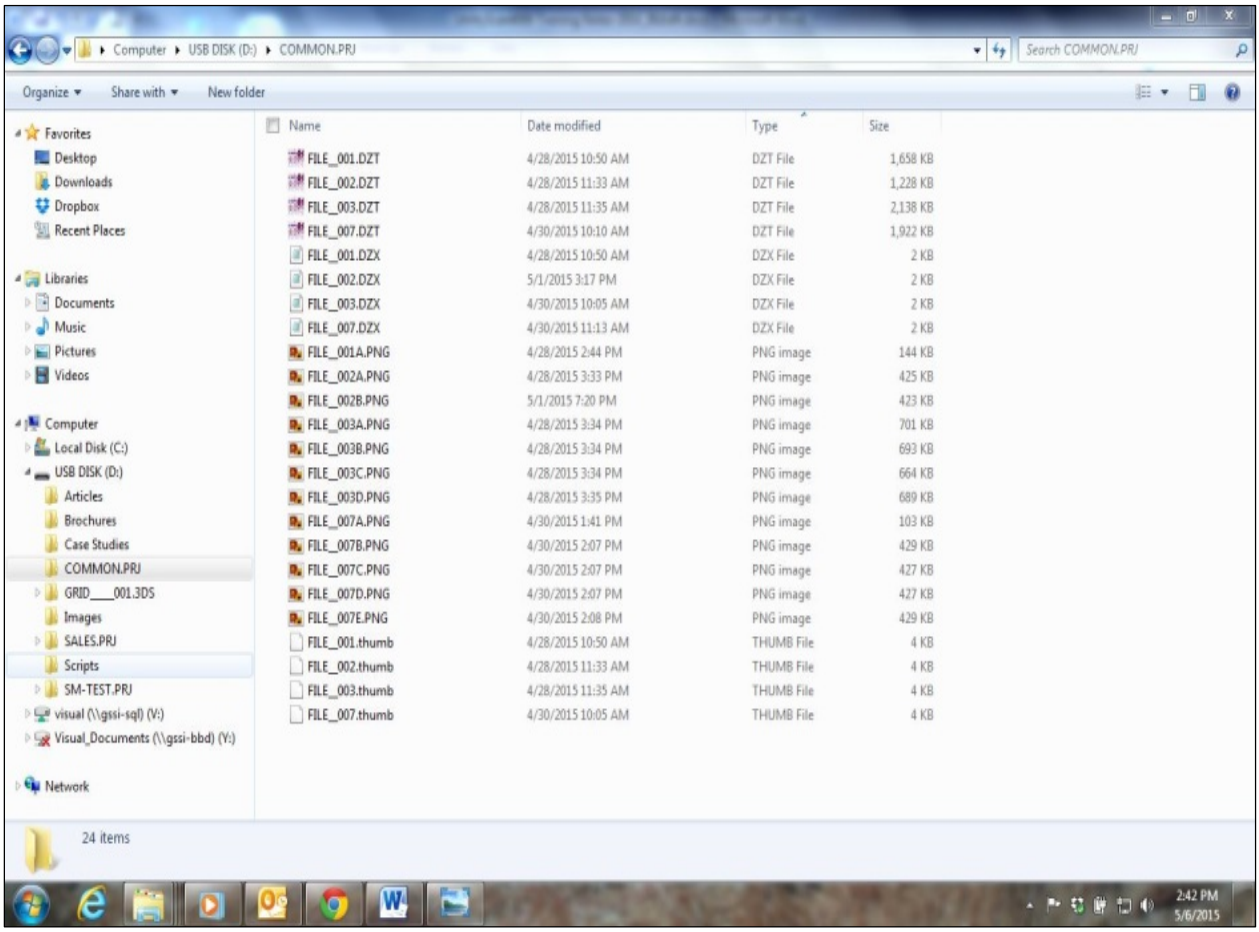

Dielectrics of Common Material

High EM Velocity

Material	Dielectric Constant	Material	Dielectric Constant
Air	1	Wet Granite	6.5
Snow Firn	1.5	Travertine	8
Dry Loamy/Clayey Soils	2.5	Wet Limestone	8
Dry Clay	4	Wet Basalt	8.5
Dry Sands	4	Tills	11
Ice	4	Wet Concrete	12.5
Coal	4.5	Volcanic Ash	13
Asphalt	5	Wet Sands	15
Dry Granite	5	Wet Sandy Soils	23.5
Frozen Sand & Gravel	5	Dry Bauxite	25
Dry Concrete	5.5	Saturated Sands	25
Dry Limestone	5.5	Wet Clay	27
Dry Sand & Gravel	5.5	Peats (saturated)	61.5
Potash Ore	5.5	Organic Soils (saturated)	64
Dry Mineral/Sandy Soils	6	Sea Water	81
Dry Salt	6	Water	81
Frozen Soil/Permafrost	6		
Syenite Porphyry	6		
Wet Sandstone	6		

Low EM Velocity